Application of Relative Response Factors in Solid-Phase Micro Extraction GC/MS for the Determination of Polycyclic Aromatic Hydrocarbons in Water

by

Tomi Schebywolok

Thesis submitted to the
University of Ottawa
in partial fulfillment of the requirements for the degree of
MSc in Chemical and Environmental Toxicology

Department of Biology
Faculty of Science
University of Ottawa

Abstract

Solid-phase microextraction (SPME) coupled with gas chromatography/mass spectrometry (GC/MS) is routinely used to analyze polycyclic aromatic hydrocarbons (PAHs) in water. A common SPME-GC/MS approach quantifies target analytes using isotopically labeled standards (IISs); one IIS is needed for each target analyte. This approach is challenging, even prohibitive since IISs are often expensive; moreover, they are generally not available for each analyte of interest. This study developed a novel SPME-GC/MS approach for the quantification of PAHs in water. The new method, which employs only a small number of IISs, uses relative response factor (RRF) (i.e., analyte corresponding to IIS) to quantify PAHs in water. Possible matrix dependency of RRFs values was examined using water that was modified concerning different physical-chemical characteristics (i.e., ionic strength, pH, suspended solids, humic acid, and biological organic carbon represented by hemoglobin). The results revealed that RRFs are not noticeably affected by changing ionic strength and pH; the other three parameters did affect the RRFs. However, the results also showed that the effect is minimal when the solution is dilute (i.e., low concentrations of suspended solids, humic acid or hemoglobin). Relatively stable RRFs for dilute water solutions indicates that this approach can be used for routine quantification of water that does not contain prohibitive amounts of suspended solids, humic acid, and biological organic matter. The developed method was employed to quantify trace levels of PAHs in three different types of water, namely river water, well water, and bottled water. PAH levels in every kind of water were less than 100 ng/L level (i.e., 0.1 ppb). Analyses of spiked water samples containing 2 ng PAHs revealed correlations between calculated RRFs and the physical-chemical

properties of the PAHs investigated (i.e., vapor pressure, boiling point, octanol/water partition coefficient, octanol/air partition coefficient, GC retention time). This implies that RRFs for PAHs not examined in this study can be predicted. Overall, the results presented herein constitute a meaningful contribution to the development of SPME-GC/MS methods for quantitative analysis of PAHs and other chemicals in dilute aqueous solutions. Moreover, the development of methods that alleviate the need for IISs corresponding to each target analyte.

Acknowledgments

I would like to acknowledge numerous people for the help that they have given to me in many ways. First and foremost I want to acknowledge my amazing wife for her patience, love, and support that she has given me throughout my time completing this thesis, without her I do not know where I would be at this point in my life. I would also honor my two supervisors, Dr. Paul White and Dr. Jiping Zhu, for allowing me to work under and sponsor me and my work. I would also like to thank Mrs. Krystyna Pipin and Mr. Mario Lacroix for their recommendation letters, without I would not have been able to do this thesis in the first place. Most importantly I would love to thank my children for keeping me grounded throughout the last four years of my life. Last and not least I have to acknowledge my late father Dr. Clifford Harold Schebywolok for giving me the initiative to go forward with "Try everything at least once! If you do not like it or succeed, at least you are far richer for the experience."

Table of Contents

List of Tables

`

List of Figures

`

`

`

`

List of Appendices

1 Chapter: Introduction

PAHs, also known as polycyclic aromatic hydrocarbons, are colorless yellow or white solid, chemically-related organic compounds. These compounds, which are generated by incomplete combustion of organic matter, are present in many contaminated environmental matrices, including urban air, vehicular exhausts, and soil. PAHs can enter the environment via a variety of natural or anthropogenic sources; they are generally found in complex mixtures. They have been deemed to be ubiquitous throughout the environment [1–3].

PAHs are comprised of carbon and hydrogen atoms formed into benzene rings of two or more rings fused together that are associated in many different arrangements (i.e., linear, angular or bunches) [3,4]. These rings usually have two or more carbon atoms that are shared between different rings within these arrangements. According to the definition of the International Agency for Research on Cancer, the smallest PAHs are anthracene and phenanthrene, which consist of three bonded aromatic rings[5]. There are hundreds of different PAHs, but the focus of research is often only on 14-20 priority PAHs. The most expansively researched PAH is benzo[*a*]pyrene (BaP) [6].

PAHs have the physical properties that include low aqueous solubility, low vapor pressure, high melting points and high boiling points[7]. The vapor pressure and aqueous solubility decrease with an increase in molecular weight (i.e., the addition of extra rings)[8,9]. Since PAHs are lipophilic, they are highly soluble in organic solvents and sparingly soluble in water. PAHs also have a variety of other properties including heat resistance, light sensitivity and electrical conductivity [10]. Many PAHs have mutagenic and carcinogenic properties; some have been found to be powerful immune-suppressants

that affect host resistance, immunities, and the overall development of immune systems [7,11].

1.1 Background

There are three sources of environmental PAHs: biological, petrogenic and pyrogenic. Pyrogenic PAHs are formed in anaerobic, or nearly anaerobic, conditions through a process of pyrolysis at high temperatures (i.e., 350^0C to 1200^0C). These can be produced intentionally through the creation of coke or coal tar from coal, and from the thermal cracking of petroleum into more widely used forms of hydrocarbons such as gasoline or diesel fuel. They can also form in internal combustion engines of cars and trucks, from incomplete burning of fuel oils, and from biomass fires (e.g., forest and wood-burning stoves). Petrogenic sources of PAHs are created in the maturation process of crude oil into crude oil products that are transported and used globally. The primary environmental sources of petrogenic PAHs come mainly from spills, large ones from oil spill disasters to small ones from vehicle refueling. They are also found in petroleum products that are used in everyday activities (e.g., lubricants). Interestingly, PAHs can also be produced biologically by specific plants and bacteria via the decomposition of vegetable matter[13–16]. It has been shown that human beings are the single most significant contributor to the formation and distribution of PAHs in the environment[17]. An interesting fact to note is that the number of rings of a PAH can differentiate whether a PAH is pyrogenic or petrogenic. For example, five ring PAHs come mainly from petrogenic sources (i.e., formed over an extended period); six-ring PAHs come from pyrogenic sources (i.e., formed over short periods of time) [15,18].

PAHs are released by anthropogenic activities such as combustion of fuels (e.g., biomass or fossil fuels), use of incinerators/smelters, and spills of materials that are treated with creosote and petroleum products[19]. They also come from natural combustion processes including biomass fires (i.e., forest fires, prairie fires) and volcanic eruptions, as well as from plant and bacterial biosynthesis[18]. PAHs, which are ubiquitous in the environment, typically bind to the surface of materials such as dust, sediments, and soil where they can be taken up by plants and in turn consumed by animals. PAHs can also enter the atmosphere where they are adsorbed to particles and fall back to earth in rainfall or via dry deposition. They can also be dispersed into natural water systems and partition to suspended particulate matter[20–22]. PAHs do not readily degrade in the environment. Through bioaccumulation, PAHs can accumulate in the tissues of organisms with a limited ability to generate and excrete PAH metabolites (e.g., bivalve mollusks). Humans are primarily exposed to PAHs via dietary ingestion (e.g., charbroiled meats, contaminated biota, etc.), non-dietary ingestion (e.g., contaminated soil), and inhalation of air containing combustion emissions (e.g., tobacco smoke, vehicular exhausts, etc.) [22–30].

Many PAHs are known, probable or possible carcinogens; many are known mutagens. PAHs experience a variety of metabolic transformations that lead to the formation of metabolites that have electrophilic properties. These include quinones, conjugated hydroxyl derivatives and diol epoxides that can generate reactive oxygen and covalently bind to nucleophilic centers in macromolecules such as proteins and nucleic acids. The process has been rigorously studied using benzo[*a*]pyrene (BaP); BaP undergoes an enzymatic transformation into the potent electrophile benzo[*a*]pyrene-7, 8-

diol-9, 10-epoxide (see Figure 1). This epoxide can interact with the amino groups of the nucleic acids (e.g., DNA); specifically, the exocyclic amino groups [30,31]. The resulting covalently-linked product is referred to as a DNA adduct. DNA adducts can disrupt the fidelity of DNA replication, and introduce mutations such as the G to T transversion mutations that have been observed in the p53 gene of tobacco smoke-induced lung cancers[32]. PAH-induced DNA adducts are also known to cause other types of genetic damage, including DNA strand breaks, small and large deletions, and alterations in chromosome structure and number [33,34]

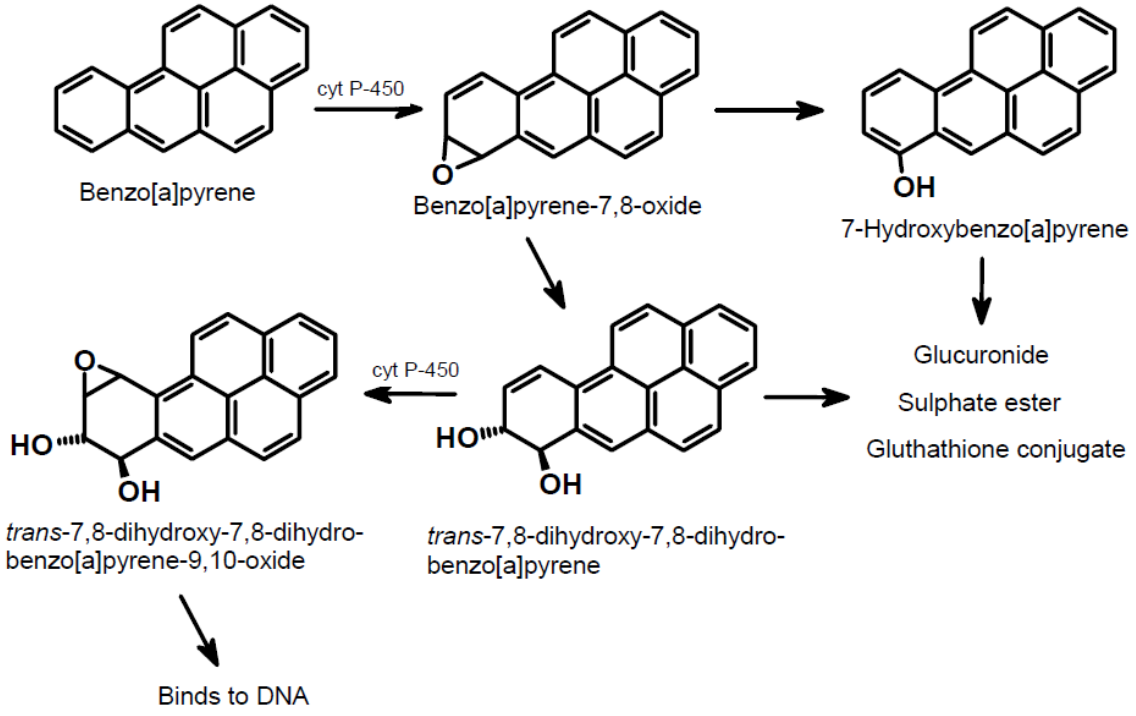

Figure 1 The metabolic conversion of benzo[*a*]pyrene to a DNA-reactive electrophile[35].

Due to their hazard, PAHs are an environmental concern; they are strictly monitored and controlled in many countries. The United States Environmental Protection Agency (USEPA) has compiled a list of 16 Priority PAHs (Figure 2). It is used as a basis for the environmental monitoring. The Canadian government's Priority Substance List

(PSL), which includes substances "that may be harmful to the environment or constitute a danger to human health," includes 13 PAHs. As such, 13 PAHs are regulated under The Canadian Environmental Protection Act (CEPA) (Figure 22)[36].

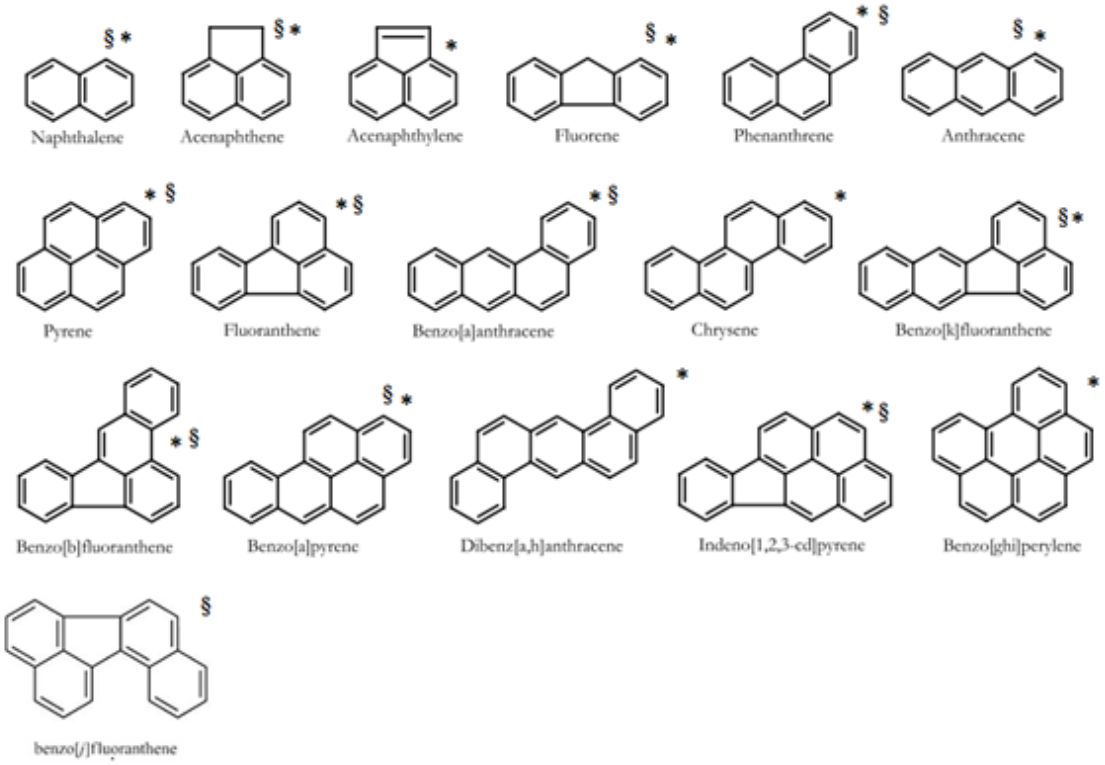

Figure 2 Structures of priority PAHs. *PAHs prioritized by the US-EPA. §prioritized under CEPA[35].

1.2 Chemical and Physical Properties of PAHs

PAHs tend to be lipophilic, and have a high affinity for organic matters. Each PAH has unique physio-chemical properties (e.g., aqueous solubility and vapor pressure). The properties of the various priority PAHs highlighted by the US EPA or Canadian CEPA (Figure 1-2) is highly variable, sometimes ranging over 5 orders of magnitude. Low molecular weight (LMW) PAHs are more water soluble and volatile than the high molecular weight (HMW) PAHs. Hydrophobicity of PAHs can be expressed as an

`

octanol-water partition coefficient (K_{ow}), with lower values indicating a stronger affinity for water and higher values indicating a stronger affinity for octanol. These properties govern the environmental behavior of PAHs (e.g., phase transfer and ultimate fate)[37]. Table 1-1 provides a list of the 15 PAHs investigated in this study, along with their density, ring number, molecular weight, boiling point, octanol/air partition coefficient, aqueous solubility, vapor pressure, and octanol/water partition coefficient[38].

Table 1-1 Some selected physical-chemical properties of the PAHs investigated in this study.

PAH Name	CAS (ǂ)	Molecular Formula (ǂ)	Rings (δ)	Molecular Weight (g/mole) (δ)
Naphthalene	91-20-3	$C_{10}H_8$	2	128
Acenaphthylene	208-96-8	$C_{12}H_8$	3	152
Acenaphthene	83-32-9	$C_{12}H_{10}$	3	154
Fluorene	86-73-7	$C_{13}H_{10}$	3	166
Phenanthrene	85-01-8	$C_{14}H_{10}$	3	178
Anthracene	120-12-7	$C_{14}H_{10}$	3	178
Pyrene	129-00-0	$C_{16}H_{10}$	4	202
Fluoranthene	206-44-0	$C_{16}H_{10}$	4	202
Chrysene	218-01-9	$C_{18}H_{12}$	4	228
Benzo[*a*]anthracene	56-55-3	$C_{18}H_{12}$	4	228
Benzo[*a*]pyrene	50-32-8	$C_{20}H_{12}$	5	252
Benzo[*b*]fluoranthene	205-99-2	$C_{20}H_{12}$	5	252
Indeno[*1,2,3-cd*]pyrene	193-39-5	$C_{22}H_{12}$	6	276
Dibenz[*a,h*]anthracene	53-70-3	$C_{22}H_{12}$	6	278
Benzo[*ghi*]perylene	191-24-2	$C_{22}H_{12}$	6	276

ǂ Physical -Chemical and Environmental Fate for Organic Chemicals Mackay D (August 1, 2006, 2nd edition)

δ Mackay D, Shiu WY Ma KC (1992) Illustrated handbook of physical-chemical properties and Michigan, USA.

Table 1-1 (continued) Physical-chemical properties of the PAHs investigated in this study.

PAH Name	Boiling Point (^{0}C) (δ)	Octanol/Air Partition Coefficient (Log Koa @ 25^{0}C)	Aqueous Solubility (mg/L @ 25^{0}C) (δ)	Vapour Pressure (Pa @ 25^{0}C)	Octanol/Water Partition Coefficient (Log Kow @ 25^{0}C) (δ)
Naphthalene	218	5.19 δ	31	1.0 x10 2 δ	3.37
Acenaphthylene	280	6.34*	16	9.0x10-1 δ	4
Acenaphthene	279	6.52*	3.8	3.0x10-1 δ	3.92
Fluorene	295	6.90*	1.9	9.0x10-2 δ	4.18
Phenanthrene	340	7.68*	1.1	2.0x10-2 δ	4.57
Anthracene	340	7.55 δ	0.045	1.0x10-3 δ	4.54
Pyrene	404	8.75 δ	0.13	6.0x10-4 δ	5.18
Fluoranthene	384	8.76*	0.26	1.2x10-3 δ	5.22
Chrysene	448	10.30*	0.006	5.7x10-7 δ	5.91
Benzo[*a*]anthracene	438	10.28*	0.011	2.8x10-5 δ	5.91
Benzo[*a*]pyrene	495	11.56*	0.0038	7.0x10-7 δ	5.91
Benzo[*b*]fluoranthene	481	11.34*	0.0015	5.0x10–8 ǂ	5.8
Indeno[*1,2,3-cd*]pyrene	536	12.43*	0.00019	1.0x10–8 ǂ	6.5
Dibenz[*a,h*]anthracene	524	12.59*	0.0006	3.7x10-10 δ	6.75
Benzo[*ghi*]perylene	525	12.55*	0.00026	1.4x10-8 δ	6.5

* M. Odabasi, et al (2006) Atmospheric Environment (40), 6615-6625

ǂ Physical -Chemical and Environmental Fate for Organic Chemicals Mackay D (August 1, 2006, 2nd edition)

δ Mackay D, Shiu WY Ma KC (1992) Illustrated handbook of physical-chemical properties and Michigan, USA.

1.3 PAHs in an aqueous environment

In an aqueous environment LMW PAHs will be partially dissolved, and therefore in the aqueous phase of natural waters. In contrast, HMW PAHs associate themselves with particles, and will therefore be found associated with the particulate phase of natural waters. A typical sink for HMW PAHs is the sediments in and around marshlands, rivers, and lakes[39]. For water purification both biological and grit chamber treatments can be used to effectively remove PAHs from surface water destined for human consumption [40].

The most common processes for removal of LMW PAHs from surface waters are evaporation and microbial degradation. Since HMW PAHs are not as soluble, they are not readily removed via biodegradation. The removal of HMW PAHs is primarily eliminated by photochemical processes[41,42]. Photolysis of a PAH occurs when light energy is absorbed[43]. These photochemical reactions, often involving OH• radicals and O_3, can lead to the creation of PAH intermediates [44]. Photochemical intermediates, such as BaP-4,5-dihydrodiol from benzo[*a*]pyrene and anthraquinone from anthracene, are more inclined to undergo biodegradation for the eventual breakdown in the environment[45,46]. Some important factors that affect the rate of photo-degradation are light intensity, dissolved oxygen, and temperature[41]. A few examples of PAHs that are degraded by photolytic processes are acenaphthene[47], acenaphthylene[48], anthracene[49,50], benzo(a)anthracene[50] and benzo[*a*]pyrene example, anthracene can be broken down by bacteria such as Nocardia, Sphingomonas, Paracoccus, Beijerinckia, and Rhodococcus; a dihydriol is the primary oxygenated intermediary [51]. The following PAHs are examples of other PAHs that are degraded by microbial metabolic processes: benzo[*a*]pyrene [52,53] and fluorene[54]. Past research shows that the half-lives of individual PAHs in surface

waters are typically in the range of several hours. More specifically, benzo[a]pyrene has a half-life of about 40 minutes and benzo[a]anthracene of five hours.[41]

1.4 Measurement Methods

1.4.1 General Analytical Method

Analysis of trace-level PAHs in water is carried out using many different methods. Typical methods for pre-analysis sample preparation include solid phase extraction (SPE), sonication, and liquid-liquid extraction (LLE) (Table 1-2). These sample preparation procedures usually consume a significant amount of organic solvent to extract and concentrate PAHs in water.

Table 1-2 Methods to extract PAHs from water

Method	Extraction Type	Method Focus	Ref
US EPA 610	LLE	Methods for organic chemical analysis of municipal and industrial wastewater - Method 610, poly-nuclear aromatic hydrocarbons	55,56
US EPA 525	SPE	Determination of Organic Compounds in Drinking Water by Liquid-Solid Extraction and Capillary Column Gas Chromatography/Mass Spectrometry	56,57
Europa -4	LLE	Polycyclic Aromatic Hydrocarbons (PAHs) analysis.	58
US-emulsification microextraction method	Sonication	Development of a novel ultrasound-assisted surfactant-enhanced emulsification microextraction method and its application to the analysis of eleven polycyclic aromatic hydrocarbons at trace levels in water	59

Solid-phase microextraction (SPME) is an extraction technique that uses a fused silica fiber coated with a thin layer of a polymer capable of selectively concentrating the chemical(s) of interest. Analytes are extracted by the fiber either through immersion of the fiber in a liquid (i.e., direct SPME), or suspension of the fiber in the space above a sample matrix (i.e., head-space SPME). The fiber is exposed to the matrix through the sheath, usually a needle. After exposure, the fiber is removed from the matrix and placed inside the injection port of the instrument being used for the analysis[60].

1.4.2 Solid-Phase Micro-Extraction GC/MS

Solid-phase microextraction (SPME) was developed by Pawliszyn in 1989 and patented in the early1990s[61]. Since then it has been applied in many different fields for the analysis of trace levels of analytes in complex matrices.

It is important to note that there is a fundamental difference between SPME and SPE. In SPME only a small amount of extraction material, usually a polymer coated fiber, is exposed to the matrix. In contrast, SPE uses a bed packed with sorbent. Originally, the term SPME was used since the method uses a small quantity of solidly fused silicon fiber[61]. Since its inception, the SPME process has evolved into many different forms and procedures.

The most crucial part of the analysis of trace analytes by SPME is the choice of the fiber used to extract the analytes from the matrix. There are many different types of coating materials used in SPME, including Polydimethylsiloxane (PDMS), Carboxen/PDMS, Polyacrylate, Polyethylene Glycol, and PDMS/Divinylbenzene (PDMS/DVB). Each coating material has unique properties, which are specifically selected for the compounds to be analyzed. The material either adsorbs (i.e., PDMS/DVB

fiber) or absorbs (i.e., PDMS fiber) the analytes. The fiber materials chosen herein for the analysis of trace amounts of lipophilic PAHs in water are PDMS and PDMS/DVB. The PDMS/DVB fiber more readily adsorbs LMW PAHs, while the PDMS fiber more readily absorbs the HMW PAHs.

Commercially available SPME fibers have the same dimensions, except for the thickness of the coating. The thickness of the fiber coating ranges from 7 µm to 100 µm, depending on the type of fibers. The commercially available PDMS/DVB fiber (i.e., adsorptive) has a fixed coating thickness of 65 µm. The PDMS fiber (i.e., absorptive) is available in coating thicknesses of 7 µm, 30 µm or 100 µm.

The instrumentation used for analyzing trace amounts of PAHs extracted from aqueous media include both high-pressure liquid chromatography (HPLC) and gas chromatography (GC). These instruments are coupled to a variety of detectors, including an ultraviolet-visible light detector (UV-Vis), mass spectrometer (MS), and a fluorescence detector for HPLC, and electron capture detector (ECD), flame ionization detector (FID), thermal conductivity detector (TCD) and MS detector for GC. One of the most effective instrumentation combinations for the analysis of trace amounts PAHs, which is also the one usually used in conjunction with the SPME approach, is GC/MS.

1.4.3 Advantages and Limitations of SPME

Compared to other sample preparation/extraction procedures like SPE, sonication, and LLE, SPME has many significant advantages. It is easy to implement and convenient, permits rapid analysis, and is almost completely solvent-free. However, to obtain accurate quantitative results with SPME GC/MS, it is generally necessary to use

an IIS (isotopically-labeled internal standard) for each analyte under investigation[62]. However, this approach can be expensive. Moreover, in some cases, the corresponding IISs for some analytes are not available. Therefore, the analyte-specific IIS requirements of SPME GC/MS approach can pose significant operational challenges.

1.5 Hypothesis

One way to minimize the need for numerous analyte-specific IISs is to use a small number of representative IISs. This might be achieved by using the relative response factor (RRF) concept, whereby the response of a chemical analyzed via SPME GC/MS is compared to the response of an IIS for a different chemical. Using RRF values to link one IIS to several target analytes will reduce the number of IISs. If this approach works, it will greatly enhance the applications of SPME GC/MS for environmental analysis of trace chemicals. Concerning this study, the following hypotheses were evaluated:

1. The relative response factor (RRF) of an analyte in a given matrix (e.g., PAHs in water), as defined above, will remain unchanged across changes in the properties of the matrix (e.g., pH, salinity, etc.), especially for analytes with similar physical-chemical properties (i.e., PAHs).
2. By employing RRFs, a quantitative SPME-GC/MS method can be established for reliable quantification of trace PAHs in water, alleviating the need for an IIS for each analyte.

1.6 Objectives

To evaluate the aforementioned hypotheses, the project had three objectives: (1) for optimized SPME GC/MS conditions, examine RRFs for several PAHs (i.e., relative to IISs) across changes in the properties of the aqueous matrix; (2) evaluate the precision of

the RRF approach for quantitation of trace PAHs in different waters via SPME GC/MS; and (3) examine the relationships between RRFs and the physical-chemical properties of PAHs.

2 Chapter: Materials and Methods

2.1 Materials and Equipment

An eVol® XR automated syringe system from SGE Analytical Science (Ringwood, Victoria, Australia), with dedicated (serial number labeled) syringes, was used throughout all experimentation. The volumes of the syringes used in the experiments were 5 µL, 50 µL, 100 µL, 500 µL and 1000 µL. A Fisher Scientific™ accumet™ Excel XL25 pH/mV/Temperature/ISE Meter (Fisher Scientific, Singapore) was used to measure pH. A VWR 575 Digital Hotplate stirrer, conductivity meter combination (Thorofare, USA) was used to measure the conductivity of solutions. Mass was measured using a Metler Toledo AE 163 balance (Metler Toledo, Switzerland). A Thermo Scientific ST16 bench top centrifuge (Thermo Scientific, USA) was used to remove suspended particulate matter.

All laboratory glassware, including beakers, volumetric flasks, bottles, was cleaned with chromic-sulfuric acid for an hour, washed with soap and water, rinsed with Milli-Q (Milli-Q advantage A, USA) water, and finally rinsed with organic solvents three times each in the following order: methanol, dichloromethane, hexane, and acetone. All glassware was then turned upside down and air-dried inside a fume hood. The 20-mL SPME vials (Agilent, Germany) were obtained from the manufacturer in a sterile condition; they were used as received.

Analytical instrumentation consisted of an Agilent 7890A gas chromatograph (GC) (Agilent Technologies, USA) connected to an Agilent 7000A Triple Quad Mass Spectrometer (Agilent Technologies, USA). The instrument was equipped with a Gerstel Multipurpose Sampler (MPS) (MPS2XL, Gerstel, USA) for sample introduction. The

MPS has options for liquid injection (using a syringe) and SPME (solid phase microextraction) fiber injection. Liquid injection, using a 10 µL Gerstel Syringe adaptor was used for the initial optimization of the GC/MS conditions.

SPME fibers used in the analyses included Supelco 23Ga 100 µm PDMS fiber (Supelco, 57342-U, red marked), 23Ga 30 µm PDMS fiber (Supelco, 57289-U, yellow marked), and 23Ga 65 µm PDMS/DVB fiber (Supelco, 57902-U, pink marked). MassHunter workstation software (Agilent) was used for data acquisition and analysis. Qualitative analysis was performed using a MassHunter Qualitative Analysis software (Version B.03.00 Build 3.0.318.0 for GCMS, Agilent). Quantitative analysis was performed using a MassHunter Quantitative Analysis software (Version B.03.01 Build 3.1.170.0 for GCMS, Agilent).

2.2 Chemicals and solvents used in sample preparation and cleaning

The following is a list of chemicals along with the information about supplier and the purity: acetone (EMD chemicals, Canada, >99% HPLC Grade), methanol (EMD chemicals, Canada, >99% HPLC Grade), dichloromethane (Sigma Aldrich, Canada, >99% HPLC Grade), sodium chloride (EMD chemicals, Canada, >99%), sodium hydroxide (Sigma Aldrich, Canada, >97%), hydrogen chloride (EMD chemicals, Canada, 36.5-38% in water), humic acid (IHSS - International Humic Substances Society, USA, Lot #1R101N-Swanee River), and hemoglobin from bovine blood (Sigma Aldrich, Canada, >85% HPC).

2.3 Preparation of PAH solutions and spiked water samples

A PAH mixture (QTM PAH Mix) containing 16 PAHs at a concentration of 2 mg/mL each PAH in dichloromethane was purchased from Supelco (Supelco, 47930-U

Lot: LB78943). This mixture was used to determine GC/MS retention times. Mass spectrum and elution order from the literature were used to help identify the PAH peaks[56,63,64]. One brominated PAH in the QTM PAH mixture, 2-bromo naphthalene, was excluded from this study. The QTM PAH mixture was also used as the stock solution for preparation of all spiking solutions employed throughout the study.

The 1,000 ng/µL stock solutions of isotope-labeled standard (IIS) of acenaphthene-d_{10} (Cambridge Isotope Laboratories, USA) and chrysene-d_{12} (Cambridge Isotope Laboratories, USA) were prepared by weighing 50.0 mg of IIS into a 50 mL class A volumetric flask and dissolving the contents in acetone. Working solutions of 10 ng/µL were prepared by diluting 100 µL of the stock solution in 10 mL acetone in a volumetric flask. IIS of $^{13}C_{12}$-benzo[*ghi*]perylene (100 ng/µL in nonane) was purchased from Cambridge Isotope Laboratories (Tewksbury, USA) as a stock solution. The 10 ng/µL working solution was made by diluting 1000 µL stock solution in 10 mL of acetone in a volumetric flask. These three IIS working solutions (10 ng/µL) were used for spiking water samples.

PAH spiking solutions were prepared from the QTM PAH mixture via a series of dilutions in acetone. More specifically, the QTM PAH mixture (2000 ng/µL) was first diluted 20 times to obtain the 100 ng/µL solution (solution A); Solution A was then further diluted to create working solutions of different concentrations for spiking the water samples At the levels of 2.0 ng/µL, 0.5 ng/ µL, 0.1 ng/ µL and blank (0.0 ng/ µL).

2.4 Instrumental analysis conditions

2.4.1 Optimization of instrument conditions - liquid injection

GC/MS transfer line temperature and MS ion source temperatures were maintained at 300 ^{0}C and 150 ^{0}C, respectively. MS was operated in electron ionization (EI) mode at 70 eV. The analytes were separated using a DB-1MS UI fused silica capillary column (30 m long × 0.25 mm internal diameter × 0.25 μm film thickness). Liquid injection was conducted in splitless mode with an injection volume of 1.0 μL, and a port temperature of 260 ^{0}C. Helium was used as the carrier gas. The oven temperature program was: 70^{0}C for 2.5 min, then 30^{0}C/min to 200^{0}C, then 8^{0}C/min to a temperature of 280^{0}C, rate 30^{0}C/min to the final temperature of 300^{0}C held for 4 min. Scan mode (40-400 amu) was used for initial optimization of MS conditions, and for obtaining a mass spectrum for PAH peak identification. Retention times (RT) and mass spectra, obtained from the literature, were used to help determine the identity of peaks [56,63–65] (see Table 3-1). Selected ion monitoring (SIM) mode was used for subsequent analysis of water sample extracts. Ions monitored in SIM are listed in Table 3-1. The selected quantification ion and their qualifiers were chosen based on information from the literature[66].

2.4.2 Optimization of instrument conditions - SPME fiber injection

2.4.3 Determination of optimal conditions for fiber cleaning

The MPS needle heater was used to clean the fiber. Cleaning conditions were determined by testing the fiber by testing the extraction procedure using a sample formulated with Milli-Q water spiked with using the 10 ng/μL PAH solution. The 100 μm PDMS fiber and the 65 μm PDMS/DVB fiber were then subjected to a bake out time by holding the exposed fiber within in the needle heater for 15 min, 20 min and 25 min, each at 250^{0}C and 260^{0}C for a total of three trials at the upper end of each fiber's

temperature range, giving six runs for bake out temperature determination. This analytical process allowed for the proper determination time needed for cleaning the fiber.

2.4.3.1 Determination of optimal conditions for fiber desorption

GC fiber desorption conditions were completed in the temperature range of 200^{0}C to 280^{0}C (using 10^{0}C increments) for the 100 µm PDMS fiber, and 200^{0}C to 270^{0}C for the 65 µm PDMS/DVB fiber. The desorption times were 60-300 seconds, in 30-second increments.

2.4.3.2 Determination of optimal conditions for SPME operation

Various extraction times and temperatures were tested to determine the best conditions for SPME extraction of target PAHs from the water. Four temperatures (i.e., 30^{0}C, 40^{0}C, 50^{0}C, and 60^{0}C) were tested, each with different extraction times (i.e., 20-90 minutes in 10-minute increments). Three different types of fibers (i.e., 100 µm PDMS, 30 µm PDMS and 65 µm PDMS/DVB) were tested for the overall method conditions needed for the final SPME extractions to be performed.

2.5 Relative response factors and quantitative method

Relative response factor (RRF) was determined using the following equation.

$$RRF = \frac{As}{Ai} / \frac{Cs}{Ci} \qquad (2\text{-}1)$$

Where, As = area of PAH peak, Ai = area of IIS peak, Cs = concentration of PAH, and Ci = concentration of IIS. The same equation can be rearranged for calculation of the PAH concentration in the tested samples (equation 2-2).

$$Cs = \frac{As*Ci}{Ai} / RRF \qquad (2\text{-}2)$$

`

Two different approaches were used to generate the RRFs. The "average" method determines the RRFs by first calculating the average of the replicate RRF values, and then using linear regression to obtain the RRF results. The "slope" method obtains the RRF values from the regression line for each set of samples, and then averages the RRF values.

2.6 Preparation of water samples for SPME GC/MS analysis

All water samples were stored at 4 °C until analysis. Before sample preparation, the water sample was warmed up to room temperature and transferred to 20-mL SPME vials. The fixed volume of water transferred to each SPME vial was set at 17.5 ml per sample vial. In all cases, the IIS concentration was set at 1.0 ng/sample.

Water samples (see section 2.8) in SPME vials were spiked with 1 µL of one of the respective PAH spiking solutions (see section 2.4) to create concentrations of 2.0 ng/sample, 0.5 ng/sample, and 0.1 ng/sample. As was done for RRF verification, water samples were analyzed in four runs: two runs using the 30 µm PDMS fiber, and two runs using the 65 µm PDMS/DVB fiber. Each run consisted of a four-sample set (i.e., spiked with PAH spiking solutions at 0.1 ng/sample, 0.5 ng/sample or 2.0 ng/sample).

2.6.1 Water samples with various pH values

Water samples with different pH values were prepared in 250-mL Kimex© media bottles. Each bottle was filled with 200 mL of Milli-Q water and then adjusted to the desired pH (i.e., from 4.5 to 9.0 in increments of 0.5) using 0.5 M HCl or 0.5 M NaOH.

2.6.2 Water samples with various ionic strength values

The ionic strength of water samples was expressed as the concentration of NaCl. NaCl salt solutions were prepared using 250-mL Kimex© media bottles. Each bottle was

filled with 200 mL of Milli-Q water, and NaCl added to prepare the required solutions (i.e., 0.10%, 1.0% to 10.0% in increments of 1 %). The solutions were agitated until complete dissolution of the NaCl.

2.6.3 Water samples with various suspended solids concentrations

Twenty grams of archived house dust was cleaned in a 50-mL glass centrifuge tube (using 20 ml of each of the following organic solvents in sequence: dichloromethane, 50/50 mix of hexane and acetone, hexane, methanol, and acetone. After adding the organic solvent, the mixture was sonicated for 10 min and then centrifuged for 5 min at 10,000 rpm. The supernatant was decanted and discarded. This process was repeated three times for each solvent wash. The cleaned dust was then left in the tube to dry for 48 hrs. in a fume hood. A portion (14 g) of the resulting dry dust was placed into a 500-mL Kimex© media bottle containing 250 mL of Milli-Q water and agitated. The resulting solution was sonicated for 30 min, shaken by hand for 1 min, and then left to settle for 90 min. The supernatant, which was slightly cloudy, was decanted into another bottle and used as the parent solution. Different concentration solutions were prepared from the parent solution by serially diluting by a factor of 3 to create 3x, 9x, 27x, 81x, 243x, 729x and 2187x dilutions in water, respectively.

2.6.4 Water samples with various humic acid concentrations

The parent solution of humic acid in water (i.e., 1.0 mg/mL) was prepared by adding 200 mg of 1R101N-Humic Acid (Suwannee River, International Humic Substances Society) to 200 mL of Milli-Q water in a 250-mL Kimex© media bottle. The solution was then stirred for at least 24 hours to dissolve the humic acid completely. This parent solution was subsequently diluted as stated in section 2.6.3.

2.6.5 Water samples with various hemoglobin concentrations

The parent solution of hemoglobin in water was prepared by adding 2.0 g of bovine hemoglobin (Sigma Aldrich, Canada) into 100 mL of Milli-Q water in a 250-mL Kimex© media bottle. The solution was stirred for 4 hours and the parent solution subsequently diluted as stated in section 2.6.3.

2.6.6 Preparation of complex water samples at pH 5.5 and pH 7.5

To create a water matrix that mimics surface and ground waters the following procedure was used. 1 L of the 5.5 pH water solution was first created using Milli-Q water, and this water was created to perform dilution to the solutions. 100 ml of complex water solution was prepared by first dissolving 100 mg of humic acid in 90 mL of deionized laboratory water. Then 10 g of NaCl and 2.0 g of hemoglobin were then added to the solution. The resulting solution was then adjusted to pH 5.5 using 0.5 M NaOH solution and left to mix for 1 hour. A series of dilutions (i.e., 3x, 9x, 27x, 81x, 243x, 729x and 2187x) were prepared from this initial solution using pH 5.5 water. The same procedure was used to create the pH 7.5 complex water sample, with the exception that dilution used pH 7.5 Milli-Q water.

2.6.7 Natural water samples

Natural water samples analyzed in this study included groundwater (i.e., well water), surface water (i.e., river water) and bottled water. The well water samples included 5 replicate samples from a single location. The surface water samples included 5 samples from 5 different locations along the Ottawa River (Figure 3), and the bottled water samples included samples from five different retail brands. Each sample was divided into four sets: original without spiking plus three spikings (at 0.1 ng

PAHs/sample, 0.5 ng PAHs/sample, and 2.0 ng PAHs/sample), with the IIS level fixed at 1.0 ng/sample for all. Each set of samples were divided into 4 replicates: two were analyzed using the 30 μm PDMS fiber (run 1 and run 2) and two using the 65 μm PDMS/DVB fiber (run 1 and run 2) (Table 2-1).

Table 2-1 Summary of samples examined for each SPME-PAH combination

	Sample number	Number of sets	Replicates of each sample	Total SPME samples
Well water	5 replicates	4	4	80
River water	5 locations	4	4	80
Bottled water	5 brands	4	4	80

2.6.8 Collection of water samples

All collected water samples were stored at 4 °C and processed within 5 days. Relative response factors (RRFs) of PAHs to the IISs were generated using both the "average" method and the "slope" method (see section 3.3).

2.6.9 River water

Each sample of river water was collected in a 250-mL Kimex© media bottle filled completely with no headspace. River water was collected from the following five locations along the Ottawa River (Figure **3**):

1. Site 1: at the entrance of the Rideau River just downstream of the "Port de Plaisance Jacques-Cartier" marina.
2. Site 2: at the entrance of the Rideau Canal.
3. Site 3: near the wooden rail bridge crossing the Ottawa River.

4. Site 4: on the northeast corner of Bate Island located approximately halfway across the Champlain Bridge.
5. Site 5: upstream from the Aylmer Marina on the north shore.

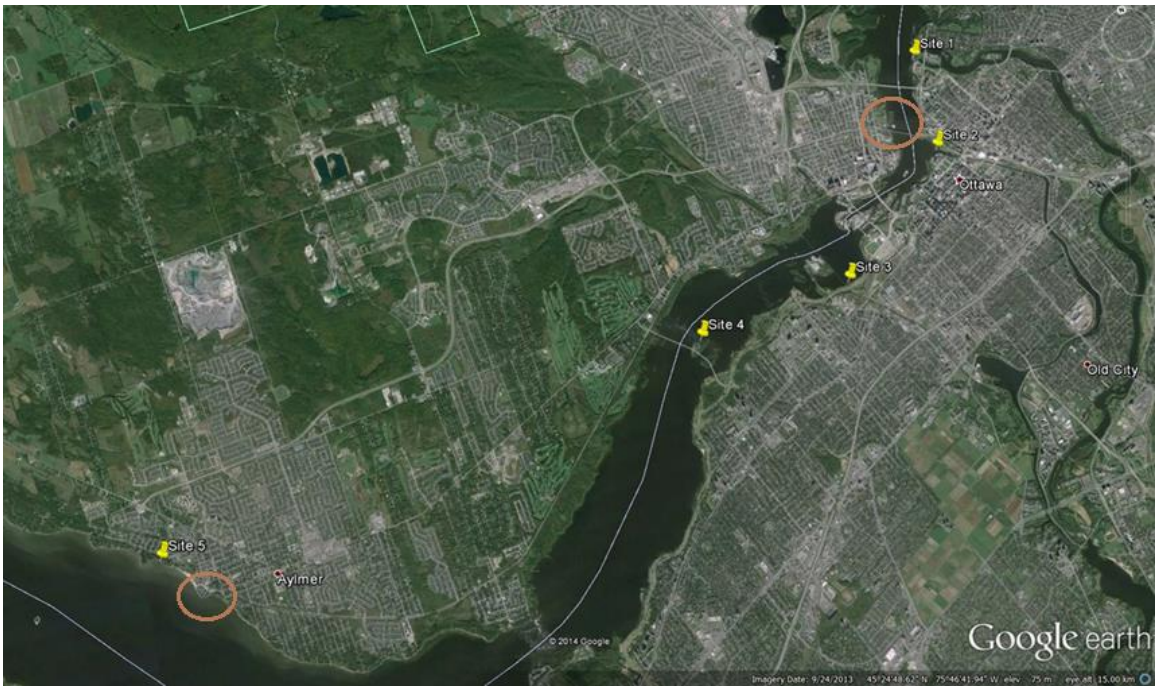

Figure 3 Five sampling locations with marinas indicated by circles (2.5 cm =1km centered on 45.408410,-75.756738 or Bate Island, Ottawa, Ontario, Canada)

2.6.10 Well water

Unaltered well water was collected from a single location Cornwall in North Stormont County. The underlying geology is a clay-like soil. Each well water sample was collected in a 250-mL Kimex© media bottle filled completely with no headspace.

2.6.11 Bottled water

Bottled water was purchased from local retailers. Bottles of 5 different brands were procured.

`

2.6.12 Laboratory water

Milli-Q water was prepared on a weekly basis. The water was verified to be free of PAHs by verifying that the blank samples run in the calibration curve contained no traces of PAHs

2.6.13 Data analysis

The data were processed in Excel to calculate linear regression, average, standard deviation, and the relative standard deviation. The coefficients of determination (i.e., r^2) values were used to measure the strength of the linear relationships. Concentrations were presented in ng/sample, except for concentrations in natural water samples (section 2.6.7), which were reported in ng/L.

3 Chapter: Results

3.1 Optimization of SPME GC/MS Analyses of PAHs in water

3.1.1 Setting instrument conditions

Typical retention times of PAHs under the SPME GC/MS condition used throughout experimentation can be seen in Table 3-1. Instrument limit of detection (LOD) in SIM mode was estimated at well below 2 pg on column for most of the PAHs. This was determined by their S/N and area as demonstrated in Figure 4, with the exception for the ions of last three eluting high molecular weight (HMW) PAHs (i.e., m/z 276 and m/z 278), which were the smallest peaks and had signal-to-noise (S/N) ratios of 1.8 for indeno[*1,2,3-cd*]pyrene (m/z = 276) and 3.6 (dibenz[*a,h*]anthracene (m/z = 278)) at 2 pg injection. At 10 pg injection, the S/N ratios for the three last eluting HMW PAHs were 9.8 for for dibenz[*a,h*]anthracene (m/z = 278, RT = 19.167 min), 15.6 for indeno[*1,2,3-cd*]pyrene (m/z = 276, T = 19.106 min), and 32.9 for benzo[*ghi*]perylene (m/z = 276, RT = 15.591 min) (Figure 5). Therefore, based on these results, LODs for this study were estimated at 10 pg injection amount or lower for all PAHs.

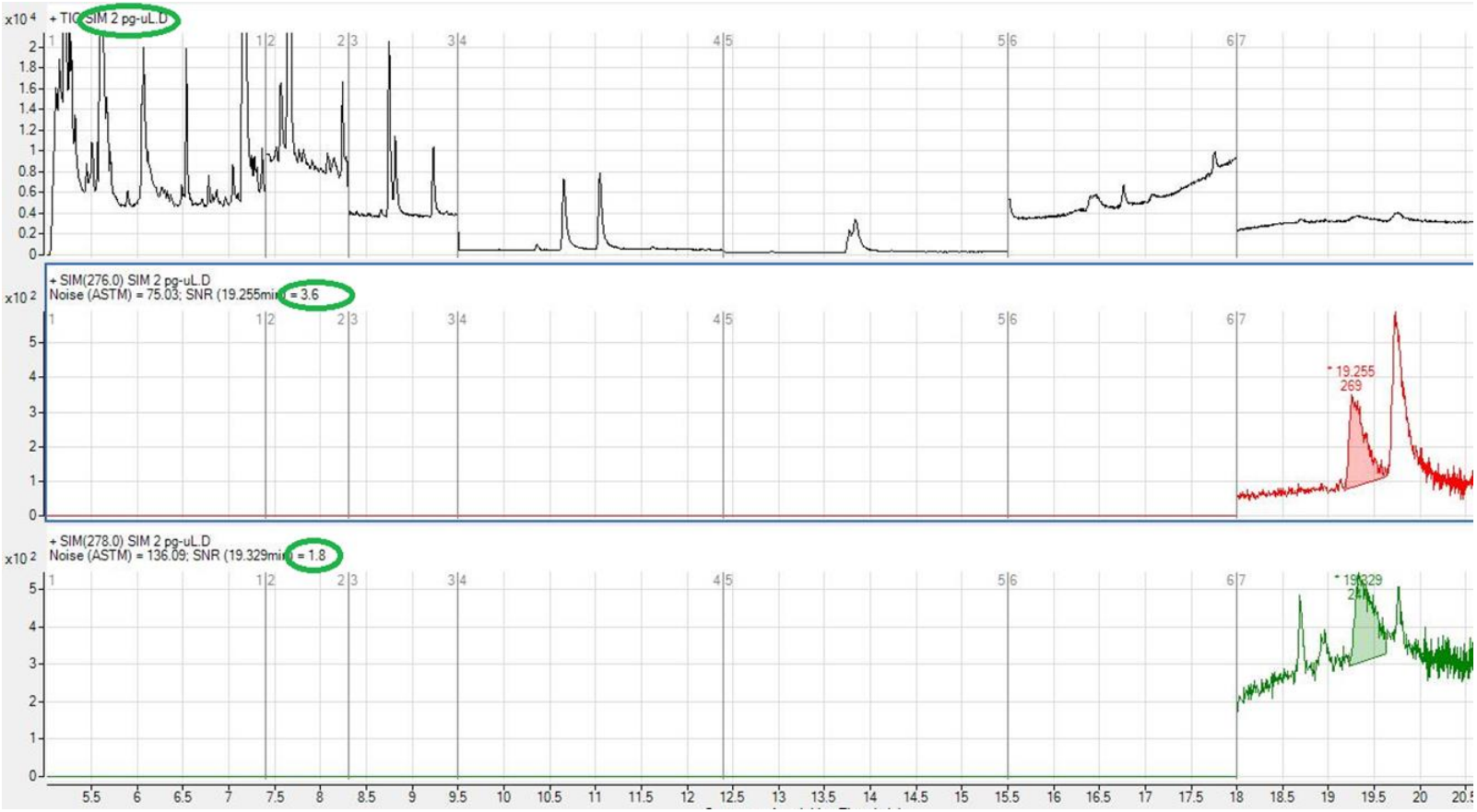

Figure 4 Chromatograms of direct liquid injection of 2 pg/µL PAH solution. The signal-to-noise (S/N) ratio of the two HMW PAHs is shown.

`

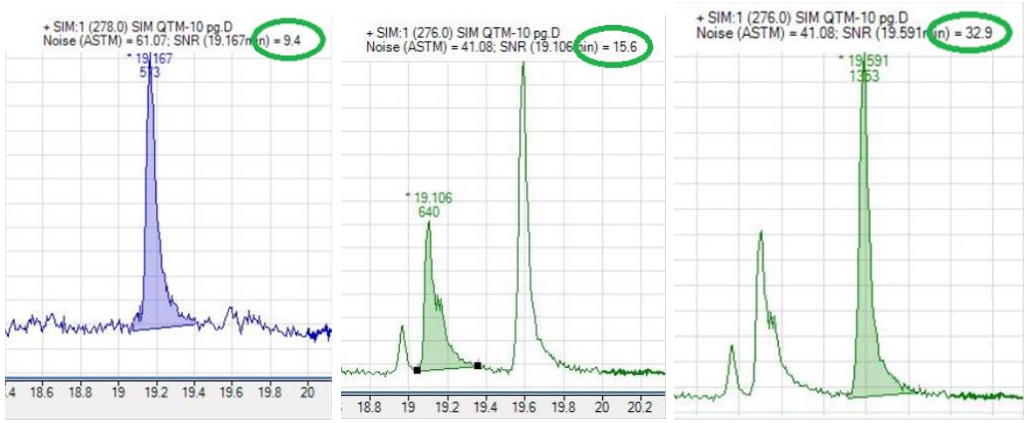

Figure 5 Chromatograms of direct liquid injection of 10 pg/µL, showing the signal-to-noise (S/N) ratio for the three smallest peaks.

`

Table 3-1 GC/MS operational parameters for the PAH analyses

Compound (2000pg/µL stock in acetone)	m/z Quantifying ion m/z Identifying ion	SIM Grouping	Retention Time (min)
naphthalene	128	1	5.594
	64	1	5.587
acenaphthylene	152.1	2	6.984
	76.3	2	6.981
acenaphthene	153.1	2	7.152
	76.5	2	7.152
acenaphthene-d_{10}	164.1	2	7.122
	163.1	2	7.122
fluorene	166	3	7.623
	82.9	3	7.623
phenanthrene	178	3	8.690
	89	3	8.692
anthracene	178	3	8.752
	89	3	8.752
pyrene	202	4	10.562
	100.9	4	10.562
fluoranthene	202	4	10.958
	100.9	4	10.961
Benzo[*a*]anthracene	228	5	13.643
	114	5	13.643
chrysene	228	5	13.711
	114	5	13.711
chrysene-d_{12}	240	5	13.658
Benzo[*k*]fluoranthene	252	6	16.264
	126	6	16.259
Benzo[*a*]pyrene	252	6	16.944
	126	6	16.937
Indeno[*1,2,3-cd*]pyrene	276	7	19.072
	138	7	19.066
Dibenz[*a,h*]anthracene	278	7	19.551
	139	7	19.551
Benzo[*ghi*]perylene	276	7	19.133
	138	7	19.133
$^{13}C_{12}$Benzo[*ghi*]perylene	288	7	19.133

`

3.1.2 Optimization of instrument conditions: general

The initial instrument conditions were determined using the 100 µm PDMS and 65 µm PDMS/DVB fibers. The 30 µm PDMS fiber was introduced to replace the 100 µm PDMS fiber, thereby reducing the SPME extraction time. As all the physical properties of the 30 µm PDMS fiber are identical to that of 100 µm PDMS fiber, except for the coating thickness, the optimized instrument conditions for the 100 µm PDMS fiber was applied to the 30 µm PDMS fiber without further validation. The only settings that needed to be taken into account for optimization, when switching from the 100 µm PDMS fiber to the 30 µm PDMS fiber, are the SPME extraction time and temperature.

The GC oven temperature and MS operating conditions were kept same for both liquid injection and the SPME fiber injection for the GC/MS analysis on the instrument. Initial optimization of instrument conditions was carried out using both 100 µm PDMS and 65 µm PDMS/DVB fibers against the PAH calibration solutions. The optimization calibrations used full scan mode for the determination of retention times (RT). Each fiber was run against the optimization parameter twice to verify results. All concentrations for injections are at 500 pg/sample (unless otherwise stated). Determination of RRF values used both the acenaphthylene-d_{10} and chrysene-d_{12} for RRF calculations.

3.1.3 Optimization of instrument conditions: Bake out of fiber

Bake out of fibers after each sample analysis is aimed at removing residual PAHs and other contaminants on the fiber. This process was carried out by baking out SPME fibers that had been used to extract PAHs from laboratory water spiked with 10 ng PAH/sample. Table 3-2 and Table 3-3 show the bake out results of the 100 µm PDMS and the 65 µm PDMS/DVB fibers, respectively. In general, longer bake out time (i.e., 25

min vs. 15 min) and higher bake out temperature (i.e., 260^{0}C vs. 250^{0}C) resulted in a lower fiber background, as indicated by the decreasing peak areas. Therefore 25 min at 260^{0}C was chosen for cleaning the fiber after each fiber injection.

Table 3-2 Post-cleaning (i.e. bake out) PAHs levels in the 100 µm PDMS fiber and the 65 µm PDMS/DVB fiber showing carry-over at 250 ºC. (RT= retention time)

			15 Min	20 Min	25 Min	
250 ºC Bakeout PDMS-DVB fiber	RT	10 ng/sample Spike	Blank-15 min Area	Blank-20 min Area	Blank-25 min Area	% carry over
Naphthalene	5.491	74520	691	616	550	0.74
Acenaphthylene	7.083	141612	1287	1133	985	0.70
Acenaphthene	7.522	123140	1557	1377	939	0.76
Fluorene	7.623	86275	192	158	157	0.18
Phenanthrene	8.554	263470	2194	1948	1333	0.51
Anthracene	8.625	255555	1339	1174	544	0.21
Pyrene	10.402	166699	2112	1909	1043	0.63
Fluoranthene	10.788	154795	2246	1966	1394	0.90
Chrysene	13.449	125474	1890	1777	1742	1.39
Benzo[*a*]anthracene	13.521	166460	2514	2392	2212	1.33
Benzo[*a*]pyrene	16.056	168891	2202	1952	1283	0.76
Benzo[*b*]fluoranthene	16.732	89543	1399	995	917	1.02
Indeno[*1,2,3-cd*]pyrene	18.845	55378	2957	2766	2405	4.34
Dibenz[*a,h*]anthracene	18.906	76689	979	896	667	0.87
Benzo[*ghi*]perylene	19.309	46758	3158	2849	2230	4.77
			15 Min	20 Min	25 Min	
250 ºC Bakeout PDMS fiber	RT	10 ng/µL spike	Blank-15 min Area	Blank-20 min Area	Blank-25 min Area	% carry over
Naphthalene	5.493	106399	339	299	176	0.17
Acenaphthylene	7.084	202192	1280	1101	792	0.39
Acenaphthene	7.521	175818	192	158	157	0.09
Fluorene	7.579	706369	1194	1037	1032	0.15
Phenanthrene	8.567	706470	2166	559	669	0.09
Anthracene	8.638	868891	1028	808	395	0.05
Pyrene	10.402	455538	2098	1616	1415	0.31
Fluoranthene	10.788	462370	2223	1809	1631	0.35
Chrysene	13.453	618410	2765	1930	1379	0.22
Benzo[*a*]anthracene	13.521	688762	3276	2755	1883	0.27
Benzo[*a*]pyrene	16.049	650198	2372	2073	1013	0.16
Benzo[*b*]fluoranthene	16.722	550198	1784	1025	717	0.13
Indeno[*1,2,3-cd*]pyrene	18.845	561867	640	528	331	0.06
Dibenz[*a,h*]anthracene	18.901	679552	774	638	400	0.06
Benzo[*ghi*]perylene	19.306	495371	1018	998	467	0.09

`

Table 3-3 Cleaning at 260 ºC for the 100 µm PDMS fiber and the 65 µm PDMS/DVB fibers (RT=retention time)

			15 Min	20 Min	25 Min	
260 °C Bakeout PDMS-DVB	RT	10 ng/µL Spike	Blank-15 min Area	Blank-20 min Area	Blank-25 min Area	% carry over
Naphthalene	5.491	75520	204	182	163	0.22
Acenaphthylene	7.085	143512	932	843	695	0.48
Acenaphthene	7.522	124792	1557	1377	953	0.76
Fluorene	7.522	84379	57	47	47	0.06
Phenanthrene	8.554	254804	649	576	394	0.15
Anthracene	8.625	155452	396	347	161	0.10
Pyrene	10.402	106699	625	565	309	0.29
Fluoranthene	10.788	113395	665	582	413	0.36
Chrysene	13.449	119474	559	526	516	0.43
Benzo[*a*]anthracene	13.521	176621	744	708	654	0.37
Benzo[*a*]pyrene	16.056	150185	651	578	380	0.25
Benzo[*b*]fluoranthene	16.732	87112	414	294	271	0.31
Indeno[*1,2,3-cd*]pyrene	18.845	58103	875	818	711	1.22
Dibenz[*a,h*]anthracene	18.906	75991	290	265	197	0.26
Benzo[*ghi*]perylene	19.309	45997	934	843	660	1.43
			15 Min	20 Min	25 Min	
260 °C Bakeout PDMS	RT	10 ng/µL spike	Blank-15 min Area	Blank-20 min Area	Blank-25 min Area	% carry over
Naphthalene	5.493	101753	202	178	105	0.10
Acenaphthylene	7.085	197231	927	819	559	0.28
Acenaphthene	7..523	174934	139	118	111	0.06
Fluorene	7.579	707495	711	617	614	0.09
Phenanthrene	8.567	712459	1289	333	398	0.06
Anthracene	8.638	888452	612	481	235	0.03
Pyrene	10.402	465338	1249	962	842	0.18
Fluoranthene	10.788	472563	1323	1077	971	0.21
Chrysene	13.453	622148	1646	1149	821	0.13
Benzo[*a*]anthracene	13.521	695111	1950	1640	1121	0.16
Benzo[*a*]pyrene	16.049	655444	1412	1234	603	0.09
Benzo[*b*]fluoranthene	16.722	561554	1062	610	427	0.08
Indeno[*1,2,3-cd*]pyrene	18.845	563155	381	314	197	0.03
Dibenz[*a,h*]anthracene	18.907	668534	453	374	234	0.04
Benzo[*ghi*]perylene	19.306	482997	606	594	278	0.06

`

3.1.4 Optimization of instrument conditions: Inlet desorption temperature

Determining the optimal desorption temperature of the inlet was conducted using laboratory water samples that were spiked with PAH spiking solution at 0.5 ng/sample, and analyzed in the range of 200^0C to 270^0C and 200^0C to 280^0C, for the 65 µm PDMS/DVB (Figure 6, see Appendix) and 100 um PDMS (Figure 7, see Appendix) fibers, respectively, using 10^0C increments. In general, a higher temperature resulted in a better instrument response (i.e., larger peak area). Therefore, the manufacturer defined maximum fiber operating temperatures of 270 ^{0}C and 280 ^{0}C were chosen for the initial testing of the 65 µm PDMS/DVB and 100 um PDMS fibers, respectively.

3.1.5 Optimization of instrument conditions: Inlet desorption duration

The range of desorption times tested was from 60 to 300 seconds. All three fibers (i.e., 65 µm PDMS/DVB, 100 µm PDMS fiber and 30 µm PDMS fiber) were tested. In general, peak areas remained relatively constant when the desorption time was 150 seconds or longer (see Figure 8, Figure 9 and Figure 10 in Appendix). Therefore, 180 seconds was chosen for the desorption time for fiber injection.

3.1.6 SPME Conditions: Extraction Time and Temperature.

The extraction of PAHs from water takes place inside an SPME vial. The tests were conducted using laboratory water containing 0.5 ng PAHs/sample. The volume of water samples in the vial was set at 17.5 mL for all SPME extractions. Relative response factor (RRF) was defined as the ratio of peak area of a given PAH against that of isotope-labeled standard (IIS). Two IISs, acenaphthylene-d_{10} and chrysene-d_{12} were used for the tests.

`

3.1.7 SPME conditions for 30 µm PDMS fiber

Figure 11, Figure 12, Figure 13 and Figure 14 in the Appendix show the peak areas of the analytes at the four different temperatures of 30^0C, 40^0C, 50^0C, and 60^0C, respectively. Figure 15, Figure 16, Figure 17 and Figure 18 in the Appendix illustrate RRF values against the acenaphthene-d_{10} internal standard, while Figure 19, Figure 20, Figure 21 and Figure 22 in the Appendix illustrate the RRF values against the chrysene-d_{12} internal standard.

3.1.8 SPME conditions for 65 µm PDMS/DVB fiber

Similar to section 3.1.3.2, Figure 23, Figure 24, Figure 25 and Figure 25 in the Appendix show the areas of the analytes extracted using 65 µm PDMS/DVB fiber at the four different temperatures of 30^0C, 40^0C, 50^0C, and 60^0C, respectively. Figure 29 and Figure 30 in the Appendix illustrate RRF values against the acenaphthene-d_{10} internal standard, while Figure 31, Figure 32, Figure 33 and Figure 34 in the Appendix illustrate RRF values against the chrysene-d_{12} internal standard.

3.1.9 Replicates of the 30 µm PDMS and 65 µm PDMS/DVB fibers.

Seven replicates under the SPME extraction conditions of 40 min at 50 ^{0}C, and 60 min at 50 ^{0}C were performed, respectively, to assess the reproducibility of the extraction method. Table 3-4 and Table 3-5 show the relative standard deviation (RSD) of the areas at 50^0C for 40 and 60 minutes, respectively. The majority of RSDs for the area counts were below or around 10%, except for the three HMW PAHs under the 50^0C/40 min extraction condition using the 30 µm PDMS fiber.

`

Table 3-4 Average, standard deviation and relative standard deviation with respect to the area of the analytes using the 30 µm PDMS fiber at 50^{0}C for 40 and 60 minutes. (SD= Standard Deviation and RSD = relative standard deviation).

Areas for the 30 µm PDMS fiber. (n = 7)	50^{0}C for 40 minutes			50^{0}C for 60 minutes		
	AVERAGE	SD	RSD	AVERAGE	SD	RSD
Naphthalene	65485	5887	9.0	50265	3182	6.3
Acenaphthylene	107252	10622	9.9	70321	6026	8.6
Acenaphthene-d$_{10}$	199842	5953	3.0	149306	3797	2.5
Acenaphthene	214003	7698	3.6	159955	3079	1.9
Fluorene	293736	12650	4.3	211659	5061	2.4
Phenanthrene	373468	25311	6.8	263363	7515	2.9
Anthracene	209275	7679	3.7	149357	6436	4.3
Pyrene	585416	39409	6.7	456365	23512	5.2
Fluoranthene	708729	29511	4.2	572181	25352	4.4
Chrysene	1409828	144534	10.3	1842015	181270	9.8
Chrysene-d$_{12}$	1137850	95755	8.4	1452259	115404	7.9
Benzo[*a*]anthracene	891880	64967	7.3	1137806	79816	7.0
Benzo[*a*]pyrene	469581	36533	7.8	740552	49137	6.6
Benzo[*b*]fluoranthene	208052	12898	6.2	317052	24204	7.6
Indeno[*1,2,3-cd*]pyrene	243698	34454	14.1	392272	37722	9.6
Dibenz[*a,h*]anthracene	455502	63905	14.0	744243	73782	9.9
Benzo[*ghi*]perylene	463942	60735	13.1	770097	66504	8.6

`

Table 3-5 Average value, standard deviation and relative standard deviation with respect to the area of the analytes using the 65 µm PDMS/DVB fiber at 50^{0}C for 40 and 60 minutes. (SD= Standard Deviation and RSD = relative standard deviation).

Areas for the 65 µm PDMS/DVB fiber. (n = 7)	50^{0}C for 40 minutes			50^{0}C for 60 minutes		
	AVERAGE	SD	RSD	AVERAGE	SD	RSD
Naphthalene	2875100	193784	6.7	4137667	106190	2.6
Acenaphthylene	1868280	44290	2.4	2801756	50600	1.8
Acenaphthene-d$_{10}$	2449937	106946	4.4	3617883	92770	2.6
Acenaphthene	2345326	111304	4.7	3382919	95310	2.8
Fluorene	2342823	123936	5.3	3431061	58634	1.7
Phenanthrene	2283178	98240	4.3	3479203	59589	1.7
Anthracene	1047656	33068	3.2	2222154	83371	3.8
Pyrene	1820739	120759	6.6	2997091	136896	4.6
Fluoranthene	2011467	129064	6.4	3244761	133045	4.1
Chrysene	1370632	93458	6.8	2402712	120443	5.0
Chrysene-d$_{12}$	1113885	40231	3.6	1793324	66274	3.7
Benzo[*a*]anthracene	928759	43823	4.7	1475773	59809	4.1
Benzo[*a*]pyrene	182802	17172	9.4	326231	27014	8.3
Benzo[*b*]fluoranthene	55134	16503	29.9	104597	9820	9.4
Indeno[*1,2,3-cd*]pyrene	29341	7265	24.8	53008	6015	11.3
Dibenz[*a,h*]anthracene	51717	17094	33.1	100935	11914	11.8
Benzo[*ghi*]perylene	55350	14094	25.5	106716	13499	12.6

For the 65 µm PDMS/DVB fiber, similar RSD values were observed for the condition of 50^{0}C/60 min, but larger RSD values for the four last eluting PAHs were observed for the extraction condition of 50^{0}C/40 min. RSDs of RRFs are summarized in Table 3-6 and Table 3-7. To assess the reproducibility, RRFs of early eluting PAHs (i.e., from naphthalene to anthracene) were calculated against acenaphthene-d$_{10}$ (Table 3-6), and later eluting PAHs (i.e., pyrene and onwards) against chrysene-d$_{12}$ (Table 3-7. RSD of single digit values were achieved except for benzo[*b*]fluoranthene and the last three eluding HMW PAHs under the extraction condition of 50^{0}C/40 min.

`

Table 3-6 Average value, standard deviation and relative standard deviation with respect to the RRFs, calculated with acenaphthene-d_{10}, for both the 65 µm PDMS/DVB fiber and 30 µm PDMS fiber at 50^{0}C for 40 and 60 minutes. (n = 7) (SD= Standard Deviation and RSD = relative standard deviation).

RRFs for the 30 µm PDMS fiber using acenaphthene-d_{10}	40 min			60 min		
	AVERAGE	SD	RSD	AVERAGE	SD	RSD
Naphthalene	0.6555	0.0563	8.6	0.6731	0.0353	5.2
Acenaphthylene	1.0726	0.0903	8.4	0.9417	0.0740	7.9
Acenaphthene-d_{10}	1.0000	0.0000	0.0	1.0000	0.0000	0.0
Acenaphthene	2.1416	0.0347	1.6	2.1431	0.0311	1.5
Fluorene	2.9416	0.1498	5.1	2.8355	0.0371	1.3
Phenanthrene	3.7417	0.2995	8.0	3.5280	0.0572	1.6
Anthracene	2.0944	0.0445	2.1	2.0005	0.0622	3.1

RRFs for the 65 µm PDMS/DVB fiber using acenaphthene-d_{10}	40 min			60 min		
	AVERAGE	SD	RSD	AVERAGE	SD	RSD
Naphthalene	2.3454	0.0720	3.1	2.2875	0.0315	1.4
Acenaphthylene	1.5266	0.0430	2.8	1.5492	0.0264	1.7
Acenaphthene-d_{10}	1.0000	0.0000	0.0	1.0000	0.0000	0.0
Acenaphthene	1.9144	0.0130	0.7	1.8702	0.0303	1.6
Fluorene	1.9120	0.0262	1.4	1.8972	0.0257	1.4
Phenanthrene	1.8643	0.0422	2.3	1.9241	0.0466	2.4
Anthracene	0.8558	0.0208	2.4	1.2293	0.0614	5.0

`

Table 3-7 Average value, standard deviation and relative standard deviation with respect to the RRFs, calculated with chrysene d_{12}, for both the 65 µm PDMS/DVB fiber and 30 µm PDMS fiber at 50^{0}C for 40 and 60 minutes. (n = 7) (SD= Standard Deviation and RSD = relative standard deviation).

RRFs for the 30 µm PDMS fiber using chrysene-d_{12}

	40 min			60 min		
	AVERAGE	SD	RSD	AVERAGE	SD	RSD
Pyrene	1.0315	0.0622	6.0	0.6312	0.0513	8.1
Fluoranthene	1.2503	0.0742	5.9	0.7907	0.0495	6.3
Chrysene	2.4752	0.0464	1.9	2.5337	0.0484	1.9
Chrysene-d_{12}	1.0000	0.0000	0.0	1.0000	0.0000	0.0
Benzo[*a*]anthracene	1.5690	0.0308	2.0	1.5680	0.0245	1.6
Benzo[*a*]pyrene	0.8258	0.0147	1.8	1.0220	0.0566	5.5
Benzo[*b*]fluoranthene	0.3665	0.0177	4.8	0.4378	0.0334	7.6
Indeno[*1,2,3-cd*]pyrene	0.4294	0.0620	14.4	0.5414	0.0509	9.4
Dibenz[*a,h*]anthracene	0.8024	0.1140	14.2	1.0272	0.0987	9.6
Benzo[*ghi*]perylene	0.8168	0.1026	12.6	1.0627	0.0840	7.9

RRFs for the 65 µm PDMS/DVB fiber using chrysene-d_{12}

	40 min			60 min		
	AVERAGE	SD	RSD	AVERAGE	SD	RSD
Pyrene	3.2702	0.2072	6.3	3.3421	0.0730	2.2
Fluoranthene	3.6110	0.1773	4.9	3.6189	0.0738	2.0
Chrysene	2.4600	0.1234	5.0	2.6786	0.0502	1.9
Chrysene-d_{12}	1.0000	0.0000	0.0	1.0000	0.0000	0.0
Benzo[*a*]anthracene	1.6673	0.0350	2.1	1.6457	0.0176	1.1
Benzo[*a*]pyrene	0.3280	0.0253	7.7	0.3634	0.0200	5.5
Benzo[*b*]fluoranthene	0.0988	0.0287	29.1	0.1165	0.0076	6.5
Indeno[*1,2,3-cd*]pyrene	0.0526	0.0124	23.6	0.0590	0.0048	8.2
Dibenz[*a,h*]anthracene	0.0927	0.0300	32.4	0.1123	0.0100	8.9
Benzo[*ghi*]perylene	0.0992	0.0243	24.5	0.1187	0.0116	9.7

`

3.1.10 Final operating conditions for SPME extraction and fiber injection

Based on the results presented in section 3.1.3, the final operating conditions for SPME extraction and analyses of PAHs in the water samples are summarized in Table 3-8. The finalized operating conditions (i.e., last column in Table 3-8) were used throughout for the rest of the sample analyses.

Table 3-8 Final instrument parameters used for all data gathered

	Range Tested	Optimal Conditions (suggested by the manufacturer)		Conditions Used on Instrument
Parameter Tested		**30 µm PDMS fiber**	**65 µm PDMS/DVB fiber**	
Bake out of Fiber:	250 ^{0}C and 260 ^{0}C (15, 20, 25 min)	260^{0}C, 25 min	260^{0}C, 25 min	260^{0}C, 25 min
Inlet Desorption Time:	60-300 secs (30 sec increment)	180 sec	150-210 sec	180 sec
Inlet Desorption Temperature:	200^{0}C-270^{0}C or 200^{0}C-280^{0}C (depending on fiber using 10^{0}C increments)	270^{0}C	280^{0}C	270^{0}C
SPME Extraction Time:	40-90 min (using 10 min increments)	40 or 60 min	40 or 60 min	60 min
SPME Extraction Temperature:	30^{0}C -60^{0}C (using 10^{0}C increments)	50^{0}C	50^{0}C	50^{0}C

It should be noted that the 100 µm PDMS fiber was replaced by the 30 µm PDMS fiber during the optimization of operating conditions. Switching of the fiber was done to bring down the SPME extraction time, and since all parameters are the same except for the thickness of the fiber, all optimal conditions for the bake out of the fiber, inlet desorption time and inlet desorption temperature were applied to 30 µm PDMS fiber without further validation.

3.2 Effects of water characteristics on SPME-determined PAH concentrations

All water samples with different parameters were tested at a PAH concentration of either 0.5 ng/sample or 2.0 ng/sample. Each parameter was tested in duplicate for each

`

fiber (i.e., 30 µm PDMS or 65 µm PDMS/DVB fiber). RRFs were calculated against the internal standards (IISs) as stated in each section.

3.2.1 Effect of pH on RRFs

The effect of pH on RRFs was tested in the pH range from 4.5 to 9.0, in 0.5 increments, using laboratory water samples that were spiked at 0.5 ng PAH/sample. Figure 36 and Figure 37 in the Appendix show the peak areas of PAHs extracted using the 30 µm PDMS fiber; Figure 38 and Figure 39 in the Appendix show the peak areas using the 65 µm PDMS/DVB fiber. Table 3-9 and Table 3-10 show the average area counts calculated from samples with different pH values (i.e., 4.5 – 9.0), and the standard deviation (SD) and relative standard deviation (RSD) for each of the compounds according to each fiber (i.e., 30 µm PDMS and 65 µm PDMS/DVB).

Table 3-9 pH area counts (averaged) for each PAH, SD and RSD determined for the 30 µm PDMS fiber for run 1 and run 2. (n=10) (SD= Standard Deviation and RSD = relative standard deviation).

30 µm PDMS fiber (Area)	Run 1 (full range)			Run 2 (full range)		
	AVERAGE	SD	RSD	AVERAGE	SD	RSD
Naphthalene	28370	1824	6.4	25178	1202	4.8
Acenaphthylene	42984	1743	4.1	39048	744	1.9
Acenaphthene-d_{10}	91956	3636	4	83843	1878	2.2
Acenaphthene	57488	1292	2.2	53014	874	1.6
Fluorene	66045	2057	3.1	60437	1793	3
Phenanthrene	146759	3752	2.6	138457	2292	1.7
Anthracene	109942	5692	5.2	102031	4876	4.8
Pyrene	302951	10522	3.5	282807	6660	2.4
Fluoranthene	330582	10648	3.2	308591	6810	2.2
Chrysene	362745	41063	11.3	322197	14308	4.4
Chrysene-d_{12}	653663	36104	5.5	581841	14223	2.4
Benzo[*a*]anthracene	494963	31876	6.4	454723	12191	2.7
Benzo[*a*]pyrene	457306	45915	10	417265	32981	7.9
Benzo[*b*]fluoranthene	265865	48195	18.1	234931	20247	8.6
Indeno[*1,2,3-cd*]pyrene	267976	63043	23.5	251867	7267	2.9
Dibenz[*a,h*]anthracene	186179	45463	24.4	239119	50307	21
Benzo[*ghi*]perylene	247094	62231	25.2	289891	56069	19.3

`

Table 3-10 pH area counts (averaged for each PAH), STD and RSD of the Area for the 65 µm PDMS/DVB fiber for run 1 and run 2. (n=10) (SD= Standard Deviation and RSD = relative standard deviation).

65 µm PDMS/DVB fiber (Area)	Run 1 (full range)			Run 2 (full range)		
	AVERAGE	SD	RSD	AVERAGE	SD	RSD
Naphthalene	1668930	29445	1.8	1482194	79238	5.3
Acenaphthylene	1367670	34037	2.5	1119343	35079	3.1
Acenaphthene-d_{10}	1690656	29561	1.7	1553607	39315	2.5
Acenaphthene	974193	33646	3.5	842582	45026	5.3
Fluorene	952002	50297	5.3	842781	39662	4.7
Phenanthrene	1245316	22181	1.8	1089695	40985	3.8
Anthracene	844741	49607	5.9	712969	25041	3.5
Pyrene	1040976	33590	3.2	923622	34504	3.7
Fluoranthene	1019390	34251	3.4	896372	31475	3.5
Chrysene	426913	30036	7.0	347409	29187	8.4
Chrysene-d_{12}	675827	40248	6.0	531550	42181	7.9
Benzo[*a*]anthracene	501495	28423	5.7	409531	29804	7.3
Benzo[*a*]pyrene	182710	26569	14.5	145610	18363	12.6
Benzo[*b*]fluoranthene	84755	11330	13.4	64000	7321	11.4
Indeno[*1,2,3-cd*]pyrene	48517	10152	20.9	34311	7987	23.3
Dibenz[*a,h*]anthracene	39133	8659	22.1	27633	6906	25.0
Benzo[*ghi*]perylene	41213	9437	22.9	31953	7468	23.4

Figure 40 and Figure 42 in the Appendix illustrate the RRFs as a function of pH values against acenaphthene-d_{10} for the 30 µm PDMS fiber and the 65 µm PDMS/DVB fiber, respectively; Figure 41 and Figure 43 in the Appendix illustrate the RRFs values against chrysene-d_{12}. Average RRF values, along with the SD and RSD for each of the compounds according to each fiber (i.e., 30 µm PDMS and 65 µm PDMS/DVB) are summarized in Table 3-11 and Table 3-12 (i.e., against acenaphthene-d_{10} and chrysene-d_{12}, respectively). Single digit RSD values for RRFs were achieved for PAHs against acenaphthene-d_{10}. Some RSDs of RRFs were larger (i.e., up to 20%); as seen for later eluting HMW PAHs (Table 3-12).

`

Table 3-11 Average RRF values against acenaphthene-d_{10} for each fiber according to the full pH range. (SD= Standard Deviation, RSD = relative standard deviation and RRF= relative response factor).

	30 µm PDMS fiber		
	AVERAGE	SD	RSD
Naphthalene	0.6095	0.0376	6.2
Acenaphthylene	0.9334	0.0158	1.7
Acenaphthene-d_{10}	1.0000	-	-
Acenaphthene	1.2582	0.0265	2.1
Fluorene	1.4394	0.0221	1.5
Phenanthrene	3.2493	0.0696	2.1
Anthracene	2.4122	0.0648	2.7

	65 µm PDMS/DVB fiber		
	AVERAGE	SD	RSD
Naphthalene	1.9422	0.0628	3.2
Acenaphthylene	1.5300	0.0315	2.1
Acenaphthene-d_{10}	1.0000	-	-
Acenaphthene	1.1187	0.0371	3.3
Fluorene	1.1059	0.0523	4.7
Phenanthrene	1.4386	0.0398	2.8
Anthracene	0.9593	0.0378	3.9

`

Table 3-12 Average RRF values against chrysene-d_{12} for each fiber according to the full pH range used. (SD= Standard Deviation, RSD = relative standard deviation and RRF= Relative response factor).

30 µm PDMS fiber

	AVERAGE	SD	RSD
Pyrene	0.9503	0.0199	2.1
Fluoranthene	1.0370	0.0271	2.6
Chrysene	1.1078	0.0528	4.8
Chrysene-d_{12}	1.0000	-	-
Benzo[*a*]anthracene	1.5386	0.0203	1.3
Benzo[*a*]pyrene	1.4155	0.0860	6.1
Benzo[*b*]fluoranthene	0.8089	0.0812	10.0
Indeno[*1,2,3-cd*]pyrene	0.8402	0.0735	8.8
Dibenz[*a,h*]anthracene	0.6926	0.1302	18.8
Benzo[*ghi*]perylene	0.8725	0.1590	18.2

65 µm PDMS/DVB fiber

	AVERAGE	SD	RSD
Pyrene	3.2881	0.1300	4.0
Fluoranthene	3.2045	0.1304	4.1
Chrysene	1.2851	0.0206	1.6
Chrysene-d_{12}	1.0000	-	-
Benzo[*a*]anthracene	1.5134	0.0335	2.2
Benzo[*a*]pyrene	0.5439	0.0540	9.9
Benzo[*b*]fluoranthene	0.2457	0.0202	8.2
Indeno[*1,2,3-cd*]pyrene	0.1360	0.0246	18.1
Dibenz[*a,h*]anthracene	0.1095	0.0204	18.6
Benzo[*ghi*]perylene	0.1208	0.0230	19.0

`

3.2.2 Effects of Ionic Strength on RRFs

Varying percentage of sodium chloride was used to measure the effect of ionic strength on RRFs (%) with a concentration range of 0.1% to 10% salt in water samples spiked with PAH the 0.5 ng/sample solution. Figure 44, Figure 45, Figure 46 and Figure 47 in the Appendix give the illustration of the area as it reflects against % sodium chloride. Table 3-13 and Table 3-14 illustrates the average area, SD, and the RSD for each of the compounds according to each fiber (30 µm PDMS and 65 µm PDMS/DVB respectively). Figure 48 and Figure 50 in the Appendix, illustrates the average RRFs using acenaphthene-d_{10} for both fibers (30 µm PDMS and 65 µm PDMS/DVB respectively) as they varied in relation to the increasing ionic strength. Figure 49 and Figure 51 in the Appendix, illustrates the average RRFs using chrysene-d_{12} for both fibers (30 µm PDMS and 65 µm PDMS/DVB respectively) as they are varying in relation to the increasing ionic strength.

Table 3-13 Peak area counts of PAHs in water solutions with different ionic strength (NaCl concentrations) extracted using the 30 µm PDMS fiber. (SD= Standard Deviation and RSD = relative standard deviation).

30 µm PDMS fiber (Area)	Run 1 (full range)			Run 2 (full range)		
	AVERAGE	SD	RSD	AVERAGE	SD	RSD
Naphthalene	28332	7349	25.9	24365	7526	30.9
Acenaphthylene	58546	15479	26.4	50676	14744	29.1
Acenaphthene-d_{10}	102813	25583	24.9	92683	26998	29.1
Acenaphthene	72932	19073	26.2	62721	17747	28.3
Fluorene	69465	19041	27.4	64895	18766	28.9
Phenanthrene	145691	36370	25	140625	36020	25.6
Anthracene	115879	28482	24.6	100864	27610	27.4
Pyrene	275557	44399	16.1	266849	44612	16.7
Fluoranthene	297848	18225	6.1	282087	44380	15.7
Chrysene	279159	26544	9.5	280276	24102	8.6
Chrysene-d_{12}	481591	29042	6	452283	33042	7.3
Benzo[*a*]anthracene	341920	19390	5.7	331146	23741	7.2
Benzo[*a*]pyrene	314671	15235	4.8	323316	15071	4.7
Benzo[*b*]fluoranthene	178121	14155	7.9	185790	10917	5.9
Indeno[*1,2,3-cd*]pyrene	231235	16765	7.3	285896	12523	4.4
Dibenz[*a,h*]anthracene	220212	6938	3.2	212482	40534	19.1
Benzo[*ghi*]perylene	216039	7468	3.5	219315	24140	11.0

`

Table 3-14 Peak area counts of PAHs in water solutions with different ionic strength (NaCl concentrations) extracted using the 65 µm PDMS/DVB fiber. (SD= Standard Deviation and RSD = relative standard deviation).

65µm PDMS/DVB fiber (Area)	Run 1 (full range)			Run 2 (full range)		
	AVERAGE	SD	RSD	AVERAGE	SD	RSD
Naphthalene	1224636	76626	6.3	1044549	87360	8.4
Acenaphthylene	978870	66291	6.8	1065261	50782	4.8
Acenaphthene-d_{10}	1114477	78135	7.0	1060254	82952	7.8
Acenaphthene	743366	44463	6.0	700411	61957	8.8
Fluorene	623701	41540	6.7	587810	39993	6.8
Phenanthrene	792496	51555	6.5	730284	41578	5.7
Anthracene	552870	58711	10.6	524566	48859	9.3
Pyrene	678378	55337	8.2	641755	20871	3.3
Fluoranthene	655428	53191	8.1	630470	19431	3.1
Chrysene	245101	32618	13.3	288572	20950	7.3
Chrysene-d_{12}	378124	47643	12.6	446438	28006	6.3
Benzo[*a*]anthracene	279030	30659	11.0	318417	24021	7.5
Benzo[*a*]pyrene	109662	23531	21.5	130100	20062	15.4
Benzo[*b*]fluoranthene	45974	14741	32.1	55171	10859	19.7
Indeno[*1,2,3-cd*]pyrene	33376	12565	37.6	36492	10247	28.1
Dibenz[*a,h*]anthracene	28996	11238	38.8	29632	8686	29.3
Benzo[*ghi*]perylene	30999	9929	32.0	31456	7670	24.4

Table 3-15 and Table 3-16 (acenaphthene-d_{10} and chrysene-d_{12} respectively) illustrates the average RRF, SD, and the RSD for each of the compounds according to each fiber (30 µm PDMS and 65 µm PDMS/DVB). The data for ionic strength from NaCl in solution is very similar to the data of pH. The tables presented here are for the illustration of the overall effect of ionic strength of PAH uptake onto both SPME fibers. To examine the resulting graphical data refer to Appendix A.1 (figures).

`

Table 3-15 Average RRF Values for the acenaphthene-d_{10} for each fiber according to ionic strength (NaCl concentrations) averaged (n=10). (SD= Standard Deviation and RSD = relative standard deviation, RRF = relative response factor)

30 µm PDMS fiber (full range)

	AVERAGE	SD	RSD
Naphthalene	0.5387	0.0186	3.5
Acenaphthylene	1.1153	0.0232	2.1
Acenaphthene-d_{10}	1.0000	-	-
Acenaphthene	1.3882	0.0259	1.9
Fluorene	1.3736	0.0329	2.4
Phenanthrene	2.9667	0.0456	1.5
Anthracene	2.2563	0.1227	5.4

65 µm PDMS/DVB fiber (full range)

	AVERAGE	SD	RSD
Naphthalene	2.0852	0.0494	2.4
Acenaphthylene	1.8864	0.0636	3.4
Acenaphthene-d_{10}	1.0000	-	-
Acenaphthene	1.3280	0.0299	2.3
Fluorene	1.1147	0.0165	1.5
Phenanthrene	1.4016	0.0274	2.0
Anthracene	0.9897	0.0301	3.0

`

Table 3-16 Average RRF values for the chrysene-d_{12} for each fiber according to ionic strength. (SD= Standard Deviation, RSD = relative standard deviation and RRF= relative response factor)

30 µm PDMS fiber (full range)

	AVERAGE	SD	RSD
Pyrene	1.1457	0.1251	10.9
Fluoranthene	1.2328	0.0587	4.8
Chrysene	1.1970	0.0329	2.7
Chrysene-d_{12}	1.0000	-	-
Benzo[*a*]anthracene	1.4446	0.0183	1.3
Benzo[*a*]pyrene	1.3750	0.0623	4.5
Benzo[*b*]fluoranthene	0.7901	0.0372	4.7
Indeno[*1,2,3-cd*]pyrene	1.1384	0.0800	7.0
Dibenz[*a,h*]anthracene	0.9475	0.1503	15.9
Benzo[*ghi*]perylene	0.9478	0.1013	10.7

65 µm PDMS/DVB fiber (full range)

	AVERAGE	SD	RSD
Pyrene	3.2289	0.1250	3.9
Fluoranthene	3.1428	0.1222	3.9
Chrysene	1.2975	0.0263	2.0
Chrysene-d_{12}	1.0000	-	-
Benzo[*a*]anthracene	1.4531	0.0266	1.8
Benzo[*a*]pyrene	0.5877	0.0451	7.7
Benzo[*b*]fluoranthene	0.2484	0.0362	14.6
Indeno[*1,2,3-cd*]pyrene	0.1733	0.0347	20.0
Dibenz[*a,h*]anthracene	0.1462	0.0317	21.7
Benzo[*ghi*]perylene	0.1550	0.0253	16.3

3.2.3 Effects of Suspended Solids on RRFs

The effect of suspended solids on RRFs was also investigated; each sample was spiked at 2.0 ng PAH/sample. Figure 52, Figure 53, Figure 54 and Figure 55 in the Appendix show peak area counts as a function of the suspended solids dilution. Figure 56 and Figure 57 in the Appendix illustrate the RRFs as a function of dilution factors from the parent solution against acenaphthene-d_{10} for both fibers (i.e., 30 µm PDMS and 65 µm PDMS/DVB). Figure 58 and Figure 59 in the Appendix illustrate the RRFs as a function of dilution factors from the parent solution against chrysene-d_{12}. Relatively

`

stable RRFs can be observed in water samples when the sample has been diluted 27 times (27x) or 81 times (81x). RRFs deviated dramatically in water samples with lower dilution factors. Table 3-17 and Table 3-18 illustrate the average RRF and RSD for the PAHs against acenaphthene-d_{10}. Large RSD values can be seen when an RRF was averaged across the entire dilution range (Table 3-18). The RSD values decreased when an RRF was averaged from the 9x – 2187x dilution range, and further decreased when averaged from the 27x – 2187x dilution range (Table 3-18). This shows that the RRFs were relatively constant for dilute solutions of suspended solids. Similar observations were observed for the RRFs against chrysene-d_{12} (Table 3-19 and Table 3-20).

Table 3-17 The average RRF values for each PAH determined for spiked water samples with suspended solids in solution. (SD= Standard Deviation and RSD = relative standard deviation)

30 µm PDMS fiber (full range)

	AVERAGE	SD	RSD
Naphthalene	0.3917	0.3548	90.6
Acenaphthylene	0.6770	0.2109	31.2
Acenaphthene-d_{10}	1.0000	-	-
Acenaphthene	1.2503	0.0268	2.1
Fluorene	1.3757	0.3480	25.3
Phenanthrene	3.1673	1.1787	37.2
Anthracene	2.7789	1.4164	51.0

65 µm PDMS/DVB fiber (full range)

	AVERAGE	SD	RSD
Naphthalene	2.2658	0.8080	35.7
Acenaphthylene	1.3117	0.2224	17.0
Acenaphthene-d_{10}	1.0000	-	-
Acenaphthene	1.0104	0.0301	3.0
Fluorene	0.7951	0.3419	43.0
Phenanthrene	0.8188	0.5141	62.8
Anthracene	0.6021	0.4515	75.0

`

Table 3-18 Average RRF Values for the acenaphthene-d_{10} for each fiber according to suspended solids calculated to respective dilution range. (SD= Standard Deviation and RSD = relative standard deviation)

	30 µm PDMS fiber					
	9x -2178x			27x -2178x		
	AVERAGE	SD	RSD	AVERAGE	SD	RSD
Naphthalene	0.2353	0.0479	20.3	0.2169	0.0180	8.3
Acenaphthylene	0.6499	0.0420	6.5	0.6350	0.0231	3.6
Acenaphthene-d_{10}	1.0000	-	-	1.0000	-	-
Acenaphthene	1.2406	0.0200	1.6	1.2419	0.0221	1.8
Fluorene	1.5367	0.2021	13.2	1.6172	0.0496	3.1
Phenanthrene	3.5922	0.9705	27.0	3.9514	0.4577	11.6
Anthracene	3.3379	1.1320	33.9	3.7421	0.6135	16.4
	65 µm PDMS/DVB fiber					
	9x -2178x			27x -2178x		
	AVERAGE	SD	RSD	AVERAGE	SD	RSD
Naphthalene	1.8354	0.1391	7.6	1.7808	0.0429	2.4
Acenaphthylene	1.4236	0.0950	6.7	1.4595	0.0398	2.7
Acenaphthene-d_{10}	1.0000	-	-	1.0000	-	-
Acenaphthene	1.0237	0.0203	2.0	1.0301	0.0144	1.4
Fluorene	0.9547	0.2030	21.3	1.0333	0.0726	7.0
Phenanthrene	1.0149	0.4282	42.2	1.1645	0.2477	21.3
Anthracene	0.7682	0.3906	50.9	0.8948	0.2656	29.7

`

Table 3-19 Average RRF Values for the chrysene-d_{12} for each fiber according to suspended solids. (SD= Standard Deviation and RSD = relative standard deviation)

30 µm PDMS fiber (full range)

	AVERAGE	SD	RSD
Pyrene	1.4013	0.5363	38.3
Fluoranthene	1.6615	0.7389	44.5
Chrysene	0.9689	0.2143	22.1
Chrysene-d_{12}	1.0000	-	-
Benzo[*a*]anthracene	1.3926	0.0932	6.7
Benzo[*a*]pyrene	1.1324	0.1880	16.6
Benzo[*b*]fluoranthene	0.8124	0.1788	22.0
Indeno[*1,2,3-cd*]pyrene	0.7669	0.3116	40.6
Dibenz[*a,h*]anthracene	0.6089	0.2342	38.5
Benzo[*ghi*]perylene	0.8087	0.2077	25.7

65 µm PDMS/DVB fiber (full range)

	AVERAGE	SD	RSD
Pyrene	2.4769	0.6108	24.7
Fluoranthene	2.7238	0.8487	31.2
Chrysene	1.0052	0.1651	16.4
Chrysene-d_{12}	1.0000	-	-
Benzo[*a*]anthracene	1.3715	0.0798	5.8
Benzo[*a*]pyrene	0.7643	0.0811	10.6
Benzo[*b*]fluoranthene	0.4960	0.0682	13.7
Indeno[*1,2,3-cd*]pyrene	0.3510	0.0843	24.0
Dibenz[*a,h*]anthracene	0.2964	0.0762	25.7
Benzo[*ghi*]perylene	0.3595	0.0616	17.1

`

Table 3-20 Average RRF Values for the chrysene-d_{12} for each fiber according to suspended solids calculated to respective dilution range. (SD= Standard Deviation and RSD = relative standard deviation)

	30 µm PDMS fiber					
	9x – 2178x			27x– 2178x		
	AVERAGE	SD	RSD	AVERAGE	SD	RSD
Pyrene	1.2147	0.4827	39.7	1.0582	0.3280	31.0
Fluoranthene	1.3475	0.5380	39.9	1.1668	0.3417	29.3
Chrysene	1.0641	0.1437	13.5	1.1155	0.0775	6.9
Chrysene-d_{12}	1.0000	-	-	1.0000	-	-
Benzo[*a*]anthracene	1.3500	0.0537	4.0	1.3357	0.0455	3.4
Benzo[*a*]pyrene	1.2187	0.1151	9.4	1.2500	0.0959	7.7
Benzo[*b*]fluoranthene	0.8913	0.1171	13.1	0.9318	0.0693	7.4
Indeno[*1,2,3-cd*]pyrene	0.9095	0.1928	21.2	0.9781	0.1054	10.8
Dibenz[*a,h*]anthracene	0.7163	0.1442	20.1	0.7665	0.0842	11.0
Benzo[*ghi*]perylene	0.9064	0.1135	12.5	0.9396	0.0887	9.4
	65 µm PDMS/DVB fiber					
	9x – 2178x			27x– 2178x		
	AVERAGE	SD	RSD	AVERAGE	SD	RSD
Pyrene	2.3149	0.6232	26.9	2.1466	0.5227	24.3
Fluoranthene	2.3757	0.6519	27.4	2.1849	0.5082	23.3
Chrysene	1.0763	0.1157	10.8	1.1154	0.0726	6.5
Chrysene-d_{12}	1.0000	-	-	1.0000	-	-
Benzo[*a*]anthracene	1.3341	0.0457	3.4	1.3261	0.0461	3.5
Benzo[*a*]pyrene	0.7795	0.0900	11.5	0.7879	0.0980	12.4
Benzo[*b*]fluoranthene	0.5035	0.0773	15.3	0.5116	0.0834	16.3
Indeno[*1,2,3-cd*]pyrene	0.3823	0.0692	18.1	0.3881	0.0757	19.5
Dibenz[*a,h*]anthracene	0.3274	0.0572	17.5	0.3332	0.0620	18.6
Benzo[*ghi*]perylene	0.3729	0.0652	17.5	0.3651	0.0697	19.1

`

3.2.4 Effects of Humic Acids on RRFs

Effects of humic acid were also examined; all samples were spiked at 2.0 ng PAH/sample. Figure 60, Figure 61 and Figure 62 in the Appendix show the peak area counts as it pertains to the concentration of humic acid in water. There was only one run of humic acid with the 30 µm PDMS fiber since the data from the second run was corrupted and consequently not available. Figure 63 and Figure 64 in the Appendix illustrate the average RRFs of PAHs against acenaphthene-d_{10} for both fibers (i.e., 30 µm PDMS and 65 µm PDMS/DVB) as a function of humic acid dilutions. Figure 65 and Figure 66 in the Appendix, illustrate the RRFs of PAHs against chrysene-d_{12}. Table 3-21, Table 3-22 and Table 3-23 summarize the average RRFs calculated for different dilution ranges. The early eluting PAHs had relatively small RSDs against acenaphthene-d_{10} (i.e., values around 10% or below), while later eluting PAHs, whose RRFs were calculated against Chrysene-d_{12}, had larger RSDs (i.e., values up to 76%) (Table 3-21 and Table 3-22). Further analysis of RRF data revealed that for the later eluting PAHs, RSD of the RRFs improved when higher humic acid samples were excluded. For example, RSDs became progressively smaller for RRFs that excluded 3-fold dilution (i.e., the range of 9x – 2178x), 3x and 9x fold dilutions (i.e., the range of 27x – 2178x) and 3x, 9x and 27x fold dilutions (i.e., the range of 81x – 2178x) (Table 3-23).

Table 3-21 RRF values for the acenaphthene-d_{10} and chrysene-d_{12} IIS for the 30µm PDMS fiber according to humic acid. (SD= Standard Deviation and RSD = relative standard deviation)

30µm PDMS fiber (acenaphthene-d_{10}) (full dilution range)

	AVERAGE	SD	RSD
Naphthalene	0.2147	0.0171	8.0
Acenaphthylene	0.7068	0.0229	3.2
Acenaphthene-d_{10}	1.0000	-	-
Acenaphthene	1.2988	0.0335	2.6
Fluorene	1.6436	0.0289	1.8
Phenanthrene	4.0228	0.3297	8.2
Anthracene	3.8803	0.5511	14.2

30µm PDMS fiber (chrysene-d_{12}) (full dilution range)

	AVERAGE	SD	RSD
Pyrene	1.3730	0.5967	43.5
Fluoranthene	1.3481	0.4344	32.2
Chrysene	1.1821	0.0664	5.6
Chrysene-d_{12}	1.0000	-	-
Benzo[*a*]anthracene	1.2353	0.0218	1.8
Benzo[*a*]pyrene	0.8768	0.3299	37.6
Benzo[*b*]fluoranthene	0.5650	0.2588	45.8
Indeno[*1,2,3-cd*]pyrene	0.5078	0.3390	66.8
Dibenzo[*a,h*]anthracene	0.4543	0.2680	59.0
Benzo[*ghi*]perylene	0.4597	0.3419	74.4

`

Table 3-22 Average RRF values for acenaphthene-d_{10} and chrysene-d_{12} IIS for 65 µm PDMS/DVB fiber according to humic acid. (SD= Standard Deviation and RSD = relative standard deviation)

65 µm PDMS/DVB fiber (full dilution range)

	AVERAGE	SD	RSD
Naphthalene	1.7933	0.2024	11.3
Acenaphthylene	1.6282	0.0583	3.6
Acenaphthene-d_{10}	1.0000	-	-
Acenaphthene	1.1014	0.0176	1.6
Fluorene	1.1070	0.0090	0.8
Phenanthrene	1.3921	0.0401	2.9
Anthracene	1.1521	0.0916	7.9

65 µm PDMS/DVB fiber (full dilution range)

	AVERAGE	SD	RSD
Pyrene	3.5344	0.9988	28.3
Fluoranthene	3.3396	0.7270	21.8
Chrysene	1.1527	0.0257	2.2
Chrysene-d_{12}	1.0000	-	-
Benzo[*a*]anthracene	1.1928	0.0322	2.7
Benzo[*a*]pyrene	0.3588	0.1325	36.9
Benzo[*b*]fluoranthene	0.1916	0.0937	48.9
Indeno[*1,2,3-cd*]pyrene	0.0756	0.0491	64.9
Dibenz[*a,h*]anthracene	0.0641	0.0403	62.9
Benzo[*ghi*]perylene	0.0623	0.0438	70.3

`

Table 3-23 RRF values for the 30µm PDMS fiber and the average RRF values for the 65 µm PDMS/DVB fiber using chrysene-d_{12} according to humic acid calculated to respective dilution factor. (SD= Standard Deviation and RSD = relative standard deviation)

30µm PDMS fiber (Chrysene-d_{12})

	9 x -2178x			27x -2178x			81x -2178x		
	AVERAGE	SD	RSD	AVERAGE	SD	RSD	AVERAGE	SD	RSD
Pyrene	1.0833	0.2851	26.3	0.9792	0.1425	14.6	0.9294	0.1029	11.1
Fluoranthene	1.1424	0.2424	21.2	1.0559	0.1316	12.5	1.0141	0.1069	10.5
Chrysene	1.1538	0.0308	2.7	1.1595	0.0307	2.6	1.1616	0.0350	3.0
Chrysene-d_{12}	1.0000	-	-	1.0000	-	-	1.0000	-	-
Benzo[*a*]anthracene	1.2298	0.0195	1.6	1.2293	0.0218	1.8	1.2277	0.0248	2.0
Benzo[*a*]pyrene	0.9775	0.3213	32.9	1.0713	0.2511	23.4	1.1820	0.0482	4.1
Benzo[*b*]fluoranthene	0.6416	0.2554	39.8	0.7153	0.2018	28.2	0.8011	0.0725	9.0
Indeno[*1,2,3-cd*]pyrene	0.6031	0.3418	56.7	0.6916	0.2956	42.7	0.8110	0.1461	18.0
Dibenz[*a,h*]anthracene	0.5299	0.2697	50.9	0.6018	0.2282	37.9	0.6973	0.0931	13.3
Benzo[*ghi*]perylene	0.5579	0.3423	61.3	0.6435	0.3025	47.0	0.7618	0.1695	22.3

65 µm PDMS/DVB fiber

	9 x -2178x			27x -2178x			81x -2178x		
	AVERAGE	SD	RSD	AVERAGE	SD	RSD	AVERAGE	SD	RSD
Pyrene	3.1026	0.7059	22.8	2.8646	0.4451	15.5	2.7525	0.4247	15.4
Fluoranthene	3.0524	0.5834	19.1	2.8664	0.4072	14.2	2.7844	0.4198	15.1
Chrysene	1.1581	0.0281	2.4	1.1650	0.0250	2.1	1.1733	0.0194	1.7
Chrysene-d_{12}	1.0000	-	-	1.0000	-	-	1.0000	-	-
Benzo[*a*]anthracene	1.2070	0.0215	1.8	1.2147	0.0117	1.0	1.2140	0.0134	1.1
Benzo[*a*]pyrene	0.3958	0.1329	33.6	0.4332	0.1077	24.9	0.4809	0.0184	3.8
Benzo[*b*]fluoranthene	0.2148	0.0975	45.4	0.2399	0.0847	35.3	0.2744	0.0399	14.5
Indeno[*1,2,3-cd*]pyrene	0.0886	0.0504	56.9	0.1012	0.0445	44.0	0.1192	0.0219	18.4
Dibenz[*a,h*]anthracene	0.0754	0.0408	54.1	0.0859	0.0353	41.1	0.1006	0.0147	14.6
Benzo[*ghi*]perylene	0.0741	0.0450	60.7	0.0851	0.0403	47.3	0.1009	0.0219	21.7

`

Table 3-24 Average RRF values of PAHs against acenaphthene-d_{10} for each fiber according to hemoglobin. (SD= Standard Deviation and RSD = relative standard deviation

30 µm PDMS fiber (full dilution range)

	AVERAGE	SD	RSD
Naphthalene	0.5819	0.2483	42.7
Acenaphthylene	0.9875	0.1027	10.4
Acenaphthene-d_{10}	1.0000	-	-
Acenaphthene	1.2746	0.0465	3.6
Fluorene	1.5539	0.0534	3.4
Phenanthrene	3.2977	0.4737	14.4
Anthracene	3.3182	0.5765	17.4

65 µm PDMS/DVB fiber (full dilution range)

	AVERAGE	SD	RSD
Naphthalene	1.9625	0.3038	15.5
Acenaphthylene	1.6638	0.0607	3.7
Acenaphthene-d_{10}	1.0000	-	-
Acenaphthene	1.1457	0.0140	1.2
Fluorene	1.2060	0.0591	4.9
Phenanthrene	1.5344	0.0960	6.3
Anthracene	1.4077	0.0935	6.6

3.2.5 Effects of Hemoglobin on RRFs

Effects of hemoglobin on RRFs were also examined (see section 2.7.5). All water samples were spiked at 2.0 ng PAH/sample. Figure 67, Figure 68, Figure 69 and Figure 70 in the Appendix show peak area counts as a function of the amount of hemoglobin in the sample RRFs of early eluting PAHs against acenaphthene-d_{10} were relatively constant over the tested hemoglobin concentration range, except for the most concentrated solution, for both 30 µm PDMS fiber (Figure 71 in Appendix) and 65 µm PDMS/DVB fiber (Figure 72 in Appendix). RRFs of later eluting PAHs against chrysene-d_{12} were less consistent over the concentration range; the RRFs only become relatively constant at diluted solutions (Figure 73 and Figure 74 in Appendix). Average RRFs of early eluting PAHs against acenaphthene-d_{10} are summarized in Table 3-25 (i.e., full dilution range of 3x – 2178x) Table 3-26 (i.e., dilution range of 9x – 2178x and 27x – 2178x). RRFs of the later eluting PAHs against chrysene-d_{12} are presented in (full range) and Table 3-28 (partial range).

`

Similar to the situations with suspended solid and humic acid, RRFs become increasingly consistent when water samples of higher levels of hemoglobin were excluded.

Table 3-25 Average RRF Values for the acenaphthene-d_{10} for each fiber according to hemoglobin. (SD= Standard Deviation and RSD = relative standard deviation)

30 µm PDMS fiber (full dilution range)

	AVERAGE	SD	RSD
Naphthalene	0.5819	0.2483	42.7
Acenaphthylene	0.9875	0.1027	10.4
Acenaphthene-d_{10}	1.0000	-	-
Acenaphthene	1.2746	0.0465	3.6
Fluorene	1.5539	0.0534	3.4
Phenanthrene	3.2977	0.4737	14.4
Anthracene	3.3182	0.5765	17.4

65 µm PDMS/DVB fiber (full dilution range)

	AVERAGE	SD	RSD
Naphthalene	1.9625	0.3038	15.5
Acenaphthylene	1.6638	0.0607	3.7
Acenaphthene-d_{10}	1.0000	-	-
Acenaphthene	1.1457	0.0140	1.2
Fluorene	1.2060	0.0591	4.9
Phenanthrene	1.5344	0.0960	6.3
Anthracene	1.4077	0.0935	6.6

`

Table 3-26 Average RRF Values for the acenaphthene-d_{10} for each fiber according to hemoglobin calculated to respective dilution factor. (SD= Standard Deviation and RSD = relative standard deviation)

	30 µm PDMS fiber					
	9x-2178x			27x-2178x		
	AVERAGE	SD	RSD	AVERAGE	SD	RSD
Naphthalene	0.4748	0.0626	13.2	0.4545	0.0426	9.4
Acenaphthylene	0.9457	0.0465	4.9	0.9317	0.0351	3.8
Acenaphthene-d_{10}	1.0000	-	-	1.0000	-	-
Acenaphthene	1.2975	0.0190	1.5	1.2940	0.0190	1.5
Fluorene	1.5730	0.0390	2.5	1.5641	0.0362	2.3
Phenanthrene	3.5080	0.0972	2.8	3.5057	0.1085	3.1
Anthracene	3.5763	0.1236	3.5	3.5780	0.1381	3.9
	65 µm PDMS/DVB fiber					
	9x-2178x			27x-2178x		
	AVERAGE	SD	RSD	AVERAGE	SD	RSD
Naphthalene	1.8251	0.0305	1.7	1.8138	0.0140	0.8
Acenaphthylene	1.6348	0.0237	1.4	1.6290	0.0213	1.3
Acenaphthene-d_{10}	1.0000	-	-	1.0000	-	-
Acenaphthene	1.1456	0.0144	1.3	1.1426	0.0138	1.2
Fluorene	1.1796	0.0391	3.3	1.1666	0.0254	2.2
Phenanthrene	1.5419	0.0837	5.4	1.5174	0.0652	4.3
Anthracene	1.4215	0.0662	4.7	1.3999	0.0446	3.2

`

Table 3-27 Average RRF Values for the chrysene-d_{12} for each fiber according to hemoglobin. (SD= Standard Deviation and RSD = relative standard deviation)

30 µm PDMS fiber (full dilution range)

	AVERAGE	SD	RSD
Pyrene	1.0645	0.3692	34.7
Fluoranthene	1.1070	0.3420	30.9
Chrysene	1.0432	0.0394	3.8
Chrysene-d_{12}	1.0000	-	-
Benzo[*a*]anthracene	1.2178	0.0411	3.4
Benzo[*a*]pyrene	0.9460	0.2342	24.8
Benzo[*b*]fluoranthene	0.5911	0.2148	36.3
Indeno[*1,2,3-cd*]pyrene	0.7650	0.2861	37.4
Dibenz[*a,h*]anthracene	0.6414	0.2443	38.1
Benzo[*ghi*]perylene	0.6906	0.2856	41.4

65 µm PDMS/DVB fiber (full dilution range)

	AVERAGE	SD	RSD
Pyrene	2.8776	0.7854	27.3
Fluoranthene	2.7868	0.6424	23.1
Chrysene	1.1655	0.0292	2.5
Chrysene-d_{12}	1.0000	-	-
Benzo[*a*]anthracene	1.2591	0.0473	3.8
Benzo[*a*]pyrene	0.4664	0.1294	27.7
Benzo[*b*]fluoranthene	0.2284	0.0850	37.2
Indeno[*1,2,3-cd*]pyrene	0.1296	0.0705	54.4
Dibenz[*a,h*]anthracene	0.1050	0.0583	55.6
Benzo[*ghi*]perylene	0.1171	0.0632	53.9

`

Table 3-28 Average RRF Values for the chrysene-d_{12} for each fiber according to hemoglobin calculated to respective dilution factor. (SD= Standard Deviation and RSD = relative standard deviation)

30 µm PDMS fiber

	9x-2178x			27x-2178x		
	AVERAGE	SD	RSD	AVERAGE	SD	RSD
Pyrene	0.8767	0.0586	6.7	0.8568	0.0362	4.2
Fluoranthene	0.9359	0.0478	5.1	0.9201	0.0311	3.4
Chrysene	1.0556	0.0379	3.6	1.0590	0.0413	3.9
Chrysene-d_{12}	1.0000	-	-	1.0000	-	-
Benzo[*a*]anthracene	1.2330	0.0335	2.7	1.2385	0.0344	2.8
Benzo[*a*]pyrene	1.0452	0.1710	16.4	1.1055	0.0963	8.7
Benzo[*b*]fluoranthene	0.6826	0.1559	22.8	0.7432	0.0533	7.2
Indeno[*1,2,3-cd*]pyrene	0.8675	0.2529	29.2	0.9522	0.1618	17.0
Dibenz[*a,h*]anthracene	0.7327	0.2084	28.4	0.8067	0.1147	14.2
Benzo[*ghi*]perylene	0.7982	0.2413	30.2	0.8830	0.1373	15.5

65 µm PDMS/DVB fiber

	9x-2178x			27x-2178x		
	AVERAGE	SD	RSD	AVERAGE	SD	RSD
Pyrene	2.4702	0.1270	5.1	2.4236	0.0623	2.6
Fluoranthene	2.4533	0.1062	4.3	2.4173	0.0664	2.7
Chrysene	1.1758	0.0236	2.0	1.1829	0.0179	1.5
Chrysene-d_{12}	1.0000	-	-	1.0000	-	-
Benzo[*a*]anthracene	1.2819	0.0238	1.9	1.2890	0.0183	1.4
Benzo[*a*]pyrene	0.5220	0.0924	17.7	0.5554	0.0484	8.7
Benzo[*b*]fluoranthene	0.2621	0.0683	26.1	0.2835	0.0489	17.2
Indeno[*1,2,3-cd*]pyrene	0.1501	0.0695	46.3	0.1687	0.0585	34.7
Dibenz[*a,h*]anthracene	0.1228	0.0565	46.0	0.1381	0.0474	34.3
Benzo[*ghi*]perylene	0.1372	0.0600	43.7	0.1542	0.0484	31.4

`

3.2.6 Effects of combined parameters on RRFs

The effects of combined parameters (i.e., ionic strength, humic acid and hemoglobin) were examined in a series of water solutions at pH of 5.5 and pH 7.5. Suspended solid was not included in the combined parameters as the actual amount of suspended solids in the parent solution could not be determined. The solutions were prepared with a 3-fold dilution from the parent solution (see section 2.6.6). All water samples were spiked at 2.0 ng PAH/sample. Examination of effects of multiple parameters against the RRFs revealed that the RRFs of latest eluting HMW PAHs against chrysene-d_{12} had the most variation (i.e., large values of RSD). Therefore, it was decided at this point to add a third IIS, $^{13}C_{12}$- benzo[*ghi*]perylene, for the generation of RRFs for the last three eluting PAHs.

3.2.6.1 Effects of combined parameters on RRFs at pH = 5

A combination of three parameters, run at a constant pH 7.5, using ionic strength, humic acid and hemoglobin were measured using a three fold serial dilution from a parent solution (see 2.7.1) with each sample spiked at 2.0 ng/sample PAH solution. Figure 85, Figure 86, Figure 87 and Figure 88 give the illustration of the area as it reflects against factors of dilution. Figure 89 and Figure 90 illustrates the RRFs using acenaphthene-d_{10} for both fibers (30 µm PDMS and 65 µm PDMS/DVB) as they varied in relation to the decreasing three factors in solution. Figure 91 and Figure 92 illustrates the RRFs using chrysene d_{12} for both fibers (30 µm PDMS and 65 µm PDMS/DVB) as they varied in relation to the decreasing three factors in solution. Figure 93 and Figure 94 illustrates the RRFs using $^{13}C_{12}$- benzo[*ghi*]perylene for both fibers (30 µm PDMS and 65 µm PDMS/DVB) as they varied in relation to the decreasing three factors in solution.

`

Table 3-29 and Table 3-30 illustrates the average RRF (acenaphthene-d_{10}), standard deviation and the relative standard deviation (RSD) for each of the compounds according to each fiber (30 µm PDMS and 65 µm PDMS/DVB) and at various dilution ranges (i.e. 9 fold and greater or 27 fold and greater. Table 3-31 and Table 3-32 illustrates the average RRF (chrysene-d_{12}), standard deviation and the relative standard deviation (RSD) for each of the compounds according to each fiber (30 µm PDMS and 65 µm PDMS/DVB) and at various dilution ranges (i.e. 9 fold and greater or 27 fold and greater). Table 3-33 and Table 3-34 illustrates the average RRF ($^{13}C_{12}$- benzo[*ghi*]perylene), SD and the RSD for each of the compounds according to each fiber (30 µm PDMS and 65 µm PDMS/DVB) and at various dilution ranges (i.e. 9 fold and greater or 27 fold and greater). The tables presented here for the illustration of the overall effect of the four parameters in solution and their effect on PAH uptake onto both SPME fibers. Figure 75, Figure 76 , Figure 77 and Figure 78 in the Appendix show the peak area amounts of PAHs as a function of the 3-fold dilutions. In general, area counts increased with increased dilution. RRFs of PAHs against acenaphthene-d_{10} for both 30 µm PDMS fiber and 65 µm PDMS/DVB fiber are presented in Figure 79 and Figure 80, respectively. RRFs of PAHs against chrysene-d_{12} are presented in Figure 81 and Figure 82, and against $^{13}C_{12}$- benzo[*ghi*]perylene in Figure 83 and Figure 84. RRFs of PAHs against acenaphthene-d_{10} are summarized in Table 3-29 (full dilution range) and Table 3-30 (9x – 2178x and 27x – 2178x dilution range) for both 30 µm PDMS and 65 µm PDMS/DVB fibers. Similarly, RRFs of PAHs against chrysene-d_{12} and PAHs against $^{13}C_{12}$- benzo[*ghi*]perylene are summarized in Table 3-31 and Table 3-32, and in Table 3-33 and Table 3-34, respectively.

`

Table 3-29 Average RRF Values (acenaphthene-d_{10}) for each fiber according to samples containing salt, humic and hemoglobin at a pH 5.5. (SD= Standard Deviation and RSD = relative standard deviation)

30 µm PDMS fiber (full range dilution)

	AVERAGE	SD	RSD
Naphthalene	3.1753	3.3853	106.6
Acenaphthylene	1.5162	0.4774	31.5
Acenaphthene-d_{10}	1.0000	-	-
Acenaphthene	1.3111	0.2215	16.9
Fluorene	1.6565	0.1771	10.7
Phenanthrene	2.7089	0.4668	17.2
Anthracene	2.5919	0.6772	26.1

65 µm PDMS/DVB fiber (full range dilution)

	AVERAGE	SD	RSD
Naphthalene	4.8906	4.8204	98.6
Acenaphthylene	1.7196	0.1471	8.6
Acenaphthene-d_{10}	1.0000	-	-
Acenaphthene	1.0459	0.3445	32.9
Fluorene	1.2132	0.1998	16.5
Phenanthrene	1.4162	0.3862	27.3
Anthracene	1.2271	0.5088	41.5

`

Table 3-30 Average RRF Values (acenaphthene-d_{10}) for each fiber according to ionic strength, humic acid and hemoglobin at a pH 5.5 at 9 fold and 27 fold dilutions. (SD= Standard Deviation and RSD = relative standard deviation)

	30 µm PDMS fiber					
	9x-2178x			27x-2178x		
	AVERAGE	SD	RSD	AVERAGE	SD	RSD
Naphthalene	1.4875	0.3732	25.1	1.3386	0.0877	6.6
Acenaphthylene	1.3154	0.0724	5.5	1.2907	0.0442	3.4
Acenaphthene-d_{10}	1.0000	-	-	1.0000	-	-
Acenaphthene	1.2384	0.0362	2.9	1.2491	0.0279	2.2
Fluorene	1.6342	0.0681	4.2	1.6524	0.0575	3.5
Phenanthrene	2.6902	0.3646	13.6	2.8171	0.2130	7.6
Anthracene	2.8260	0.5708	20.2	3.0281	0.3175	10.5
	65 µm PDMS/DVB fiber					
	9x-2178x			27x-2178x		
	AVERAGE	SD	RSD	AVERAGE	SD	RSD
Naphthalene	2.4510	0.7277	29.7	2.1614	0.1813	8.4
Acenaphthylene	1.7474	0.0721	4.1	1.7214	0.0378	2.2
Acenaphthene-d_{10}	1.0000	-	-	1.0000	-	-
Acenaphthene	1.1850	0.0222	1.9	1.1905	0.0197	1.7
Fluorene	1.3126	0.0406	3.1	1.3178	0.0432	3.3
Phenanthrene	1.5993	0.2181	13.6	1.6819	0.0915	5.4
Anthracene	1.4714	0.2668	18.1	1.5722	0.1132	7.2

`

Table 3-31 Average RRF Values (chrysene-d_{12}) for each fiber according to ionic strength, humic acid, and hemoglobin at a pH 5.5. (SD= Standard Deviation and RSD = relative standard deviation)

30 µm PDMS fiber (full dilution range)

	AVERAGE	SD	RSD
Pyrene	0.9429	0.2492	26.4
Fluoranthene	0.9335	0.2136	22.9
Chrysene	0.7216	0.0523	7.2
Chrysene-d_{12}	1.0000	-	-
Benzo[*a*]anthracene	1.1466	0.0601	5.2
Benzo[*a*]pyrene	0.7319	0.1273	17.4
Benzo[*b*]fluoranthene	0.3924	0.1053	26.8

65 µm PDMS/DVB fiber (full dilution range)

	AVERAGE	SD	RSD
Pyrene	3.9404	1.3446	34.1
Fluoranthene	3.4872	0.9674	27.7
Chrysene	0.9654	0.0652	6.8
Chrysene-d_{12}	1.0000	-	-
Benzo[*a*]anthracene	1.1322	0.0497	4.4
Benzo[*a*]pyrene	0.3766	0.1309	34.8
Benzo[*b*]fluoranthene	0.1749	0.0651	37.2

`

Table 3-32 Average RRF Values (chrysene-d_{12}) for each fiber according to ionic strength, humic acid and hemoglobin at a pH 5.5 at 9 fold and 27 fold dilutions. (SD= Standard Deviation and RSD = relative standard deviation)

30 µm PDMS fiber

	9x-2178x			27x-2178x		
	AVERAGE	SD	RSD	AVERAGE	SD	RSD
Pyrene	0.9023	0.2600	28.8	0.8552	0.2605	30.5
Fluoranthene	0.8984	0.2044	22.8	0.8674	0.2121	24.5
Chrysene	0.7451	0.0283	3.8	0.7528	0.0237	3.1
Chrysene-d_{12}	1.0000	-	-	1.0000	-	-
Benzo[*a*]anthracene	1.1767	0.0244	2.1	1.1815	0.0240	2.0
Benzo[*a*]pyrene	0.7410	0.1433	19.3	0.7477	0.1592	21.3
Benzo[*b*]fluoranthene	0.4098	0.1140	27.8	0.4187	0.1251	29.9

65 µm PDMS/DVB fiber

	9x-2178x			27x-2178x		
	AVERAGE	SD	RSD	AVERAGE	SD	RSD
Pyrene	3.6405	1.4329	39.4	3.2397	1.1667	36.0
Fluoranthene	3.3300	1.0850	32.6	3.0352	0.9054	29.8
Chrysene	0.9377	0.0094	1.0	0.9371	0.0103	1.1
Chrysene-d_{12}	1.0000	-	-	1.0000	-	-
Benzo[*a*]anthracene	1.1190	0.0369	3.3	1.1215	0.0407	3.6
Benzo[*a*]pyrene	0.3141	0.0718	22.9	0.3151	0.0803	25.5
Benzo[*b*]fluoranthene	0.1432	0.0324	22.6	0.1419	0.0361	25.4

`

Table 3-33 Average RRF Values ($^{13}C_{12}$- benzo[*ghi*]perylene) for each fiber according to ionic strength, humic acid, and hemoglobin at a pH 5.5. (SD= Standard Deviation and RSD = relative standard deviation)

30 µm PDMS fiber (full dilution range)

	AVERAGE	SD	RSD
Indeno[*1,2,3-cd*]pyrene	1.1442	0.1706	14.9
Dibenz[*a,h*]anthracene	0.9182	0.0610	6.6
Benzo[*ghi*]perylene	0.9220	0.0446	4.8
$^{13}C_{12}$- Benzo[*ghi*]perylene	1.0000	-	-

65 µm PDMS/DVB fiber (full dilution range)

	AVERAGE	SD	RSD
Indeno[*1,2,3-cd*]pyrene	1.2398	0.4287	34.6
Dibenz[*a,h*]anthracene	0.8321	0.0525	6.3
Benzo[*ghi*]perylene	0.9596	0.0527	5.5
$^{13}C_{12}$- Benzo[*ghi*]perylene	1.0000	-	-

`

Table 3-34 Average RRF Values ($^{13}C_{12}$- benzo[*ghi*]perylene) for each fiber according to ionic strength, humic acid and hemoglobin at a pH 5.5 at 9 fold and 27 fold dilutions. (SD= Standard Deviation and RSD = relative standard deviation)

30 µm PDMS fiber

	9x-2178x			27x-2178x		
	AVERAGE	SD	RSD	AVERAGE	SD	RSD
Indeno[*1,2,3-cd*]pyrene	1.0703	0.0628	5.9	1.1442	0.1706	14.9
Dibenzo[*a,h*]anthracene	0.9354	0.0608	6.5	0.9182	0.0610	6.6
Benzo[*ghi*]perylene	0.9306	0.0460	4.9	0.9220	0.0446	4.8
$^{13}C_{12}$- Benzo[*ghi*]perylene	1.0000	-	-	1.0000	-	-

65 µm PDMS/DVB fiber

	9x-2178x			27x-2178x		
	AVERAGE	SD	RSD	AVERAGE	SD	RSD
Indeno[*1,2,3-cd*]pyrene	1.0410	0.0574	5.5	1.0196	0.0256	2.5
Dibenzo[*a,h*]anthracene	0.8101	0.0375	4.6	0.8165	0.0381	4.7
Benzo[*ghi*]perylene	0.9399	0.0431	4.6	0.9415	0.0480	5.1
$^{13}C_{12}$- Benzo[*ghi*]perylene	1.0000	-	-	1.0000	-	-

`

3.2.6.2 Effects of combined parameters on RRFs at pH = 7.5

A parallel experiment was carried out to examine the effects on RRFs at a constant pH of 7.5. Figure 85, Figure 86, Figure 87 and Figure 88 in the Appendix, show peak area counts of PAHs as a function of the dilutions. Similar to the situation for pH 5.5 water solutions, peak area counts increased with increased dilution. RRFs of PAHs against acenaphthene-d_{10} for both 30 μm PDMS fiber and 65 μm PDMS/DVB fiber are presented in Figure 89 and Figure 90 in the Appendix, respectively. RRFs of PAHs against chrysene-d_{12} are presented in (Figure 91 and Figure 92, in Appendix, A.1), and RRFs of PAHs against $^{13}C_{12}$- benzo[*ghi*]perylene are presented in Figure 93, and Figure 94 (in Appendix, A.1) demonstrate RRFs of PAHs against acenaphthene-d_{10} are summarized in Table 3-35 (full dilution range) and Table 3-36 (9x – 2178x and 27x – 2178x dilution range) for both 30 μm PDMS and 65 μm PDMS/DVB fibers. Similarly, RRFs of PAHs against chrysene-d_{12} and PAHs against $^{13}C_{12}$- benzo[*ghi*]perylene are summarized in Table 3-37 and Table 3-38, and in Table 3-39 and Table 3-40 in the Appendix, respectively.

Table 3-35 Average RRF Values (acenaphthene-d_{10}) for each fiber according to ionic strength, humic acid, and hemoglobin at a pH 7.5. (SD= Standard Deviation and RSD = relative standard deviation)

30 µm PDMS fiber (full dilution range)

	AVERAGE	SD	RSD
Naphthalene	1.1536	1.1340	98.3
Acenaphthylene	1.0337	0.2719	26.3
Acenaphthene-d_{10}	1.0000	-	-
Acenaphthene	1.1407	0.2448	21.5
Fluorene	1.5471	0.2991	19.3
Phenanthrene	3.6527	0.9083	24.9
Anthracene	3.4717	1.4586	42.0

65 µm PDMS/DVB fiber (full dilution range)

	AVERAGE	SD	RSD
Naphthalene	8.1899	13.3308	162.8
Acenaphthylene	1.8461	0.2293	12.4
Acenaphthene-d_{10}	1.0000	-	-
Acenaphthene	1.1702	0.0434	3.7
Fluorene	1.4095	0.0679	4.8
Phenanthrene	1.6999	0.2997	17.6
Anthracene	1.5488	0.5215	33.7

`

Table 3-36 Average RRF Values (acenaphthene-d_{10}) for each fiber according to ionic strength, humic acid and hemoglobin at a pH 7.5 at 9 fold and 27 fold dilutions. (SD= Standard Deviation and RSD = relative standard deviation)

	30 µm PDMS fiber					
	9x-2178x			27x-2178x		
	AVERAGE	SD	RSD	AVERAGE	SD	RSD
Naphthalene	0.5477	0.1643	30.0	0.4924	0.1040	21.1
Acenaphthylene	0.9388	0.1392	14.8	0.8993	0.1122	12.5
Acenaphthene-d_{10}	1.0000	-	-	1.0000	-	-
Acenaphthene	1.2352	0.0744	6.0	1.2512	0.0708	5.7
Fluorene	1.6694	0.1678	10.1	1.7149	0.1402	8.2
Phenanthrene	3.9176	0.8561	21.9	4.2504	0.2916	6.9
Anthracene	4.1128	1.0015	24.4	4.4788	0.4987	11.1
	65 µm PDMS/DVB fiber					
	9x-2178x			27x-2178x		
	AVERAGE	SD	RSD	AVERAGE	SD	RSD
Naphthalene	2.5264	0.8123	32.2	2.2140	0.3043	13.7
Acenaphthylene	1.7364	0.0666	3.8	1.7140	0.0423	2.5
Acenaphthene-d_{10}	1.0000	-	-	1.0000	-	-
Acenaphthene	1.1567	0.0124	1.1	1.1604	0.0096	0.8
Fluorene	1.4108	0.0411	2.9	1.4199	0.0386	2.7
Phenanthrene	1.7905	0.2484	13.9	1.8830	0.1136	6.0
Anthracene	1.7764	0.3634	20.5	1.9054	0.2007	10.5

`

Table 3-37 Average RRF Values (chrysene-d_{12}) for each fiber according to ionic strength, humic acid, and hemoglobin at a pH 7.5. (SD= Standard Deviation and RSD = relative standard deviation)

30 µm PDMS fiber (full dilution range)

	AVERAGE	SD	RSD
Pyrene	1.4946	0.6147	41.1
Fluoranthene	1.6270	0.6759	41.5
Chrysene	0.7748	0.1098	14.2
Chrysene-d_{12}	1.0000	-	-
Benzo[*a*]anthracene	1.3207	0.0872	6.6
Benzo[*a*]pyrene	0.7445	0.1972	26.5
Benzo[*b*]fluoranthene	0.3751	0.1615	43.0

65 µm PDMS/DVB fiber (full dilution range)

	AVERAGE	SD	RSD
Pyrene	3.7493	1.0425	27.8
Fluoranthene	3.4076	0.8122	23.8
Chrysene	0.9186	0.0510	5.5
Chrysene-d_{12}	1.0000	-	-
Benzo[*a*]anthracene	1.1593	0.0410	3.5
Benzo[*a*]pyrene	0.3103	0.0606	19.5
Benzo[*b*]fluoranthene	0.1477	0.0404	27.4

`

Table 3-38 Average RRF Values (chrysene-d_{12}) for each fiber according to ionic strength, humic acid and hemoglobin at a pH 7.5 at 9 fold and 27 fold dilutions. (SD= Standard Deviation and RSD = relative standard deviation)

30 µm PDMS fiber

	9x-2178x			27x-2178x		
	AVERAGE	SD	RSD	AVERAGE	SD	RSD
Pyrene	1.3362	0.6213	46.5	1.1921	0.5716	48.0
Fluoranthene	1.3999	0.5616	40.1	1.2770	0.5301	41.5
Chrysene	0.8234	0.0689	8.4	0.8432	0.0548	6.5
Chrysene-d_{12}	1.0000	-	-	1.0000	-	-
Benzo[*a*]anthracene	1.3061	0.0191	1.5	1.3106	0.0173	1.3
Benzo[*a*]pyrene	0.7605	0.2210	29.1	0.7992	0.2230	27.9
Benzo[*b*]fluoranthene	0.4077	0.1772	43.5	0.4398	0.1776	40.4

65 µm PDMS/DVB fiber

	9x-2178x			27x-2178x		
	AVERAGE	SD	RSD	AVERAGE	SD	RSD
Pyrene	3.6501	1.2063	33.0	3.3509	1.0713	32.0
Fluoranthene	3.3228	0.9351	28.1	3.0806	0.8083	26.2
Chrysene	0.9341	0.0362	3.9	0.9353	0.0404	4.3
Chrysene-d_{12}	1.0000	-	-	1.0000	-	-
Benzo[*a*]anthracene	1.1779	0.0246	2.1	1.1832	0.0234	2.0
Benzo[*a*]pyrene	0.2943	0.0626	21.3	0.2974	0.0695	23.4
Benzo[*b*]fluoranthene	0.1374	0.0413	30.0	0.1396	0.0458	32.8

`

Table 3-39 Average RRF Values ($^{13}C_{12}$- benzo[*ghi*]perylene) for each fiber according to ionic strength, humic acid, and hemoglobin at a pH 7.5. (SD= Standard Deviation and RSD = relative standard deviation)

30 µm PDMS fiber (full dilution range)

	AVERAGE	SD	RSD
Indeno[*1,2,3-cd*]pyrene	1.1670	0.2570	22.0
Dibenz[*a,h*]anthracene	0.8324	0.0561	6.7
Benzo[*ghi*]perylene	0.9845	0.0419	4.3
$^{13}C_{12}$- Benzo[*ghi*]perylene	1.0000	-	-

65 µm PDMS/DVB fiber (full dilution range)

	AVERAGE	SD	RSD
Indeno[*1,2,3-cd*]pyrene	1.1731	0.3771	32.1
Dibenz[*a,h*]anthracene	0.7931	0.0676	8.5
Benzo[*ghi*]perylene	0.8612	0.0657	7.6
$^{13}C_{12}$- Benzo[*ghi*]perylene	1.0000	-	-

`

Table 3-40 Average RRF Values ($^{13}C_{12}$- benzo[*ghi*]perylene) for each fiber according to ionic strength, humic acid and hemoglobin at a pH 7.5 at 9 fold and 27 fold dilutions. (SD= Standard Deviation and RSD = relative standard deviation)

30 µm PDMS fiber

	9x-2178x			27x-2178x		
	AVERAGE	SD	RSD	AVERAGE	SD	RSD
Indeno[*1,2,3-cd*]pyrene	1.0506	0.1454	13.8	1.1670	0.2570	22.0
Dibenz[*a,h*]anthracene	0.8197	0.0375	4.6	0.8324	0.0561	6.7
Benzo[*ghi*]perylene	0.9745	0.0408	4.2	0.9845	0.0419	4.3
$^{13}C_{12}$- Benzo[*ghi*]perylene	1.0000	-	-	1.0000	-	-

	9x-2178x			27x-2178x		
	AVERAGE	SD	RSD	AVERAGE	SD	RSD
Indeno[*1,2,3-cd*]pyrene	0.9828	0.0704	7.2	0.9565	0.0321	3.4
Dibenz[*a,h*]anthracene	0.7588	0.0219	2.9	0.7569	0.0239	3.2
Benzo[*ghi*]perylene	0.8824	0.0382	4.3	0.8899	0.0375	4.2
$^{13}C_{12}$- Benzo[*ghi*]perylene	1.0000	-	-	1.0000	-	-

`

3.3 Analysis of natural water samples using RRFs

The concept of RRFs was applied to the determination of PAHs in natural water. Natural water samples were collected from three different sources to represent three types of waters that exist in the environment. Well water was collected as a representative of a groundwater, river water as a surface water and bottled water as an anthropogenic source of water.

All natural water samples (17.5 mL) were spiked with PAHs at four levels of PAH spiking solution (0.0, 0.1, 0.5 and 2.0 ng/sample), and with three IISs (acenaphthene-d_{10}, chrysene-d_{12} and $^{13}C_{12}$- benzo[*ghi*]perylene) at 1.0 ng/sample. The three spiked levels permitted examination of the consistency of RRFs for samples that are slightly different for each type of natural waters, while the results of unspiked samples (i.e., 0.0 ng/sample) demonstrated the applicability of the SPME-GC/MS methods using RRFs. Samples were analyzed in duplicate for each fiber (i.e., PDMS/DVB-1, PDMS/DVB-2, PDMS-1, and PDMS-2, see section 2.6.7). The levels in the water samples were then determined using two different methods. The first method used average RRFs from the calibration standards (i.e., laboratory water spiked at 0.1 ng/sample, 0.5 ng/per sample and 2.0 ng/sample) to determine PAH levels in each sample. The second method used RRF value from the slope of RRFs against the levels in calibration standards (i.e., laboratory water spiked at 0.1 ng/sample, 0.5 ng/per sample and 2.0 ng/sample) to determine PAH levels in each sample. An S/N ratio of 3 was used to determine if a peak is present in the chromatogram.

3.3.1 Well Water

Well water from the same well source was divided into five well water samples. Table 3-43 shows the average PAH values from four runs (i.e., PDMS/DVB-1, PDMS/DVB-2, PDMS-1, and PDMS-2) along with associated variation expressed as SD and RSD. It can be seen that the values between the two runs, using the same type of fiber, were quite close to each other, while the values between the two types of the fiber had larger differences.

3.3.2 River Water

River water samples from five sampling locations were analyzed; Table 3-44 summarizes the river water results. The mean value presented in the table is the average of four set of runs (i.e., PDMS/DVB-1, PDMS/DVB-2, PDMS-1, and PDMS-2). Large RSDs were observed, likely due to low concentration levels of PAHs and averaging of values from different fibers.

3.3.3 Bottled Water

Five different brands of bottled waters were analyzed. Similar to river water, results of the five bottled water samples are summarized in Table 3-45. Again, low concentration levels of PAHs were detected, and this contributed to the large RSD values.

3.4 Correlations of RRFs and physical properties of PAHs

Physical properties of PAHs may be used to examine relationships with RRFs. And by taking these properties and examining them by plotting the RRF values against selected physical or chromographic attributes a relationship was to be discovered. The RRF comparison was either a direct comparison of RRF to physical property, or as a ratio of $RRF_{sample}/RRF_{direct}$ (RRF_{ratio}), where RRF_{sample}

refers to RRFs of PAHs in a sample that was measured using SPME extraction followed by GC/MS analysis, and RRF_{direct} refers to RRFs of PAHs from a direct liquid injection. Different fibers have different properties that could affect the uptake of PAHs as they are either adsorbed onto the fiber surface, as for the 65 µm PDMS/DVB fiber, or absorbed into the fiber, as for the 30 µm PDMS fiber. In the process of examining the relationships of RRFs and physical and chromatographic properties of PAHs, all RRFs were generated against one single IIS, in this case, the acenaphthene-d_{10} to provide continuity.

3.4.1 Relationship of vapor pressure and RRFs

The relationship between log-transformed vapor pressure (Log v.p.) and RRF_{direct} is illustrated in Figure 95. Relationships of Log v.p. and RRF_{sample} are illustrated in Figure 96 for laboratory water, Figure 98 for well water, Figure 100 for river water, and Figure 102 for bottled water. The relationship of Log v.p. and RRF_{ratio} ($RRF_{sample}/RRF_{direct}$) are illustrated in Figure 97 for laboratory water, Figure 99 for well water, Figure 101 for river water and Figure 103 for bottled water. All figures can be found in Appendix, A1.

3.4.2 Relationship of octanol/water partition coefficient and

The relationship of the log-transformed octanol/water partition coefficient ($\log K_{ow}$) and RRF_{direct} is shown in Figure 104. Relationships of $\log K_{ow}$ and RRF_{sample} are shown in Figure 105 for laboratory water, Figure 107 for well water, Figure 109 for river water and Figure 111Figure 111 for bottled water. The relationships of $\log K_{ow}$ and $RRF_{sample}/RRF_{direct}$ are shown in Figure 106 for

laboratory water, Figure 108 for well water, Figure 110 for river water and Figure 112 for bottled water. All figures can be found in Appendix, A1.

3.4.3 Relationship of retention time and RRF

The relationship of the GC/MS retention time (RT) and RRF_{direct} is shown in Figure 113. Relationships of RT and RRF_{sample} are shown in Figure 114 for laboratory water, Figure 116 for well water, Figure 118 for river water and Figure 120 for bottled water. Relationships of RT and $RRF_{sample}/RRF_{direct}$ are shown in Figure 115 for laboratory water, Figure 117 for well water, Figure 119 for river water and Figure 121 for bottled water. All figures can be found in Appendix, A1.

3.4.4 The octanol/air partition coefficient (log K_{oa}) relationship

The relationship of log-transformed octanol/air coefficient (log K_{oa}) and RRF_{direct} is shown in Figure 122. Relationships of log K_{oa} and RRF_{sample} are shown in Figure 123 for laboratory water, Figure 125 for well water, Figure 127 for river water and Figure 129 for bottled water. Relationships of log K_{oa} and $RRF_{sample}/RRF_{direct}$ are shown in Figure 124 for laboratory water, Figure 126 for well water, Figure 128 for river water and Figure 130 for bottled water. All figures can be found in Appendix, A1.

3.4.5 Relationship of boiling point and RRFs

The relationship of boiling point of the studied PAHs and RRF_{direct} can be seen in Figure 131. Relationships of the boiling point and RRF_{sample} are shown in Figure 132 for laboratory water, Figure 134 for well water, Figure 136 for river water, and Figure 138 for bottled water. Relationships of the boiling point and $RRF_{sample}/RRF_{direct}$ are shown in Figure 133 for laboratory water, Figure 135 for

well water, Figure 137 for river water, and Figure 139 for bottled water. All figures can be found in Appendix, A1.

3.4.6 Summary of relationships of the physical properties and RRFs

The compiled results of all comparisons between the RRFs of the studied PAHs and their respective physical and chromatographic properties are summarized in Table 3-41 and Table 3-42, with a regression equation for each relationship along with the coefficient of determination (r^2) and the p values as it associates with the F value. The correlation can be described by its r^2 value, with a statistical significance of the correlation indicated by the p values. It can be seen that the analysis of the PDMS/DVB fiber data yielded the highest correlation values with the r^2 values and p values for all the physical properties of water. The PDMS fiber is also well correlated with the RRF ratios, then p values are all statistically significant with $p<0.01$ for all parameters investigated. The correlation for values for the RRFs against the physical properties yielded $r^2 < 0.5$ for about half of the parameters, with corresponding p values of around 0.5 (i.e., relationship not statistically significant).

Table 3-41 Summary of the regression results of RRFs of PAHs in various types of samples as they pertain to the physical properties and chromatographic behaviors of PAHs.

	Log Vapor Pressure			Log K_{ow}			Retention Time		
RRF Type*	Equation	r^2	P-Value (P <)	Equation	r^2	P-Value (P <)	Equation	r^2	P-Value (P <)
Direct Injection	y = 0.2217x + 2.2226	0.6289	0.5	y = -0.5982x + 4.4645	0.4856	0.01	y = -0.1448x + 3.0985	0.6620	0.001
Lab water									
RRF PDMS/DVB	y = 0.1846x + 1.5032	0.8501	0.00001	y = -0.5544x + 3.6708	0.8129	0.0001	y = -0.1207x + 2.2337	0.8961	0.00001
RRF PDMS	y = -1.2715x + 3.0295	0.3859	0.02	y = 4.6946x - 16.587	0.5578	0.005	y = 0.8642x - 2.4186	0.4396	0.01
RRF Ratio PDMS/DVB	y = 0.1245x + 1.0508	0.8009	0.0001	y = -0.3917x + 2.6081	0.8409	0.00001	y = -0.0790x + 1.5136	0.7962	0.0001
RRF Ratio PDMS	y = -4.8308x - 4.0429	0.7563	0.0001	y = 15.8755x - 69.0789	0.6883	0.0005	y = 3.628x - 30.101	0.8360	0.00001
Well Water									
RRF PDMS/DVB	y = 0.1964x + 1.6440	0.8557	0.0001	y = -0.5734x + 3.8622	0.7734	0.0001	y = -0.1272x + 2.4054	0.8847	0.000001
RRF PDMS	y = -0.6156x + 4.6171	0.1453	0.5	y = 2.8802x - 8.1291	0.3372	0.1	y = 0.4496x + 1.5841	0.1911	0.5
RRF Ratio PDMS/DVB	y = 0.1236x + 1.1245	0.7984	0.00001	y = -0.3868x + 2.6592	0.8288	0.00001	y = -0.0778x + 1.5754	0.7798	0.0001
RRF Ratio PDMS	y = -3.3766x - 3.3688	0.8157	0.00001	y = 9.7401x - 40.8754	0.7196	0.0005	y = 2.23x - 17.013	0.8773	0.000001
River Water									
RRF PDMS/DVB	y = 0.1791x + 1.4612	0.8303	0.00001	y = -0.5233x + 3.4859	0.7512	0.0001	y = -0.1158x + 2.1539	0.8563	0.00001
RRF PDMS	y = -0.3870x + 5.1262	0.0439	0.5	y = 2.3613x - 5.8323	0.1732	0.5	y = 0.3055x + 2.9297	0.0675	0.5
RRF Ratio PDMS/DVB	y = 0.1236x + 1.0246	0.8166	0.00001	y = -0.3799x + 2.5225	0.8180	0.00001	y = -0.0738x + 1.4129	0.7947	0.0001
RRF Ratio PDMS	y = -2.4917x - 1.4519	0.8128	0.0001	y = 7.3915x - 30.2204	0.7583	0.00003	y = 1.5968x - 10.7474	0.8839	0.00001
Bottled Water									
RRF PDMS/DVB	y = 0.1687x + 1.4484	0.8114	0.00001	y = -0.4888x + 3.3339	0.7225	0.0001	y = -0.1104x + 2.1175	0.8574	0.0001
RRF PDMS	y = -0.1711x + 4.9318	0.0106	0.7	y = 1.5316x - 2.5217	0.0898	0.5	y = 0.1510x + 3.7590	0.0203	0.6
RRF Ratio PDMS/DVB	y = 0.1026x + 0.9775	0.7976	0.00001	y = -0.3201x + 2.2466	0.8238	0.00001	y = -0.0650x + 1.3572	0.7898	0.00001
RRF Ratio PDMS	y = -1.7479x - 0.3094	0.6172	0.001	y = 5.4472x - 21.8921	0.6355	0.001	y = 1.1936x - 7.8698	0.7098	0.0001

`

Table 3-42 (continued) Summary of the regression results of RRFs as they pertain to the physical properties and chromatographic behaviors of PAHs.

	K_{oa}			Boiling Point		
RRF Type*	Equation	r^2	P-Value (P <)	Equation	r^2	P-Value (P <)
Direct Injection	y = -0.2765x + 3.9024	0.5920	0.01	y = -0.0065x + 3.9525	0.5370	0.01
Lab water						
RRF PDMS/DVB	y = -0.2425x + 3.0184	0.8873	0.000001	y = -0.0059x + 3.1269	0.8496	0.000001
RRF PDMS	y = 1.8533x - 9.1534	0.4959	0.005	y = 0.0463x - 10.5407	0.5039	0.005
RRF Ratio PDMS/DVB	y = -0.1634x + 2.0713	0.8346	0.00001	y = -0.0041x + 2.2054	0.8600	0.000001
RRF Ratio PDMS	y = 7.0131x - 51.0563	0.7663	0.0001	y = 0.1682x - 53.4655	0.7185	0.0001
Well Water						
RRF PDMS/DVB	y = -0.2542x + 3.2197	0.8671	0.00001	y = -0.0061x + 3.3188	0.8206	0.0001
RRF PDMS	y = 1.0547x - 2.7832	0.2579	0.1	y = 0.0277x - 4.1374	0.2901	0.05
RRF Ratio PDMS/DVB	y = -0.1612x + 2.1280	0.8213	0.00001	y = -0.0040x + 2.2583	0.8443	0.00001
RRF Ratio PDMS	y = 4.3500x - 30.2690	0.8189	0.00001	y = 0.1051x - 32.0918	0.7796	0.0001
River Water						
RRF PDMS/DVB	y = -0.2313x + 2.8931	0.8372	0.00001	y = -0.0056x + 2.9863	0.7945	0.0001
RRF PDMS	y = 0.7909x - 0.7461	0.1109	0.5	y = 0.0211x - 1.9138	0.1292	0.2
RRF Ratio PDMS/DVB	y = -0.1598x + 2.0151	0.8261	0.00001	y = -0.0040x + 2.1411	0.8460	0.0001
RRF Ratio PDMS	y = 3.2714x - 21.8877	0.8475	0.00001	y = 0.0791x - 23.2811	0.8080	0.00001
Bottled Water						
RRF PDMS/DVB	y = -0.2186x + 2.8044	0.8243	0.00001	y = -0.0052x + 2.8793	0.7728	0.0001
RRF PDMS	y = 0.4523x + 1.3566	0.0447	0.5	y = 0.0127x + 0.4479	0.0572	0.5
RRF Ratio PDMS/DVB	y = -0.1336x + 1.8083	0.8181	0.00001	y = -0.0034x + 1.9156	0.8403	0.0001
RRF Ratio PDMS	y = 2.3695x - 15.3566	0.6860	0.0005	y = 0.0572x - 16.3230	0.6517	0.0005

`

Table 3-43 Concentrations (ng/L) of PAHs in well water

	PDMS/DVB-1			PDMS/DVB-2			PDMS-1			PDMS-2		
Compound	Mean	SD	RSD	Mean	SD	RSD	Mean	SD	RSD	Mean	SD	RSD
RRF using "slope" method												
Naphthalene	2.7	1.1	42	2.7	1.1	42	11.7	7.9	67	23.1	10.8	46
Acenaphthylene	0.26	0.1	44	0.26	0.11	43	ND			0.032	0.07	224
Acenaphthene	0.052	0.02	47	0.047	0.02	51	0.36	0.35	97	0.069	0.16	224
Fluorene	0.27	0.11	42	0.27	0.11	42	1.2	1.4	114	0.60	0.34	57
Phenanthrene	1.0	0.49	47	1.1	0.53	49	2.7	1.24	46	2.1	1.06	51
Anthracene	ND			ND			0.29	0.24	84	0.28	0.19	67
Pyrene	1.00	0.43	43	1.0	0.45	43	70.9	94.5	133	2.6	1.33	50
Fluoranthene	3.03	1.3	43	3.2	1.4	44	85.4	109.5	128	5.9	2.79	47
Chrysene	0.26	0.24	92	0.18	0.25	137	24.8	40.3	162	1.1	0.53	47
Benzo[*a*]anthracene	0.20	0.15	75	0.15	0.17	112	32.4	47.2	145	1.7	0.9	52
Benzo[*a*]pyrene	0.26	0.21	81	0.19	0.23	122	29.0	46.3	160	1.0	0.6	59
Benzo[*b*]fluoranthene	0.63	1.4	224	1.3	1.7	137	23.1	38.9	168	0.53	0.31	58
Indeno[*1,2,3-cd*]pyrene	1.2	0.9	74	0.89	1.0	113	28.0	42.0	150	2.2	1.25	57
Dibenz[*a,h*]anthracene	1.1	0.8	75	0.75	0.86	115	26.6	41.2	155	1.4	0.77	54
Benzo[*ghi*]perylene	1.6	1.23	74	1.2	1.4	113	22.4	30.9	138	2.4	1.4	58
RRF using "Average" method												
Naphthalene	2.4	1.0	42	2.4	1.0	42	11.7	7.9	67	23.2	10.8	46
Acenaphthylene	0.27	0.12	44	0.27	0.12	43	ND			0.015	0.030	224
Acenaphthene	0.05	0.02	47	0.045	0.020	51	0.18	0.17	97	0.034	0.080	224
Fluorene	0.27	0.11	42	0.27	0.11	42	0.55	0.63	114	0.27	0.15	57
Phenanthrene	1.1	0.50	47	1.1	0.54	49	1.2	0.54	46	0.90	0.46	51
Anthracene	ND			ND			0.13	0.11	84	0.13	0.08	67
Pyrene	0.94	0.40	43	0.98	0.42	43	28.0	37.3	133	1.04	0.53	50
Fluoranthene	2.8	1.2	43	2.9	1.27	44	33.5	42.9	128	2.31	1.09	47
Chrysene	0.31	0.28	92	0.21	0.29	137	7.5	12.1	162	0.34	0.16	47
Benzo[*a*]anthracene	0.21	0.16	75	0.16	0.18	112	13.8	20.1	145	0.73	0.38	52
Benzo[*a*]pyrene	0.31	0.25	81	0.22	0.27	122	14.4	23.0	160	0.50	0.3	59
Benzo[*b*]fluoranthene	0.87	1.9	224	1.7	2.4	137	12.9	21.6	168	0.30	0.17	58
Indeno[*1,2,3-cd*]pyrene	1.5	1.1	74	1.1	1.2	113	16.4	24.5	150	1.3	0.73	57
Dibenz[*a,h*]anthracene	1.5	1.1	75	1.1	1.2	115	17.6	27.2	155	0.95	0.51	54
Benzo[*ghi*]perylene	2.2	1.6	74	1.6	1.8	113	11.7	16.1	138	1.2	0.72	58

Note:ND = peaks with S/N ratio <3

`

Table 3-44 PAHs levels (ng/L) in five sites along Ottawa River

River Water	Site 1			Site 2			Site 3			Site 4			Site 5		
	Mean	SD	RSD	Mean	SD	RSD	Mean	SD	RSD	Mean	SD	RSD	Mean	SD	RSD
RRF (slope)															
Naphthalene	4.6	5.8	126	3.5	6.3	182	8.4	9.6	114	3.4	6.0	177	0.48	1.0	200
Acenaphthylene	ND			1.4	2.8		0.40	0.73	182	0.033	0.066	200	0.009	0.018	200
Acenaphthene	0.084	0.15	179	0.006	0.013	200	0.23	0.28	123	0.14	0.22	160	0.006	0.007	117
Fluorene	0.67	0.55	83	0.32	0.12	38	0.48	0.26	53	0.47	0.15	32	0.088	0.068	77
Phenanthrene	1.1	0.68	64	1.0	0.64	63	1.27	0.80	63	1.2	0.51	41	0.25	0.12	46
Anthracene	0.12	0.10	83	0.11	0.11	98	0.22	0.24	107	0.20	0.17	86	0.043	0.037	86
Pyrene	10.9	17.2	158	23.8	46.2	194	20.7	39.8	192	0.91	0.17	18	0.40	0.068	17
Fluoranthene	9.4	14.0	149	25.6	49.9	195	19.2	36.7	192	0.83	0.21	25	0.34	0.043	13
Chrysene	3.1	5.0	162	9.2	17.8	193	8.3	16.1	193	0.58	0.084	15	0.17	0.046	27
Benzo[*a*]anthracene	7.9	12.9	163	26.7	52.4	196	25.8	50.3	195	0.97	0.42	43	0.39	0.14	37
Benzo[*a*]pyrene	6.7	10.9	164	28.7	56.0	195	19.8	38.3	194	1.0	0.55	55	0.30	0.17	58
Benzo[*b*]fluoranthene	4.3	7.0	163	12.9	25.1	194	11.2	21.6	193	0.47	0.23	50	0.14	0.090	63
Indeno[*1,2,3-cd*]pyrene	5.0	6.3	128	25.9	45.6	176	29.7	49.1	165	4.9	2.87	58	1.7	1.2	71
Dibenz[*a,h*]anthracene	4.8	5.5	115	26.3	46.2	175	36.4	62.8	173	5.9	3.9	67	2.0	1.4	72
Benzo[*ghi*]perylene	7.3	9.9	136	31.6	53.8	170	36.2	58.9	163	6.7	4.0	60	2.2	1.3	60
RRF (Average)															
Naphthalene	3.9	4.9	128	2.8	5.06	181	6.2	6.9	110	2.7	4.8	175	0.39	0.77	200
Acenaphthylene	ND			1.7	3.31		0.47	0.86	184	0.033	0.067	200	0.009	0.018	200
Acenaphthene	0.081	0.14	179	0.006	0.012	200	0.25	0.30	121	0.14	0.23	163	0.006	0.007	116
Fluorene	0.72	0.63	87	0.35	0.16	45	0.51	0.30	57	0.50	0.19	37	0.095	0.078	82
Phenanthrene	1.1	0.76	66	1.1	0.67	62	1.3	0.82	61	1.3	0.61	46	0.27	0.14	52
Anthracene	0.14	0.11	80	0.13	0.12	92	0.25	0.25	100	0.23	0.20	87	0.052	0.049	94
Pyrene	9.9	15.6	157	22.2	43.2	194	19.4	37.2	192	0.86	0.17	20	0.38	0.064	17
Fluoranthene	8.6	12.8	148	23.6	46.0	195	17.7	33.9	192	0.76	0.20	26	0.31	0.039	12
Chrysene	4.0	6.2	155	11.4	21.6	190	10.3	19.6	190	0.94	0.52	55	0.26	0.045	17
Benzo[*a*]anthracene	7.6	12.5	164	24.3	47.6	196	23.5	45.8	195	0.92	0.36	39	0.37	0.12	33
Benzo[*a*]pyrene	7.9	13.1	165	31.3	60.9	195	21.6	41.7	193	1.1	0.57	50	0.34	0.18	53
Benzo[*b*]fluoranthene	6.2	10.1	163	16.8	32.5	193	14.6	28.0	192	0.64	0.27	42	0.19	0.11	55
Indeno[*1,2,3-cd*]pyrene	5.6	7.2	127	28.2	49.0	174	32.6	52.7	162	5.8	3.4	59	2.0	1.4	74
Dibenz[*a,h*]anthracene	5.0	5.9	117	25.3	42.5	168	35.3	57.7	163	7.2	5.9	82	2.4	2.2	88
Benzo[*ghi*]perylene	7.3	10.3	141	27.7	44.0	159	32.4	47.9	148	7.8	6.2	80	2.5	2.0	80

Note:ND = peaks with S/N ratio <3

`

Table 3-45 PAHs levels (ng/L) in five brands of bottled water

Bottled water	Bottle 1			Bottle 2			Bottle 3			Bottle 4			Bottle 5		
	Mean	SD	RSD	Mean	SD	RSD	Mean	SD	RSD	Mean	SD	RSD	Mean	SD	RSD
RRF (slope)															
Naphthalene	5.7	5.3	94	10.3	8.4	82	8.9	9.9	111	16.6	8.1	49	2.3	3.2	136
Acenaphthylene	ND			ND			ND			ND			ND		
Acenaphthene	0.27	0.32	119	0.29	0.34	118	0.25	0.29	116	0.25	0.22	85	0.028	0.055	200
Fluorene	0.32	0.29	91	0.31	0.33	105	0.29	0.34	117	1.6	0.21	13	0.13	0.036	28
Phenanthrene	1.1	1.1	93	0.99	0.95	96	6.0	10.3	171	1.4	1.1	73	0.22	0.21	95
Anthracene	5.9	9.8	165	0.35	0.42	119	0.4	0.49	123	0.46	0.41	88	0.094	0.089	95
Pyrene	0.62	0.57	92	0.54	0.46	85	0.35	0.33	95	0.65	0.57	87	0.13	0.11	86
Fluoranthene	0.75	0.75	100	0.69	0.69	100	0.41	0.42	101	0.73	0.71	97	0.15	0.14	98
Chrysene	0.55	0.47	86	0.35	0.26	75	0.27	0.25	91	0.37	0.26	71	0.063	0.045	71
Benzo[*a*]anthracene	1.4	1.4	97	1.2	0.99	86	0.67	0.60	90	1.1	0.81	73	0.22	0.15	69
Benzo[*a*]pyrene	1.4	1.3	93	1.0	0.88	84	0.61	0.64	106	0.94	0.81	85	0.15	0.12	79
Benzo[*b*]fluoranthene	1.2	1.1	98	0.78	0.63	81	0.33	0.39	119	0.56	0.46	83	0.12	0.093	81
Indeno[*1,2,3-cd*]pyrene	1.2	1.6	141	1.3	1.8	141	0.86	1.2	142	1.2	1.4	118	0.49	0.49	101
Dibenz[*a,h*]anthracene	1.4	2.0	142	1.6	2.2	138	0.84	1.1	126	1.0	1.2	121	0.12	0.14	115
Benzo[*ghi*]perylene	3.5	3.2	90	4.3	3.6	84	3.1	3.0	95	4.4	3.8	85	0.78	1.0	133
RRF (Average)															
Naphthalene	4.2	3.7	88	7.7	5.5	72	6.5	6.8	106	12.7	5.0	40	1.7	2.2	126
Acenaphthylene	ND			ND			ND			ND			ND		
Acenaphthene	0.27	0.32	118	0.29	0.34	117	0.25	0.29	116	0.26	0.22	87	0.029	0.058	200
Fluorene	0.33	0.31	92	0.34	0.36	107	0.31	0.37	119	1.7	0.30	18	0.14	0.040	29
Phenanthrene	1.3	1.2	93	1.1	1.1	100	6.3	10.6	169	1.6	1.2	75	0.24	0.23	95
Anthracene	6.5	10.8	166	0.35	0.41	116	0.42	0.54	129	0.47	0.39	82	0.096	0.090	94
Pyrene	0.61	0.57	93	0.54	0.46	86	0.35	0.33	95	0.64	0.57	88	0.13	0.11	87
Fluoranthene	0.69	0.69	100	0.63	0.64	100	0.37	0.36	98	0.67	0.65	97	0.13	0.13	98
Chrysene	0.95	0.88	93	0.57	0.46	81	0.41	0.33	81	0.62	0.49	79	0.10	0.070	69
Benzo[*a*]anthracene	1.5	1.4	98	1.2	1.1	89	0.67	0.61	92	1.1	0.86	76	0.22	0.16	72
Benzo[*a*]pyrene	2.1	2.0	97	1.5	1.4	90	0.88	1.0	116	1.4	1.3	92	0.22	0.19	85
Benzo[*b*]fluoranthene	2.1	2.1	99	1.4	1.2	87	0.58	0.76	132	1.0	0.88	89	0.20	0.17	85
Indeno[*1,2,3-cd*]pyrene	1.9	2.9	149	2.0	3.1	153	1.4	2.2	154	1.9	2.4	126	0.64	0.57	90
Dibenz[*a,h*]anthracene	2.1	3.1	151	2.4	3.6	151	1.2	1.7	138	1.5	1.9	130	0.17	0.20	119
Benzo[*ghi*]perylene	3.6	3.3	91	4.4	3.7	84	3.2	3.0	94	4.5	3.8	84	0.79	1.0	131

Note:ND = peaks with S/N ratio <3

`

4 Chapter: Discussion

This project was designed to evaluate the utility of RRFs in an SPME-based method for the determination of polycyclic aromatic hydrocarbons (PAHs) in water. The evaluation investigated the performance of two different fibers (i.e., a PDMS fiber and a PDMS/DVB fiber) regarding the applicability of RRFs. RRFs were first evaluated using laboratory water that was adjusted for various water parameters, namely the pH, ionic strength, suspended solids and organic carbon (i.e., humic acid and hemoglobin). Subsequently, the RRFs were examined under combined parameters at two pH values. Finally, the use of RRFs was applied to quantifying PAHs in natural water samples (i.e., river water, groundwater and bottled water). The data generated from the natural water samples were used to examine relationships between RRFs and the physical-chemical and chromatographic characteristics of PAHs (i.e., K_{ow}, K_{oa}, vapor pressure, boiling point, chromatographic retention time).

4.1 Instrument methods that use SPME

Different instrumentation and method protocols are used in SPME-based quantification of PAHs in water. Work performed by Chen used SPME and HPLC/FLD, giving similar values to this research, with RSD values around 10% and the detection level was in the ug/L range[67]. Work by Kernis et al. showed the use of a GC/MS coupled with SPME obtained concentrations in the 0.05-10.0 ng/mL range, with RSD values of 10-20 %.[68] Work by Zuazagoitia et al., which analysed water leached from contaminated soil samples, showed that by utilizing an SPME coupled with a GC/FID it is possible to obtain a LOD value around 0.1

µg/L (LOD).[69] The resulting data gave RSD values between 5 and 20% (at 50 µg/L). The work of López-Darias et al. used SPME-GC/FID instrumentation, with a 30 µm PDMS fiber, and obtained good recoveries (i.e., around 80% and low RSD values) with bottled water samples spiked with PAH, parabens, and alkylphenols. The resulting data showed RSD values ranging from 3.7 to 14%, with LODs for specific PAHs in the range of 0.37 ng/mL for low molecular weight PAHs to 10 ng/mL for the heavier PAHs.[70] In comparison, the detection sensitivity in the current study is substantially lower. Although the LOD was not specifically measured, judging from the S/N ratios for both 2 and 10 pg injections, the LOD for the current study can be conservatively estimated at 10 pg/sample or lower. This value translates into a LOD of 0.57 ng/L, a value that is at least 100 times lower than the detection sensitivities reported in the literature. Using three IISs, RSD values of RRFs ranged from as low as 3, to values around 20-30 for different PAHs.

4.2 Optimization for the use of SPME GC/MS

The use of the 100 µm PDMS fiber in method development was problematic due to the very long extraction time required to achieve equilibration. By careful examination of the data, the extraction times were shortened when the 30 µm PDMS fiber was used instead of the 100 µm PDMS fiber (i.e., the thinner coating of the 30 µm PDMS fiber reduced the overall time required to reach equilibrium). Optimization of each parameter, for both fibers, is shown in Table 3-8. This table demonstrates the optimal operating conditions for both fibers. By examining the relative response factor (RRF) results acquired using

acenaphthylene-d_{10} and chrysene-d_{12} at each condition set point, it was determined that optimal operating conditions were needed. These conditions included a fiber bake out at 260^0C (for 25 min), an SPME extraction temperature of 50^0C, desorption temperature of 270^0C, desorption time of 180 seconds, and an extraction time of 40 or 60 minutes. A total of 7 replicates were run twice for each fiber using the optimal conditions (listed in Table 3-8) for two different SPME extraction times, namely 40 min and 60 min. The peak areas and RRF values were examined and compared using average, standard deviation (SD) and relative standard deviation (RSD) for the 40 and 60 minute extraction times. The optimal extraction time for both fibers was determined to be 60 minutes. The desorption temperature listed above (i.e., 270^0C), was chosen because both peaks and RRFs are more reproducible using 60 min, when compared to the 40 min extraction, and the temperature lies within the upper end of the manufacturer's suggested upper limit.

4.3 The effects of water properties on the RRFs

The common practice in quantitative SPME is to use a corresponding IIS for each target analyte. However, one of the main purposes of this study was to use only a few IISs for the quantification of a large number of PAHs, alleviating the need to have a corresponding IIS for each PAH studied using SPME-GC/MS. Since it is not possible or very hard to obtain a corresponding IIS for each target analyte, the use of a single IIS for a group of PAHs to calculate concentrations is needed to overcome this problem. When calculations are performed, the relative response factor (RRF) must be introduced to alleviate error. The error is that there

is a matrix effect that affects the analysis of water samples, so a relationship of the IIS to each analyte (i.e., RRFs) has to be studied to permit generation of accurate and precise results.

In this study, the following five water parameters were examined: pH, ionic strength (i.e., NaCl concentration), suspended solids (i.e., suspended dust), humic acid concentration, and hemoglobin concentration. The selected range of each parameter covered a range that reflects different waters that exist in the environment.

Initial use of acenaphthene-d_{10} and chrysene-d_{12} was used for determining the parameters needed to start the initial analysis of the method. These two IISs were used as a basis for the initial method development. The use of just two IISs in this method development justified the analysis of RRFs for the determination of PAH concentration in water. Looking at the results of the initial data analysis, they showed that a addition of a third IIS, $^{13}C_{12}$- benzo[*ghi*]perylene, was needed for the accurate quantification of the higher molecular weight (HMW) PAHs.

There are benefits and pitfalls for the use of a single IIS for a group of similar PAHs. To determine the best IIS to use for a group of PAHs it is essential that an IIS has properties that are similar to the PAHs you want to analyze, and that they cover the mass range of the compounds being studied. Some other primary qualifications for the use of an IIS are that it must be stable, be available in pure form, have a compatible detector response, and a structure similar to the analytes being studied[65]. The main benefit obtained, using this single IIS, is that the accuracy and precision are improved when using the method. The

improvement to the results obtained is due to the fact that the IIS is used to compensate for the loss of an analyte in the preparation and injection part of the analysis. The IIS is of a known concentration and has gone through the same procedure as the analyte, giving an assurance to the results. The analyte concentration is determined when you divide the related responses; this eliminates errors that edge into the analysis when calculating results using this method. The main problem of using a single IIS for each PAH is that they are not available for all compounds studied; moreover, they can co-elute with the unlabelled targeted compound.

It is important to consider how the physical-chemical properties of the matrix (i.e., water), which affect the properties of PAHs and fibers in aqueous solution, impact the ability to employ SPME-based approaches to quantify PAHs in water. For example, pH can affect the coating of the fiber and affect the ability of the fiber to uptake PAHs from solution. pH can also affect PAH partition coefficients, particularly when other parameters such as humic acid, suspended solids or organic carbon are also variable and come into consideration. Ionic strength can also affect the ability to quantify PAHs in aqueous solution. The salting out effect of ionic compounds can cause SPME fibers to increase the amount of analyte taken up into or onto the fiber. This salting out effect can also be a major factor in the analysis of PAHs from water samples. Although the results presented herein failed to show that pH and ionic strength affect the quantification of PAHs in water, the overall effect of these two parameters has been observed in other studies[68,71]. Suspended solids, humic acids, and organic

carbon can also affect the uptake of PAHs from solution[72–75]. These agents can bind PAHs and exclude them from the aqueous matrix via π bonding with humic acids[76], adsorption onto the surface or absorption into the matrix of suspended solids[72,77], and interactions between PAHs and the micropores on the organic carbon matrix[78]. Each of the aforementioned parameters of an aqueous matrix can influence the analysis of PAHs in water[79]. These relevant studies will be outlined below.

4.3.1 pH and Ionic Strength

The pH of the studied water samples was examined in the context of the natural range of water pH (i.e., 4.5-9.0). Peak area counts of PAHs showed consistency across the whole pH range studied for all PAHs; RRF values were consistent throughout the entire range of pH values studied for both the PDMS and the PDMS/DVB fibers. Thus, the results indicated that there is little impact of natural water pH range on RRFs. There are however, contradictory ideas on the effect of pH on the uptake of PAHs from water by extraction fibers. Nevertheless, the results described herein are consistent with studies that showed that the effect of pH on the uptake of PAHs from water depends on the fiber used for analysis. As seen with the MIL-53(Al) fiber, PAH uptake has been shown to be barely affected by pH [80], whereas the 100μm PDMS fiber is affected by pH.[81,82] The differences in the observed effects of pH are most likely related to the stability of the SPME coating. With the stability of the coating compromised, the adsorption processes can be adversely affected leading to decreased extraction efficiency and

fiber life. With the PDMS fibers, pH has been shown to decrease the absorption of PAHs into the fiber coating[71].

The ionic strength of solution, expressed as percentage of salt (i.e., 0.1 to 10% w/v), impacted the results obtained and show that ionic strength of the solution affects the uptake of PAHs onto the fiber, and is totally dependent on the fiber. The HMW PAHs are affected by the addition of salt, the addition of salt decreases the extraction of HMW PAHs, reducing PAH solubility in the aqueous sample. The PAHs are pushed to the water/headspace interface (i.e., oil effect), and this has a limiting effect on PAH interactions with the immersed fiber.[83] The results presented herein indicate that the ionic strength of water solutions enhances the uptake of PAHs into/onto the PDMS fiber. Research shows that for the 65 µm PDMS/DVB fiber the exact opposite effect was observed (i.e., hindering PAH uptake via adsorption) by taking up fiber binding sites where PAH adsorption occurs[61,84]. Those effects are, however, quite minor. When examining the RRF values for both fibers, it can be seen that they remain quite consistent with very little deviation in the RRF value across the ionic strength range studied. This data shows that although ionic strength can affect the uptake of PAHs from solution, and can promote or hinder the adsorption or absorption from solution, it does not affect the resulting RRFs.

Referring to the results presented in Tables 3-9 to 3-16 (section 3.2.1), the data indicates that these two parameters (i.e., pH and ionic strength) do not appear to have a noticeable effect on the RRFs over the tested concentration range. More specifically, as the ionic strength or pH changes, there is little impact on the

uptake of the PAH onto the fibers. This likely indicates that the competition for active sites on the fiber is not adversely impacted by increasing salt concentration. Similarly, pH does not appear to affect the adsorption process significantly. Between pH values of 2 and 8, the uptake differences were minimal, presumably because the PAHs are stable and chemically inert.

4.3.2 Suspended Solids

Suspended solids can affect the concentration of PAHs dissolved in solution by either adsorption or absorption.[82] A few test methods were initially examined to determine if a linear range of suspended solids could be tested. When performing these tests the results quickly revealed that by directly adding the dust into a sample of water, the resulting data were not useful. For our analysis the concentration of suspended dust could not be determined because only a fraction of the initial amount of dust was suspended in the water. A way had to be found to circumvent the problem, so an initial solution was prepared (section 2.6.3) and diluted for analysis. Although the exact concentration of suspended solid was not known, the results showed that the amount of suspended solids present in the solution affected the amount of dissolved PAHs. The suspended particulate matter had a different effect on each class of PAH (i.e., low molecular weight (LMW), HMW, and mid-range molecular weight PAHs). However, the effect on LWM PAHs differed from the effect on HMW PAHs. The heaviest PAHs were absorbed/adsorbed onto the suspended solids, and could only be determined in solutions containing very low concentrations of suspended solids. The mid-range PAHs, such as pyrene, chrysene, and benzo[*a*]pyrene were not absorbed/adsorbed

as extensively as explained by work done by Patrolecco et al. [85]. This showed that the analysis HMW PAH in solutions containing amounts of suspended solids of a concentration above the range, as discussed in section 3.2.3, is possible. The concentration of the suspended solids has to be low enough so as to not affect the HMW PAHs in solution. The concentration of the lightest PAHs can be determined at higher levels of suspended solids as seen in the results in section 3.2.3. These results are consistent with the work performed by Rügner et al. [86], which indicated that the effects of suspended solid concentration vary across PAHs analyzed. However, when one looks at the RRF values determined herein, for both fibers investigated, it can be seen that the values are consistent at 27x and higher dilution levels for the 30 μm PDMS fiber, and 9x and higher dilution levels for the 65 μm PDMS/DVB fiber. It was also observed that for the 65 μm PDMS/DVB fiber, the RRFs of LMW PAHs are less sensitive to changes in suspended solid concentration, which was also seen in the work done by Rügner et al[86].

The results obtained show that RRFs are consistent if the suspended solid concentrations are relatively low. The effect of high concentrations of suspended solids affecting PAH concentration is consistent with the work done by Countway et al.[87] The property of suspended solids in solution that can affect the uptake, transport, and release of PAHs has been investigated[85,88], and the results indicate that analysis of PAHs in waters with high levels of suspended solids is impractical. Suspended solids affect the concentration of PAHs within solution whereby fine particles can become PAH enriched, affecting the concentration of

PAH in the aqueous phase. The literature research shows that an increase in temperature of around 20°C can increase the desorption of PAHs from suspended solids. Thus, an increase in extraction temperature from 50°C to 60°C or even 50°C to 70°C could enhance the adsorption of suspended solids.[72,77] Due to their hydrophobic nature, HMW PAHs in solution are generally more attached to suspended solids, and hence adsorbed onto the surfaces of the dust particles within the water solutions. In other words, the dust can act as an adsorptive material and temporarily binds the PAHs in the solution. The PAHs can later be released back into solution over time, or locked into sedimented material where they can be degraded over an extended period.

4.3.3 Humic Acid

Humic acid was chosen to represent natural organic matter in water. At the time of this study there was some research that showed the effect of humic acid on SPME uptake of PAHs from the water[82]. Humic acids can promote the dissolution of LMW PAHs into aqueous solution, but they usually hinder the dissolution of HMW PAHs; moreover, humic acids can compete with HMW PAHs for binding sites on the SPME fibers as seen in the work done by de Perre et al.[89] where humic acids can be seen to affect PAH uptake by the fiber. However, the results in this study were not affected by the fiber used in the analysis, and consistent RRFs for all PAHs were observed. These results support the findings of others who have examined similar scenarios; such as the work done by Chiou et al.[90]. Concerning the current study, the results show that humic acid affects the uptake of PAHs from water. More specifically, the consistent

results obtained in this study verify that the method is suitable for waters that contain humic acid. The results show that when the humic acid levels are low enough within solution, the resulting data obtained are acceptable. Humic acid likely affects the concentration of PAHs in water since PAHs are nonpolar aromatic compounds and are capable of interaction with the π electrons in the aromatic portion of humic acids[76]. These π electrons affect the bonding by being attracted to the bonds contained within the humic substances themselves[64,90]. Since LMW PAHs have a proportionally lower number of π electrons they are desorbed more easily than HMW PAHs, and thus more likely to be dissolved in the aqueous phase.[76] It was also stated in the literature that the aliphatic section of humic acids could also act as a binding site for PAHs.[76]

4.3.4 Hemoglobin

Hemoglobin was chosen to represent organic carbon of biological origin. The uptake of PAHs from water has been shown to be dependent on the type of biologically-derived organic material present in solution, as discussed in the work of Krüger et al. and Countway et al.[82,87]. The results obtained here indicate that absorption/adsorption on organic material such as hemoglobin can affect the RRFs values, with higher concentrations of hemoglobin showing a tendency to retain PAHs. More specifically, increased concentrations of hemoglobin prevented accurate calculation of RRFs for the PAHs in water, thereby preventing accurate PAH analysis. With respect to lower levels of hemoglobin, the RRFs are consistent and more usable for analysis. Overall, hemoglobin, and therefore organic matter of biological origin, should not affect determination of RRFs for

PAHs, as long as the concentrations are low. This result is consistent with the literature that examined the effect of this property of water, again as seen in the works of Krüger et al. and Countway et al .[82,87].

4.3.5 Combined water parameters at pH 5.5 or 7.5

To obtain a better overall picture as to what will happen to results when real water samples are used, the four parameters, namely pH, ionic strength, humic acid, and biological organic carbon were examined as a mixture. This was done by combining all of the parameters into one solution, and by keeping the pH constant at either 5.5 or 7.5. Suspended solids were not included in the mixture because of the dramatic effect on the level of dissolved PAHs, relative to the other parameters examined (i.e., severe impact on the ability to accurately determine RRFs). The parent solutions that were created were at the extreme end of the concentrations that would likely be found naturally. Nevertheless, the dilutions permitted the preparation of solutions that mimic natural waters that exist in the environment. Another consideration before the analysis of multiple parameters was to add a third isotopically labeled standard (IIS). This IIS was chosen to improve the precision of RRFs for the three HMW PAHs.

At this point, there is no literature that examined RRFs in such a comprehensive manner, and this examination is the first of its kind. The RRFs of PAHs can be affected to some extent by certain water parameters, but as long as the parameter is in low concentrations, it will not affect the uptake of PAHs by the fiber in a significant way. Thus RRFs allow for determination of PAHs in typical

water samples as long as the IIS is similar to the examined analytes (i.e., ring structure, molecular weight, and other properties).

In summary, three IISs were used to examine how water parameters affect RRF values of PAHs. Suspended solids, humic acid and organic carbon of biological origin (i.e., hemoglobin) affect the RRF values, but pH and ionic strength do not impact RRFs. The results also show that even if a parameter does affect the RRF values, the impact of that parameter could be greatly reduced as demonstrated by the relatively constant RRFs in diluted water solutions; approximately 10 times dilution for the 65 μm PDMS/DVB fiber and 27 times dilution for the 30 μm PDMS fiber from the concentrated parent solution. When a combination of the four water parameters is examined, such a dilution depended effect can also be seen. Therefore, when the concentration levels of these water parameters are elevated, it can affect the consistency of the RRF values, and hence the ability to measure PAH concentrations in water. Thus, analysis of PAHs using RRFs can be best performed when these parameters are in low concentrations. With the dilutions done to the parent solution that mimics natural waters, the RRF calculation for PAHs should work on a broad range of natural waters. RSD values were less than 40% and are adequate, so the determination of RRFs, and hence the calculation of PAH concentration, can be performed in natural water samples.

The use of two different IISs, one for LMW PAHs and one for HMW PAHs was usable for RRF calculation for all PAHs except for the last eluting PAHs that have the highest molecular weights. In general, acenapthene-d_{10} can

serve as a good IIS for naphthalene, acenaphthylene, acenaphthene, and fluorene, providing reproducible RRFs with a range of RSD at ~13.0 to 75. There are some issues with phenanthrene and anthracene, which give higher RSDs because the structural similarities start to deviate from acenaphthene-d_{10}. Chrysene-d_{12} is a good choice of IIS for pyrene, fluoranthene, chrysene, benzo[*a*]anthracene, benzo[*a*]pyrene and benzo[*b*]fluoranthene, but not as good for indeno[*1,2,3 cd*]pyrene, dibenz[*a,h*]anthracene and benzo[*ghi*]perylene. The RSDs of indeno[*1,2,3 cd*]pyrene, dibenz[*a,h*]anthracene and benzo[*ghi*]perylene were also well out of RSD range (RSD > 40) with RSDs at 10 to 74%. The inclusion of a third IIS, $^{13}C_{12}$- benzo[*ghi*]perylene, for the three last eluting PAHs (i.e., indeno[*1,2,3 cd*]pyrene, di- benzo[*a,h*]anthracene and benzo[*ghi*]perylene), significantly improved reproducibility of RRFs for these three PAHs. It is therefore concluded that use of three IISs would be a good choice for the quantitative determination of all 15 target PAHs; this is a significant reduction in the IISs that are currently used for the SPME GC/MS analysis of PAHs.

4.4 Analyses of Natural Water Samples

Three types of natural water were analyzed. The results demonstrated that the SPME-GC/MS method using RRFs could be used to detect PAHs in various types of water. Large variations observed in the results are largely due to the fact that PAHs are present at low levels in natural water in general, as seen in the research by Zuazagoitia et al. where such variations also occured[69]. The results obtained when using the standard addition, when analyzing data, for each set of samples showed similar recoveries of PAH that are similar to the work of

Zuazagoitia et al. The variations of three PAHs that have their corresponding IISs (i.e., acenaphthene, chrysene, and benzo[*ghi*]perylene) had similar variations as other PAHs whose RRFs are calculated against one of the three IISs. The other important observation is that the values for PAHs in natural water are close to the "average" and "slope" calculation method. This indicated that only one calculation method is necessary for the calculation of PAH levels in water.

To study the effect of RRFs on surface water, river water was obtained from 5 different locations along the Ottawa River. The locations were chosen to show the variability of RRFs as they are affected by the different conditions presented by each site. The levels of PAHs in Ottawa river are similar to values observed in the works by Cheng et al., Zhu et al. and Planas et al., which also examined PAHs in river waters[88,91,92]

4.5 Influence of the physical-chemical and chromatographical properties on the analysis of PAHs and the utility of the SPME approach.

The properties examined in this study are relevant to the SPME analysis of PAHs in water. Vapor pressure is an essential aspect of how much of a PAH moves from the substrate to the air contained within the vial. The boiling point is important as it determines what temperature would be needed to vaporize or change the PAH into a gaseous state. The K_{ow} (i.e., octanol/water coefficient) is a critical parameter as it reflects the ability for a PAH to diffuse from the water to the immersed SPME fiber. The K_{oa} (i.e., octanol air coefficient) determines the rate at which the PAHs diffuse from the air to the SPME fiber suspended inside the air portion of a vial. The results presented herein indicate a relationship to the

physical-chemical properties of PAHs [93]. GC retention times (RT) of PAHs were also examined to examine the relationship between the RT and the RRF. Every one of these properties is important to some aspect of SPME analysis, and by determining if there is a relationship between a particular property and the RRF, it could be used to predict RRF values of other PAHs in water.

When looking at the r^2 and their corresponding p values, the results obtained for each property showed a pattern between the RRF and the parameter examined which was unique to each particular PAH and it's RRF. The correlation is considered statistically significant if the corresponding p value is less than 0.05 ($p<0.05$). A single IIS was used to generate RRF values to examine the relationship between RRFs and properties of PAHs. Acenaphthene-d_{10} was chosen as this it is the only IIS used for initial injections on the instrumentation, upon which RRF values of PAHs under direct liquid injection were available. The RRF from a direct injection (RRF_{direct}) was initially compared to each of the properties of PAHs in the hopes that some correlation would be observed. The resulting coefficient of determination (r^2) values were between 0.60 and 0.66 for log vapor pressure ($r^2 = 0.63$), log K_{oa} ($r^2 = 0.60$) and the retention time ($r^2 = 0.66$). The other two parameters, boiling point, and log K_{ow} had lower r^2 values below 0.5. The correlations between physical-chemical properties and RRF were statistically significant ($p< 0.05$), except for log $K_{oa.}$ The correlation between the RRFs and a particular property of PAHs in spiked natural water samples was also examined. The results are summarized in Table 3-41 and Table 3-42. The results show that RRF from the 65 µm PDMS/DVB fiber had a downward slope with the physical-

chemical property value, for all properties except vapor pressure. The opposite trend was found for the 30 µm PDMS fiber, which had an upward trend of the regression line. RRFs from PDMS/DVB fiber also had a stronger correlation (i.e., larger r^2 value) than those from PDMS fiber in general. The tables for the initial water parameter show that 30 µm PDMS fiber is more likely to absorb heavier PAHs than the 65 µm PDMS/DVB fiber (Table 3-41 and Table 3-42). There is a trend with all of the RRF results for the PDMS/DVB fiber showing $p < 0.0001$, and there is a strong correlation between the RRF_{ratio} and the chosen properties of PAHs.

Use of RRF ratio ($RRF_{sample}/RRF_{direct}$) to correlate with properties minimizes the impact of GC/MS response to PAHs. By removing the differences in instrument response, the correlation improves (Table 3-41 and Table 3-42). The r^2 values in this case stay relatively consistent with the 65 µm PDMS/DVB fiber and show great improvement with the 30 µm PDMS fiber. All correlations between RRF_{ratio} and properties were statistically significant with p values below 0.001. The results indicate that RRFs of other PAHs that were not determined in this study may be estimated. As for the prediction, the PDMS/DVB fiber may produce better results than PDMS does, as the former has higher r^2 values and better p values. Therefore, physical properties and chromatographic behaviors of PAHs can be used at least to predict RRFs within the group of PAHs. It therefore needs to be determined whether or not the relationships between RRFs and physical and chromatographic properties of PAHs can be applied to other types of chemicals.

5 Chapter: Conclusion

Revisiting the hypothesis and objectives outlined in sections 1.5 and 1.6, the results indicate that use of an isotopically labeled standard (IIS) to calculate a relative response factor (RRF) of an analyte in a given matrix can be used for quantitative SPME GC/MS. Using this approach, PAHs in natural water were quantified in this study. Our study shows that use of three IISs is sufficient for the quantification of PAHs in water. The use of a single IIS alleviates the need for an IIS for every target PAH.

The objectives of this study were successfully fulfilled; the calculation of the amount of PAH in solution, using RRFs, with a single IIS for a group of PAHs was successful. The RRFs responded to changes in matrix parameters, under the optimized SPME conditions, and remained stable under the right conditions. The accuracy of employing RRFs in quantitative SPME-GC/MS analysis of PAHs in different waters was successfully evaluated. More specifically, the work examined accuracy of the results, repeatability of determined RRFs, and concentrations of PAHs in different types of natural waters. The objective to examine the relationships between RRFs and physical-chemical and chromographic properties of PAHs was also successfully fulfilled; when employing a ratio of RRFs ($RRF_{sample}/RRF_{direct}$) the regression values obtained all have an $r^2 > 0.6$. Using the RRF_{ratio} to determine of PAH concentrations is viable.

There are some limitations of the approach that employs a limited number of IISs in the SPME-GC/MS analysis of PAHs in water samples. One limitation is the impact of matrix effect on the consistency of RRFs when the water samples

contain high levels of suspended solids, humic acids or organic carbon; the consistency of RRFs can only be achieved by examining dilute water samples.

Relationships between RRFs and single (or possibly multiple) physical or chromatographic properties of PAHs and their behavior in water samples can be observed, especially when the relative response factors are presented in the form of an RRF ratio ($RRF_{sample}/RRF_{direct}$). The use of RRF ratios minimizes the impact of instrument responses, thus revealing a more robust relationship between the physical and chromatographic properties of PAHs and their behavior in the SPME process examined herein.

Use of RRFs in the calculation of aqueous PAH concentrations will likely increase since it can readily be applied to a wide range of source waters. Another reason that RRFs used in the calculation of aqueous PAH concentrations, via SPME/GC-MS, is the removal of high quantities of solvents in the analysis process. The application of this method to other contaminants is an obvious next step. Also, the use of this method to other matrices such a serum for the use in human biomonitoring would be an ideal starting point for applications related to PAHs and other toxic organic substances.

With the availability of this new method, which uses RRF for SPME-driven determination of PAHs in aqueous matrices, we hope that more research groups will employ this powerful analytical technique.

Appendices

A.1 Figures

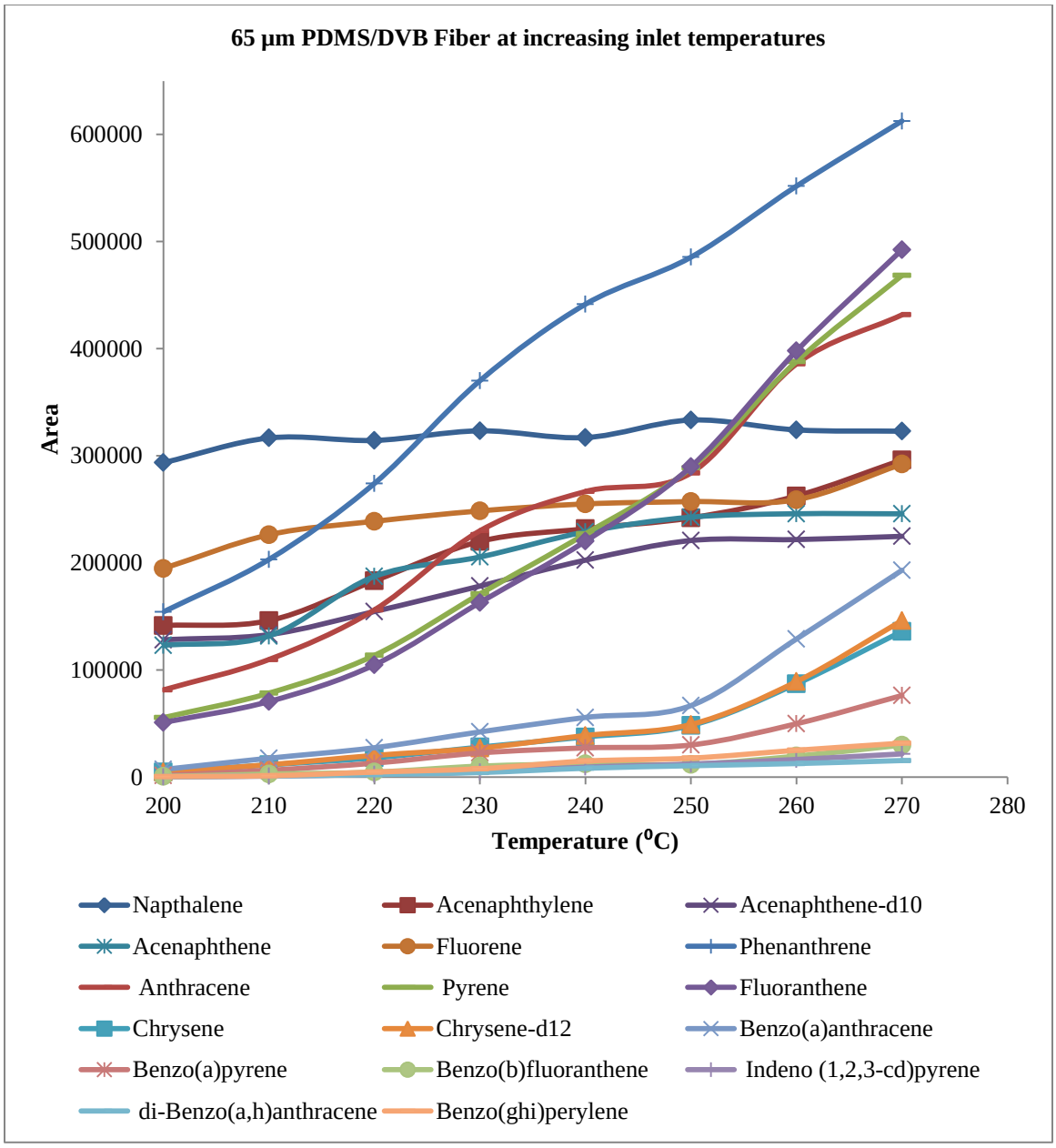

Figure 6 Area results of the increasing inlet desorption temperature for the PDMS/DVB fiber.

`

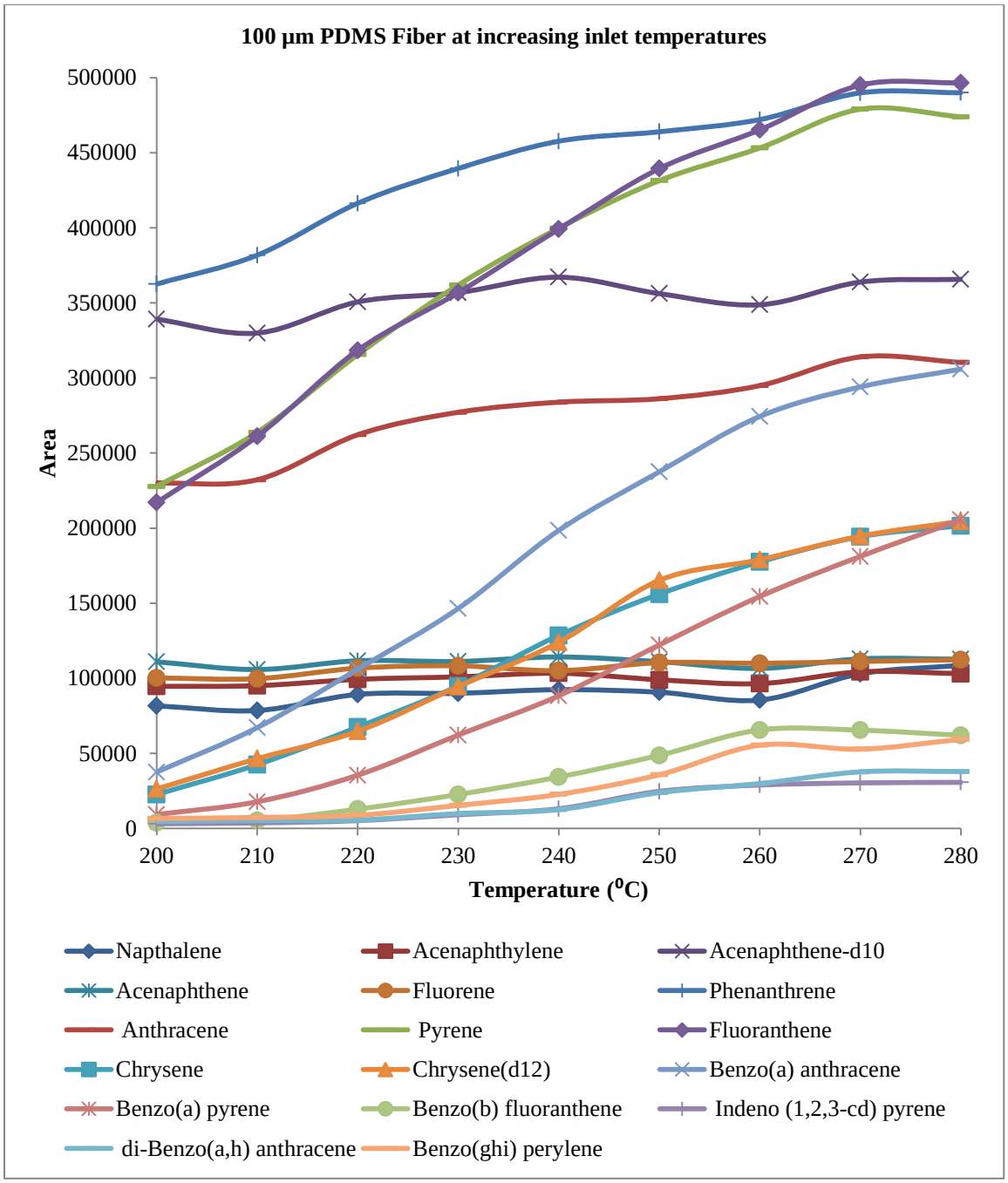

Figure 7 Area results of the increasing inlet desorption temperature for the 100 µm PDMS fiber.

`

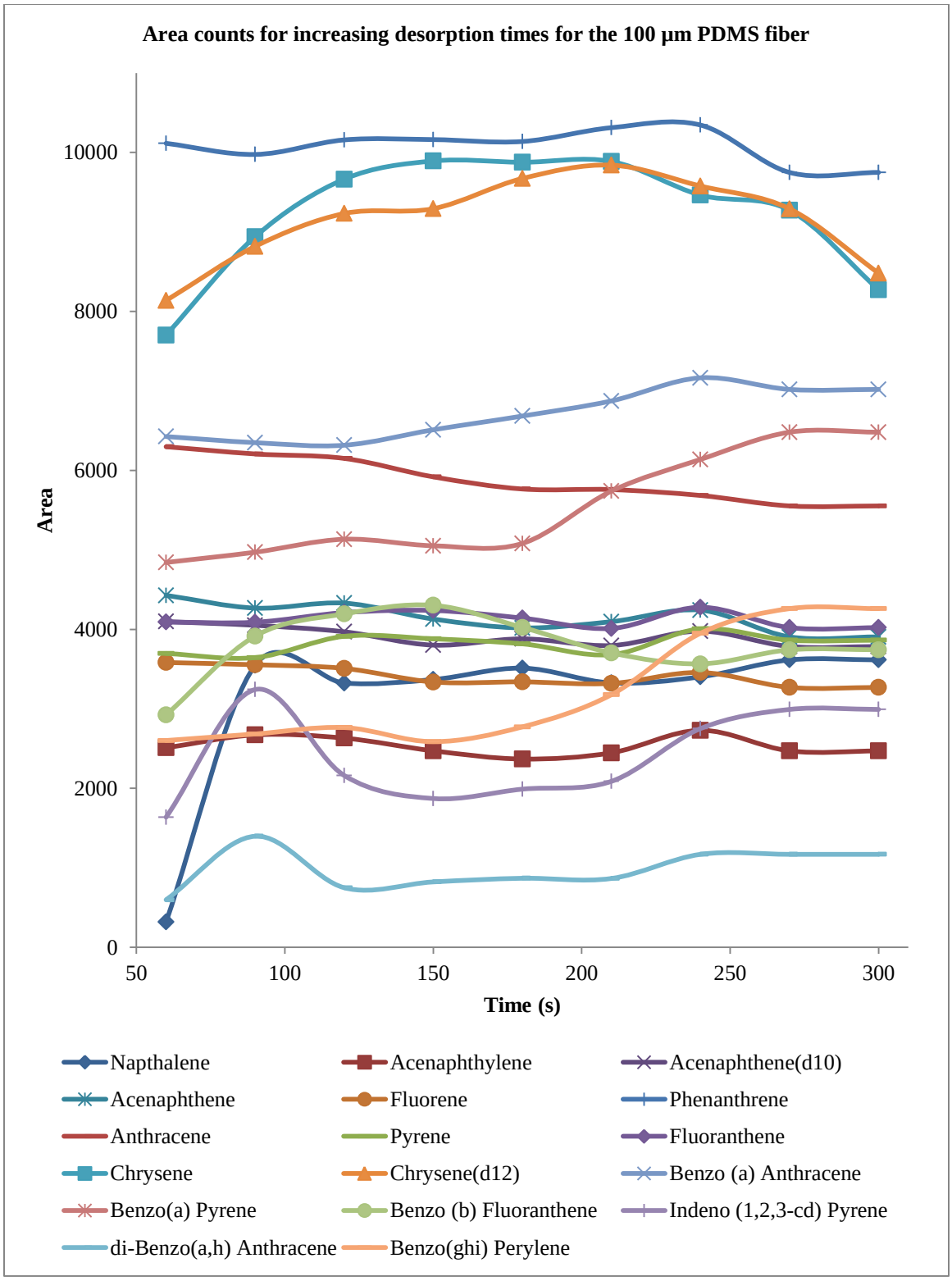

Figure 8 Amount detected for the 100 um PDMS fiber with increasing desorption times.

`

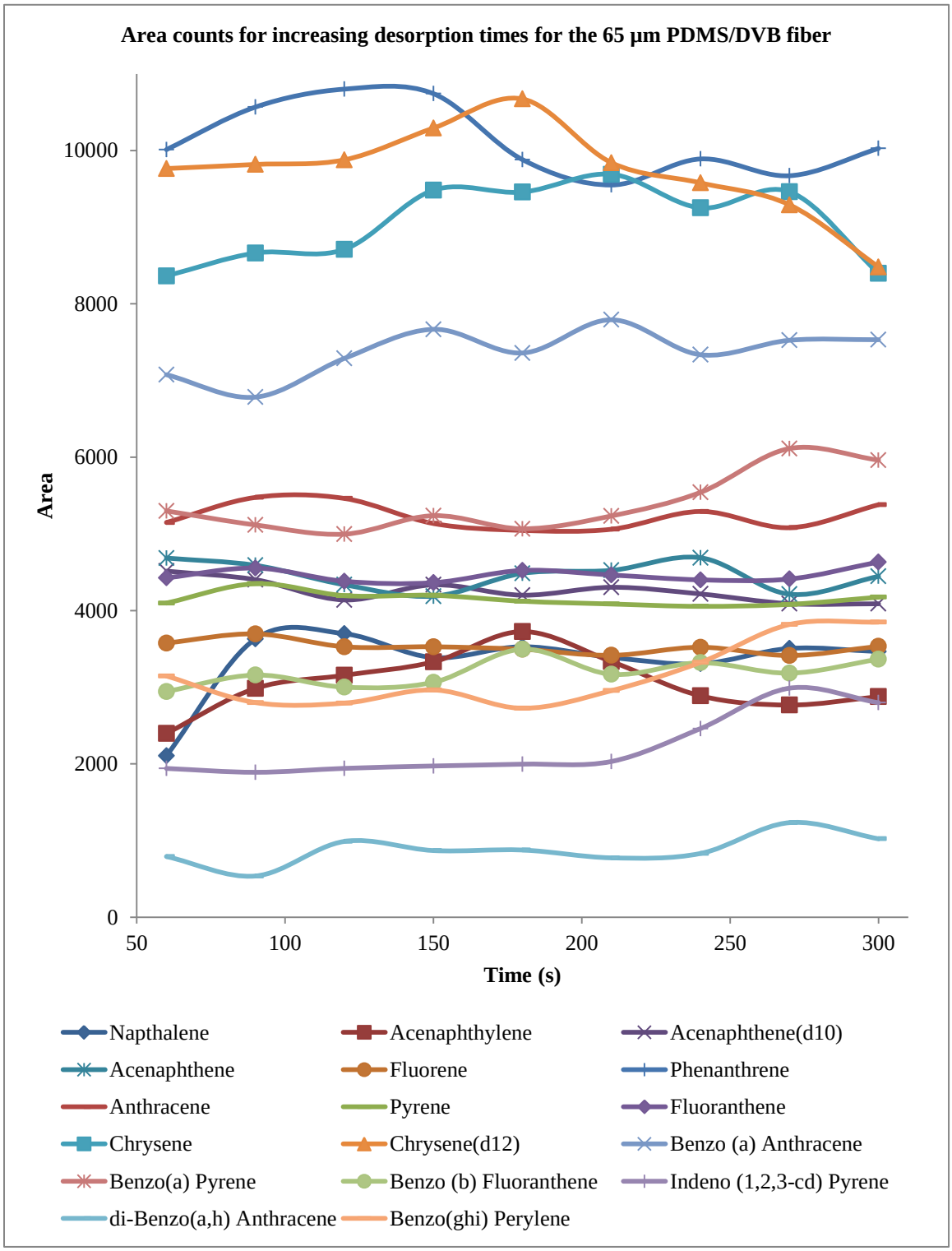

Figure 9 Amount detected for the 65 µm PDMS/DVB fiber for increasing desorption times.

`

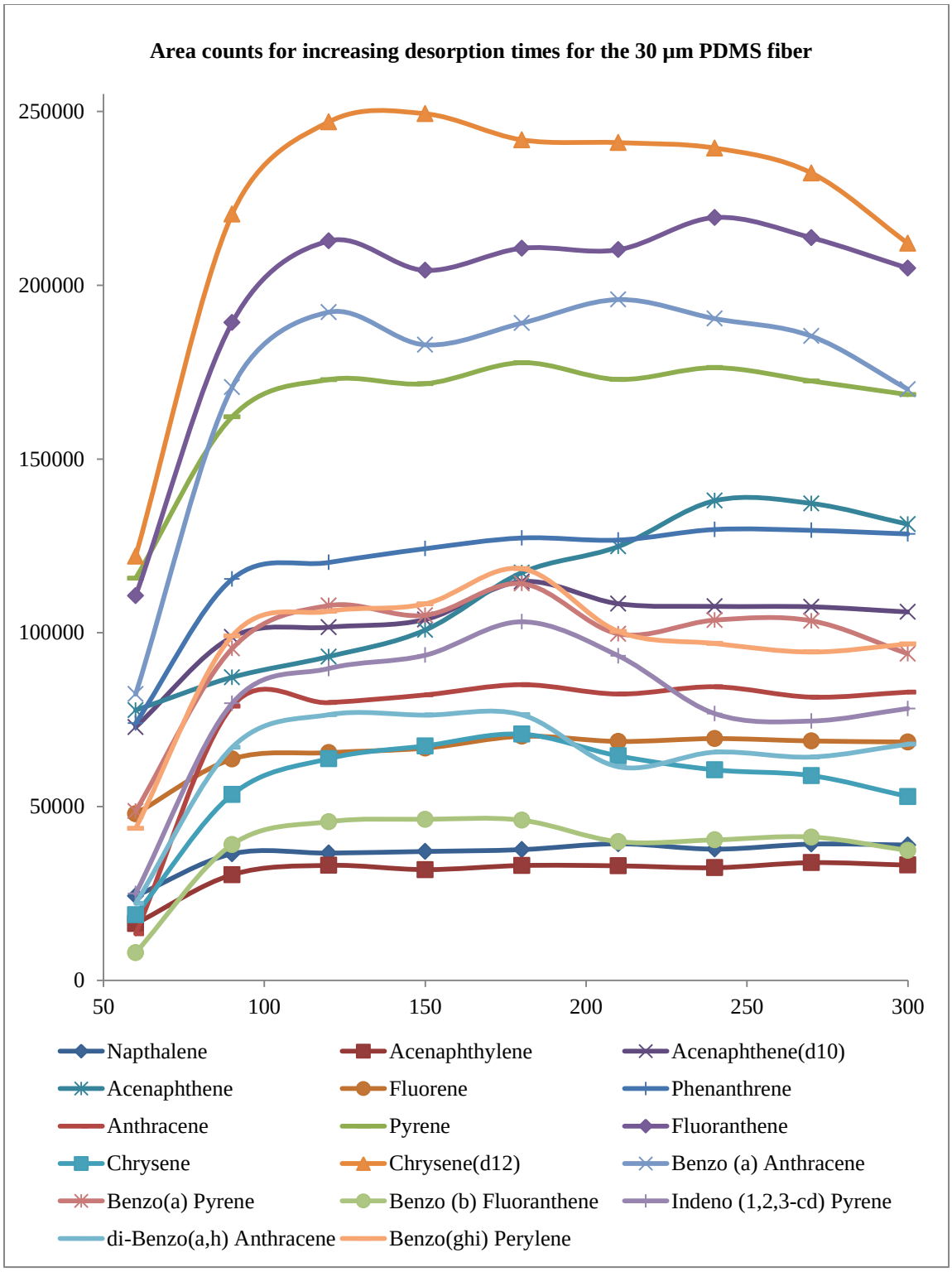

Figure 10 Amount detected for the 30 µm PDMS fiber for increasing desorption times.

`

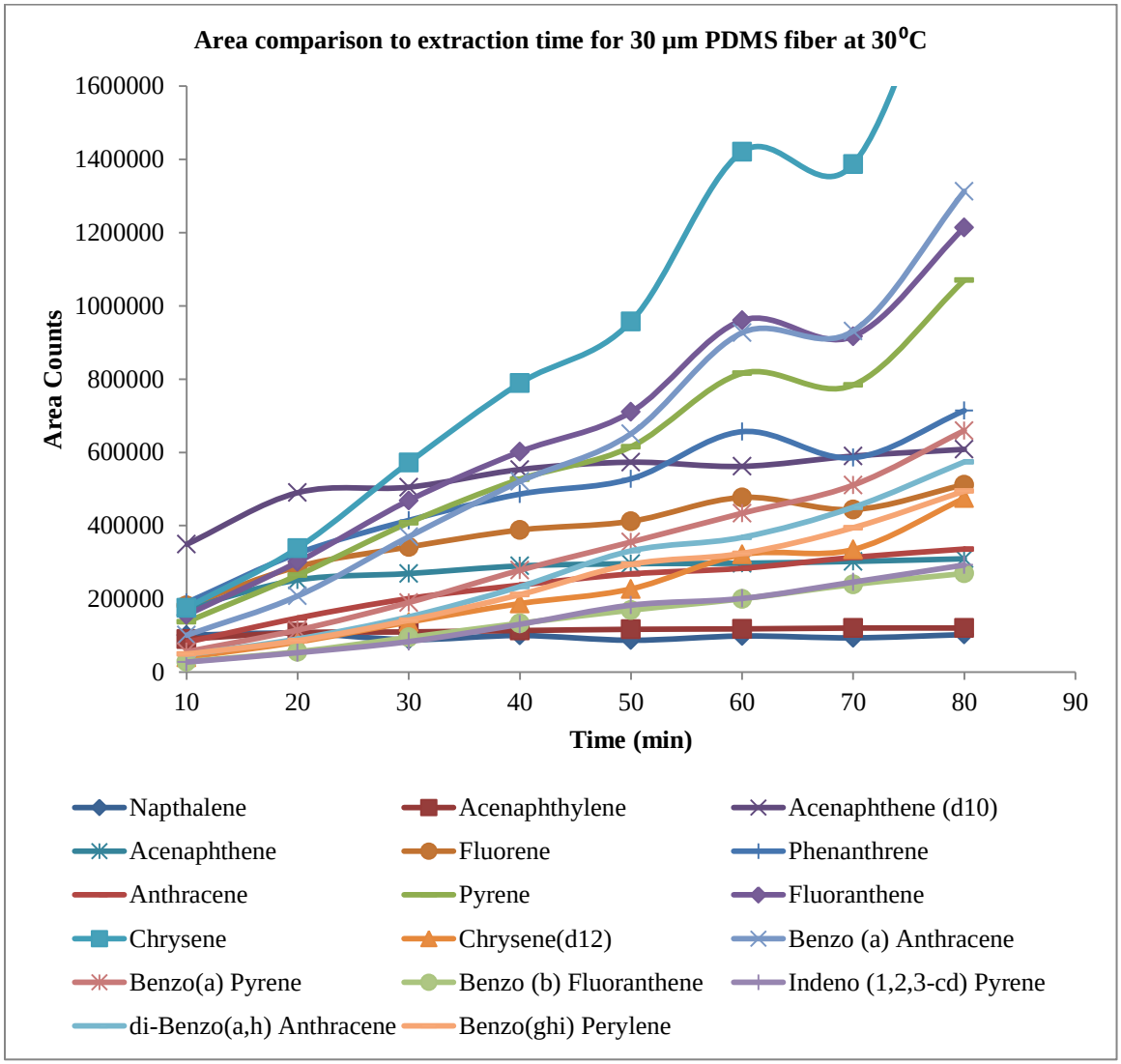

Figure 11 Area comparison to extraction time for 30 µm PDMS fiber at 30°C (10-80 minutes).

`

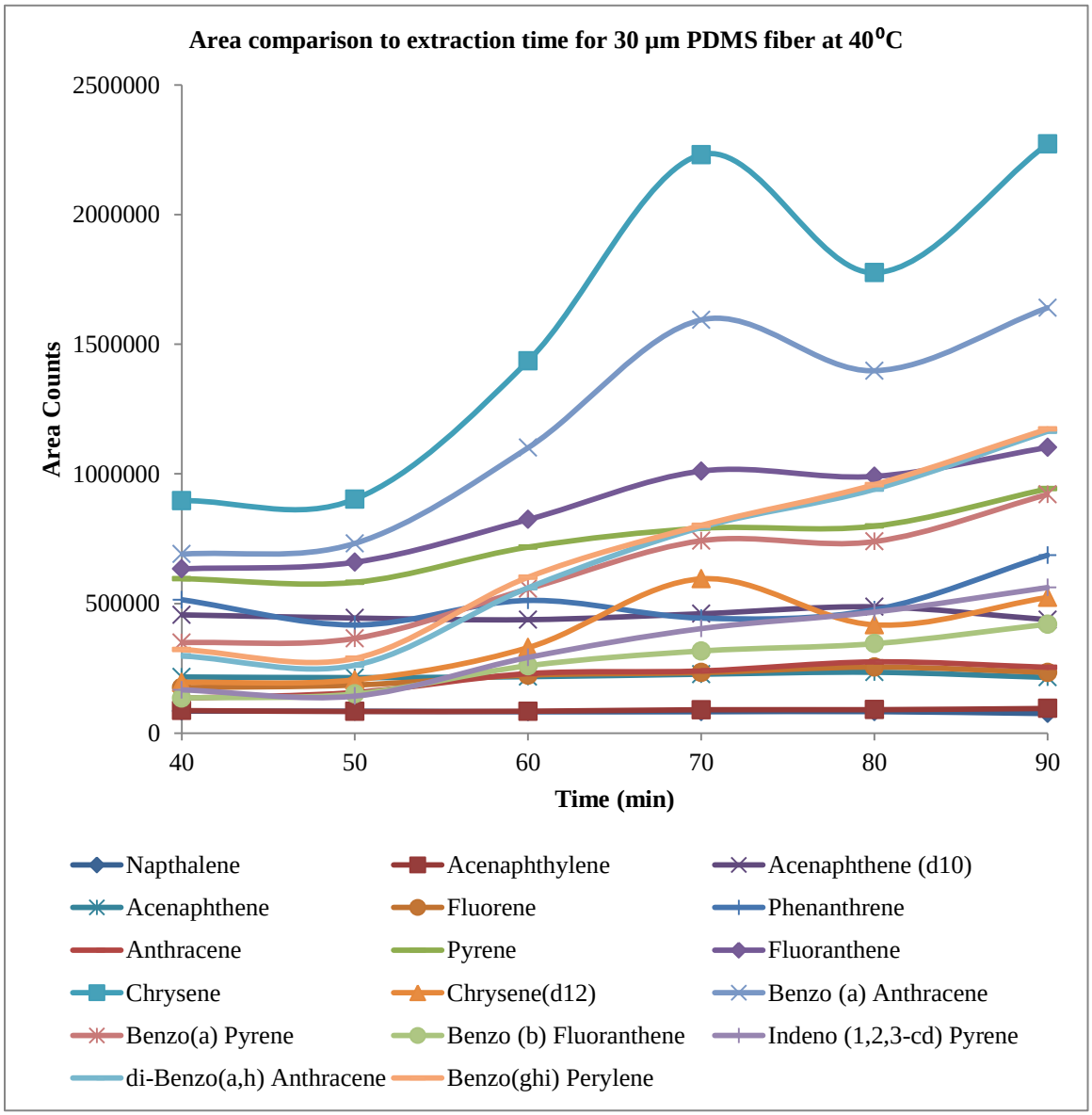

Figure 12 Area comparison to extraction time for 30 µm PDMS fiber at 40°C (40-90 minutes).

`

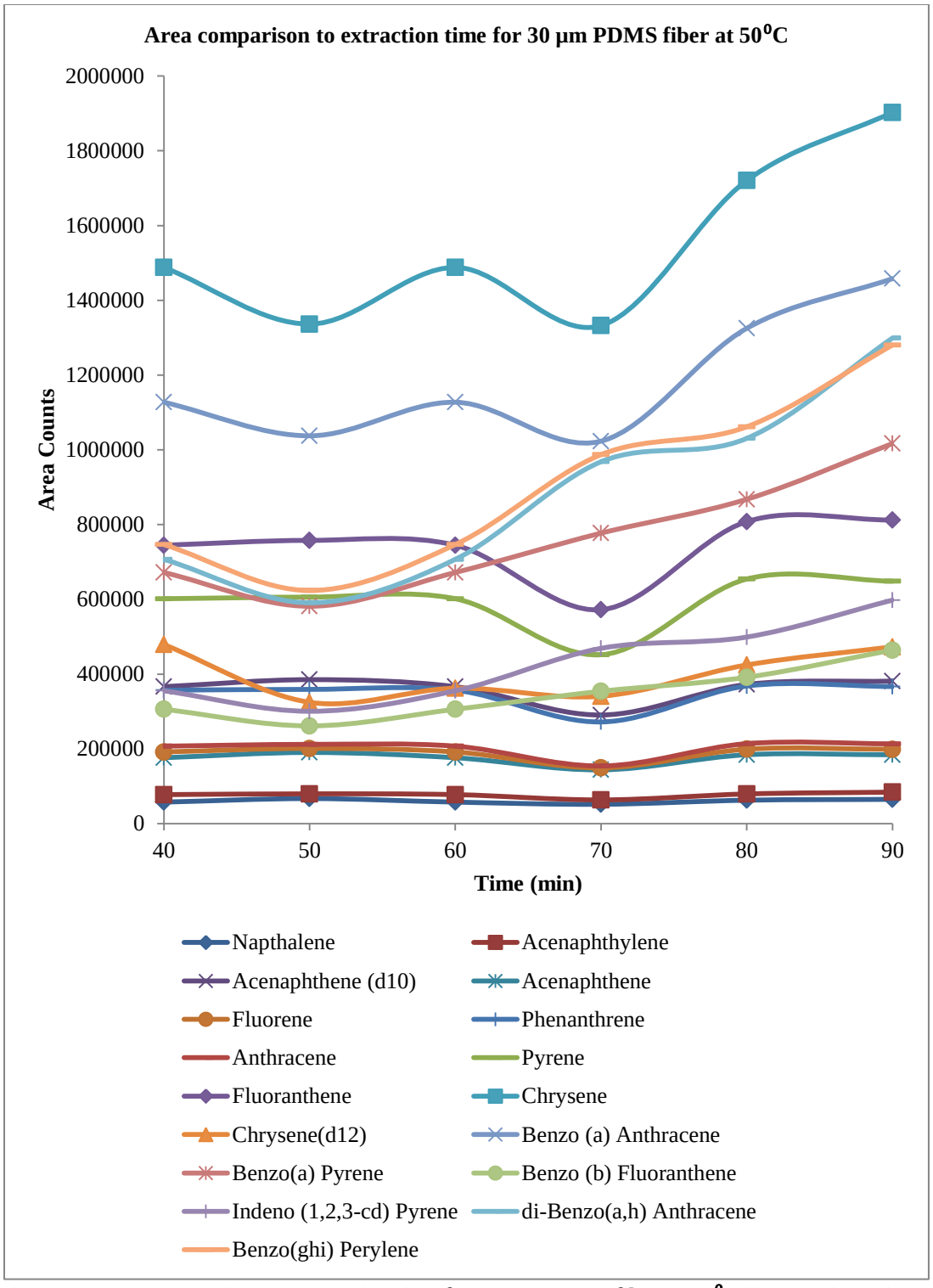

Figure 13 Area comparison to extraction time for 30 µm PDMS fiber at 50°C (40-90 minutes).

`

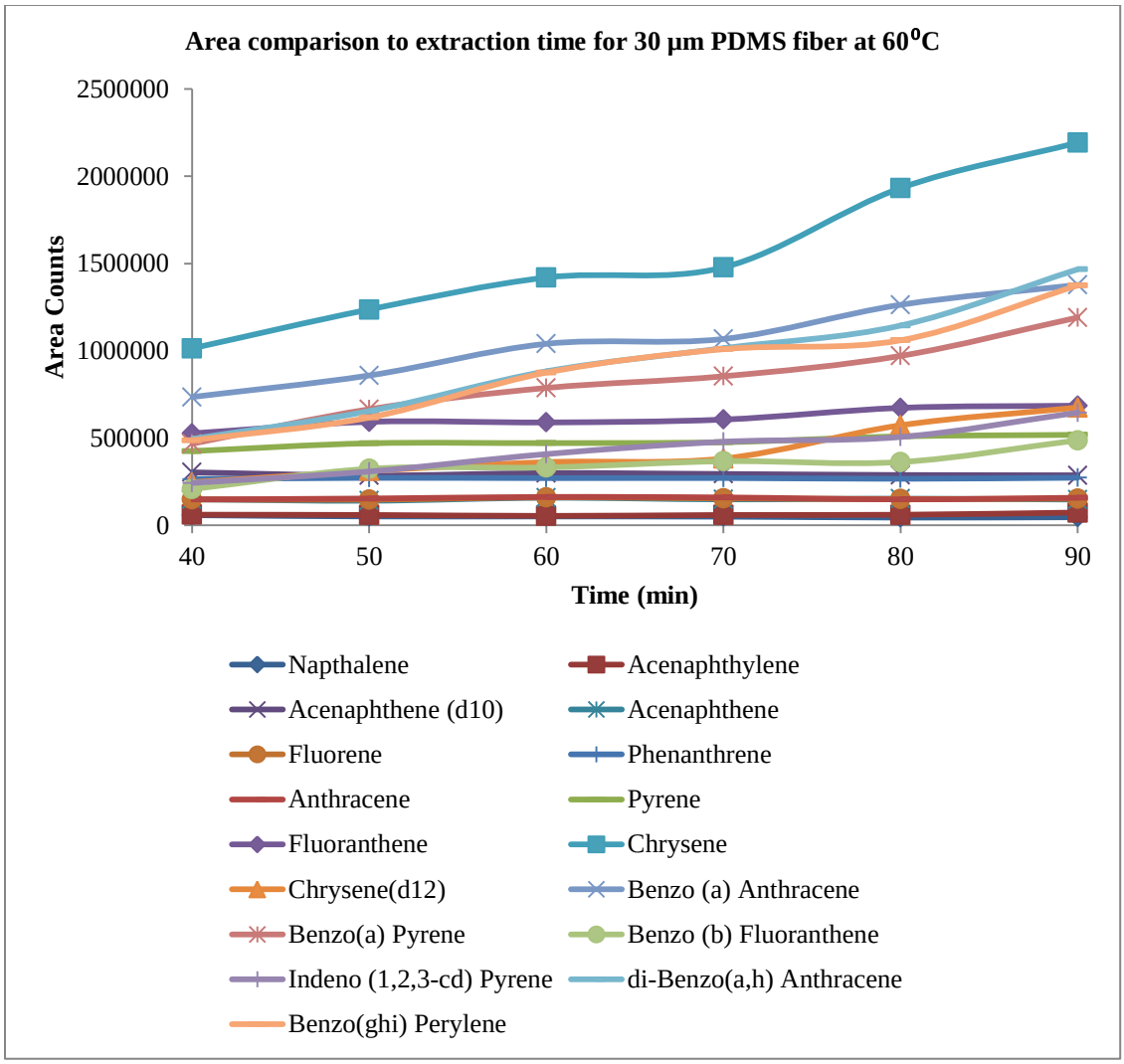

Figure 14 Area comparison to extraction time for 30 µm PDMS fiber at 60°C (40-90 minutes).

`

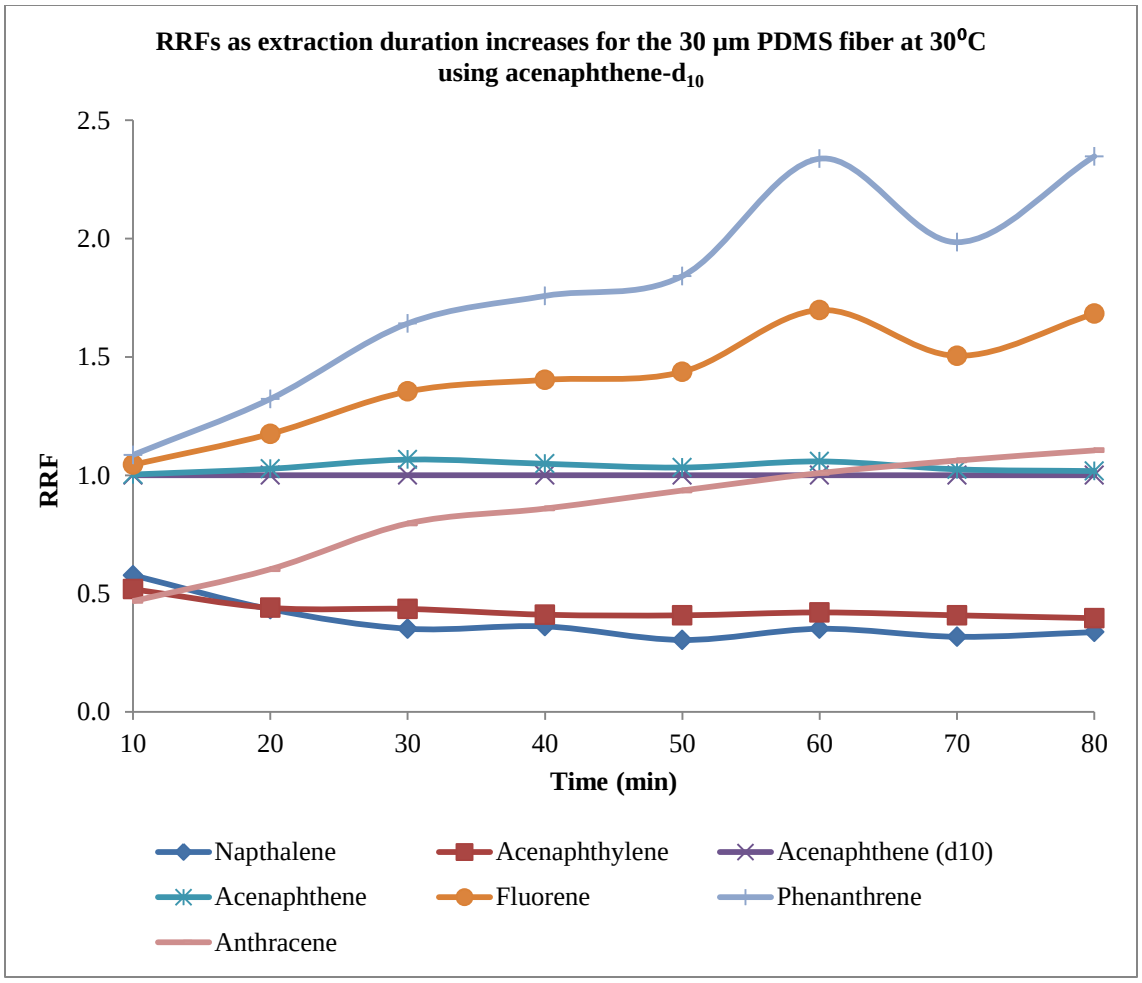

Figure 15 RRF values with respect to extraction times for 30 µm PDMS fiber at 30°C using acenaphthene-d_{10} for RRF calculation.

`

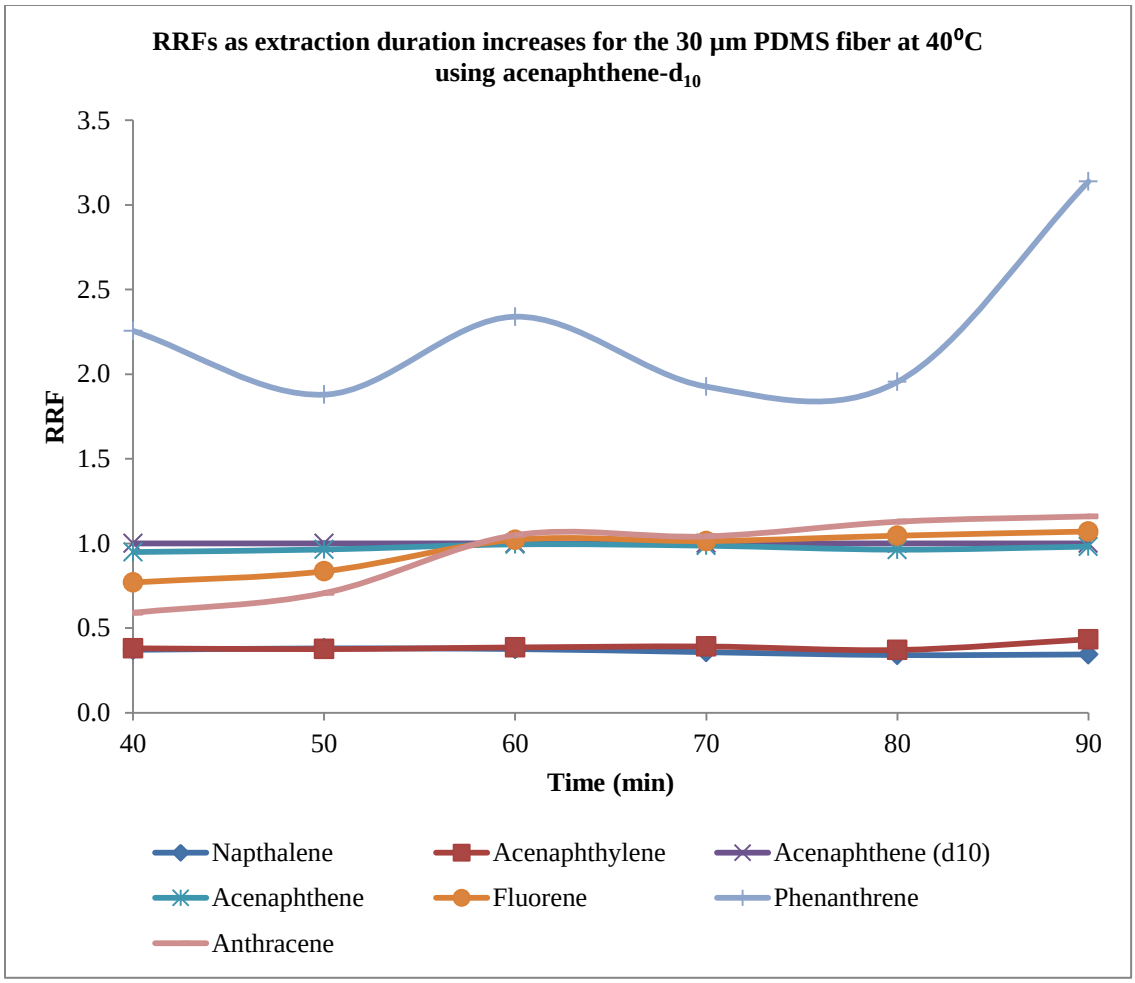

Figure 16 RRF values with respect to extraction times for 30 µm PDMS fiber at 40°C using acenaphthene-d_{10} for RRF calculation.

`

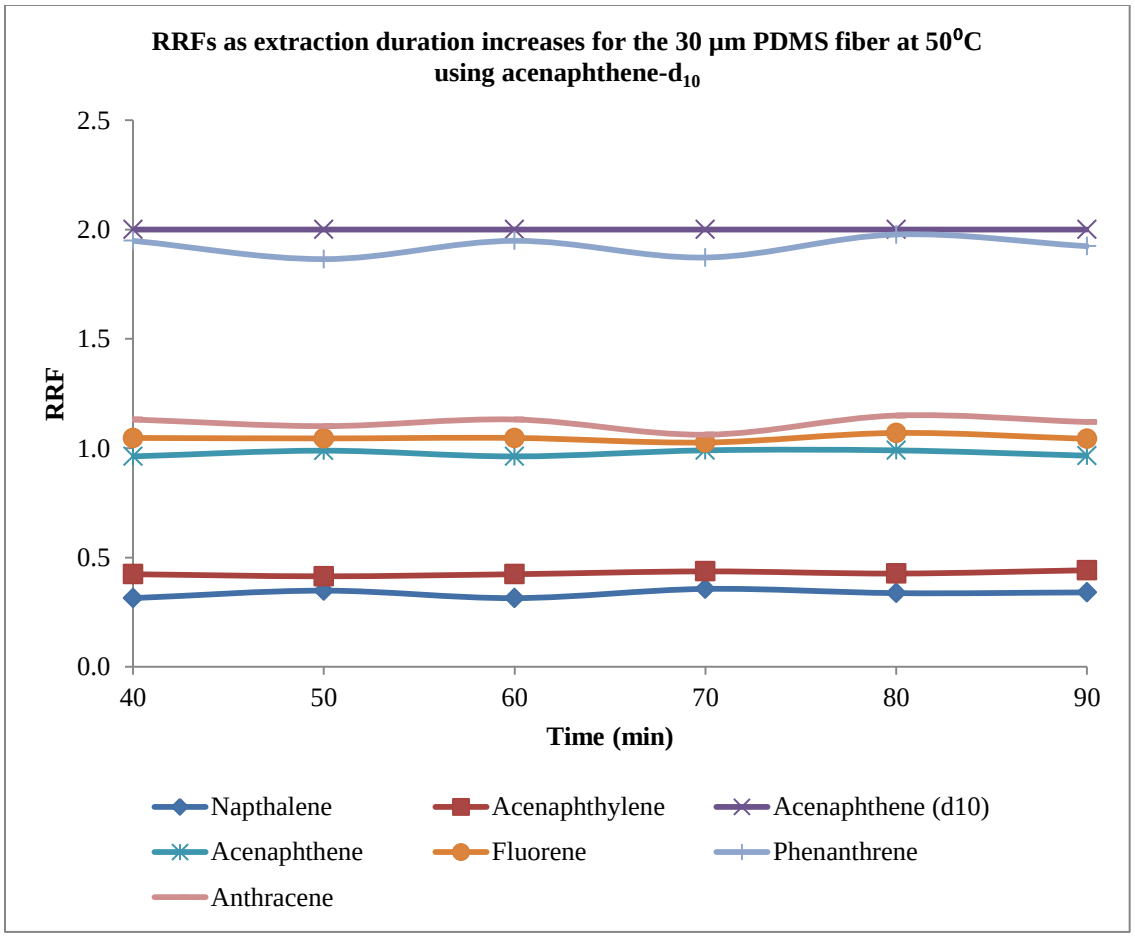

Figure 17 RRF values with respect to extraction times for 30 µm PDMS fiber at 50°C using acenaphthene-d_{10} for RRF calculation.

`

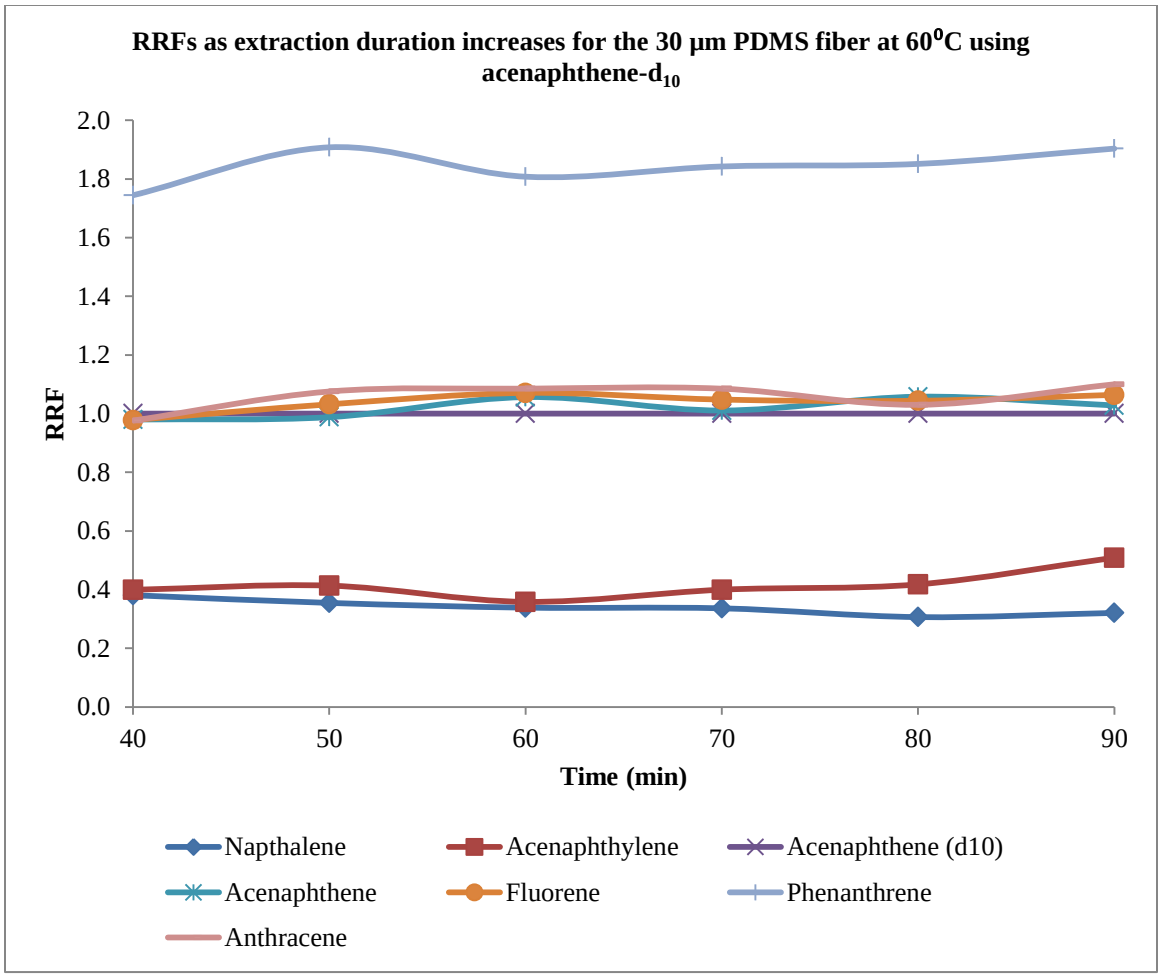

Figure 18 RRF values with respect to extraction times for 30 µm PDMS fiber at 60°C using acenaphthene-d_{10} for RRF calculation.

`

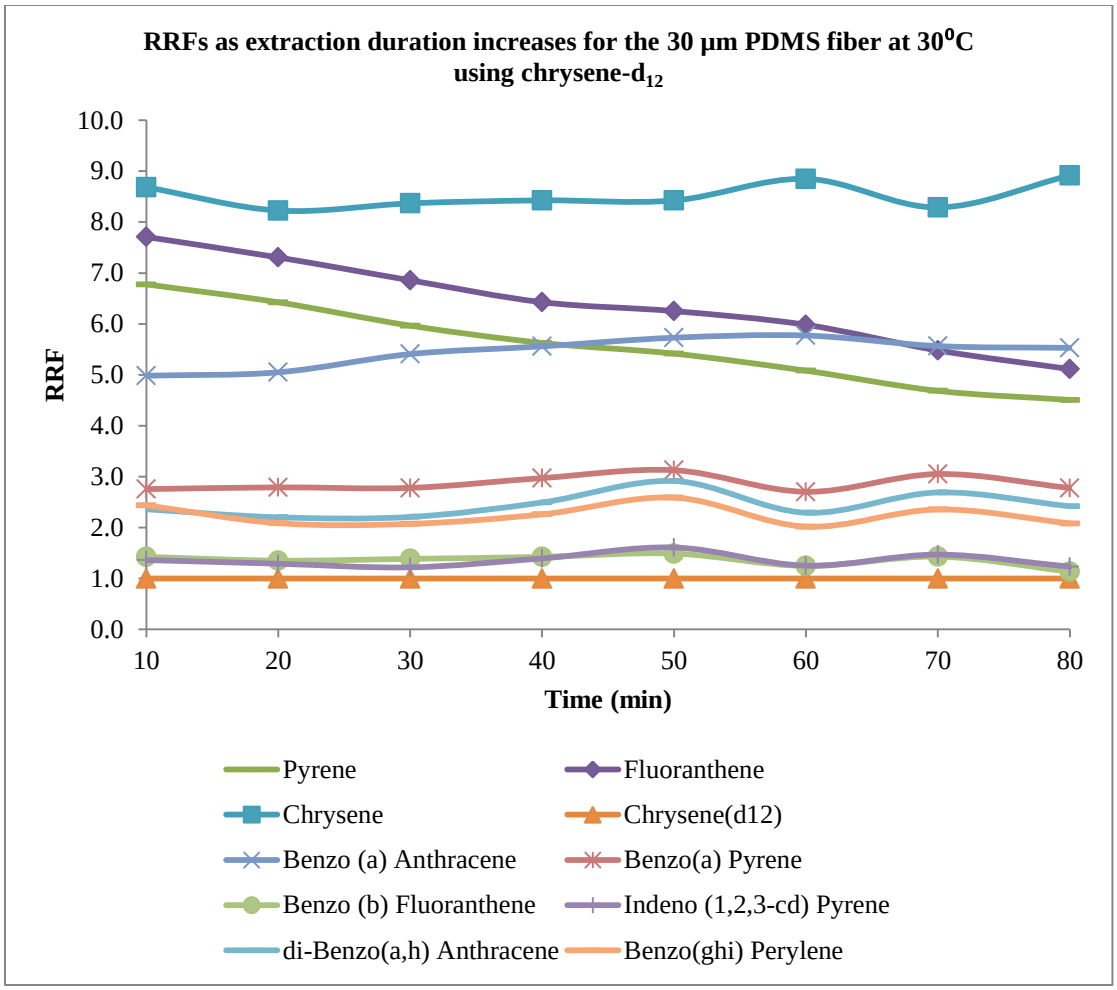

Figure 19 RRF values with respect to extraction times for 30 µm PDMS fiber at 30°C using chrysene-d_{12} for RRF calculation.

`

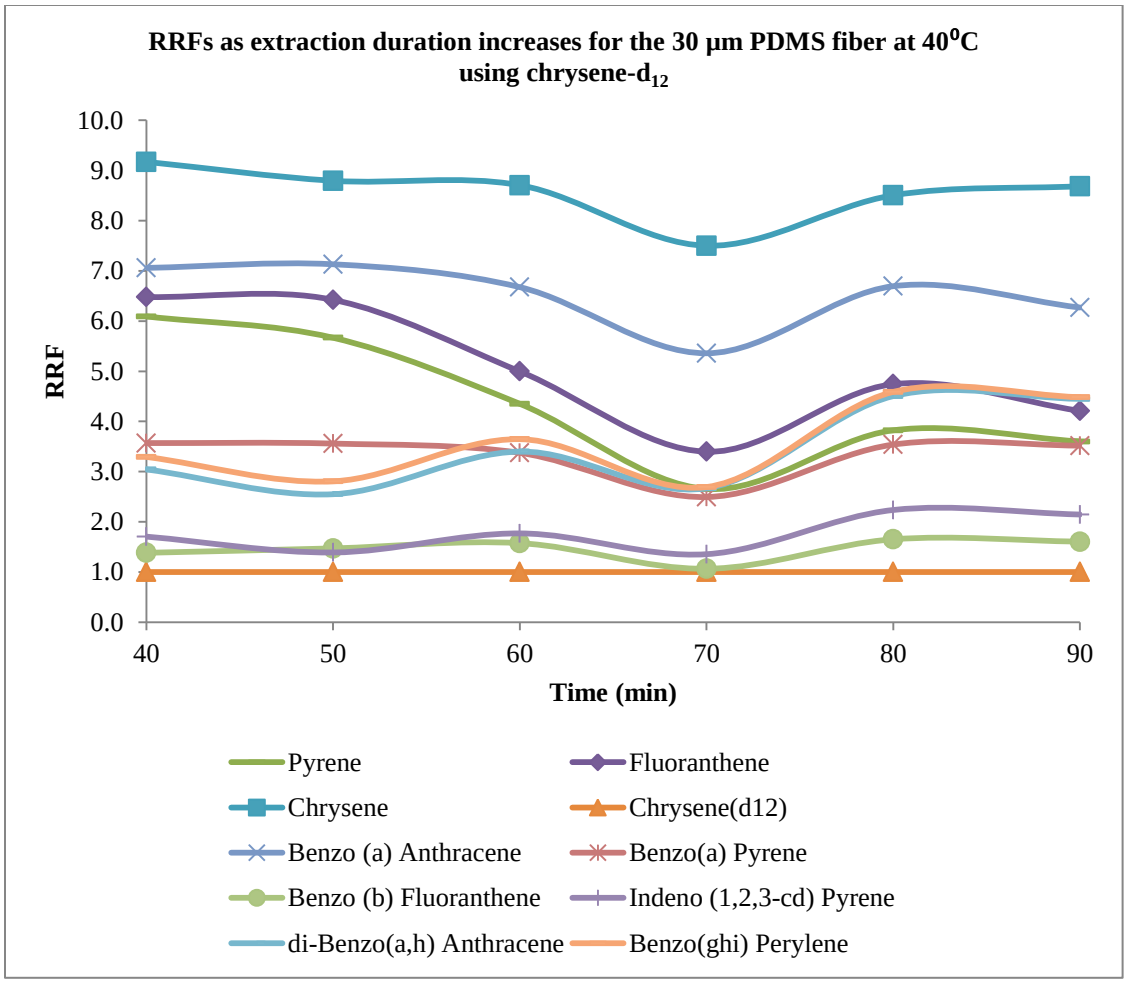

Figure 20 RRF values with respect to extraction times for 30 µm PDMS fiber at 40°C using chrysene-d_{12} for RRF calculation.

`

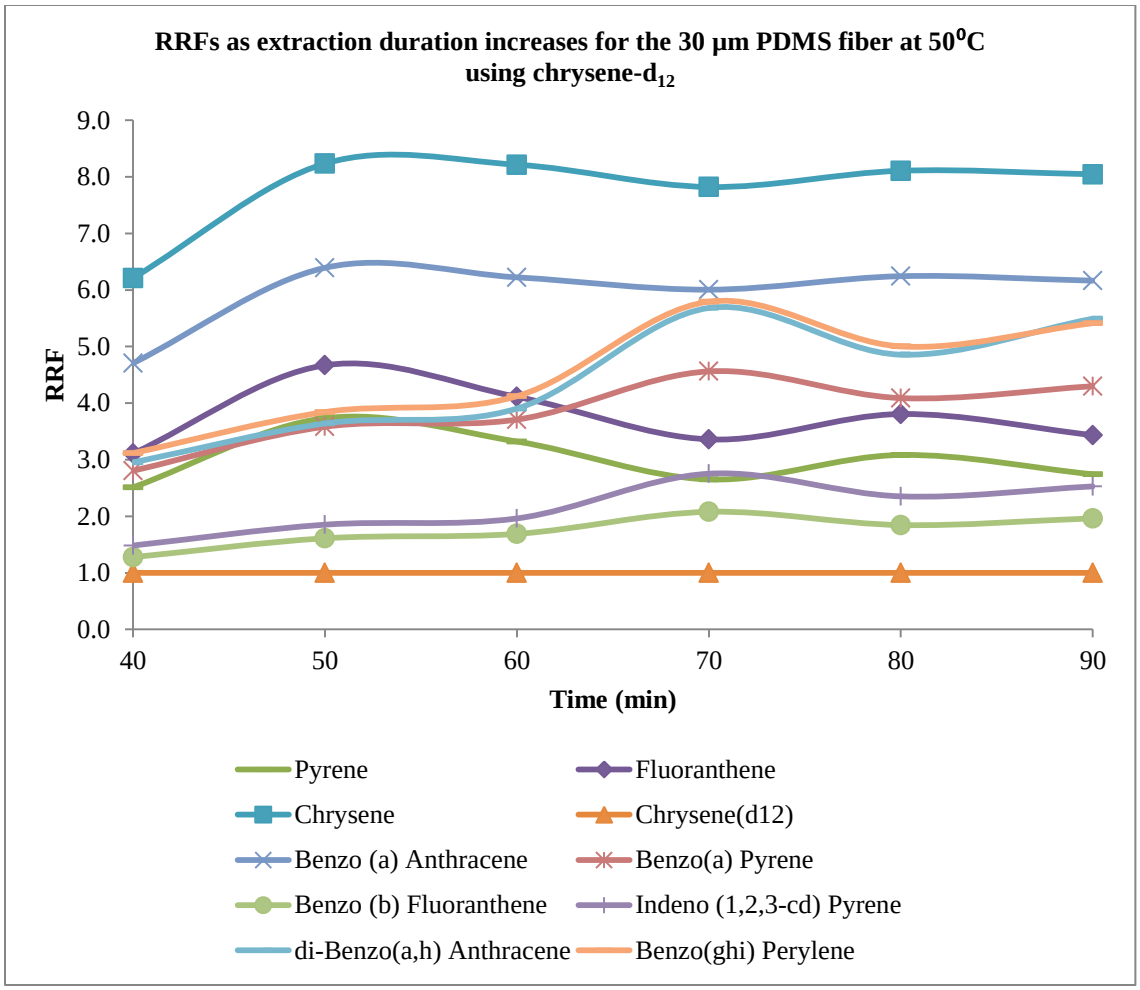

Figure 21 RRF values with respect to extraction times for 30 µm PDMS fiber at 50°C using chrysene-d_{12} for RRF calculation.

`

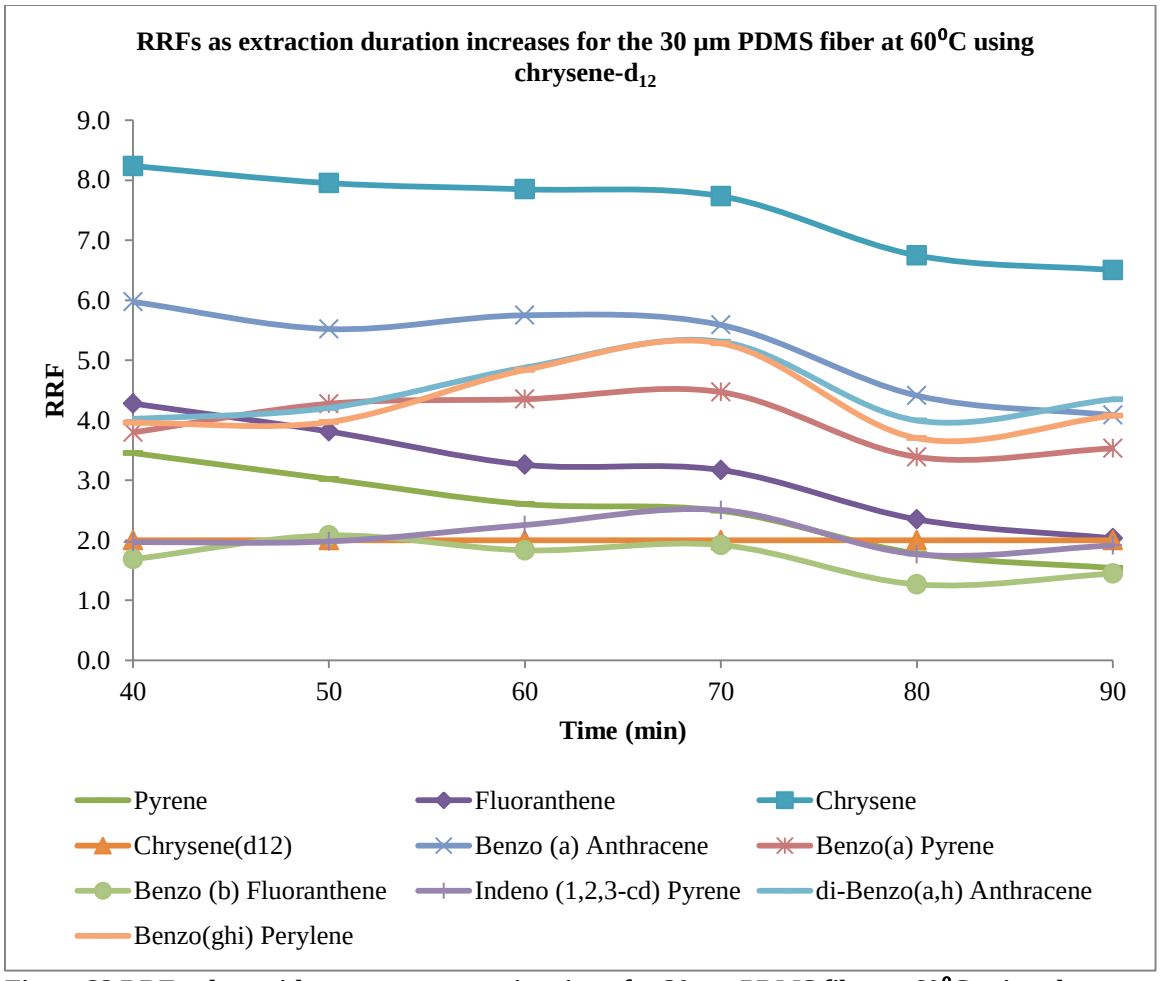

Figure 22 RRF values with respect to extraction times for 30 µm PDMS fiber at 60°C using chrysene-d_{12} for RRF calculation. (RRF=relative response factor).

`

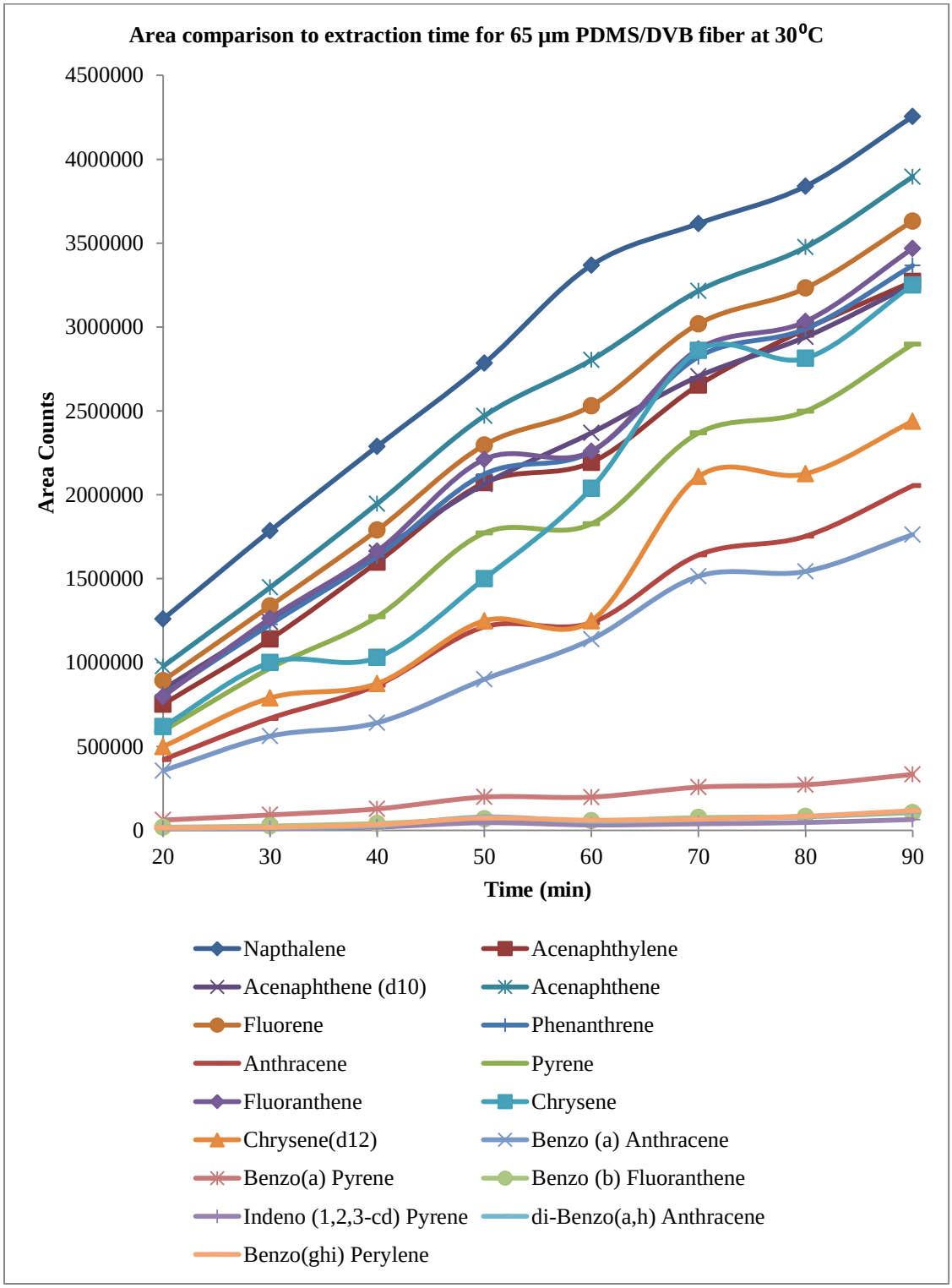

Figure 23 Area comparison to extraction time using the 65 µm PDMS/DVB fiber at 30°C (20-90 minutes).

`

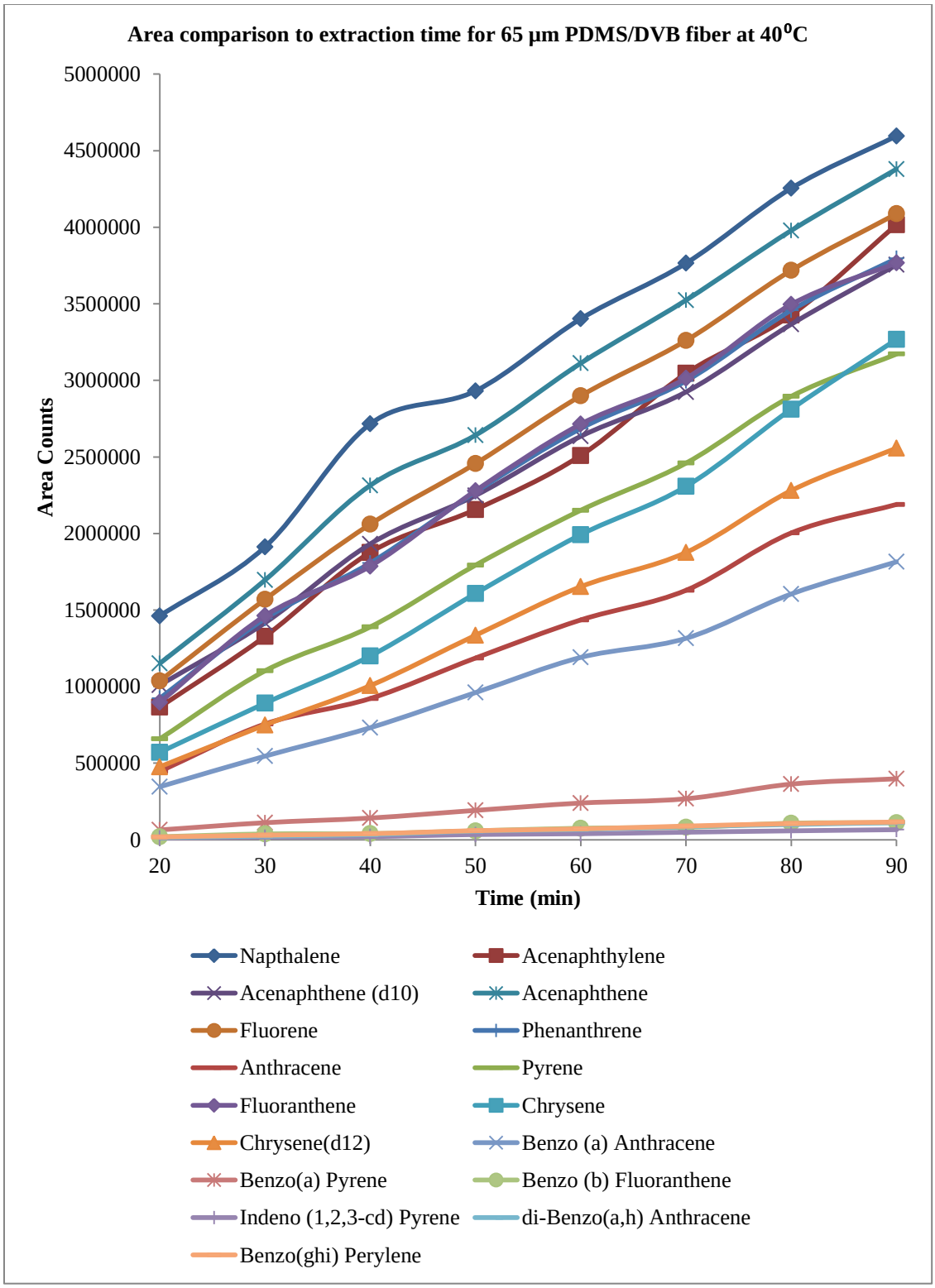

Figure 24 Area comparison to extraction time using the 65 µm PDMS/DVB fiber at 40°C (20-90 minutes).

`

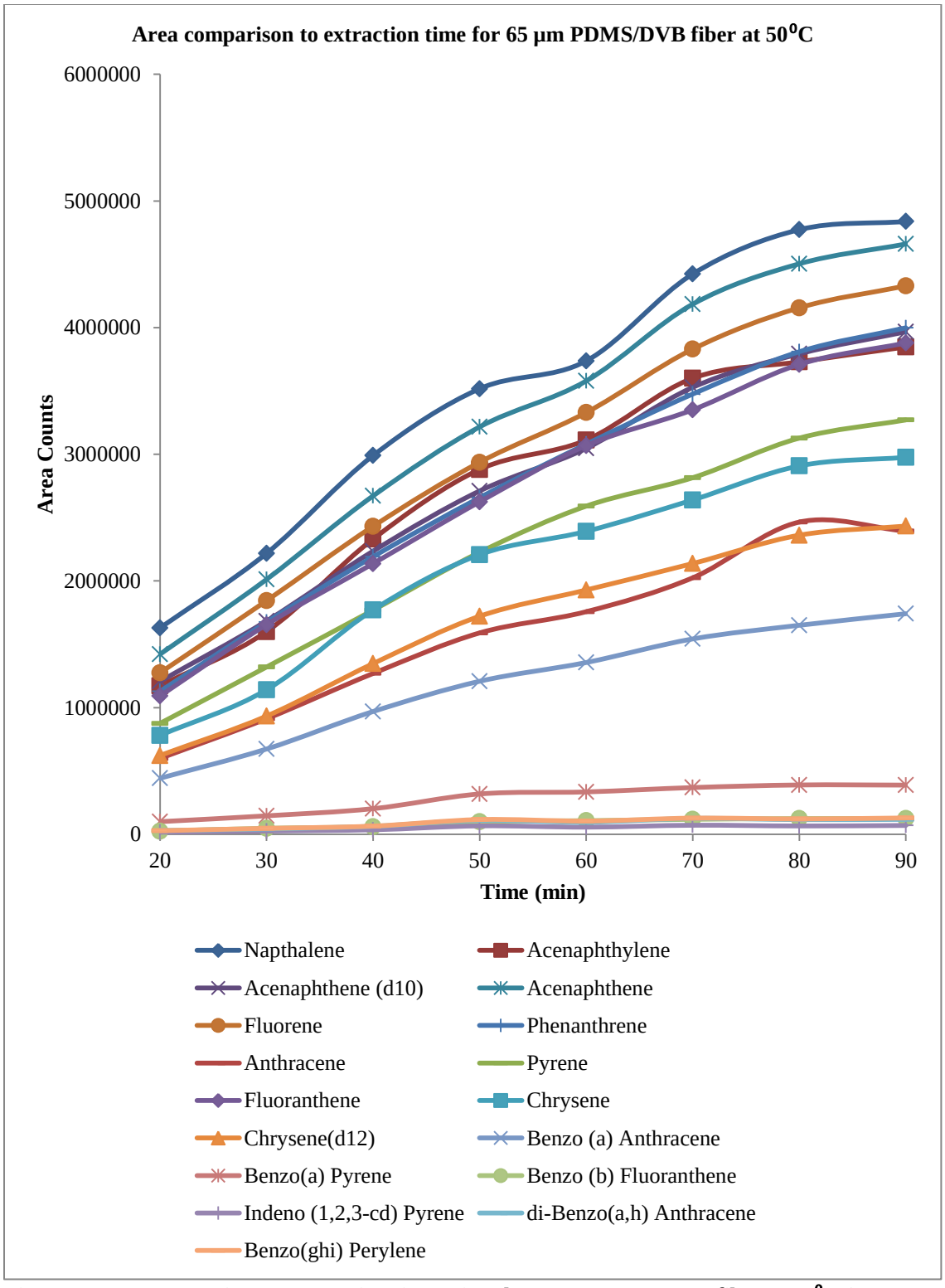

Figure 25 Area comparison to extraction time using the 65 µm PDMS/DVB fiber at 50°C (20-90 minutes).

`

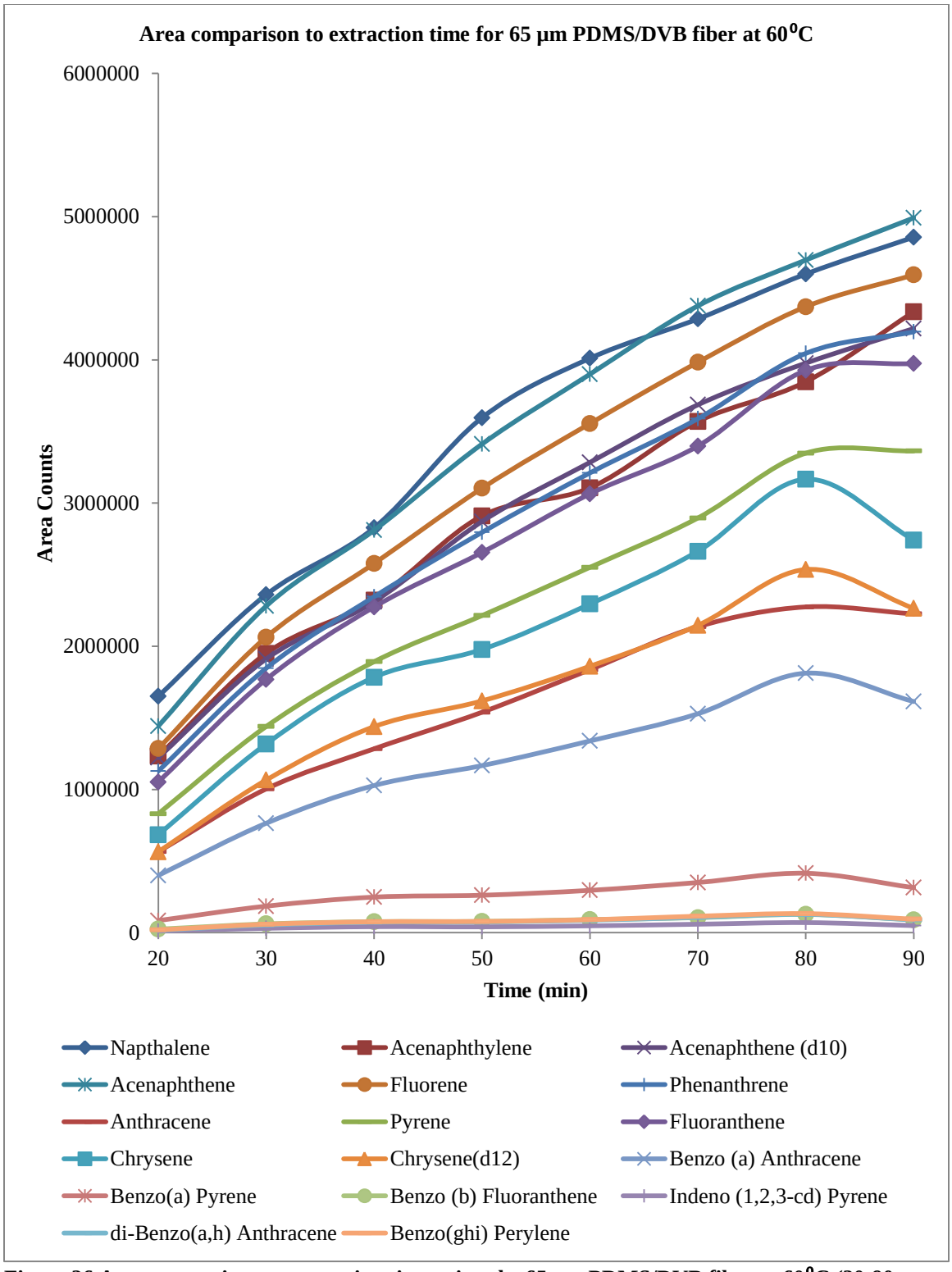

Figure 26 Area comparison to extraction time using the 65 µm PDMS/DVB fiber at 60°C (20-90 minutes).

`

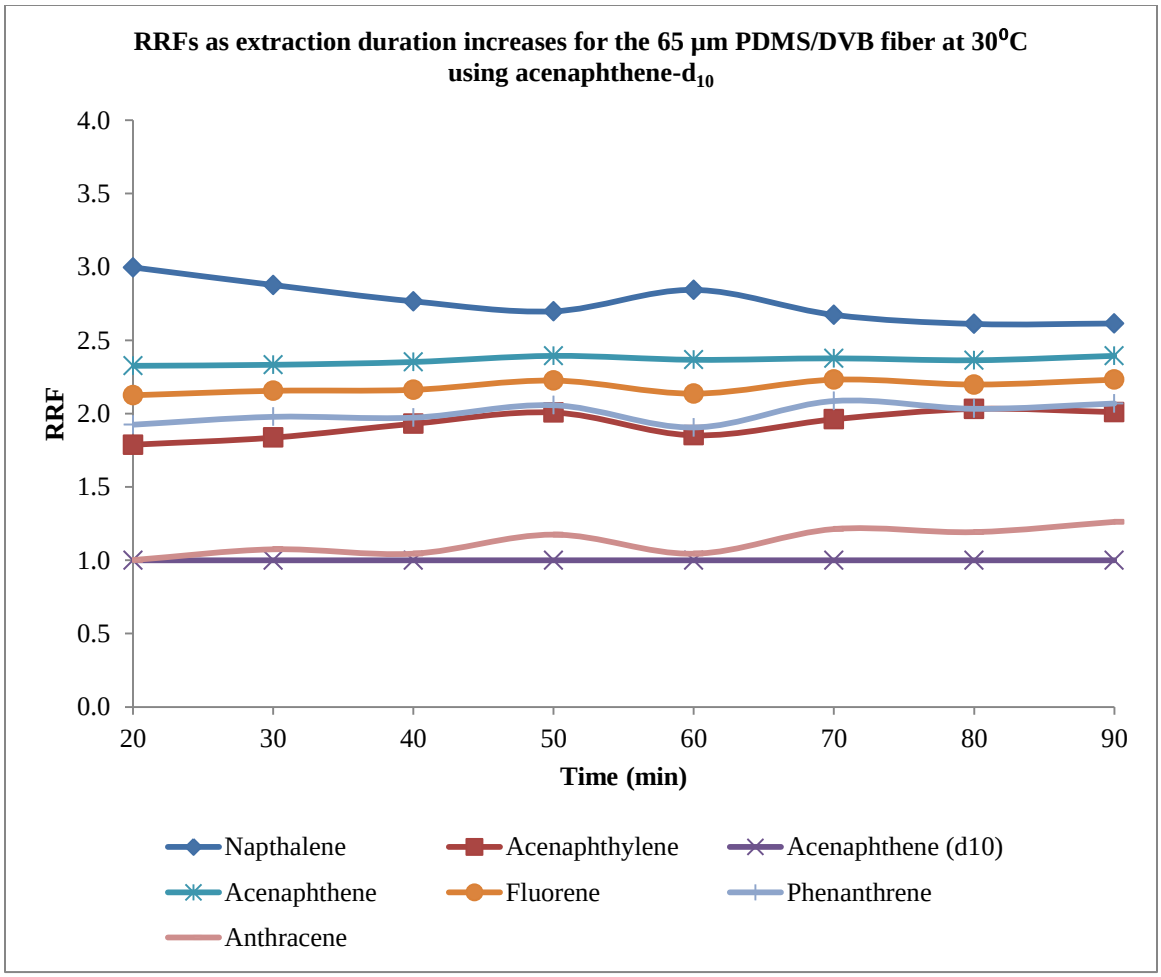

Figure 27 RRF values with respect to extraction times using the 65 µm PDMS/DVB fiber at 30°C using acenaphthene-d_{10} for RRF calculation. (RRF = relative response factor)

`

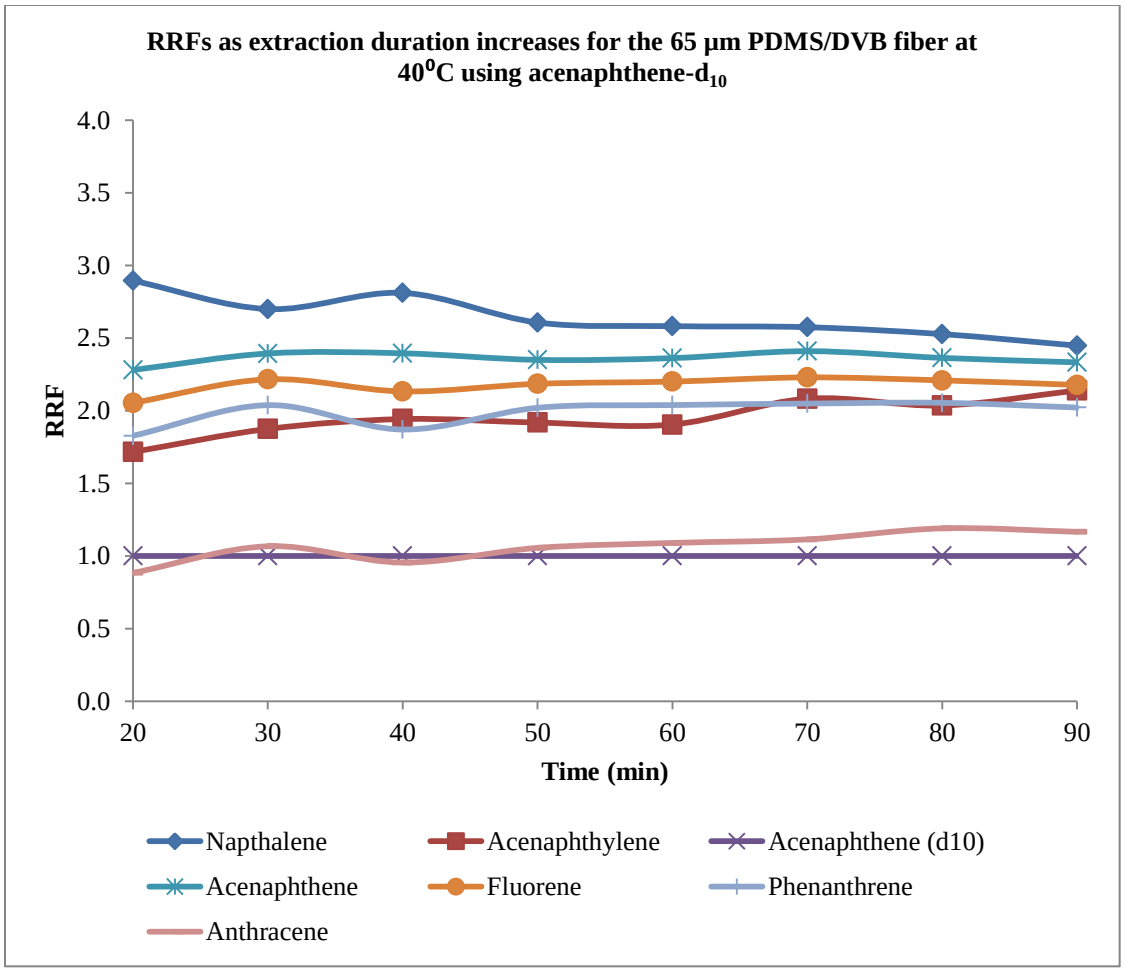

Figure 28 RRF values with respect to extraction times using the 65 µm PDMS/DVB fiber at 40°C using acenaphthene-d_{10} for RRF calculation. (RRF = relative response factor)

`

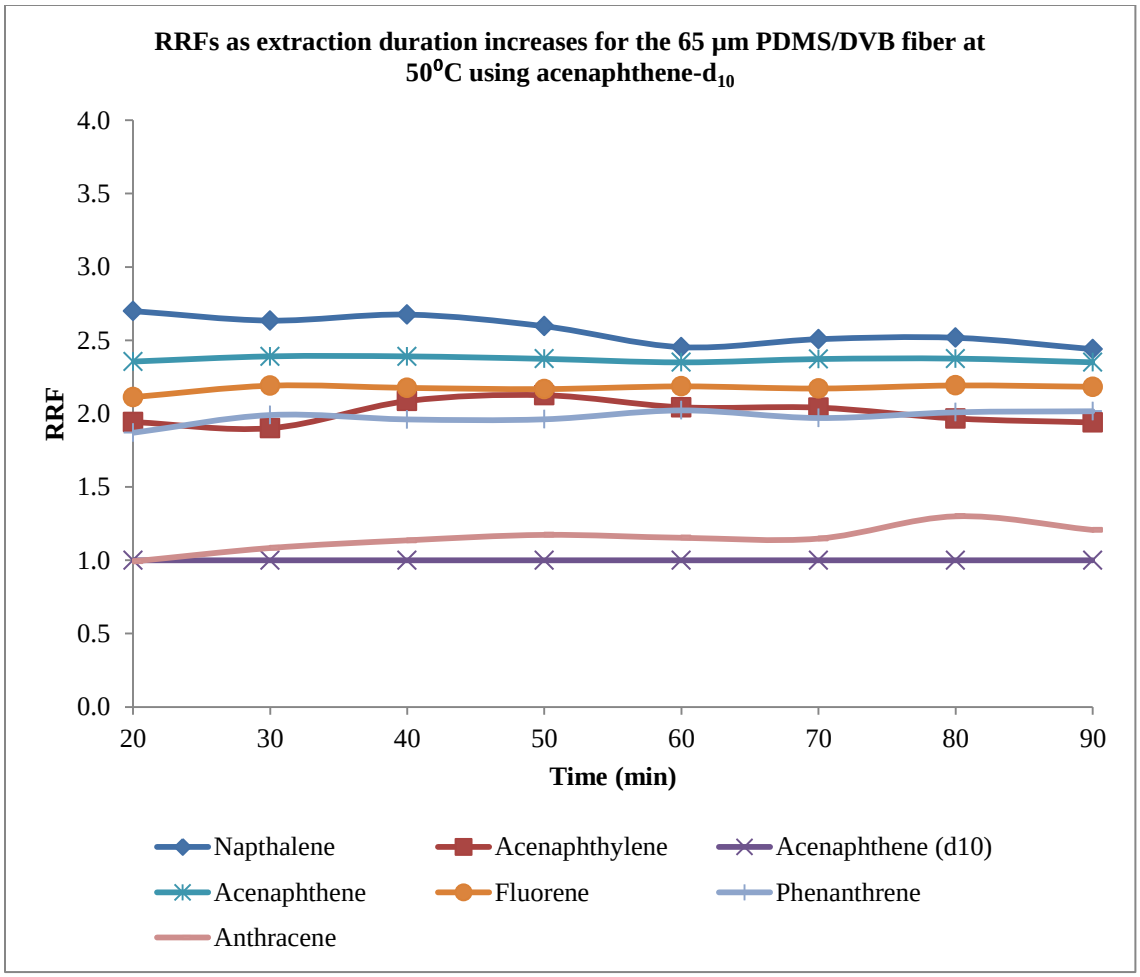

Figure 29 RRF values with respect to extraction times using the 65 µm PDMS/DVB fiber at 50°C using acenaphthene-d_{10} for RRF calculation. (RRF = relative response factor)

`

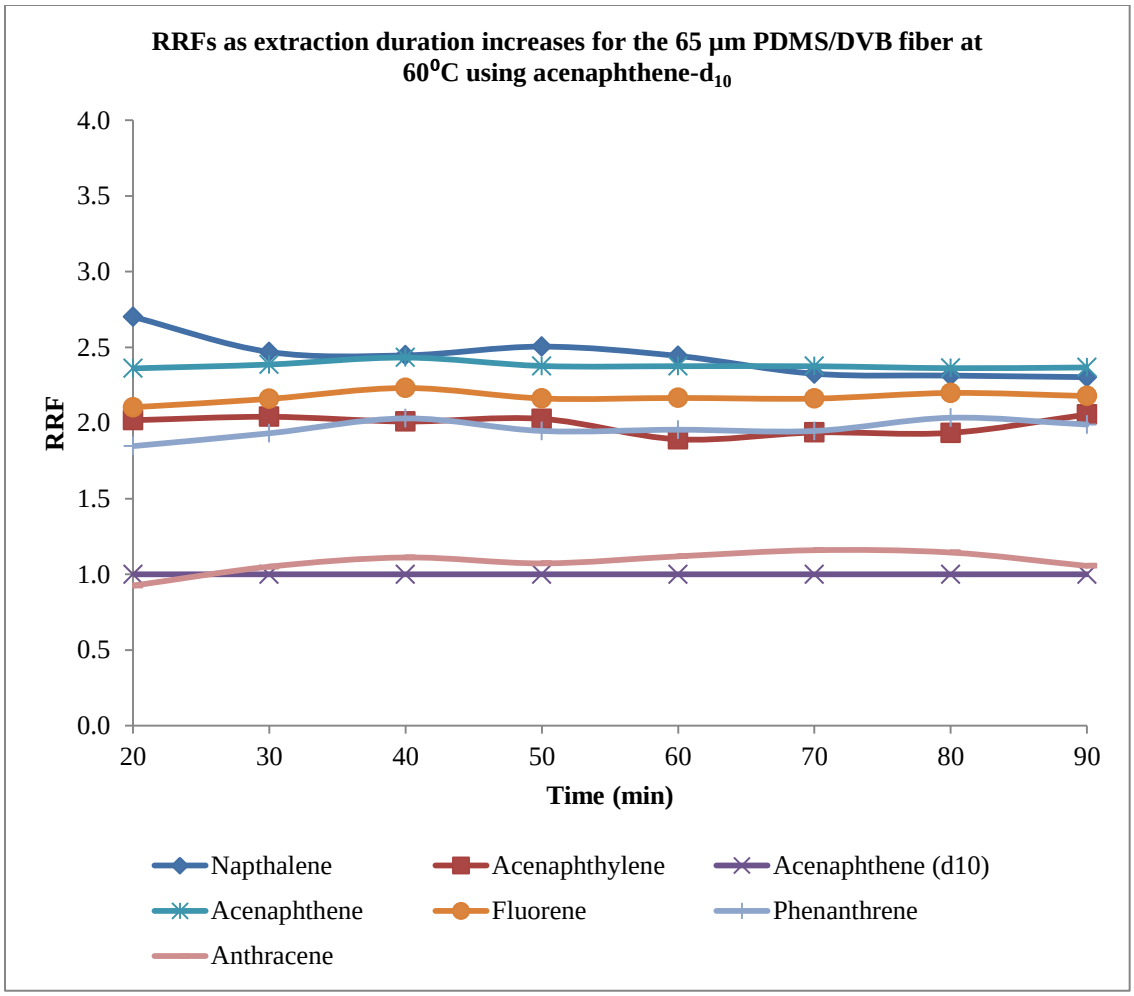

Figure 30 RRF values with respect to extraction times using the 65 µm PDMS/DVB fiber at 60°C using acenaphthene-d_{10} for RRF calculation. (RRF = relative response factor)

`

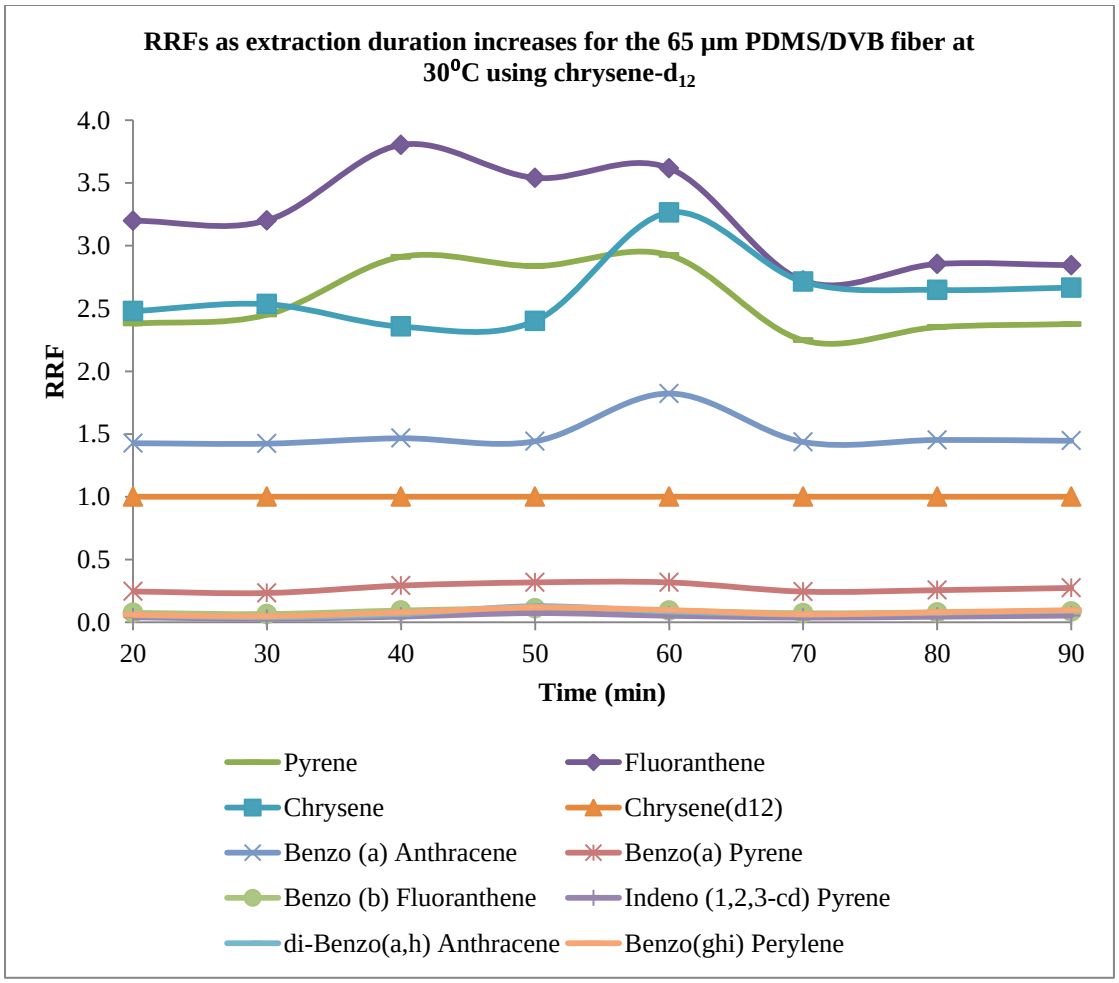

Figure 31 RRF values with respect to extraction times using the 65 µm PDMS/DVB fiber at 30°C using chrysene-d_{12} for RRF calculation. (RRF = relative response factor)

`

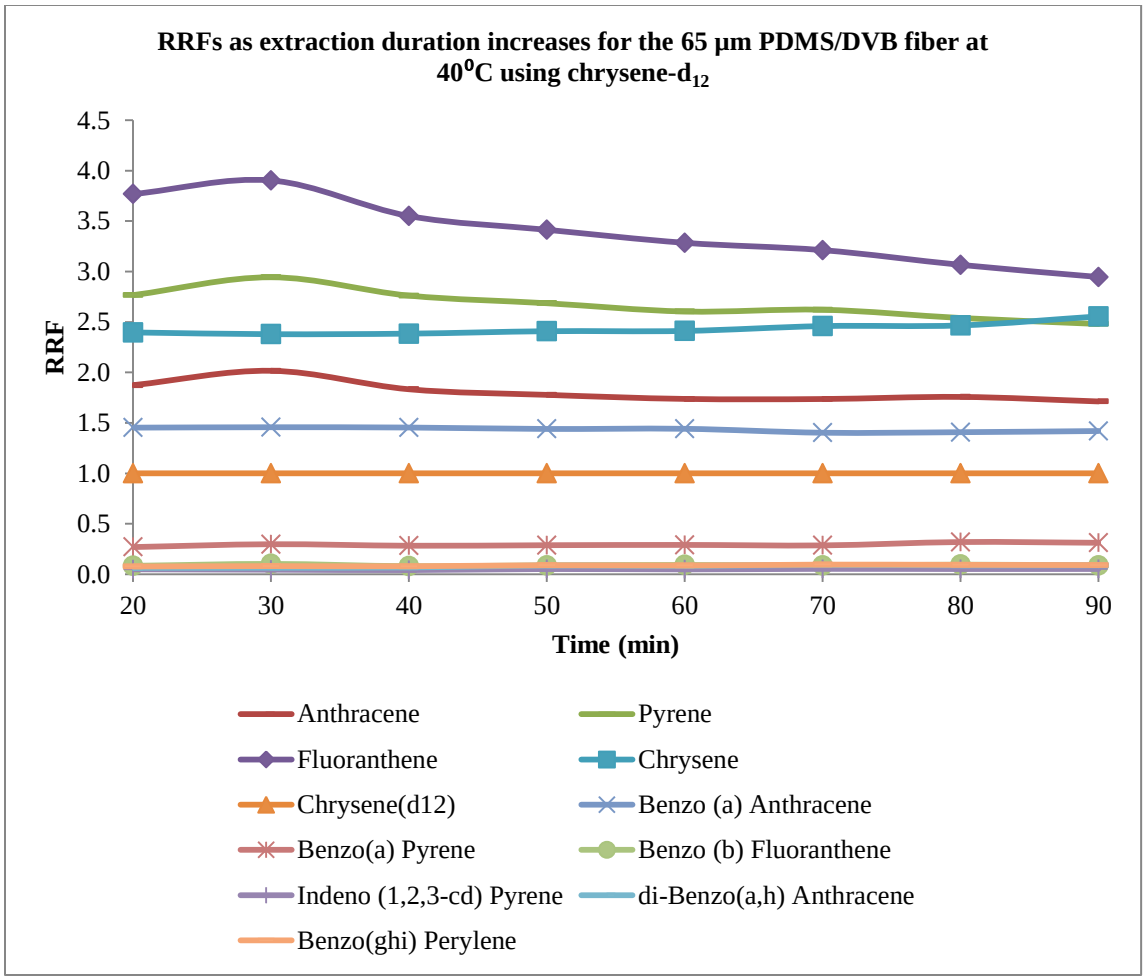

Figure 32 RRF values with respect to extraction times using the 65 µm PDMS/DVB fiber at 40°C using chrysene-d_{12} for RRF calculation. (RRF = relative response factor)

`

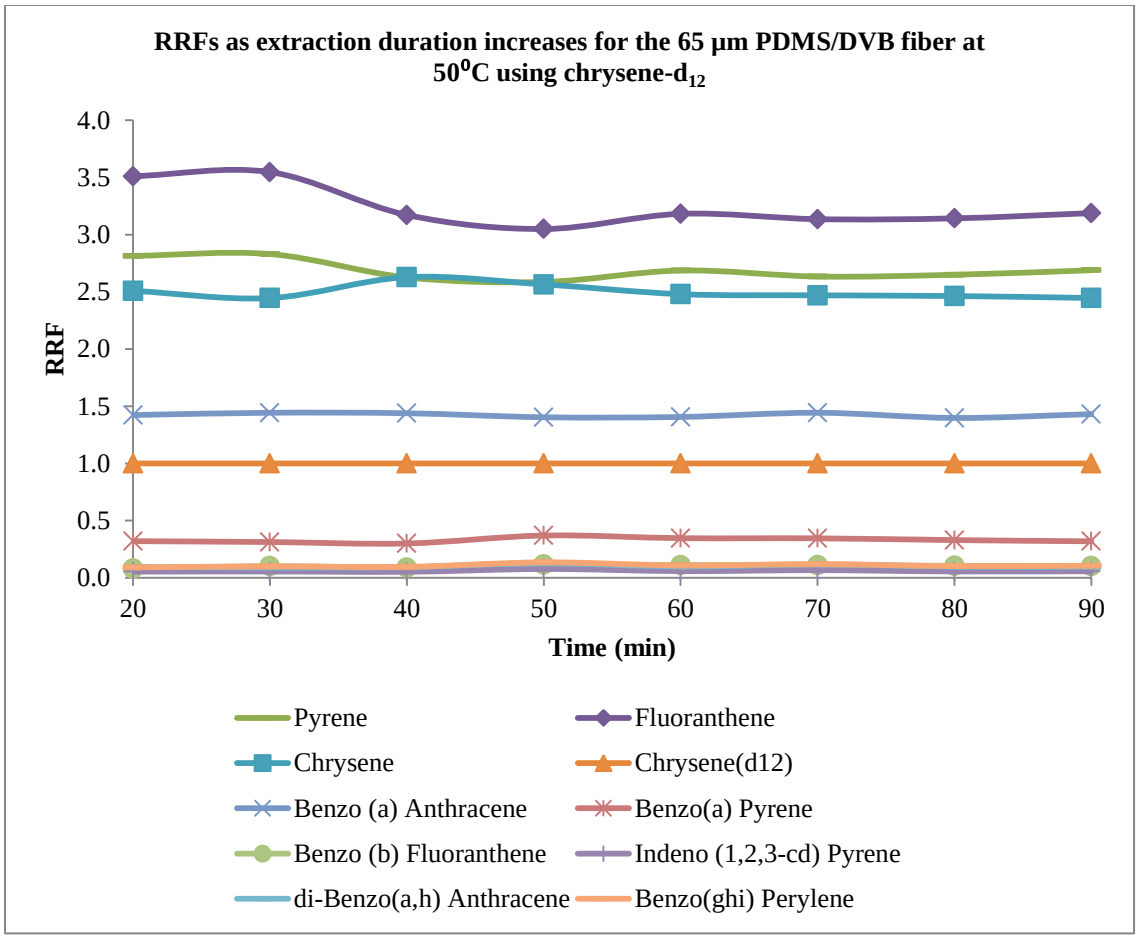

Figure 33 RRF values with respect to extraction times using the 65 µm PDMS/DVB fiber at 50°C using chrysene-d_{12} for RRF calculation. (RRF = relative response factor)

`

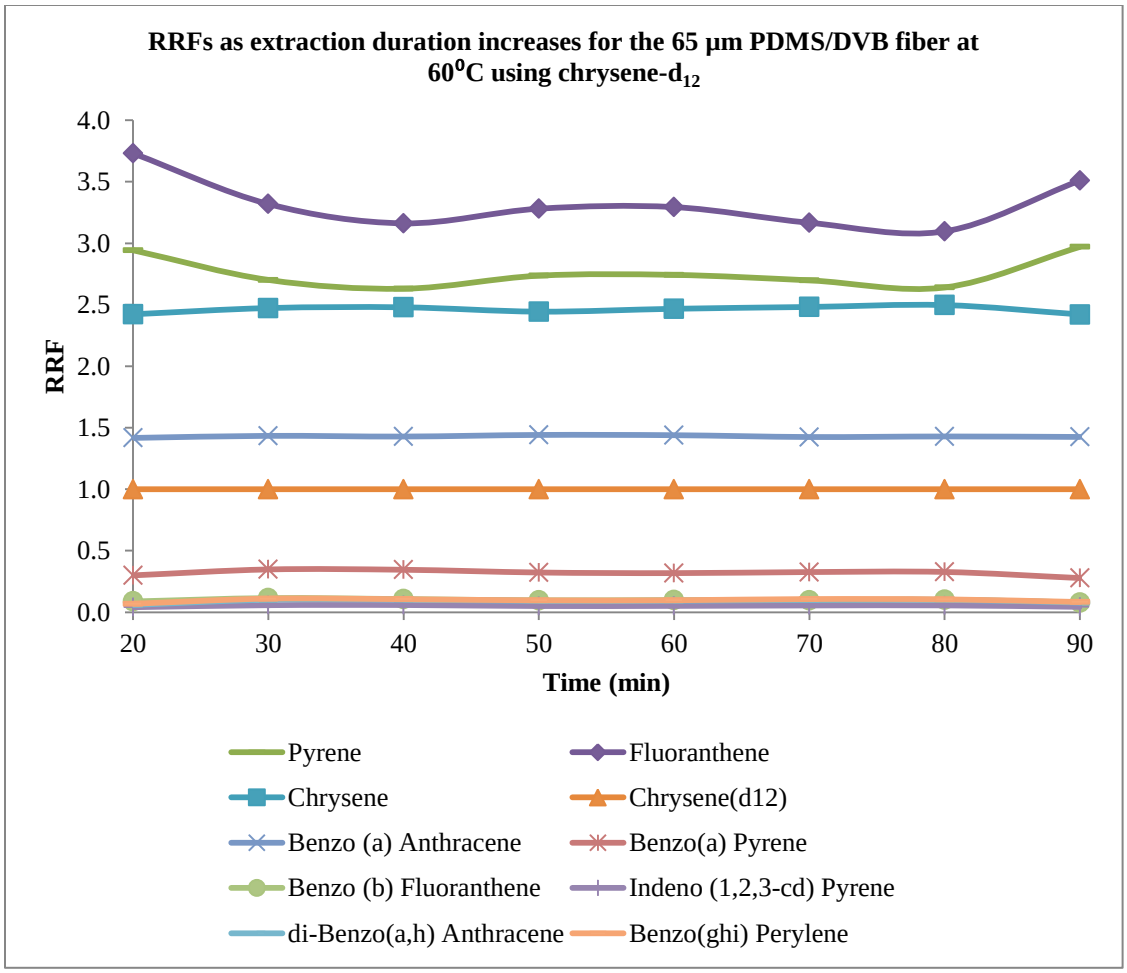

Figure 34 RRF values with respect to extraction times using the 65 µm PDMS/DVB fiber at 60°C using chrysene-d_{12} for RRF calculation. (RRF = relative response factor)

`

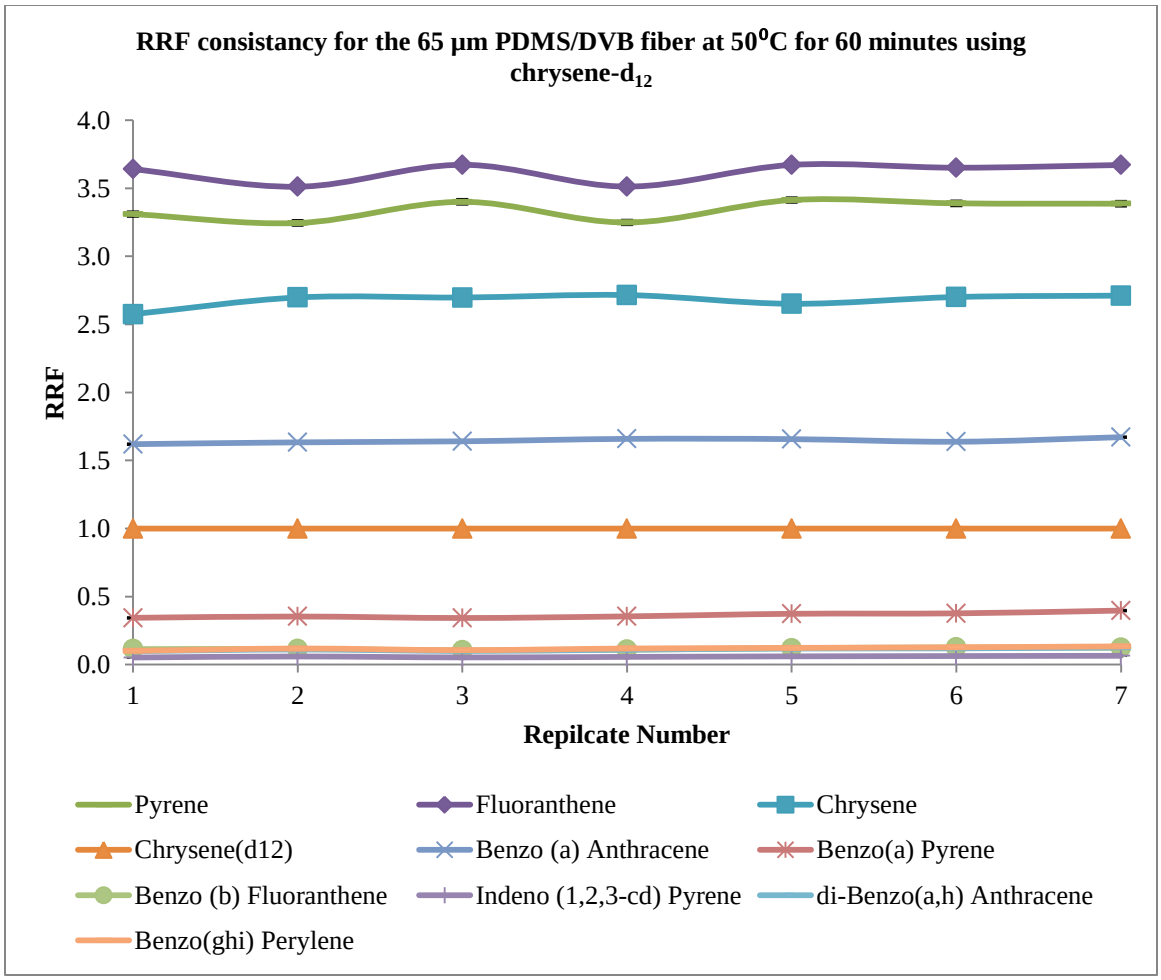

Figure 35 RRF repeatability using the 65 µm PDMS/DVB fiber for 60 minute extraction at 50 °C using chrysene-d_{12} for calculation. (RRF = relative response factor)

`

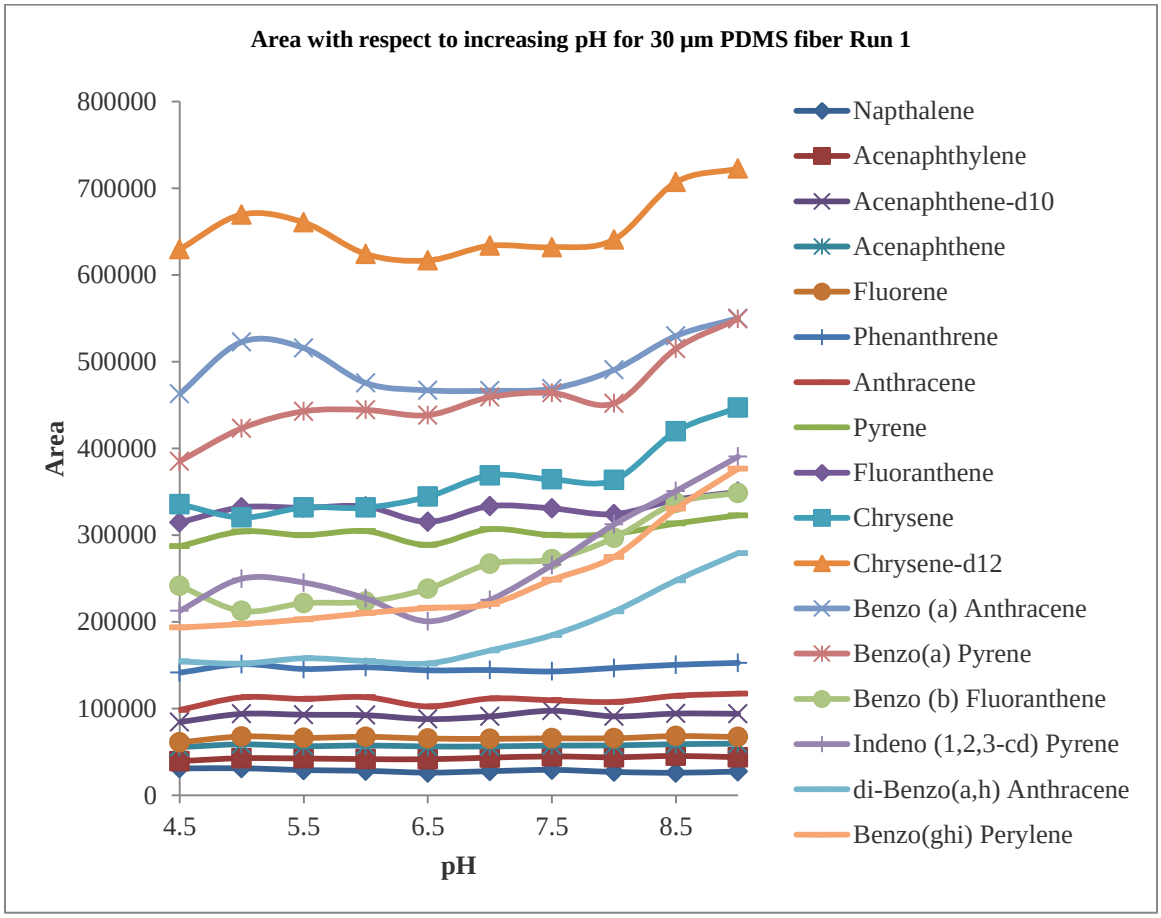

Figure 36 Area with respect to increasing pH using the 30 µm PDMS fiber run 1.

`

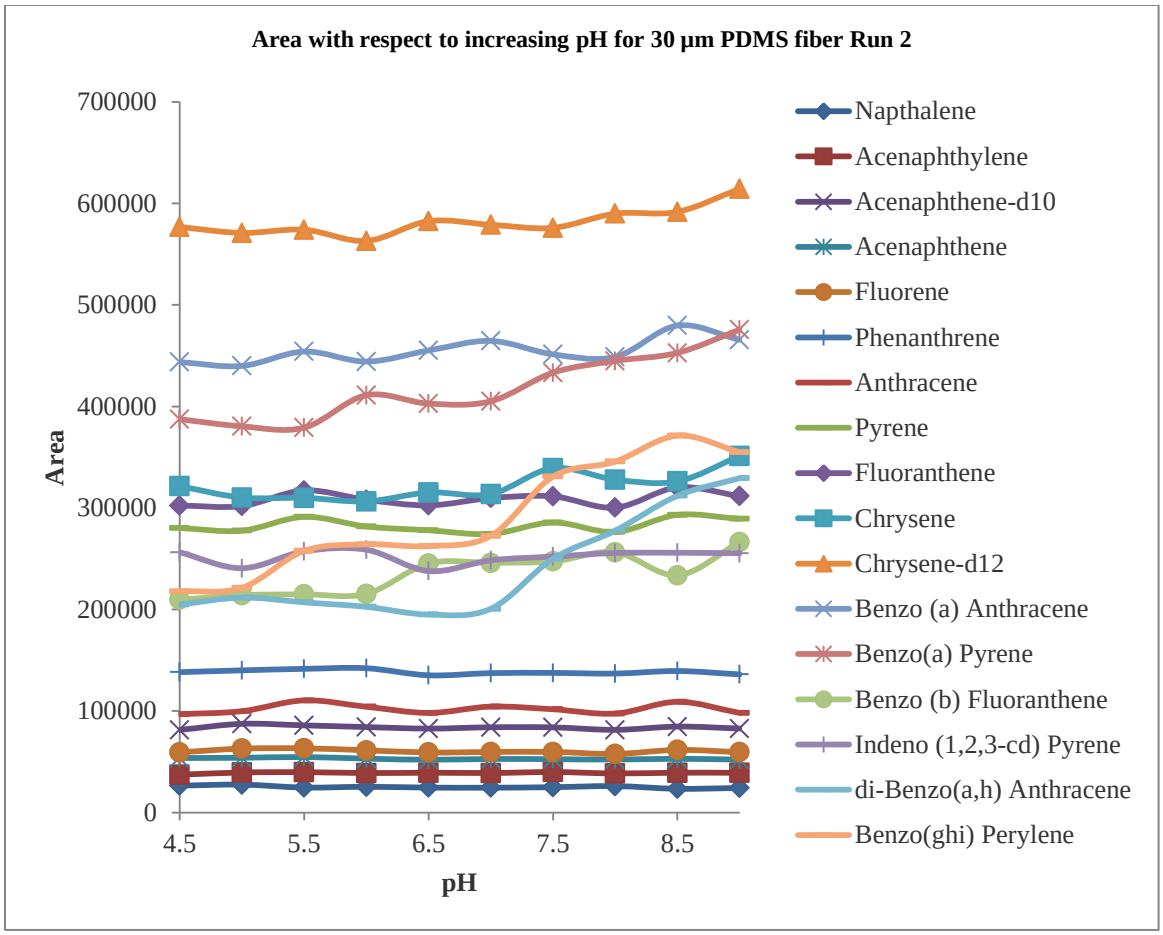

Figure 37 Area with respect to increasing pH using the 30 µm PDMS fiber run 2.

`

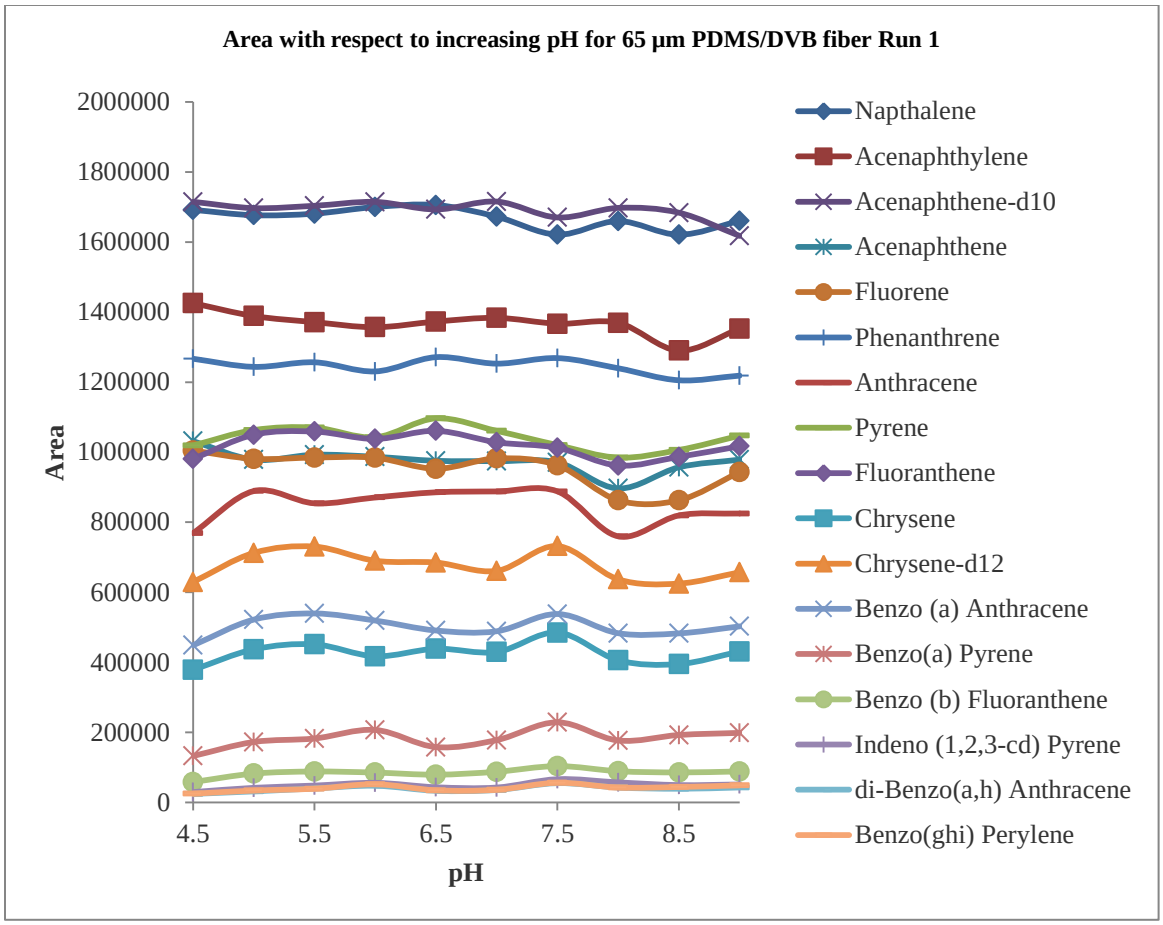

Figure 38 Area with respect to increasing pH using the 65 µm PDMS/DVB fiber run 1.

`

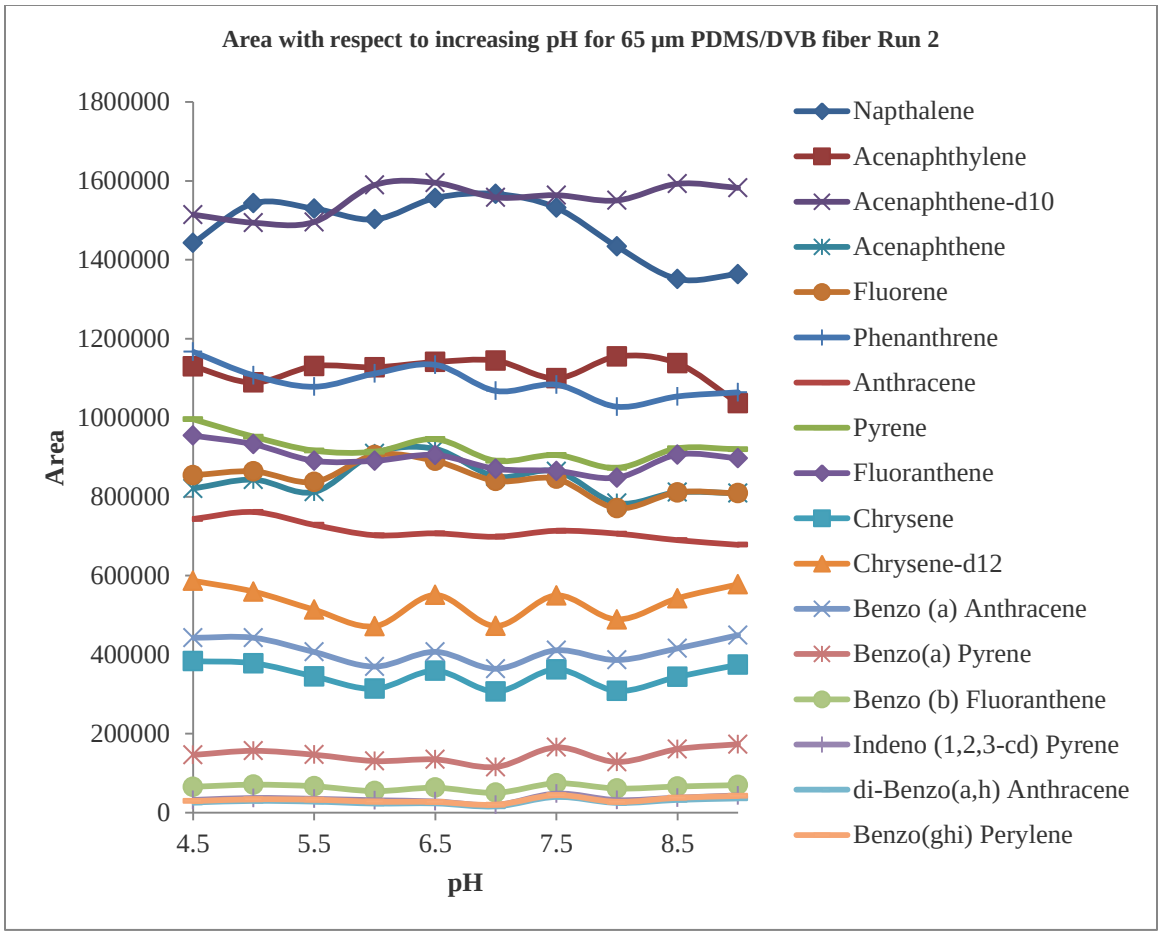

Figure 39 Area with respect to increasing pH using the 65 µm PDMS/DVB fiber run 2.

`

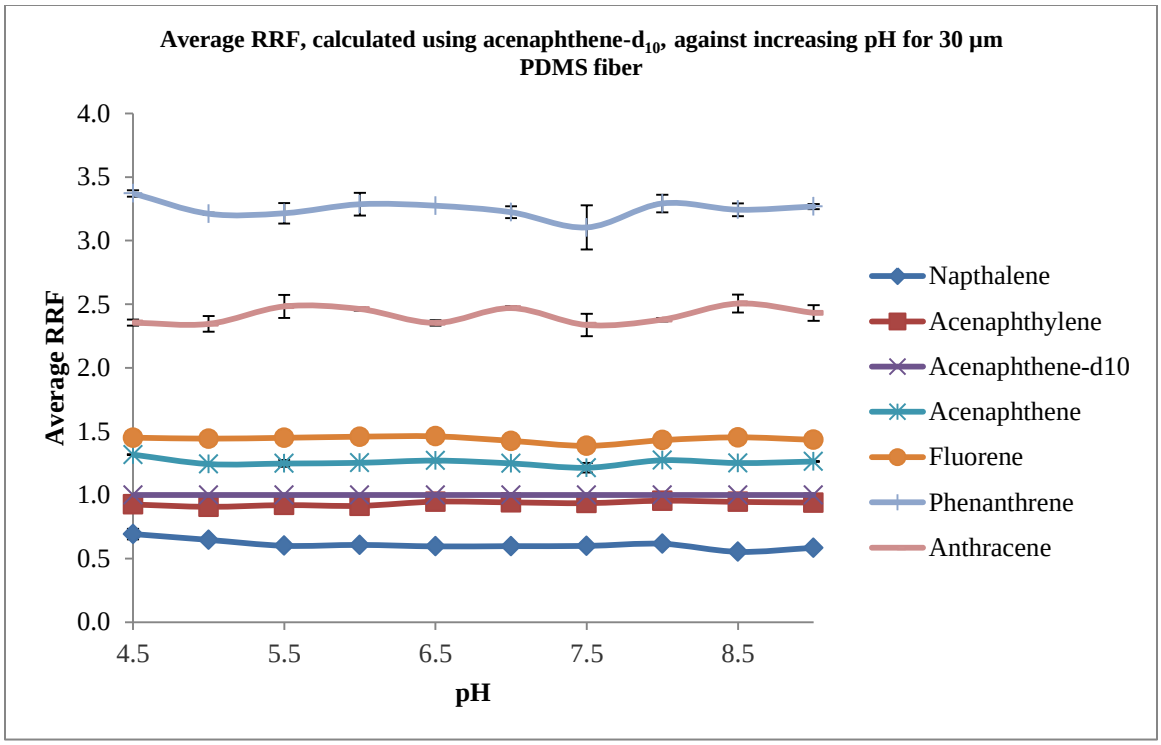

Figure 40 Average RRF, using acenaphthene-d_{10}, using the 30 µm PDMS fiber for pH. (RRF = relative response factor)

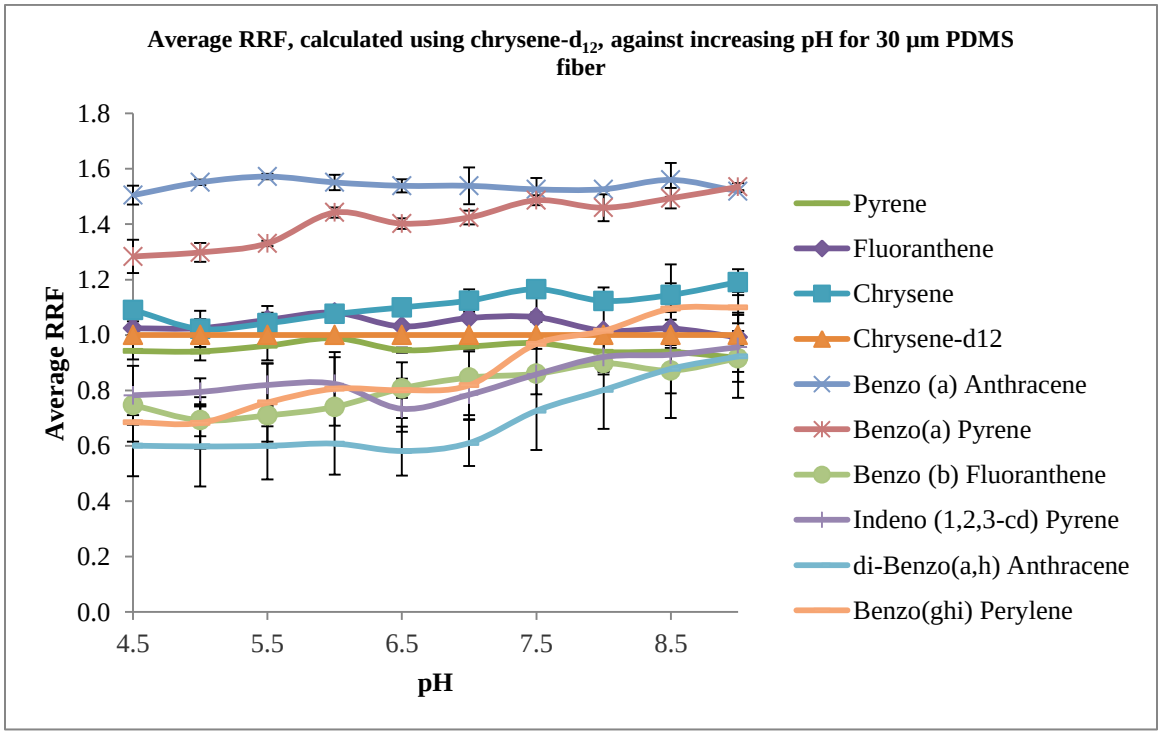

Figure 41 Average RRF, using chrysene-d_{12}, using the 30 µm PDMS fiber for pH.

`

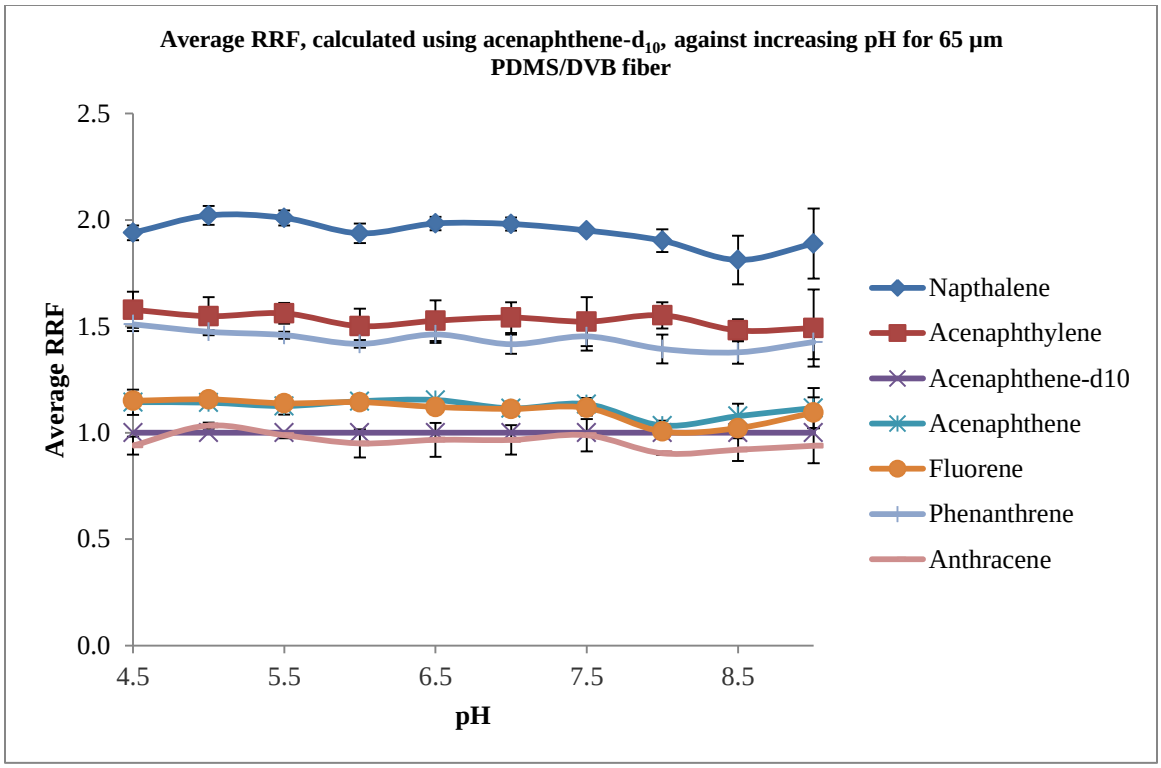

Figure 42 Average RRF, using Acenaphthene-d_{10}, using the 65 µm PDMS/DVB fiber for pH. (RRF = relative response factor)

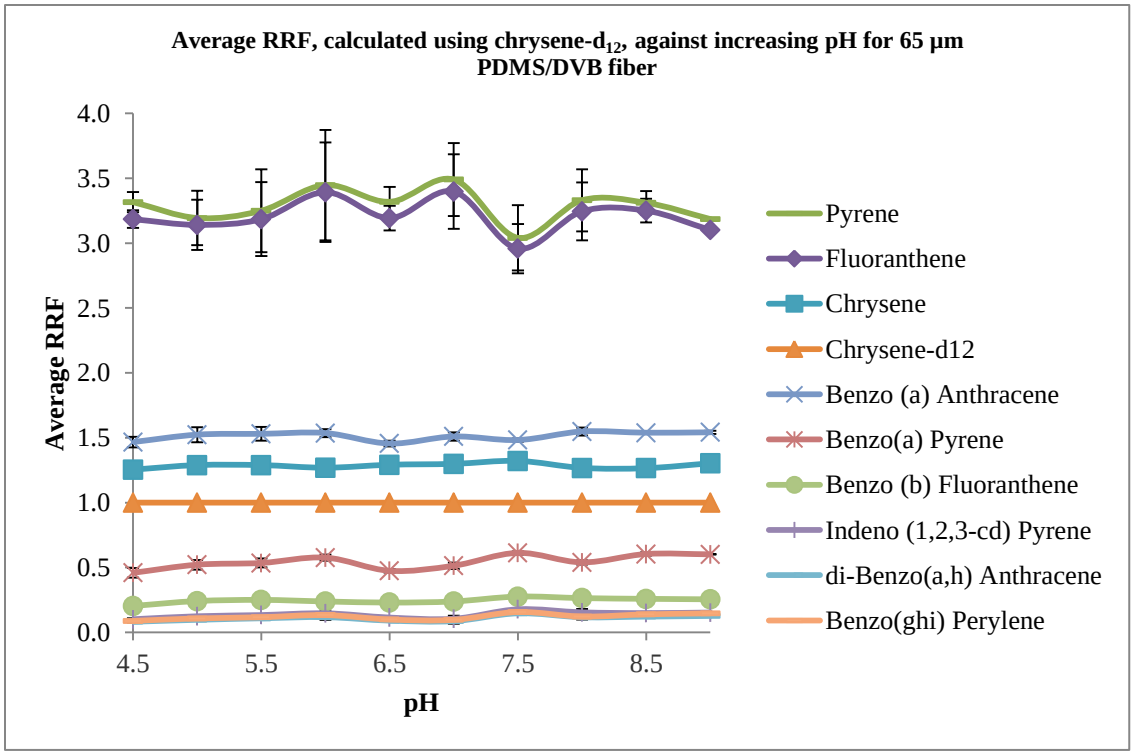

Figure 43 Average RRF, using chrysene-d_{12}, using the 65 µm PDMS/DVB fiber for pH.

`

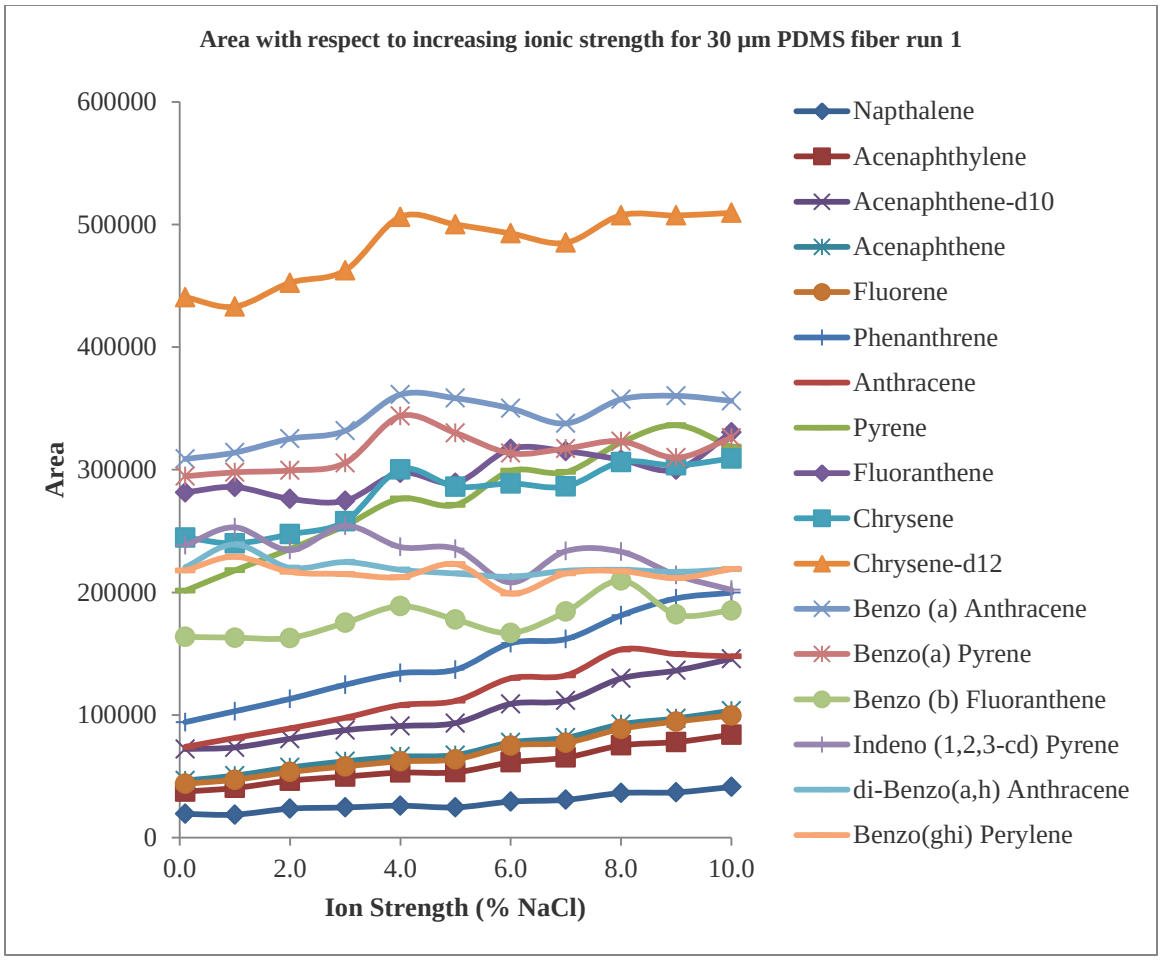

Figure 44 Area with respect to increasing ionic strength using the 30 µm PDMS fiber run 1.

`

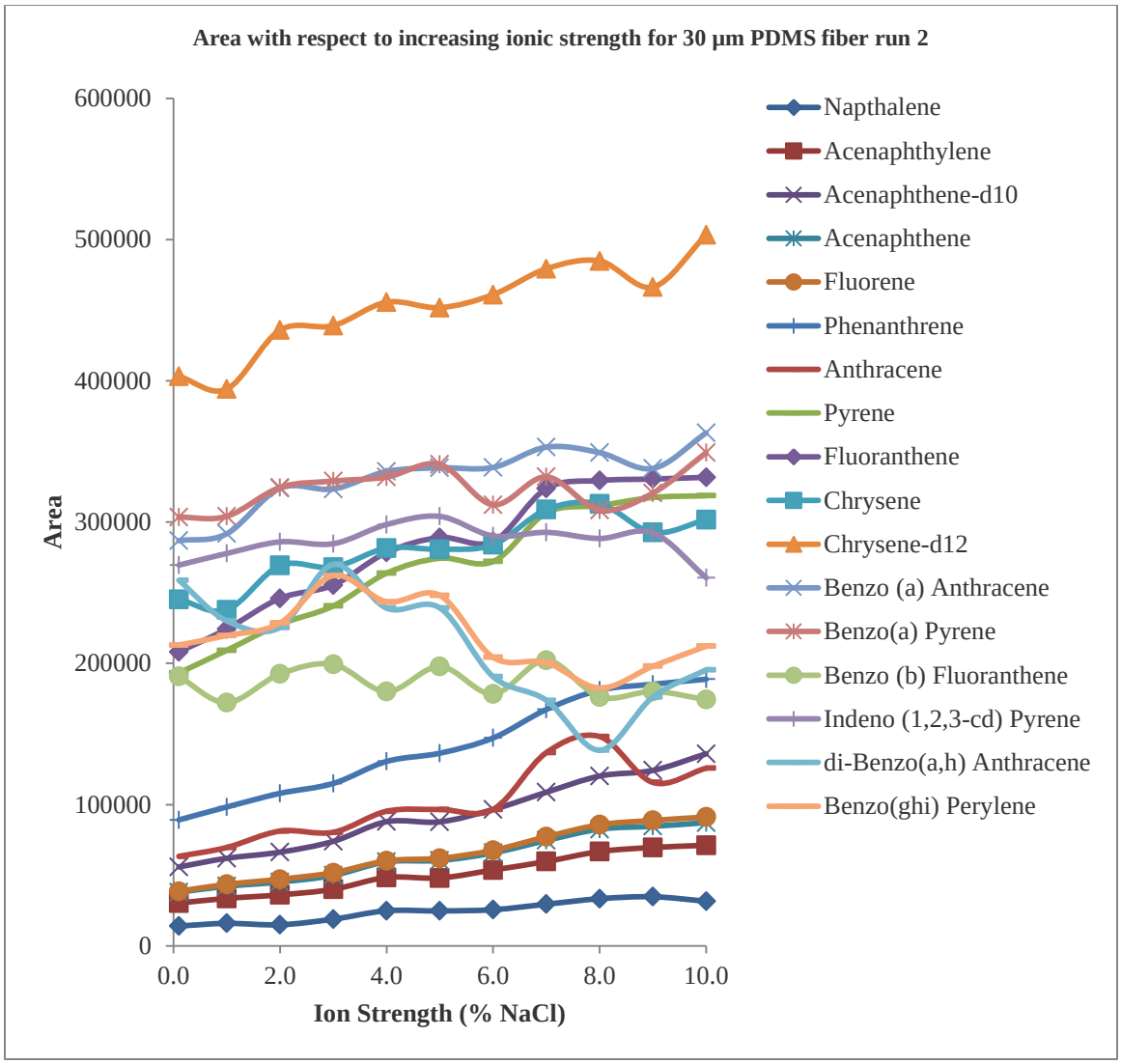

Figure 45 Area with respect to increasing ionic strength using the 30 µm PDMS fiber run 2.

`

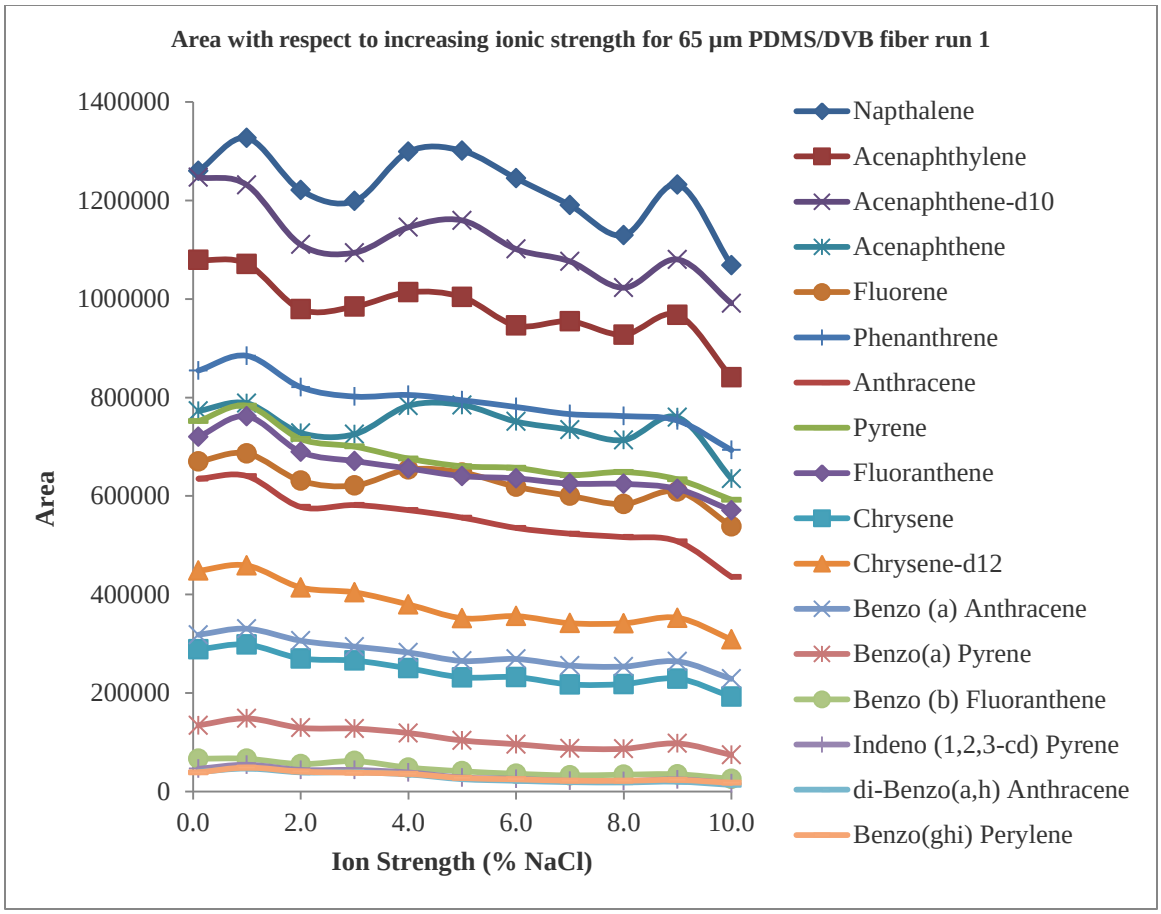

Figure 46 Area with respect to increasing ionic strength using the 65 µm PDMS fiber run 1.

`

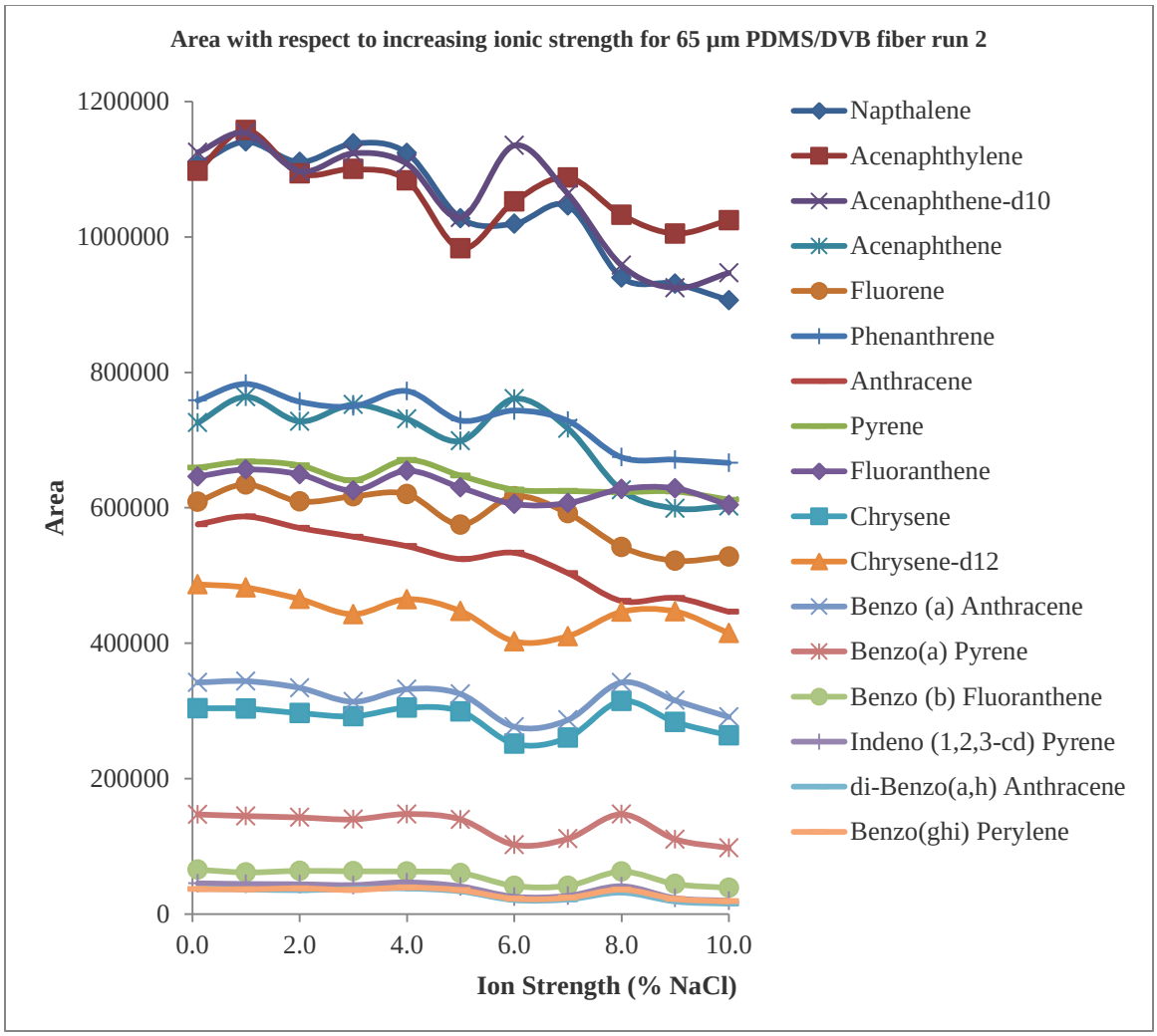

Figure 47 Area with respect to increasing ionic strength using the 65 µm PDMS fiber run 2.

`

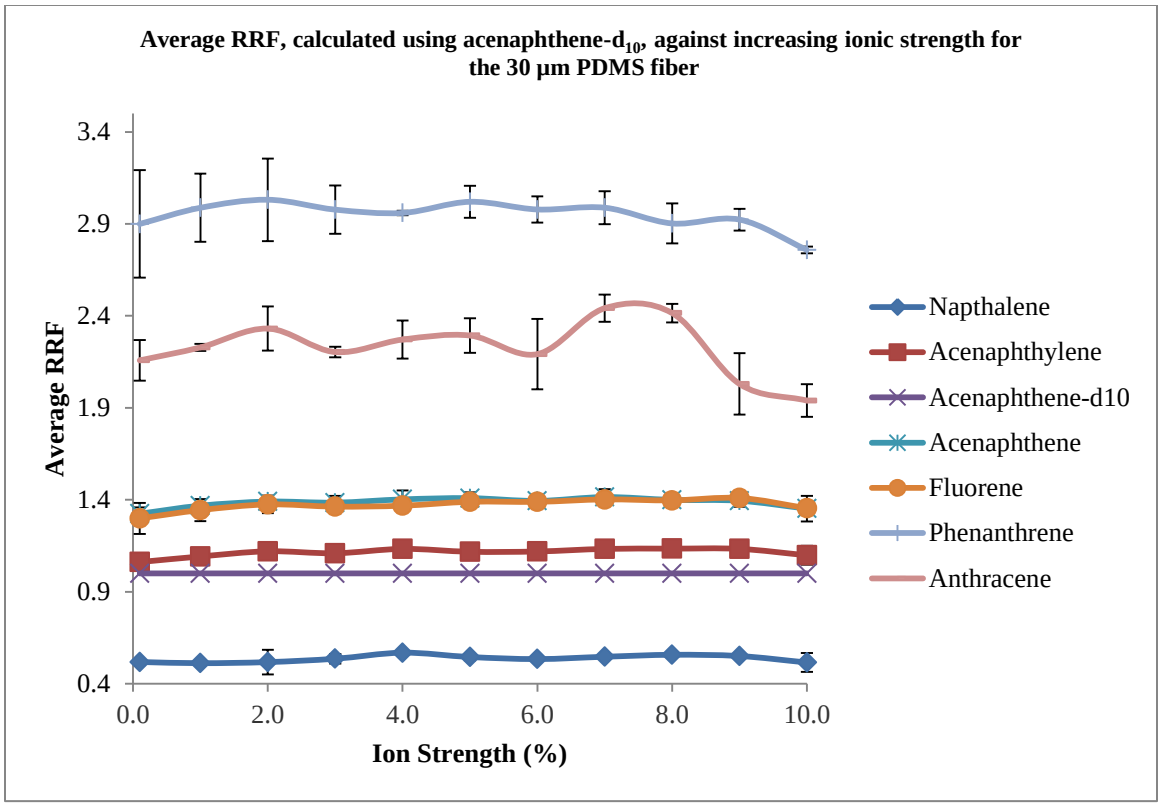

Figure 48 Average RRF, using acenaphthene-d_{10}, using the 30 µm PDMS fiber for ionic strength. (RRF = relative response factor)

`

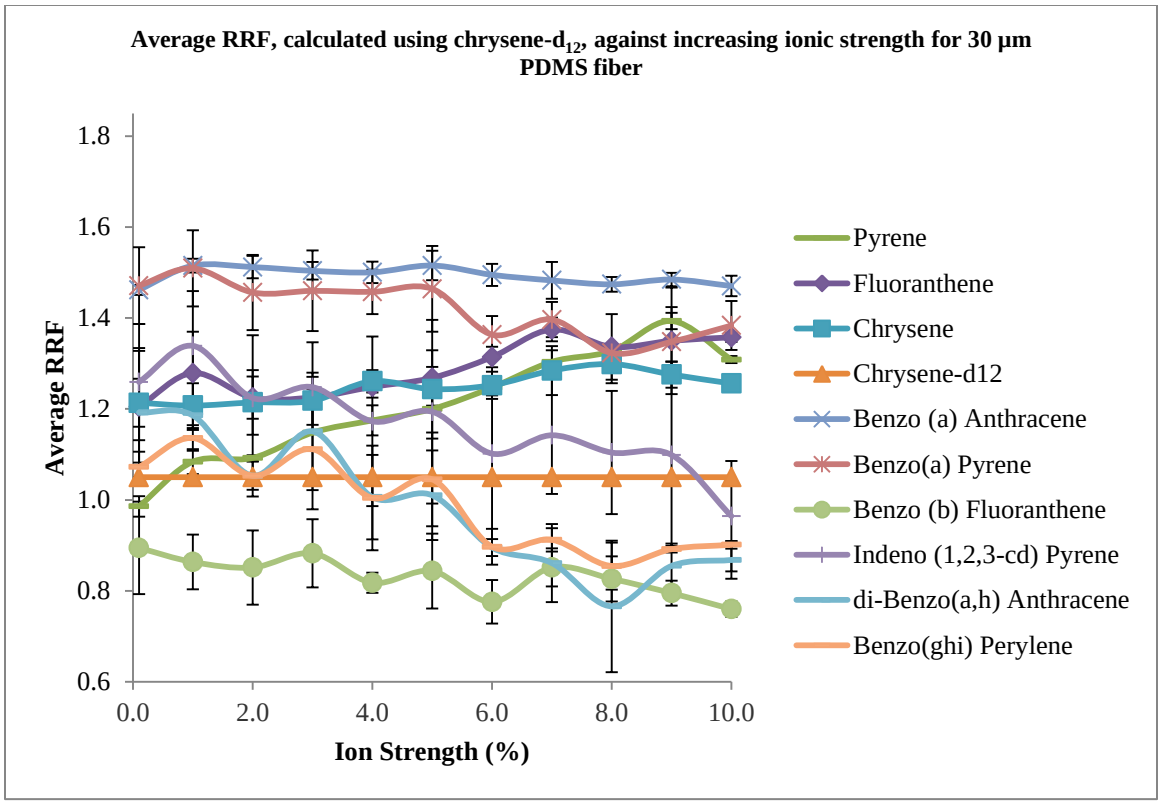

Figure 49 Average RRF, using chrysene-d_{12}, using the 30 µm PDMS fiber for ionic strength. (RRF = relative response factor)

`

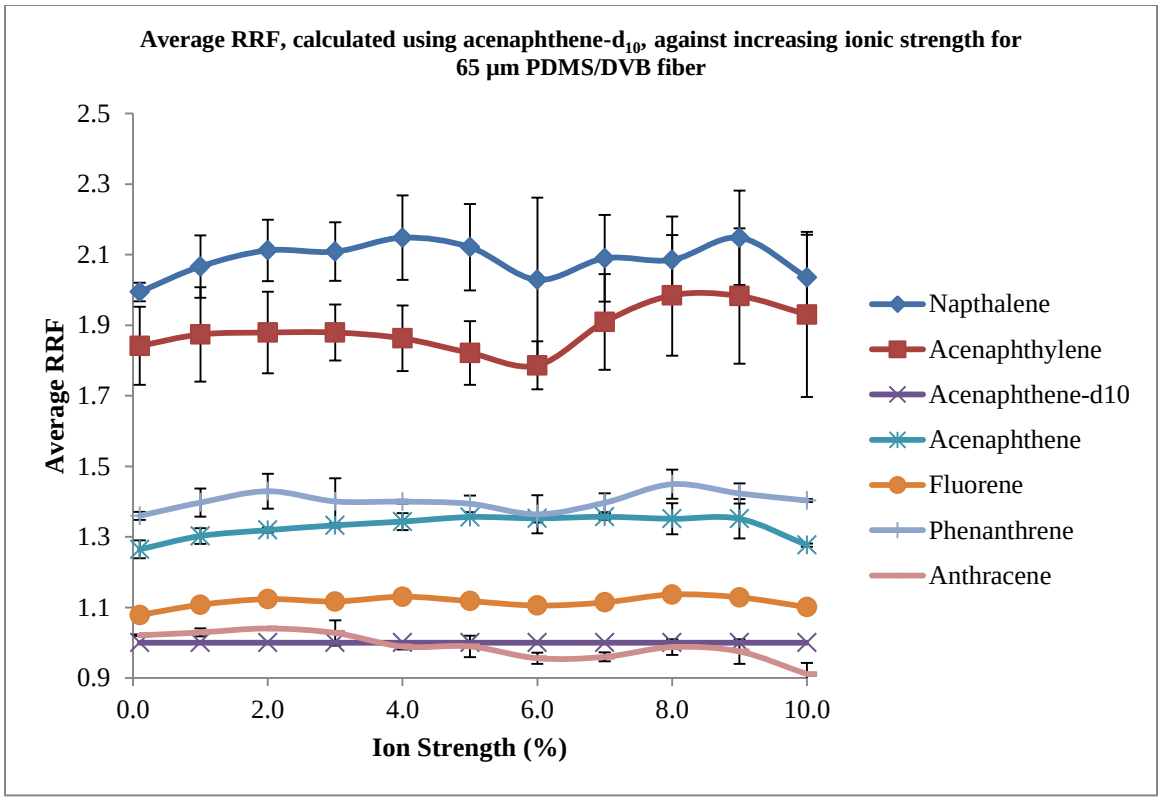

Figure 50 Average RRF, using acenaphthene-d_{10}, using the 65 µm PDMS/DVB fiber for ionic strength. (RRF = relative response factor)

`

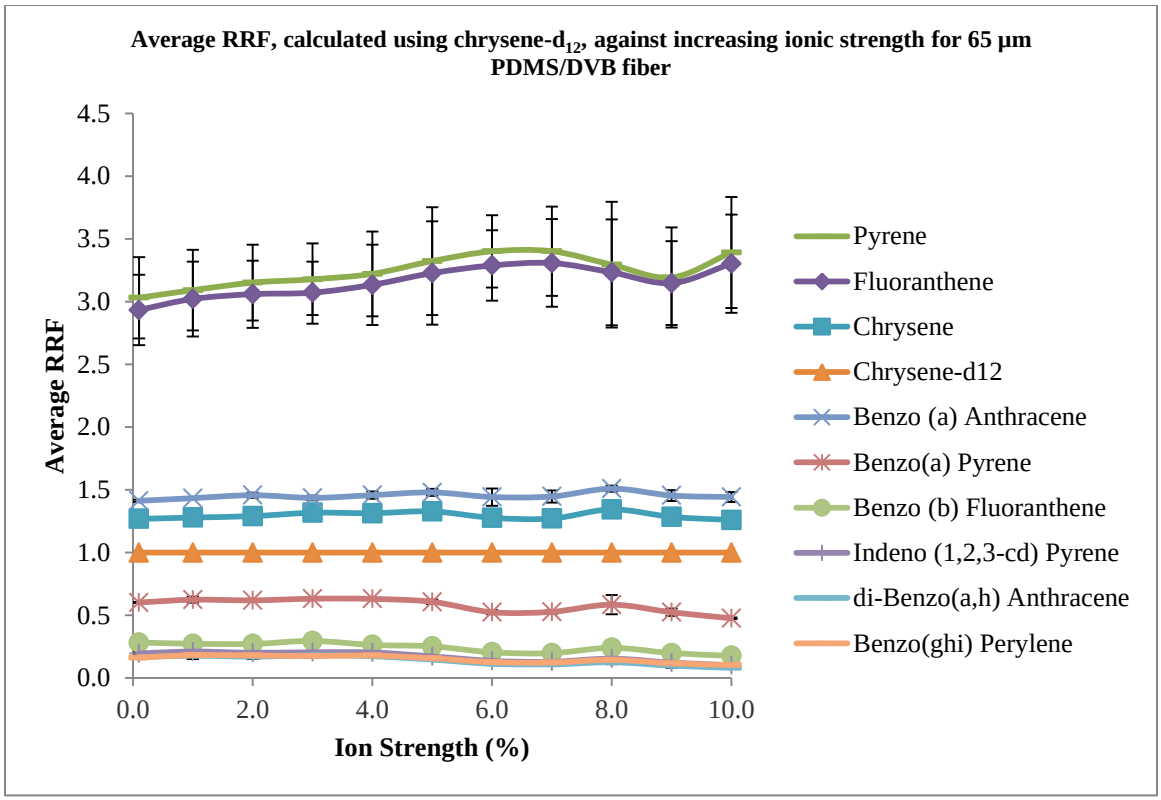

Figure 51 Average RRF, using chrysene-d_{12}, using the 65 µm PDMS/DVB fiber for ionic strength. (RRF = relative response factor)

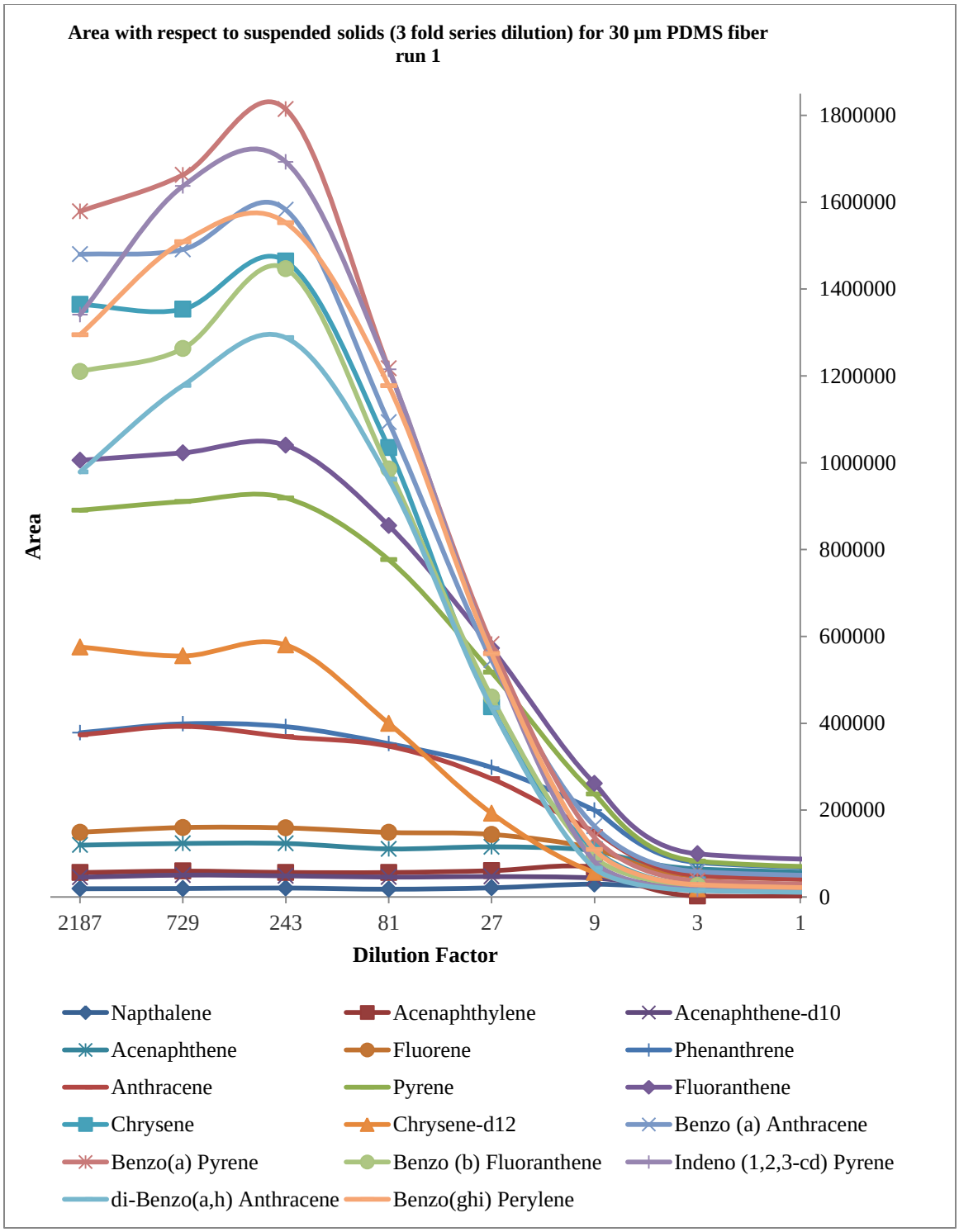

Figure 52 Area of PAHs with respect to suspended solids, by increasing concentration, using the 30 µm PDMS fiber run 1.

`

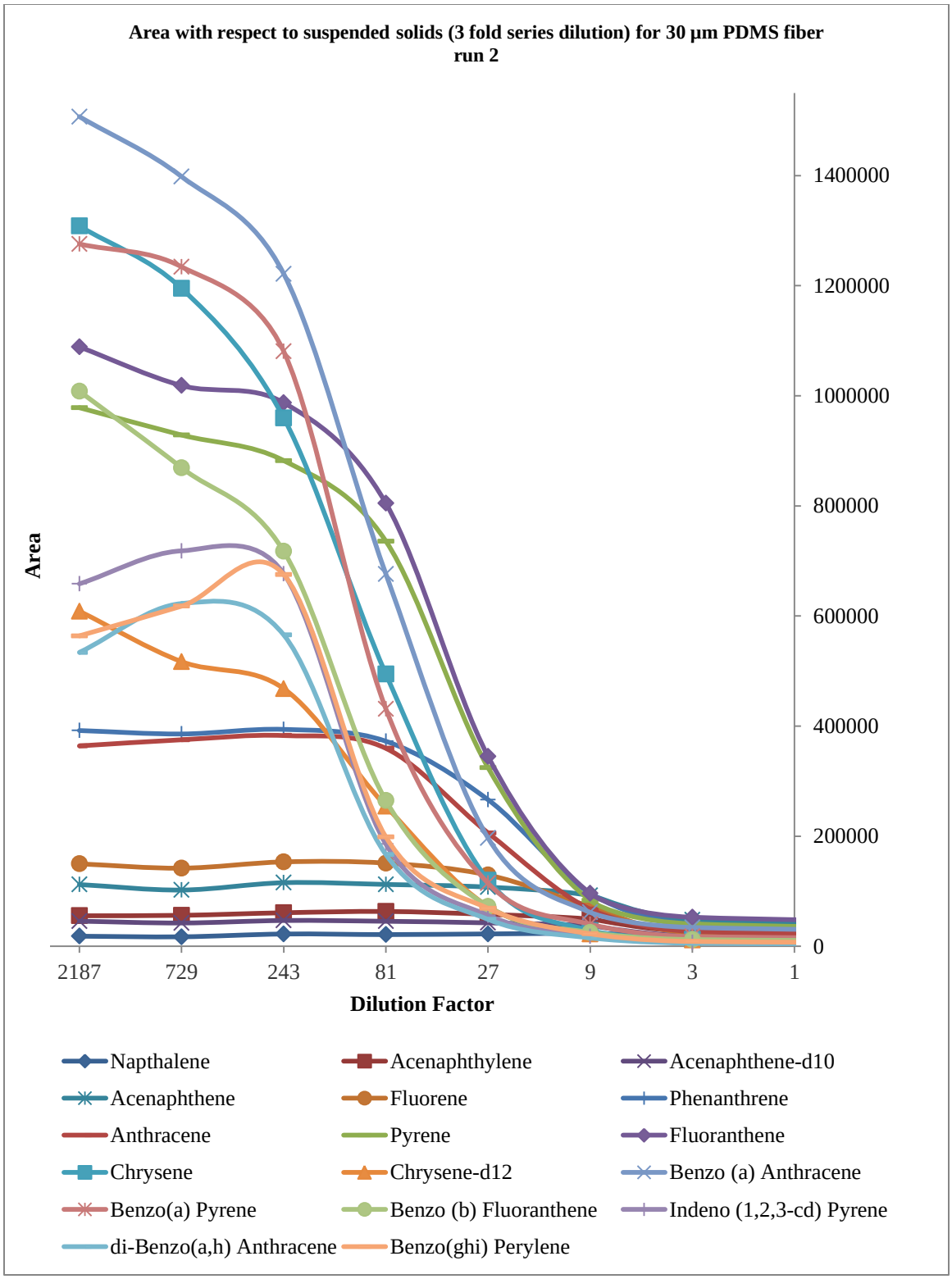

Figure 53 Area of PAHs with respect to suspended solids, by increasing concentration, using the 30 µm PDMS fiber run 2.

`

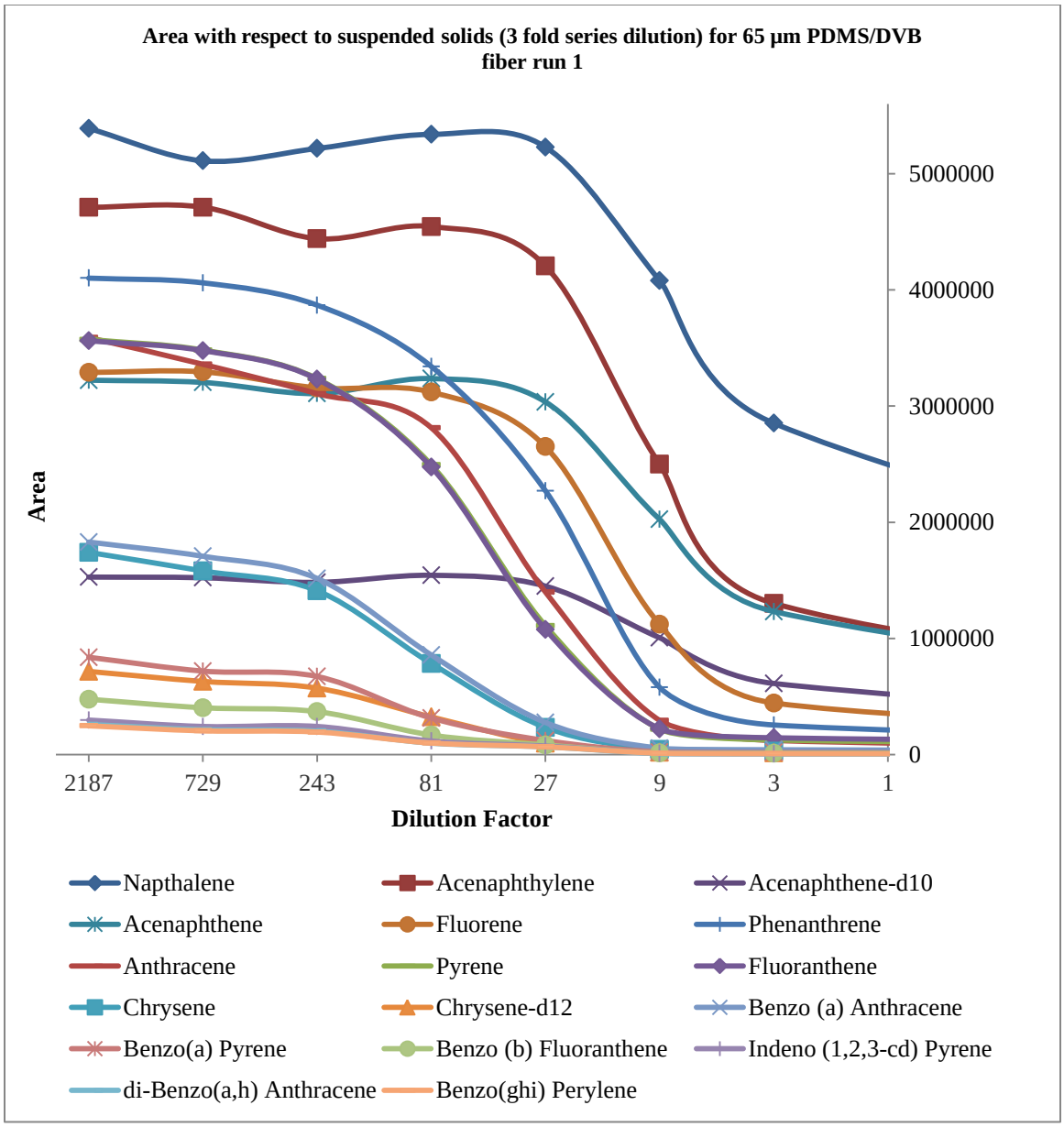

Figure 54 Area of PAHs with respect to suspended solids, by increasing concentration, using the 65 µm PDMS/DVB fiber run 1.

`

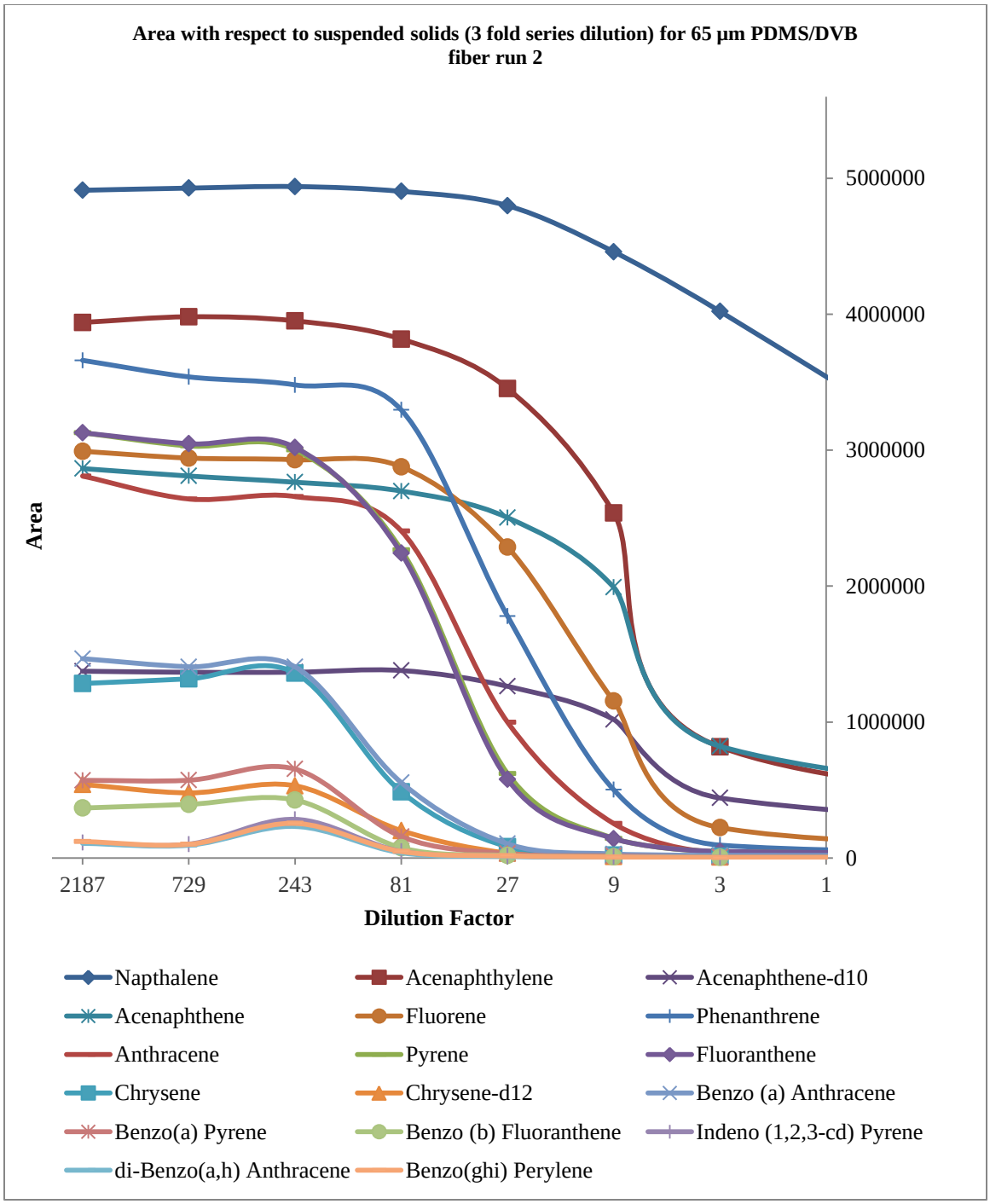

Figure 55 Area of PAHs with respect to suspended solids, by increasing concentration, using the 65 µm PDMS/DVB fiber run 2.

`

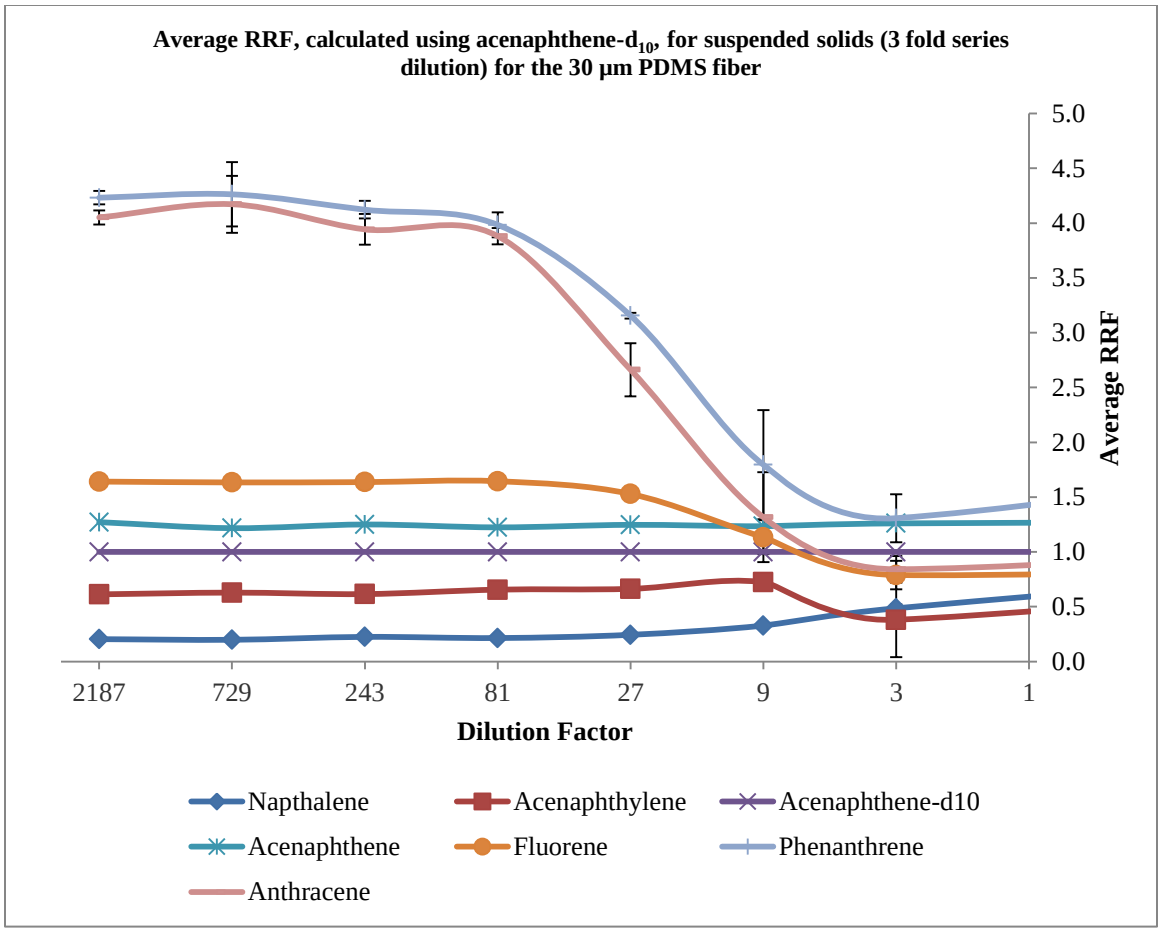

Figure 56 Average RRF, using acenaphthene-d_{10}, using the 30 µm PDMS fiber for suspended solids. (RRF = relative response factor)

`

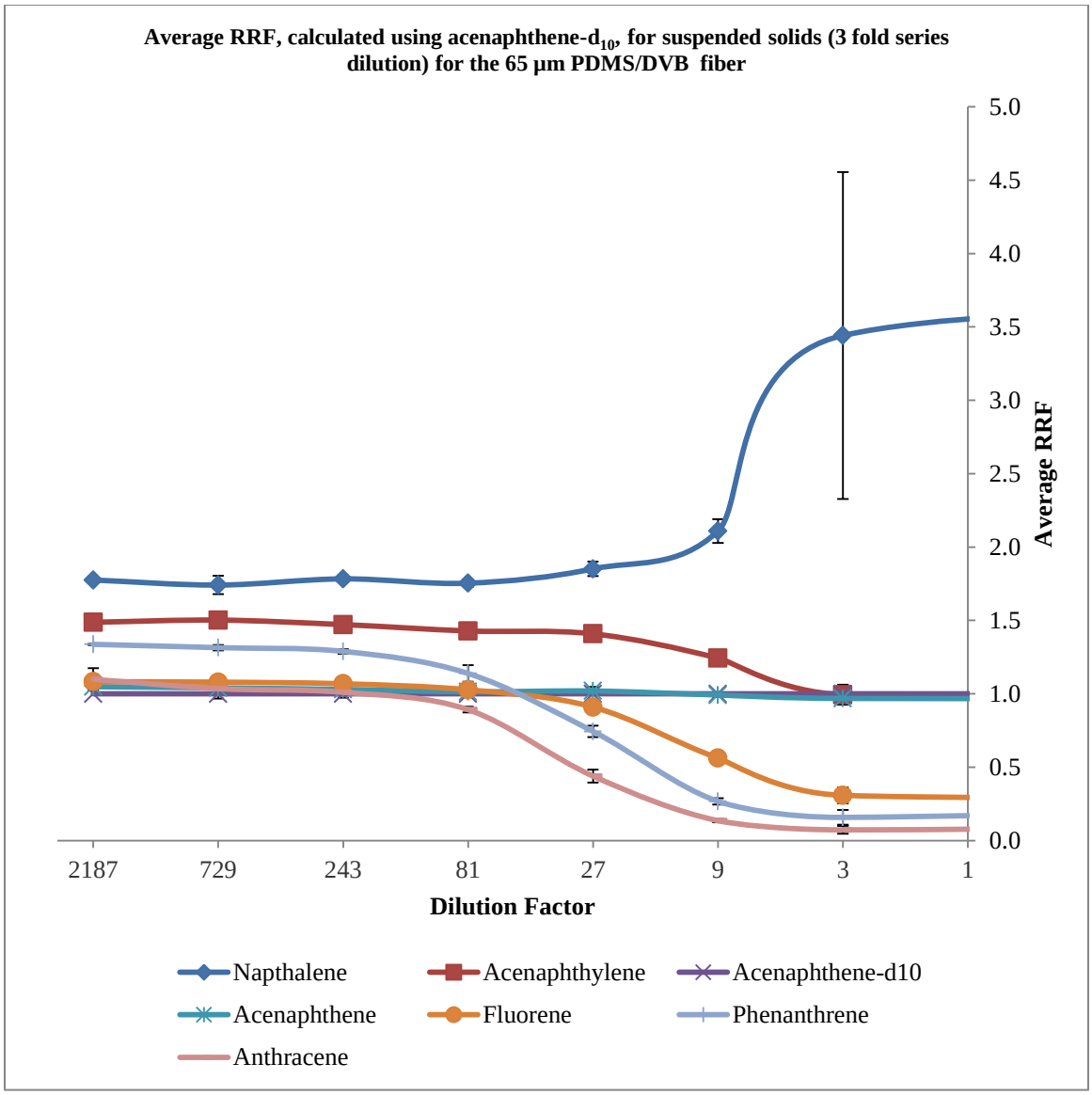

Figure 57 Average RRF, using acenaphthene-d_{10}, using the 65 µm PDMS/DVB fiber for suspended solids. (RRF = relative response factor)

`

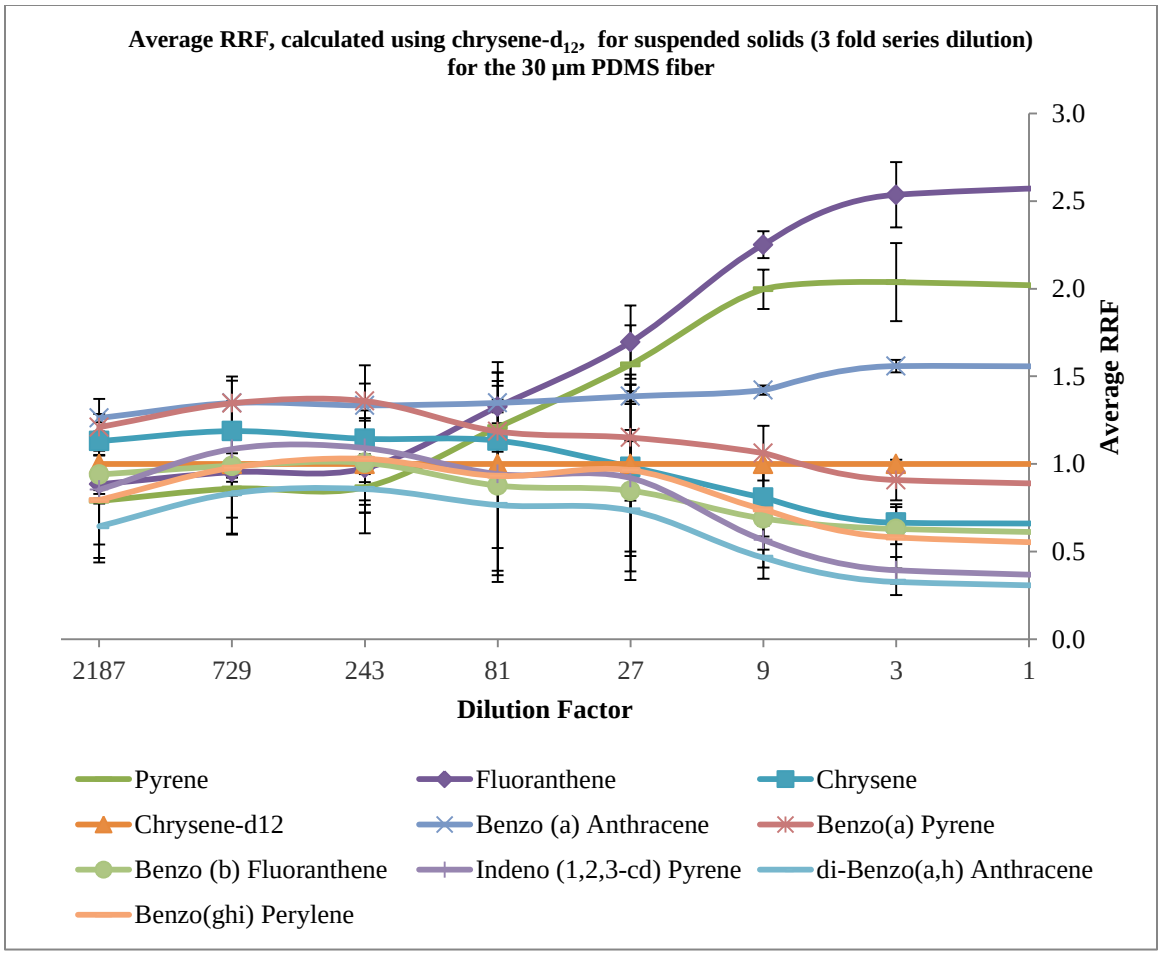

Figure 58 Average RRF, using chrysene-d_{12}, for the 30 µm PDMS fiber for suspended solids. (RRF = relative response factor)

`

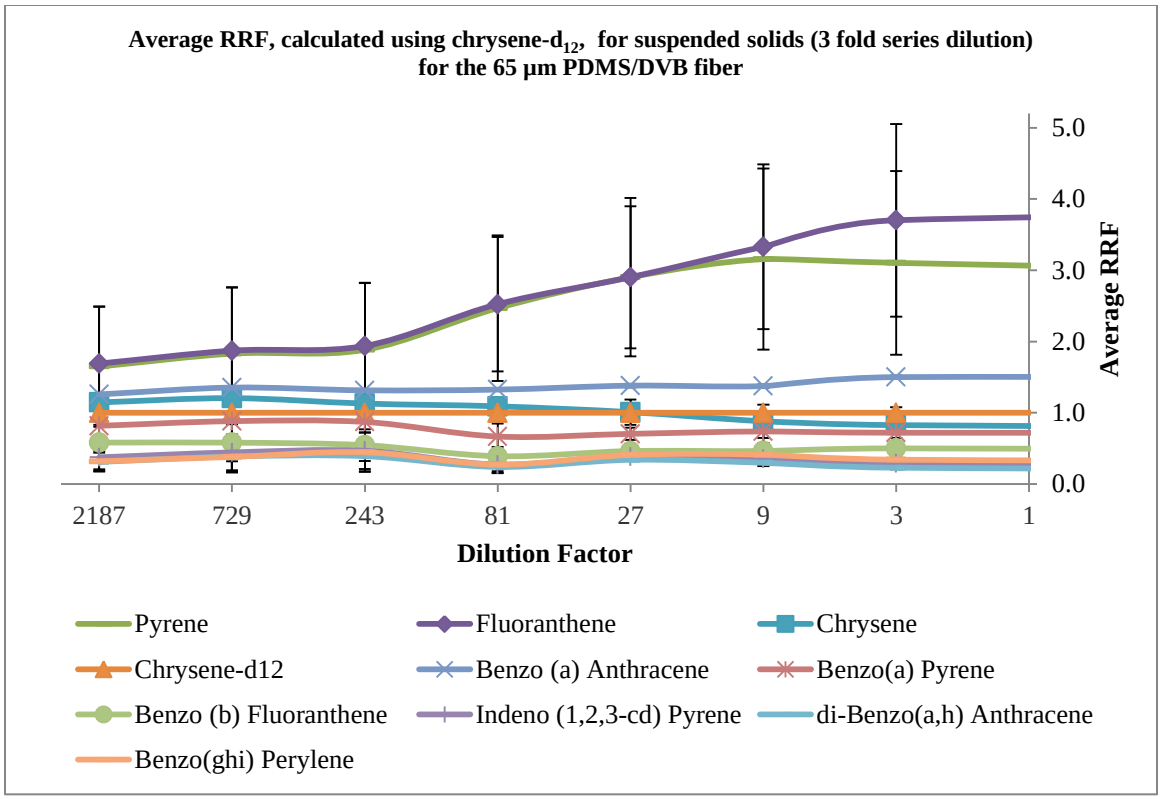

Figure 59 Average RRF, using chrysene-d_{12}, for the 65 µm PDMS/DVB fiber for suspended solids. (RRF = relative response factor)

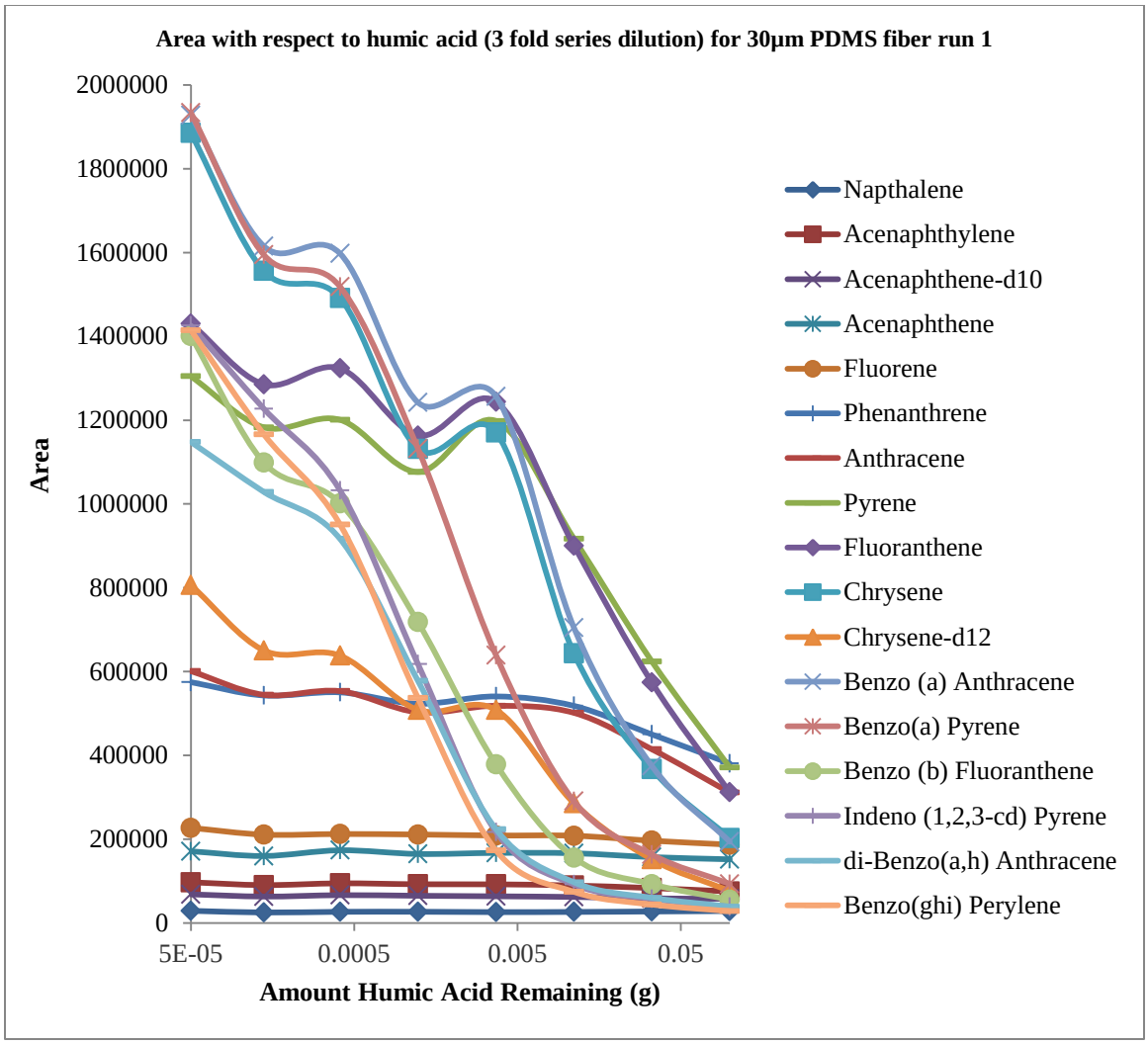

Figure 60 Area with respect to humic acid (3 fold series dilution) for 30 µm PDMS fiber run 1.

`

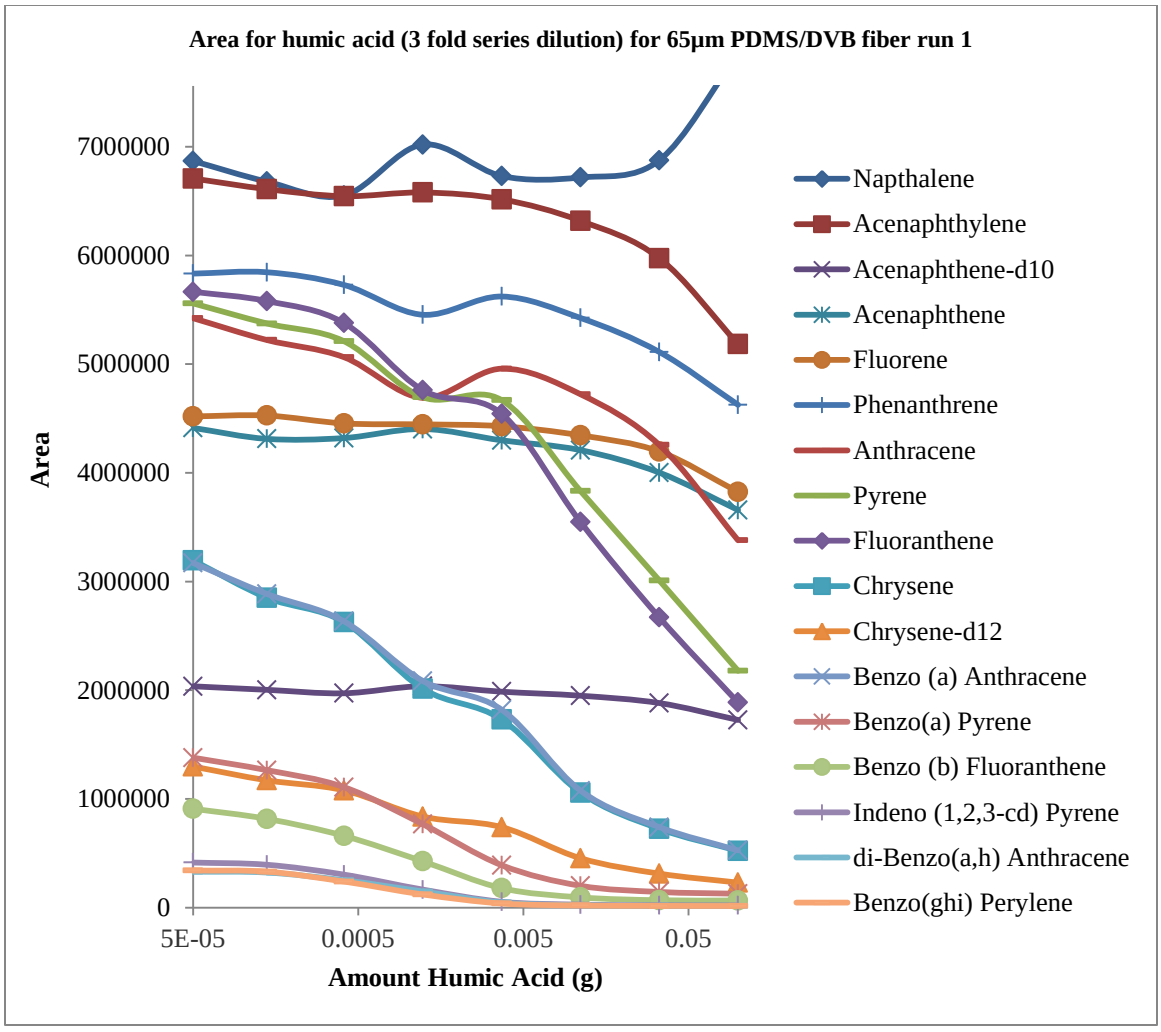

Figure 61 Area with respect to humic acid (3 fold series dilution) for 65 µm PDMS/DVB fiber run 1.

`

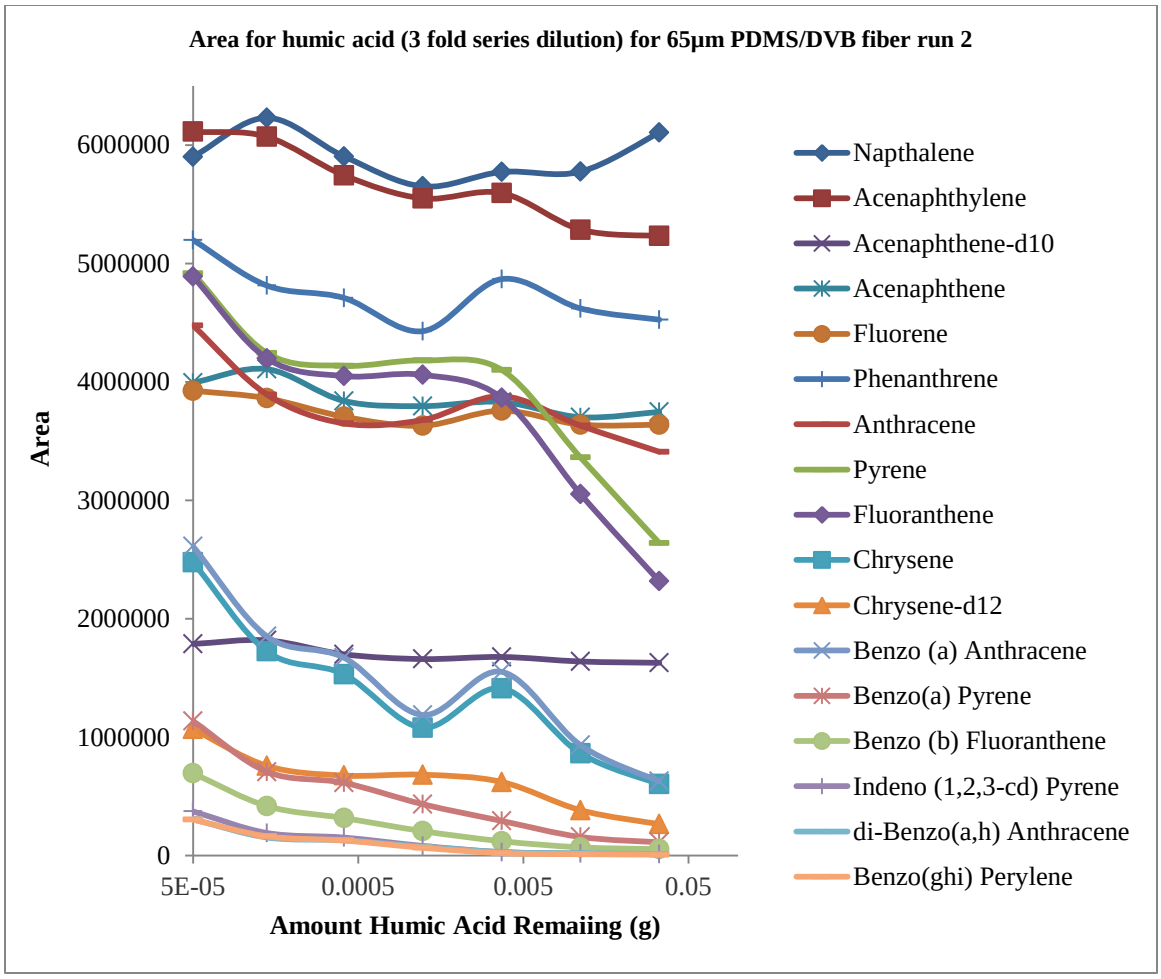

Figure 62 Area with respect to humic acid (3 fold series dilution) for 65 µm PDMS/DVB fiber run 2.

`

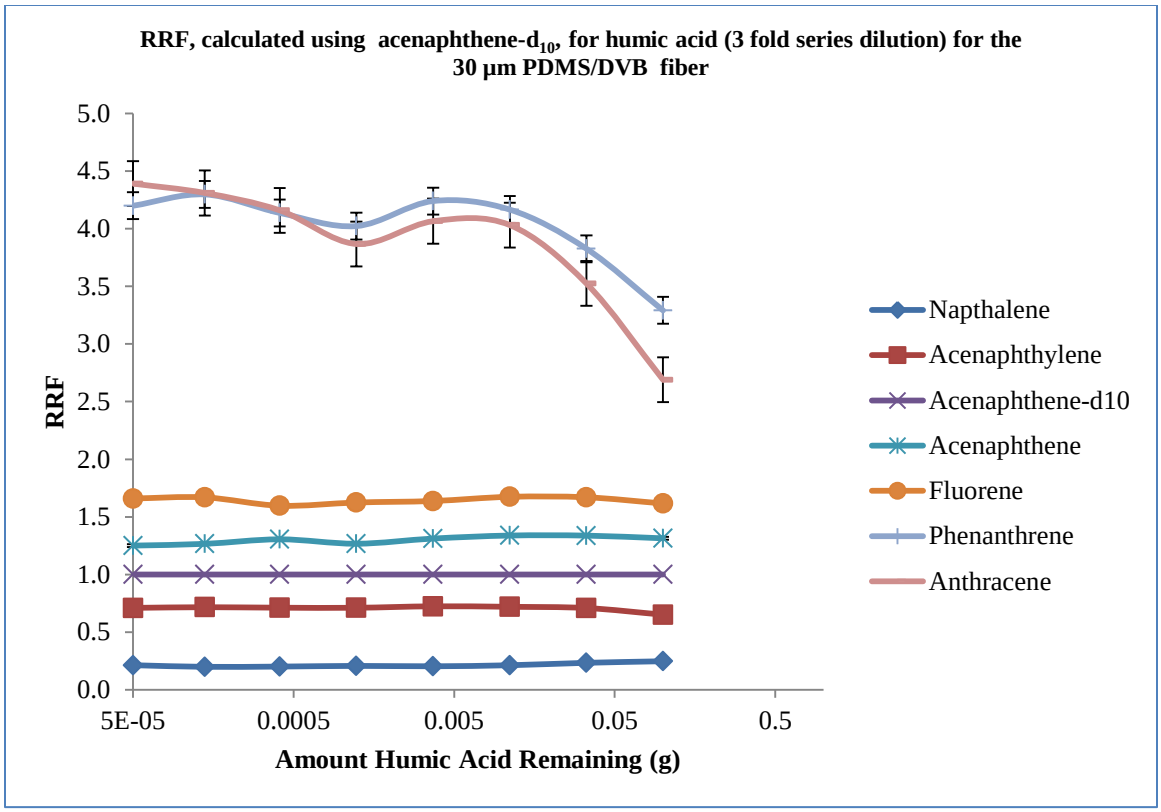

Figure 63 Average RRF, using acenaphthene-d_{10}, for the 30 µm PDMS fiber for humic acid. (RRF = relative response factor)

`

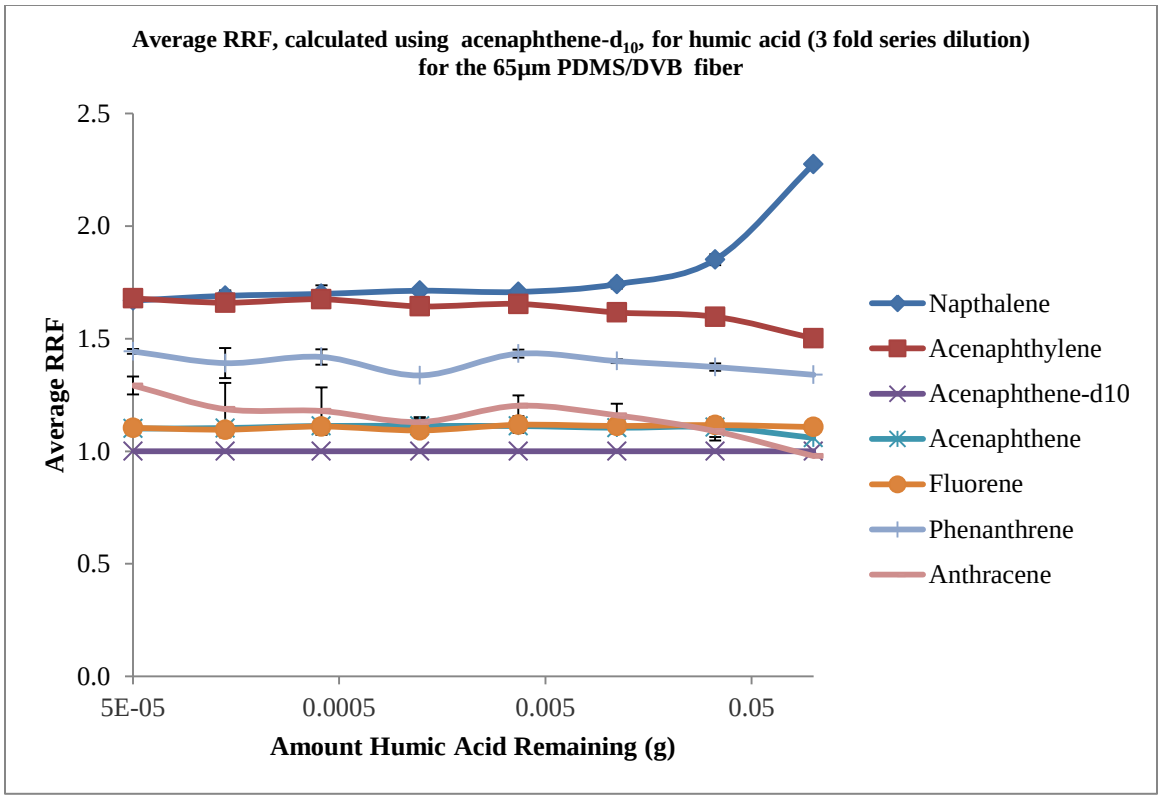

Figure 64 Average RRF, using acenaphthene-d_{10}, for the 65 µm PDMS/DVB fiber for humic acid. (RRF = relative response factor)

`

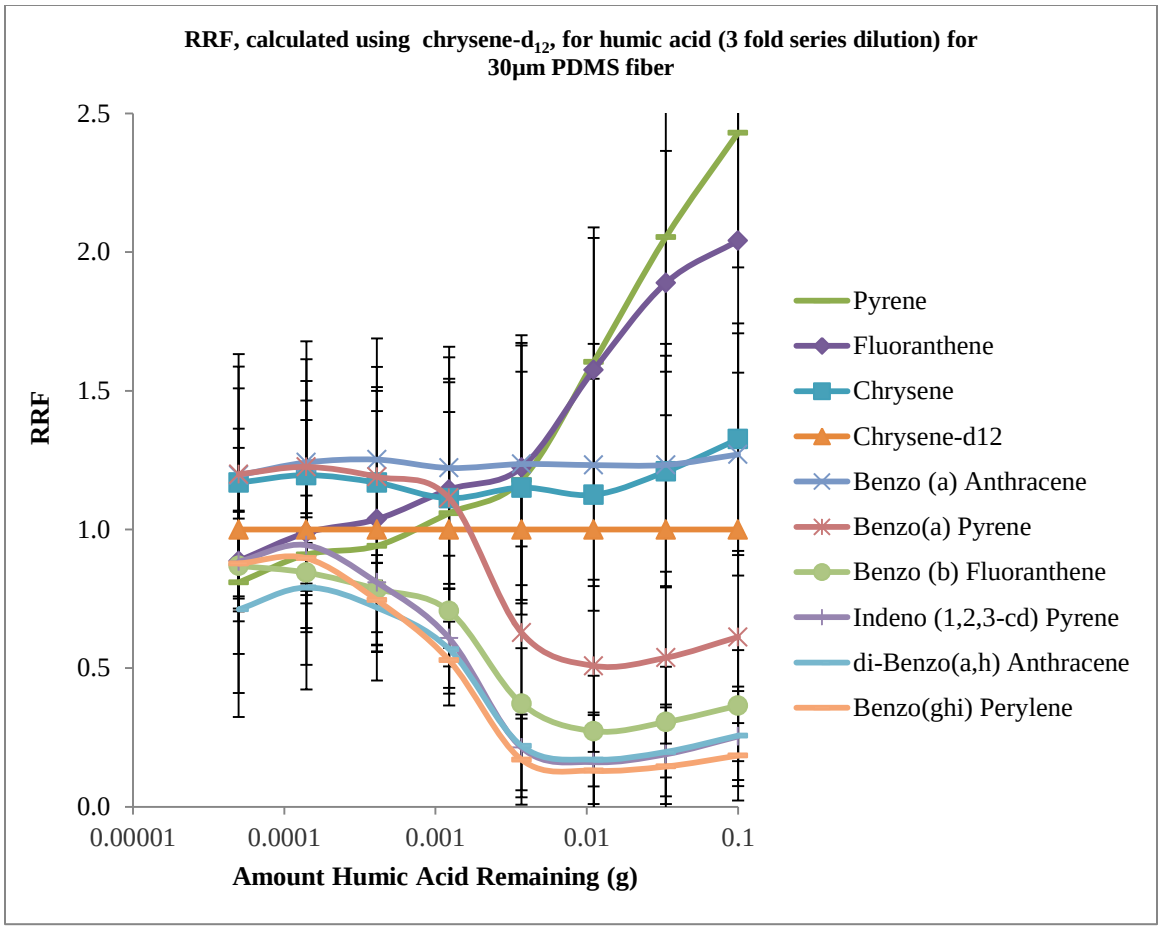

Figure 65 Average RRF, using chrysene-d_{12}, for the 30 µm PDMS fiber for humic acid. (RRF = relative response factor)

`

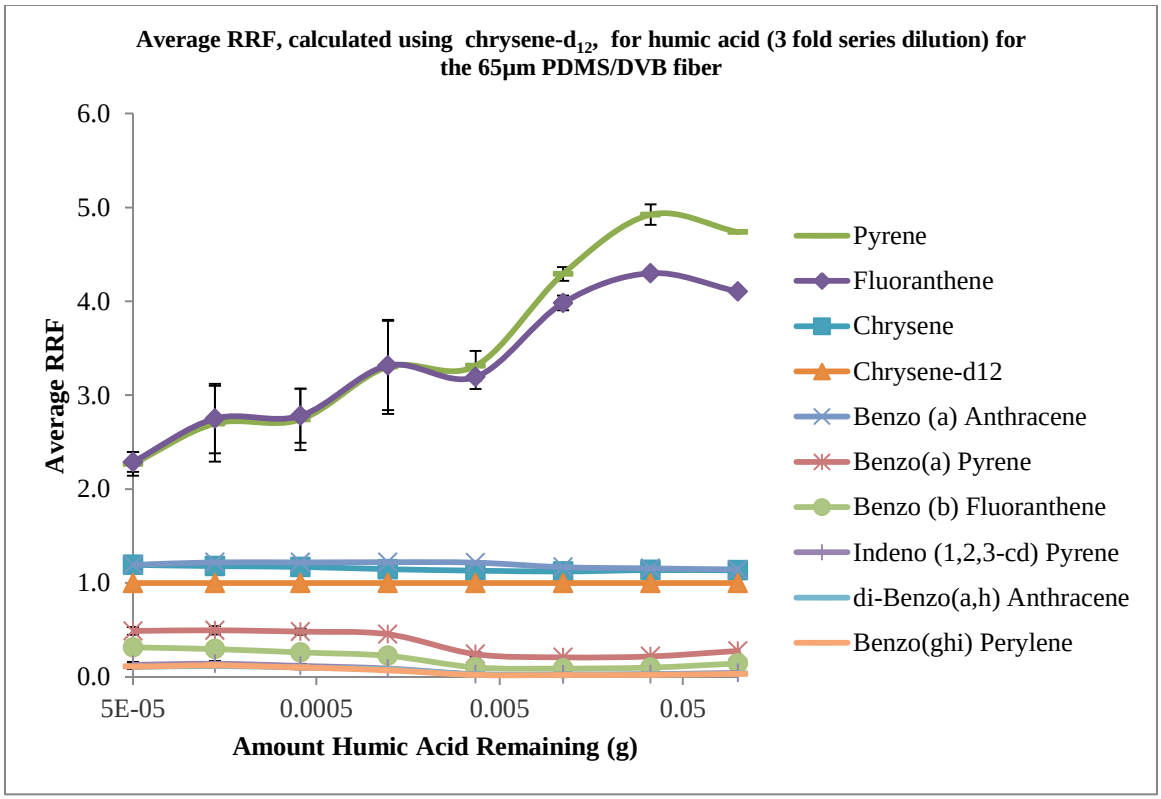

Figure 66 Average RRF, using chrysene-d_{12}, for the 65 µm PDMS/DVB fiber for humic acid. (RRF = relative response factor)

`

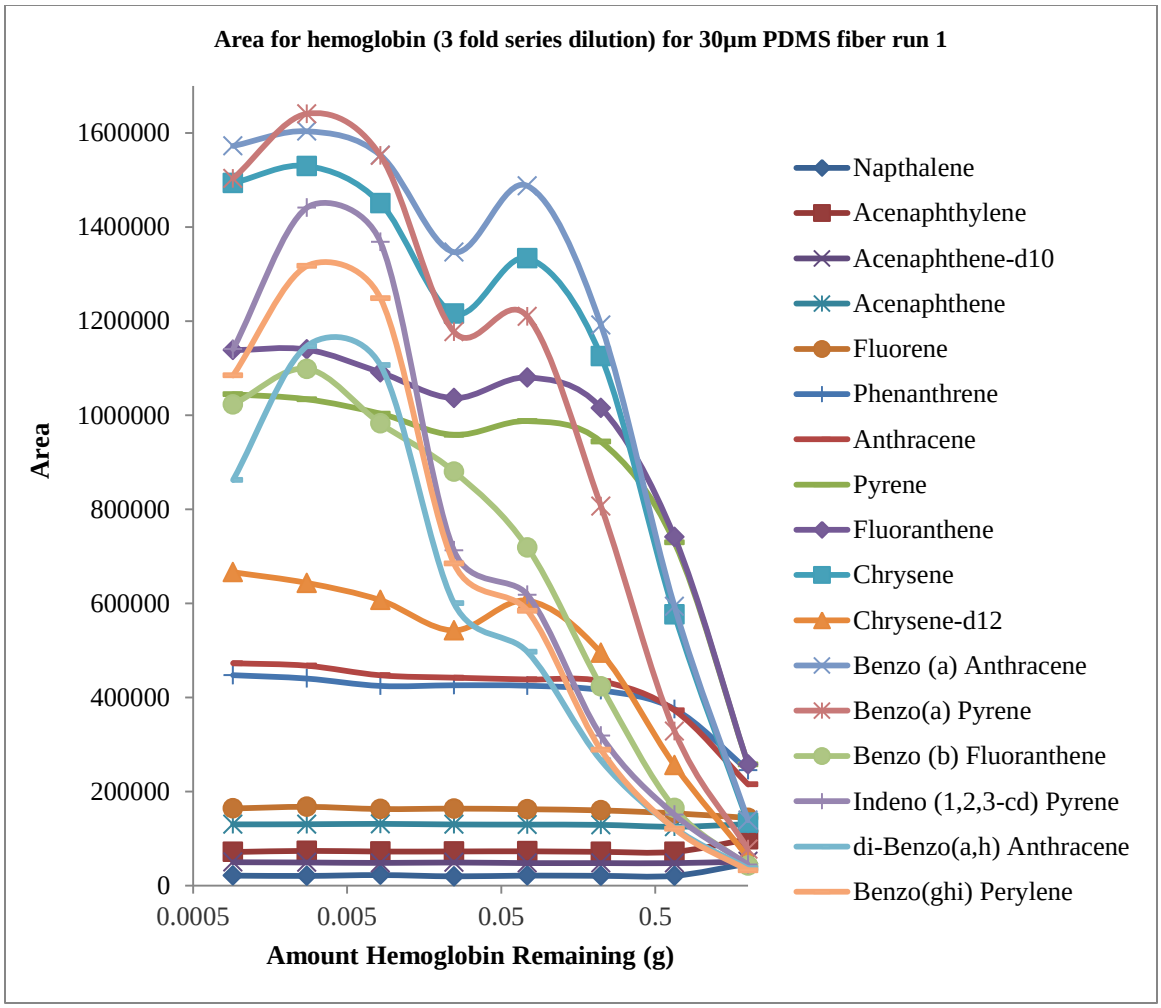

Figure 67 Area with respect to hemoglobin (3 fold series dilution) for 30 µm PDMS fiber run 1.

`

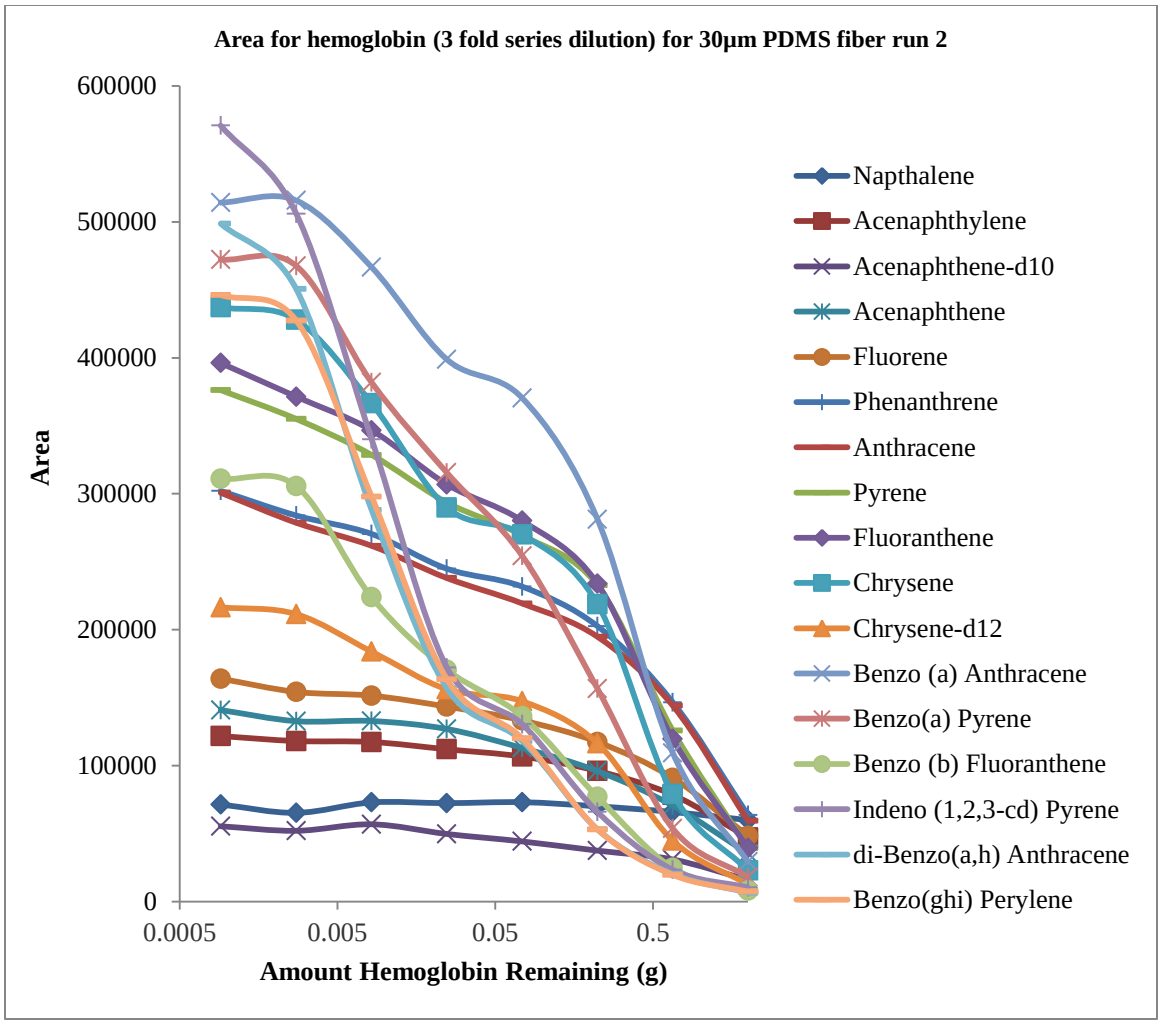

Figure 68 Area with respect to hemoglobin (3 fold series dilution) for 30 µm PDMS fiber run 2.

`

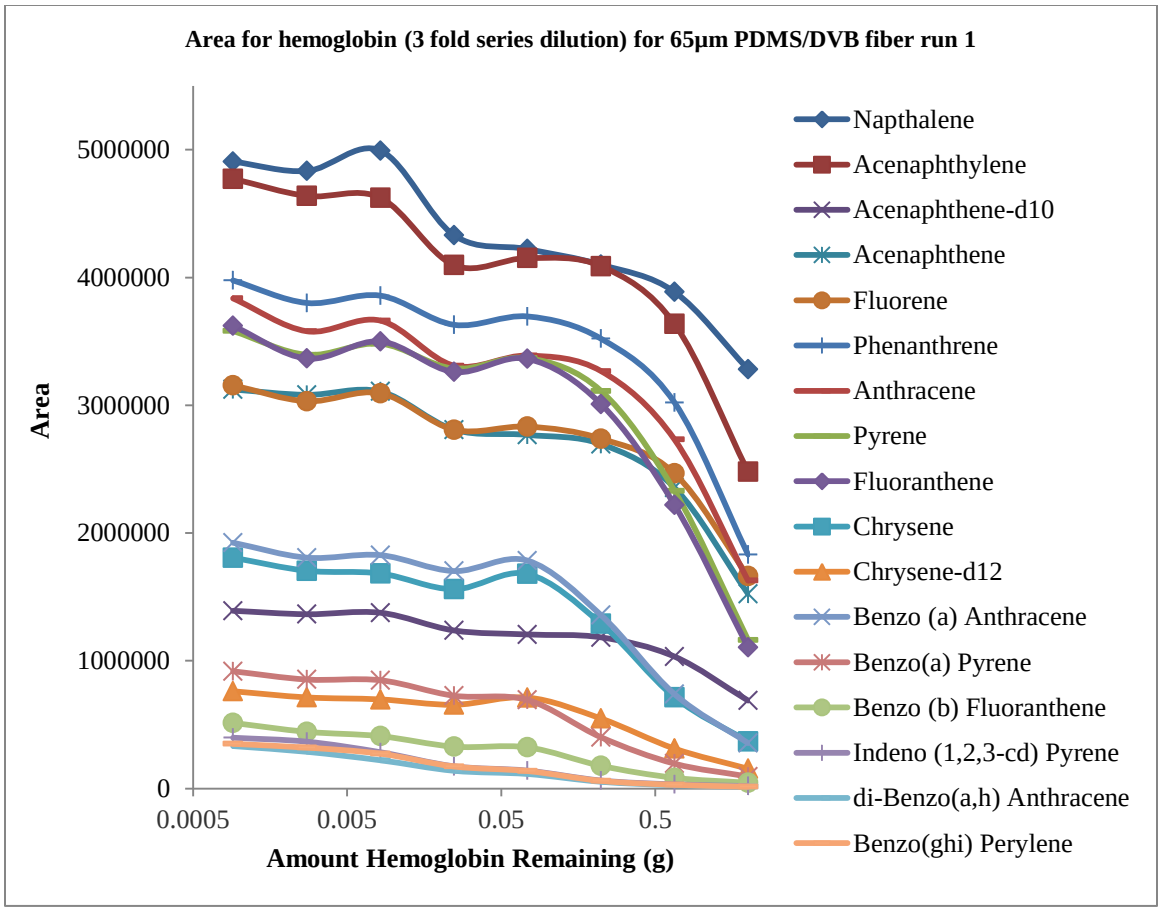

Figure 69 Area with respect to hemoglobin (3 fold series dilution) for 65 µm PDMS/DVB fiber run 1.

`

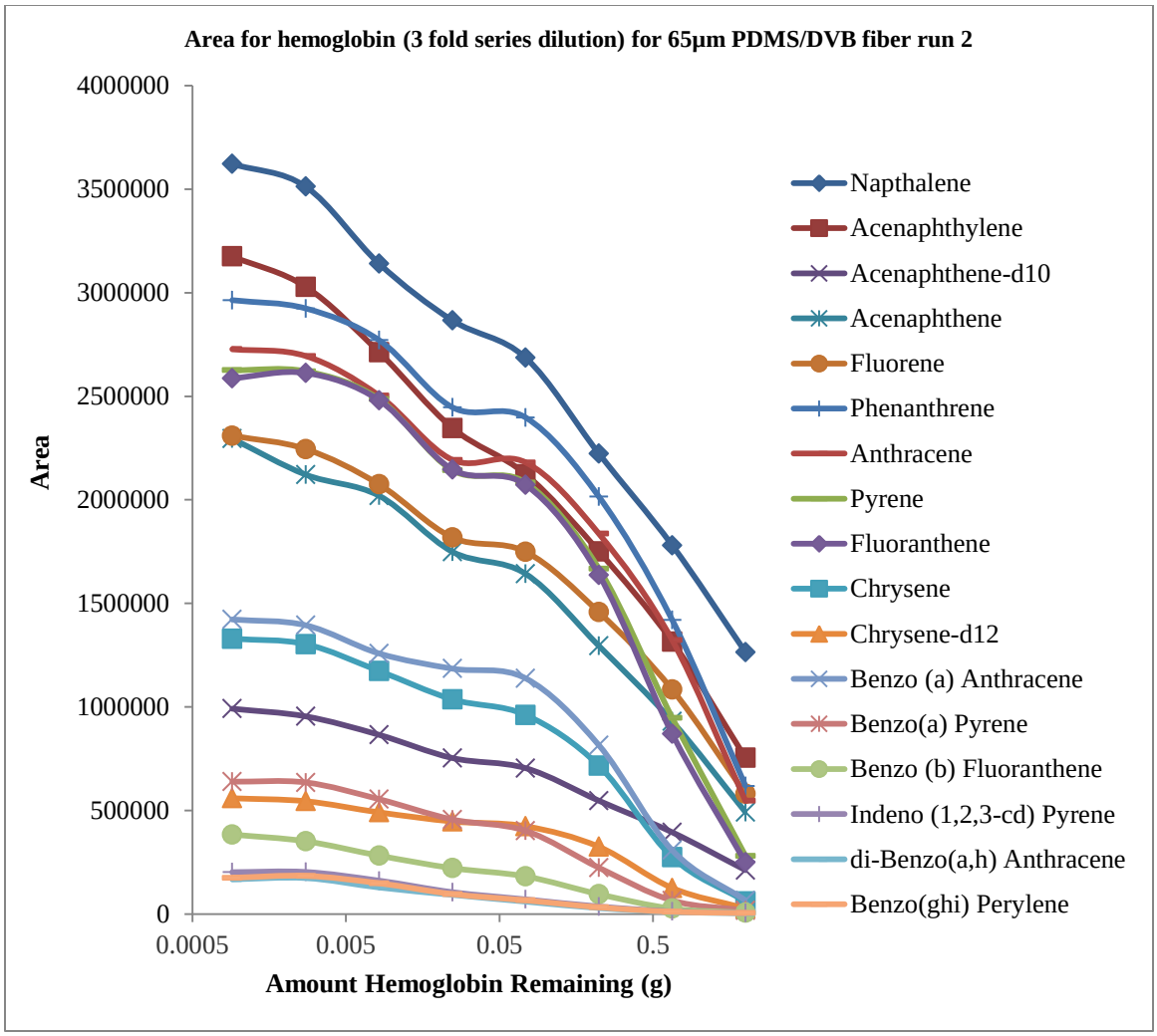

Figure 70 Area with respect to hemoglobin (3 fold series dilution) for 65 µm PDMS/DVB fiber run 2.

`

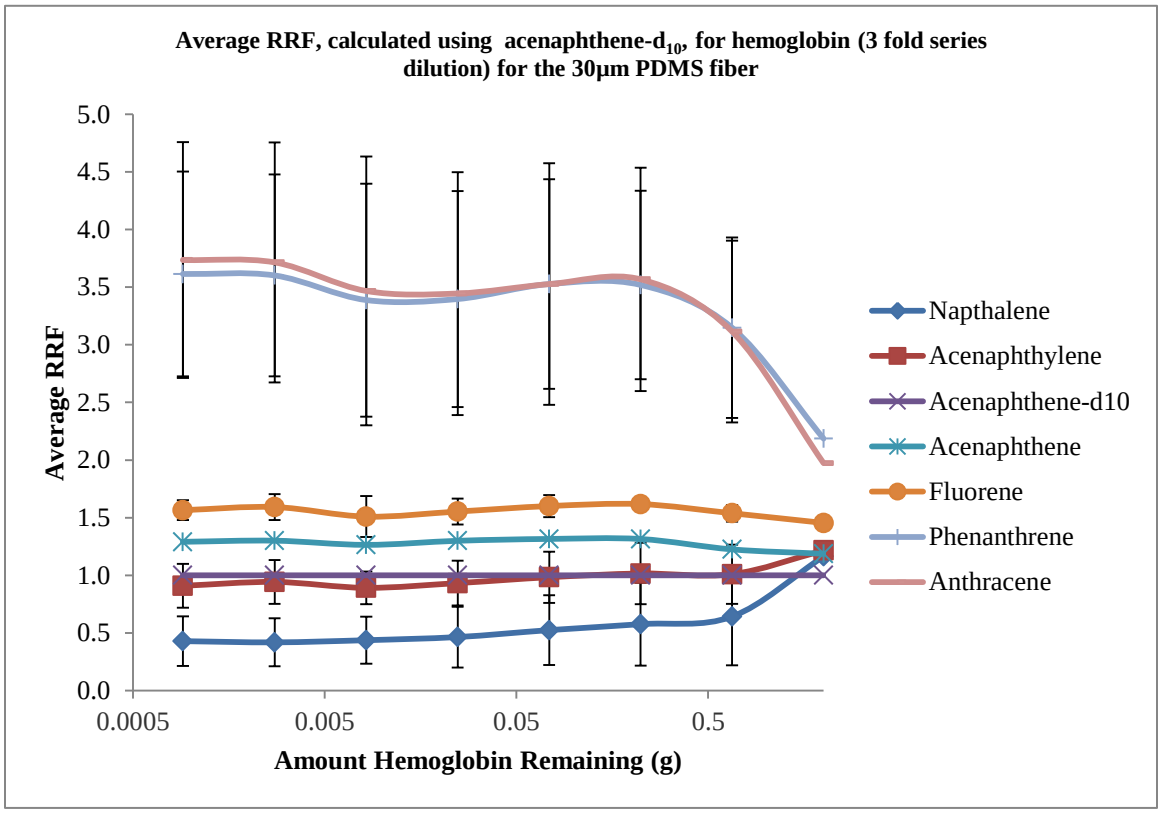

Figure 71 Average RRF, using acenaphthene-d_{10}, using the 30 µm PDMS fiber for hemoglobin. (RRF = relative response factor)

`

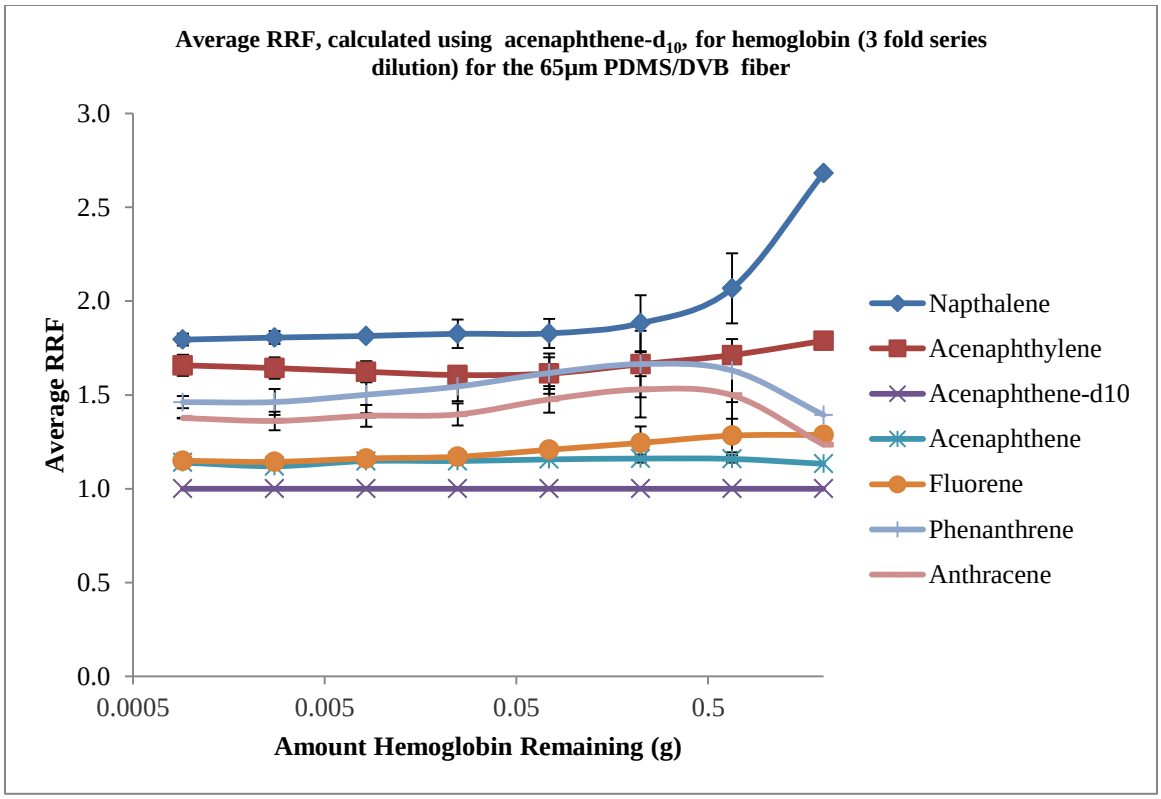

Figure 72 Average RRF, using acenaphthene-d_{10}, using the 65 µm PDMS/DVB fiber for hemoglobin. (RRF = relative response factor)

`

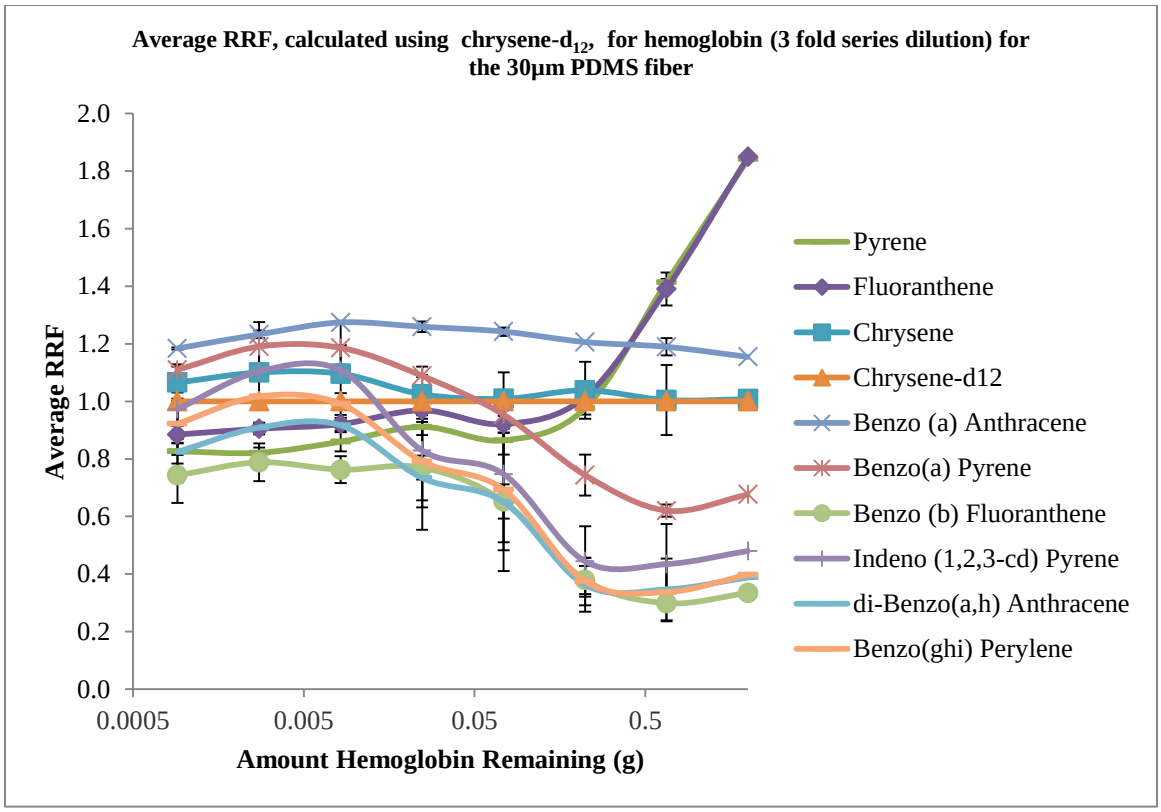

Figure 73 Average RRF, using chrysene-d_{12}, using the 30 µm PDMS fiber for hemoglobin. (RRF = relative response factor)

`

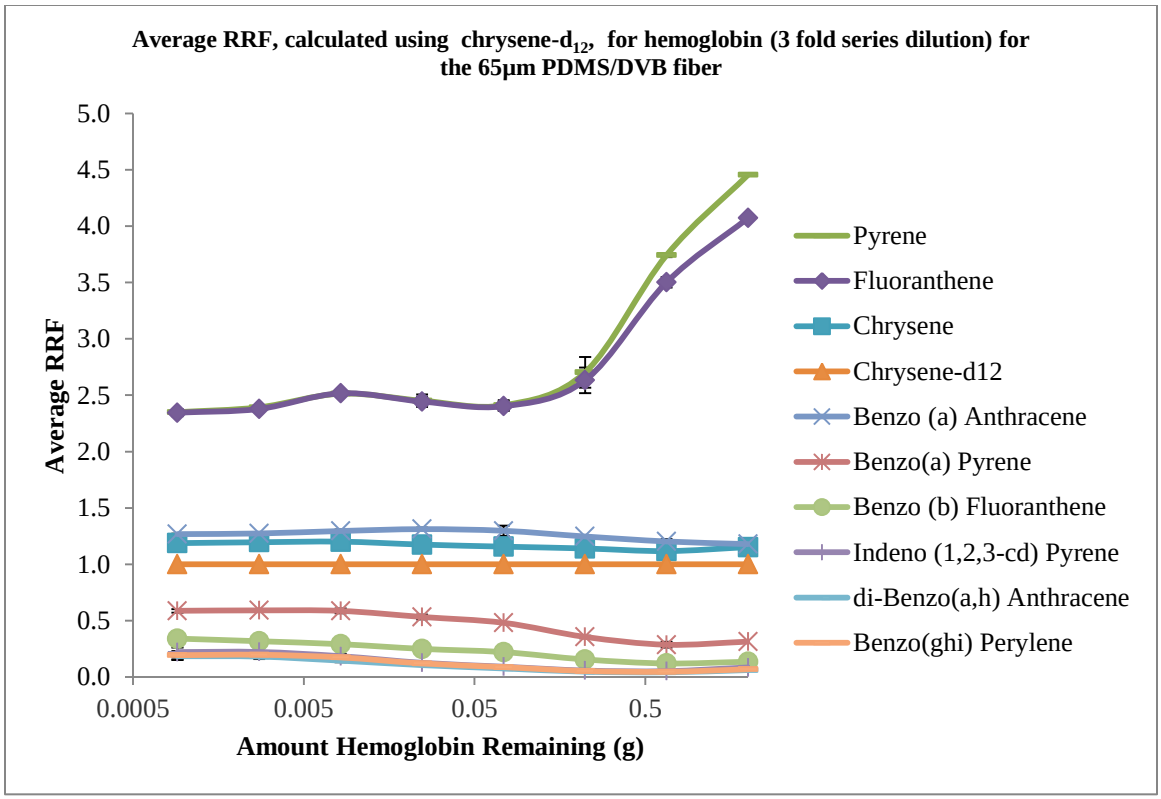

Figure 74 Average RRF, using chrysene-d_{12}, using the 65 µm PDMS/DVB fiber for hemoglobin. (RRF = relative response factor)

`

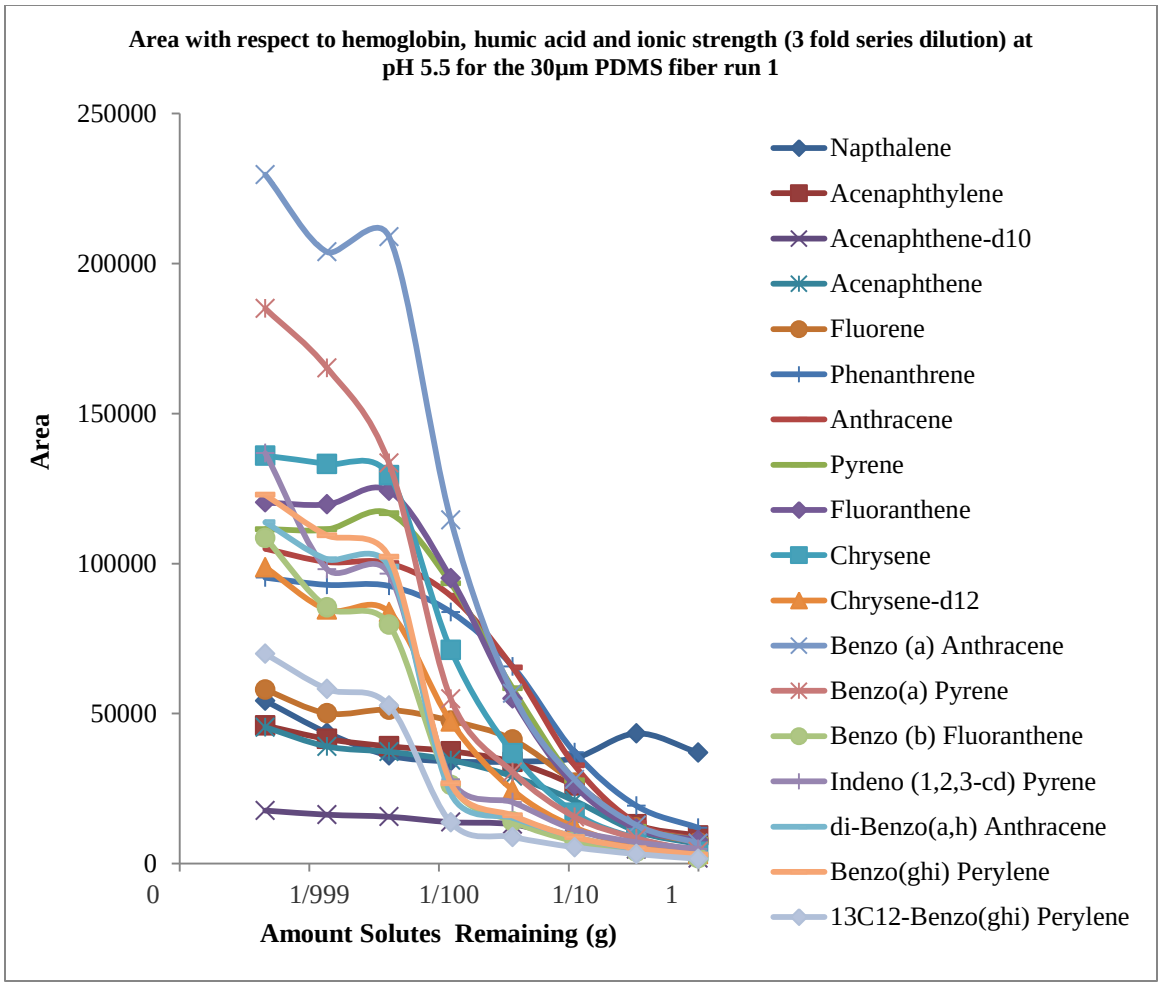

Figure 75 Area with respect to ion strength, humic acid and hemoglobin at a pH 5.5 (3 fold series dilution) using the 30 µm PDMS fiber run 1.

`

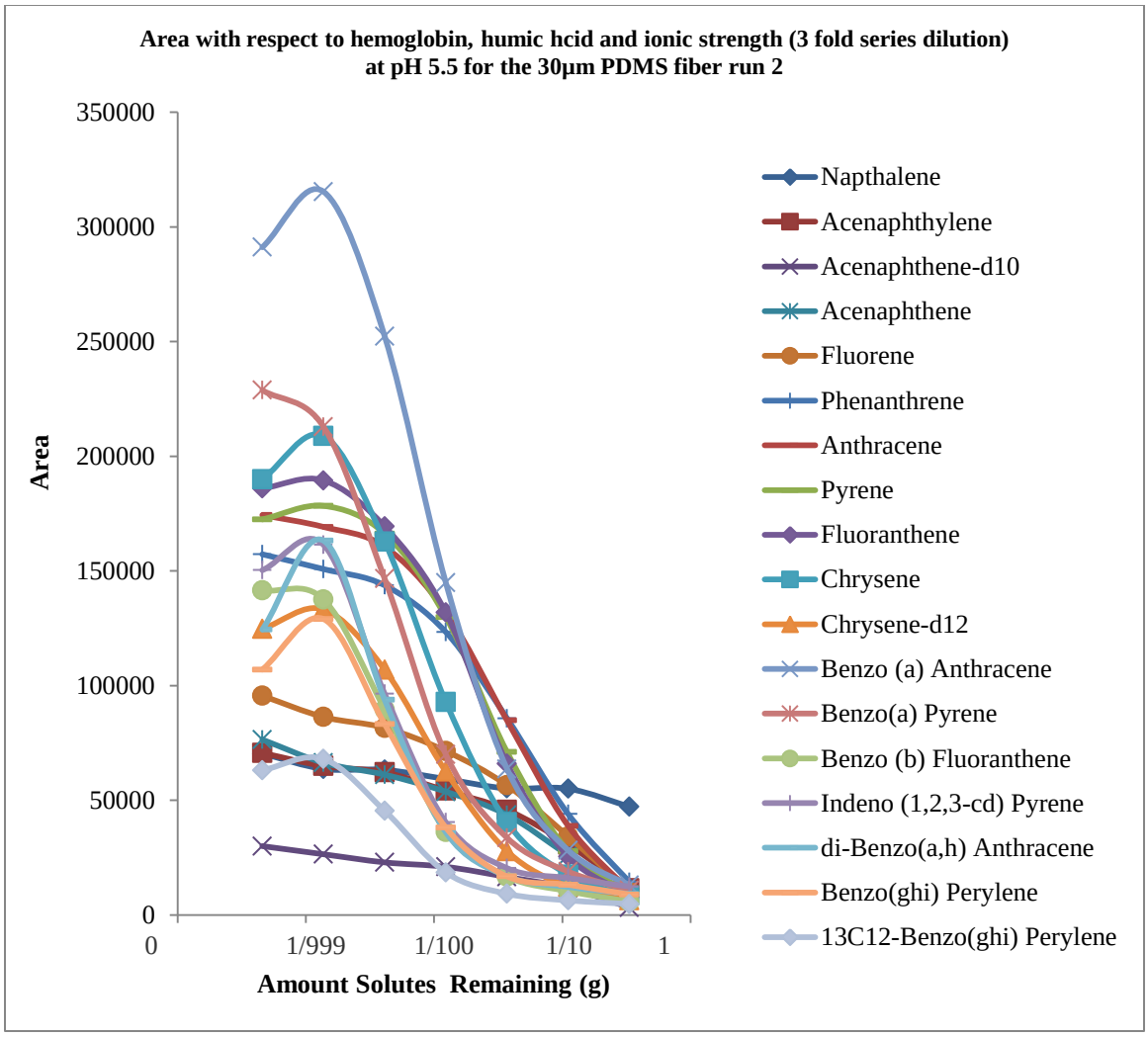

Figure 76 Area with respect to ionic strength, humic acid and hemoglobin at a pH 5.5 (3 fold series dilution) using the 30 µm PDMS fiber run 2.

`

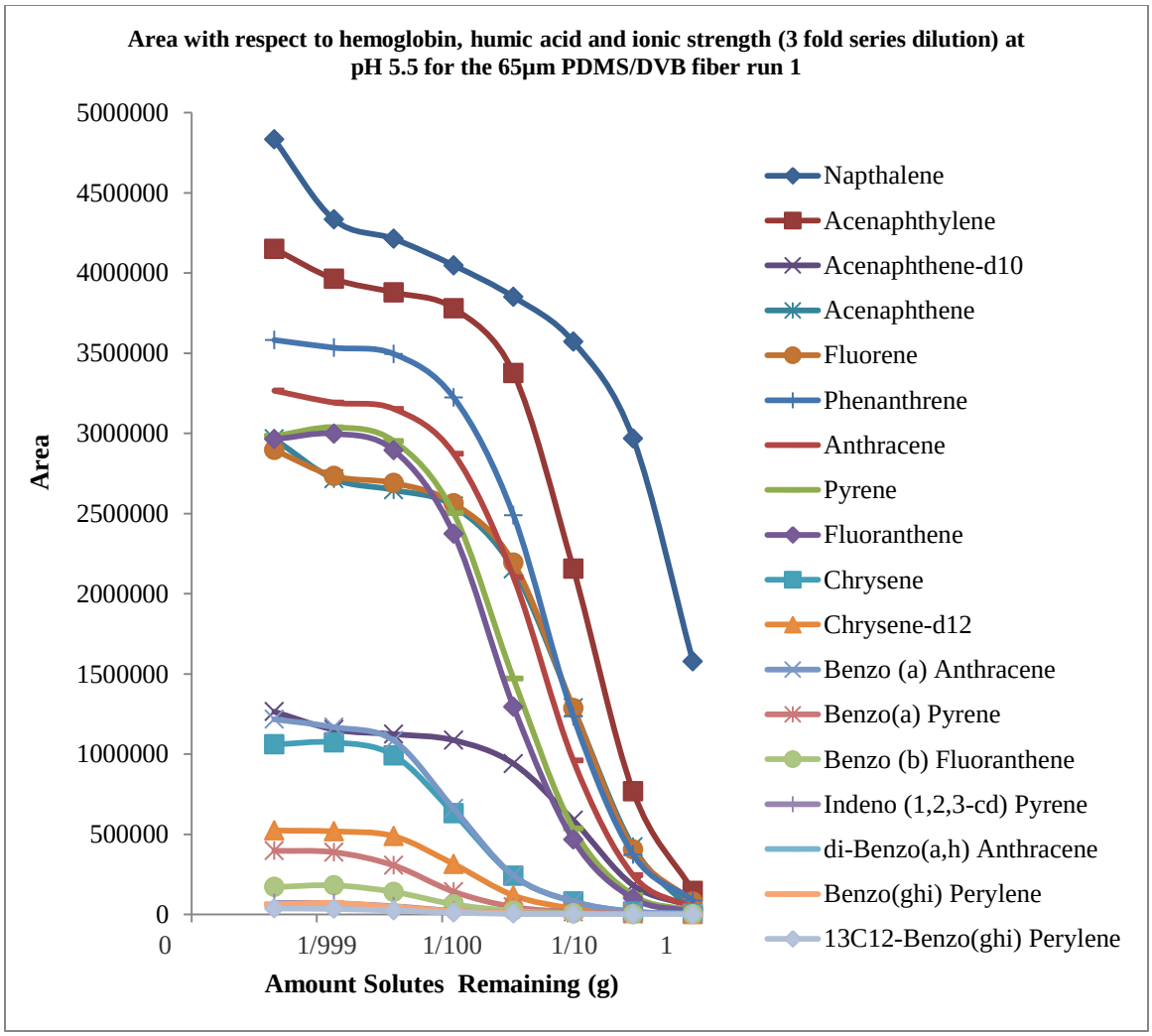

Figure 77 Area with respect to ionic strength, humic acid and hemoglobin at a pH 5.5 (3 fold series dilution) using the 65 µm PDMS/DVB fiber run 1.

`

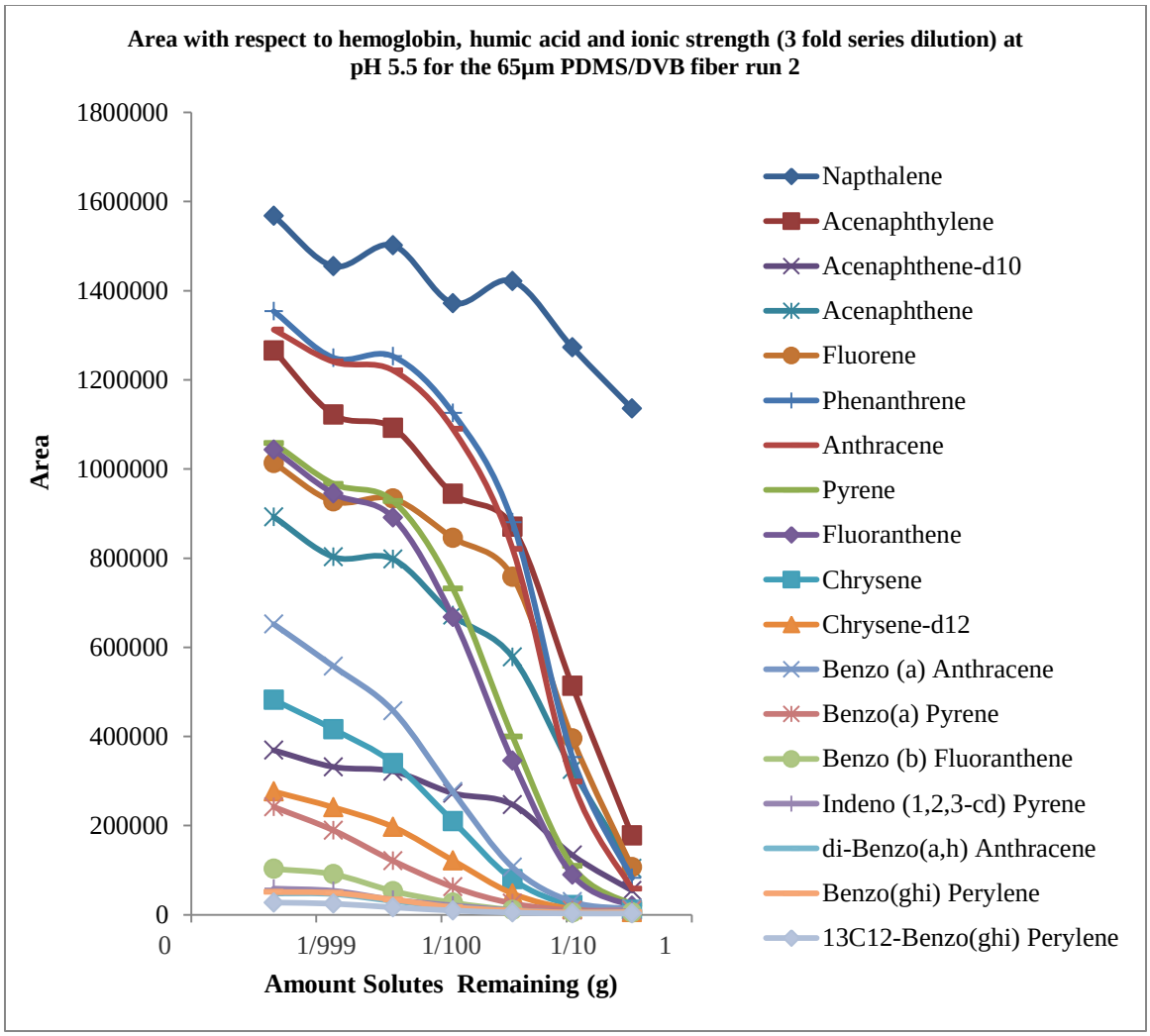

Figure 78 Area with respect to ionic strength, humic acid and hemoglobin at a pH 5.5 (3 fold series dilution) using the 65 µm PDMS/DVB fiber run 2.

`

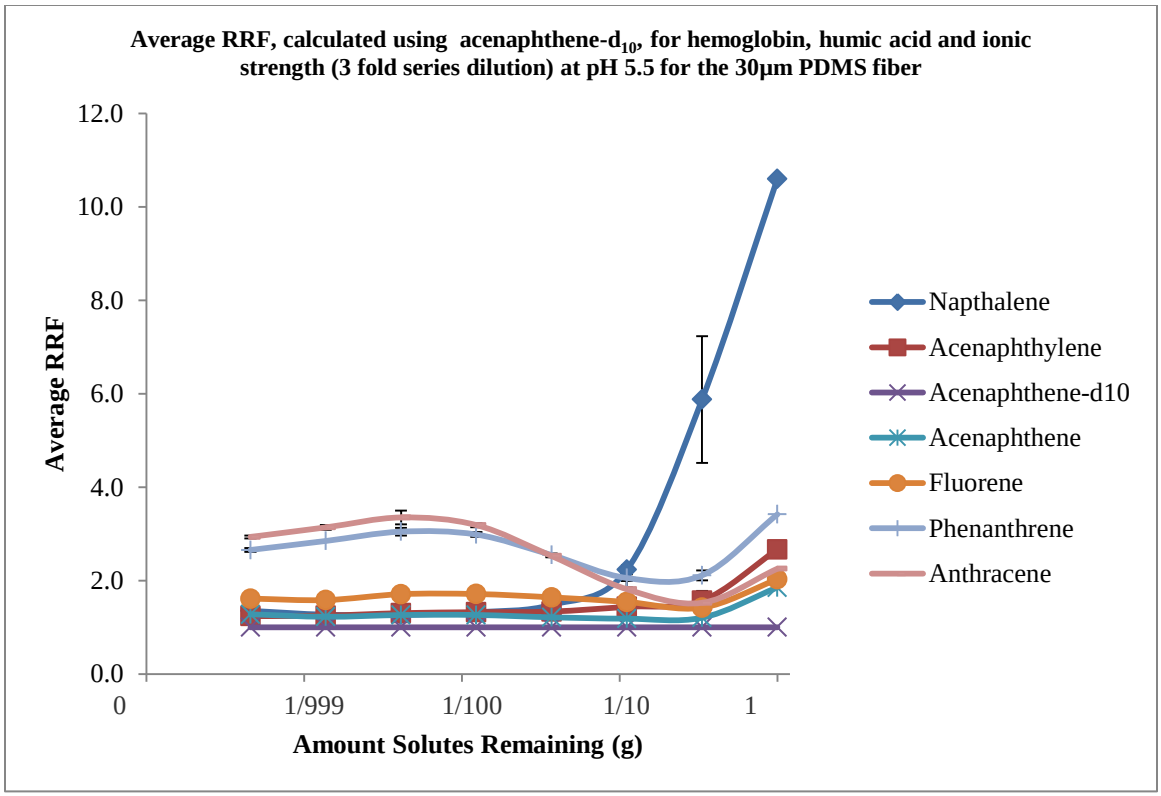

Figure 79 Average RRF (acenaphthene-d_{10}), using the 30 µm PDMS fiber for hemoglobin, humic acid and ionic strength (3 fold series dilution) at pH 5.5. (RRF = relative response factor)

`

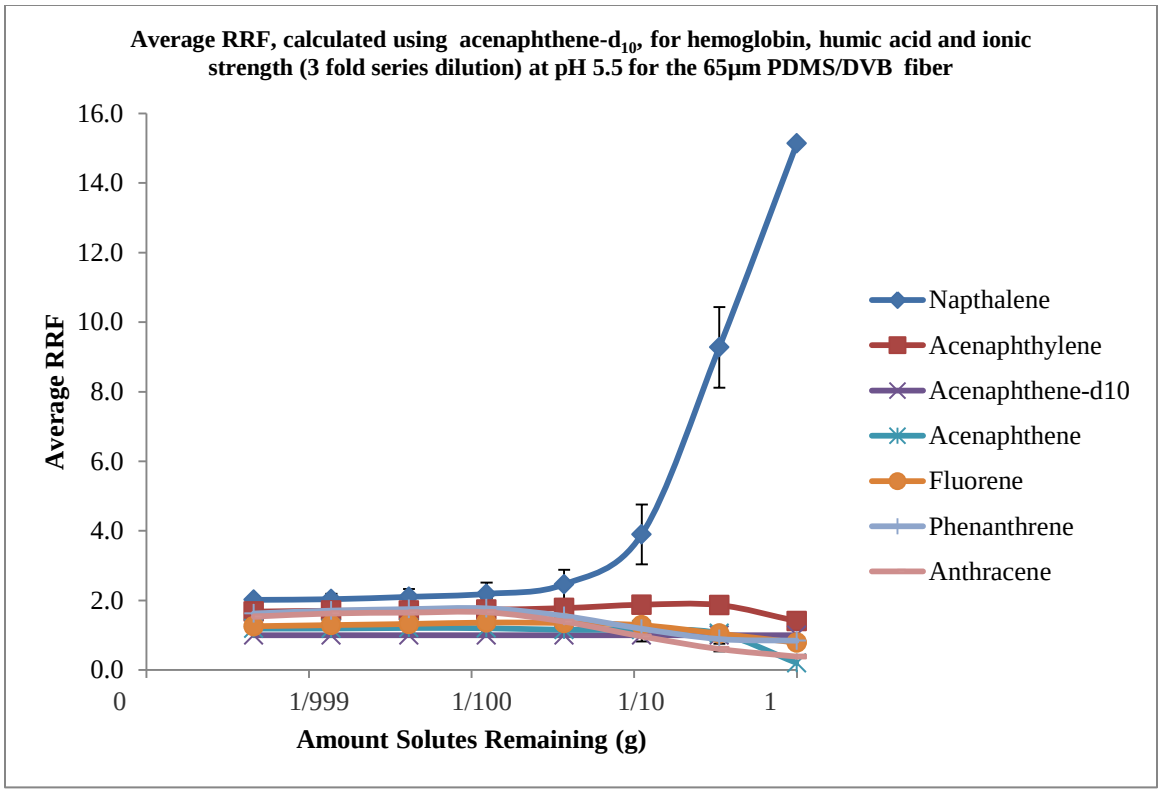

Figure 80 Average RRF (acenaphthene-d_{10}), using the 65 µm PDMS/DVB fiber for hemoglobin, humic acid and ionic strength (3 fold series dilution) at pH 5.5. (RRF = relative response factor)

`

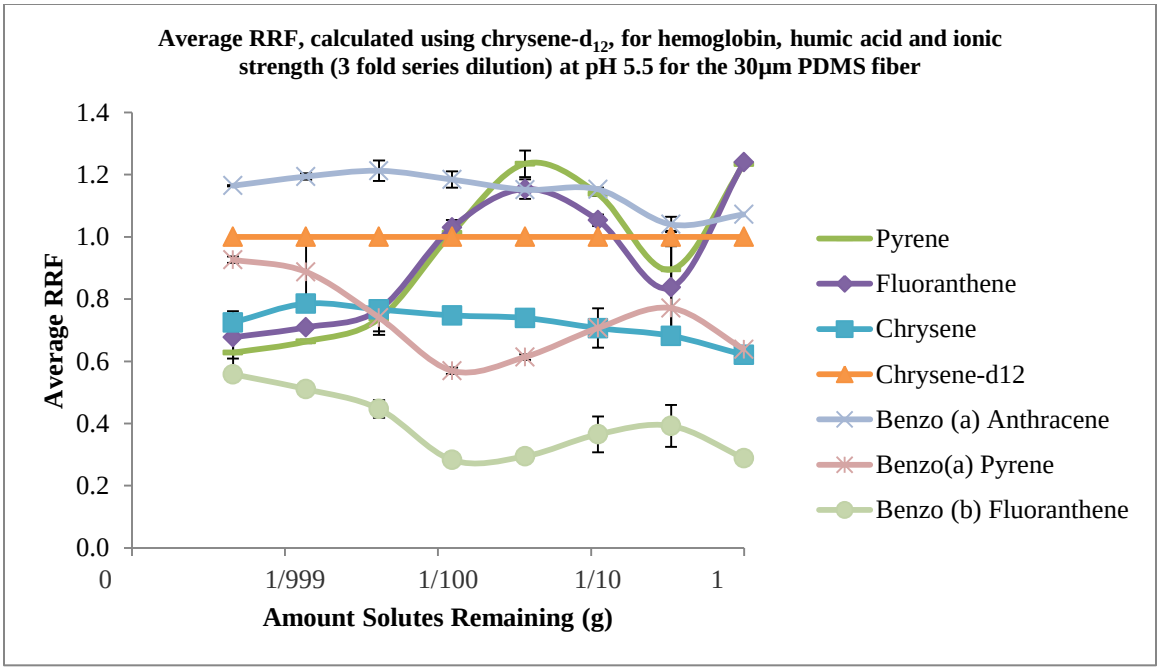

Figure 81 Average RRF (chrysene-d_{12}), using the 30 µm PDMS fiber for hemoglobin, humic acid and ionic strength (3 fold series dilution) at pH 5.5. (RRF = relative response factor)

`

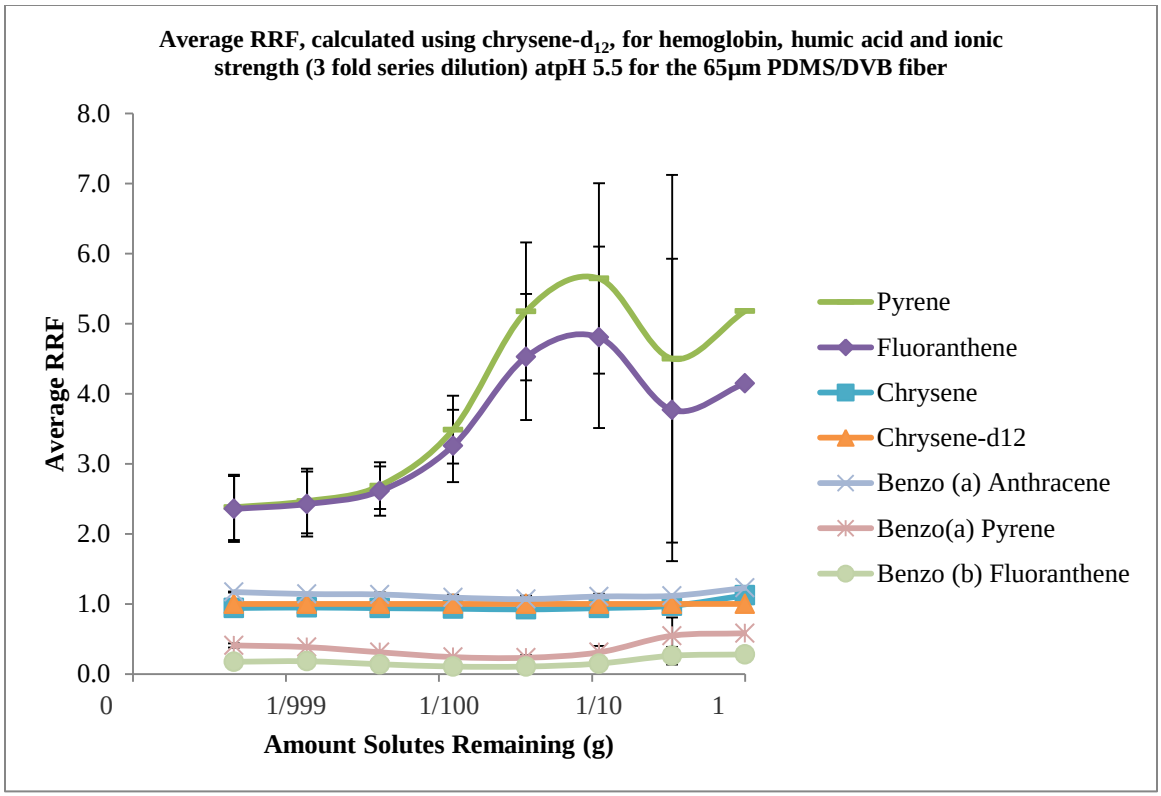

Figure 82 Average RRF (chrysene-d_{12}), using the 65 µm PDMS/DVB fiber for hemoglobin, humic acid and ionic strength (3 fold series dilution) at pH 5.5. (RRF = relative response factor)

`

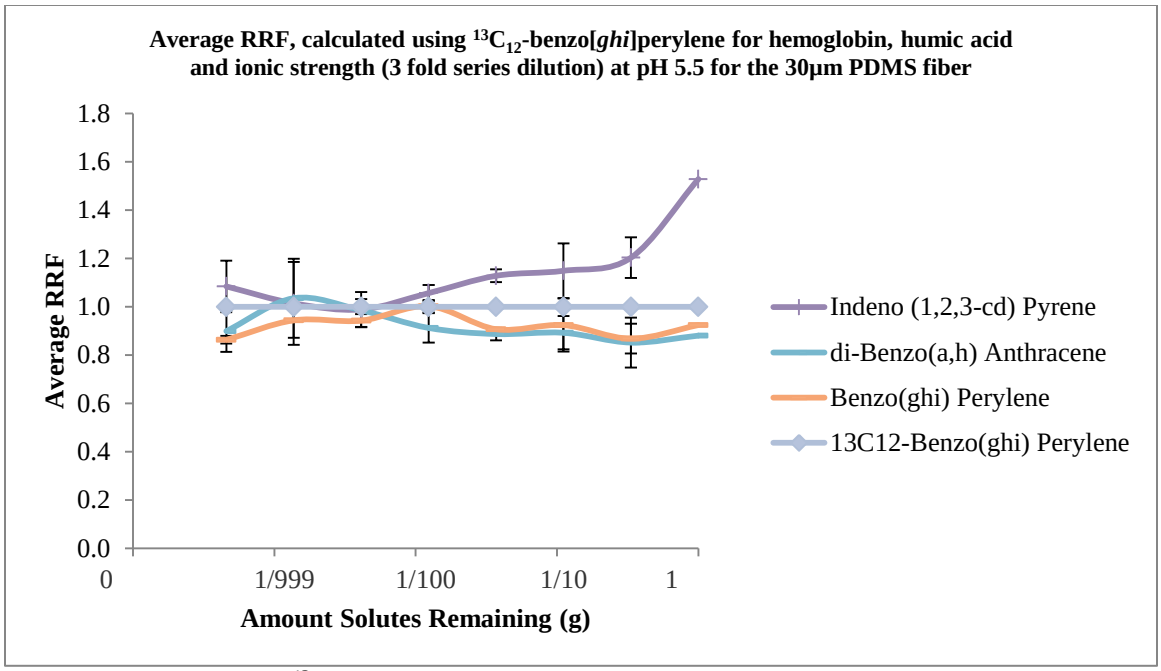

Figure 83 Average RRF ($^{13}C_{12}$-benzo[*ghi*]perylene), using the 30 µm PDMS fiber for hemoglobin, humic acid and ion strength (3 fold series dilution) at pH 5.5. (RRF = relative response factor)

`

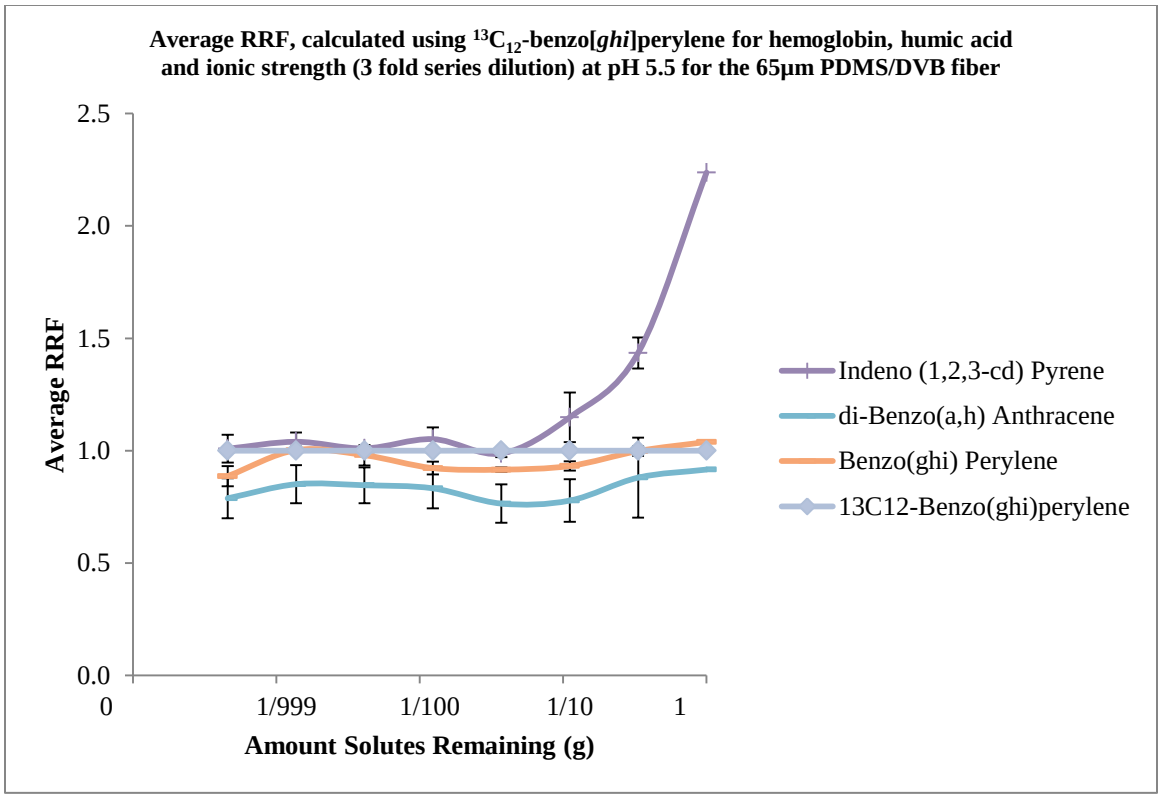

Figure 84 Average RRF ($^{13}C_{12}$-benzo[*ghi*]perylene), using the 65 µm PDMS/DVB fiber for hemoglobin, humic acid and ionic strength (3 fold series dilution) at pH 5.5. (RRF = relative response factor)

`

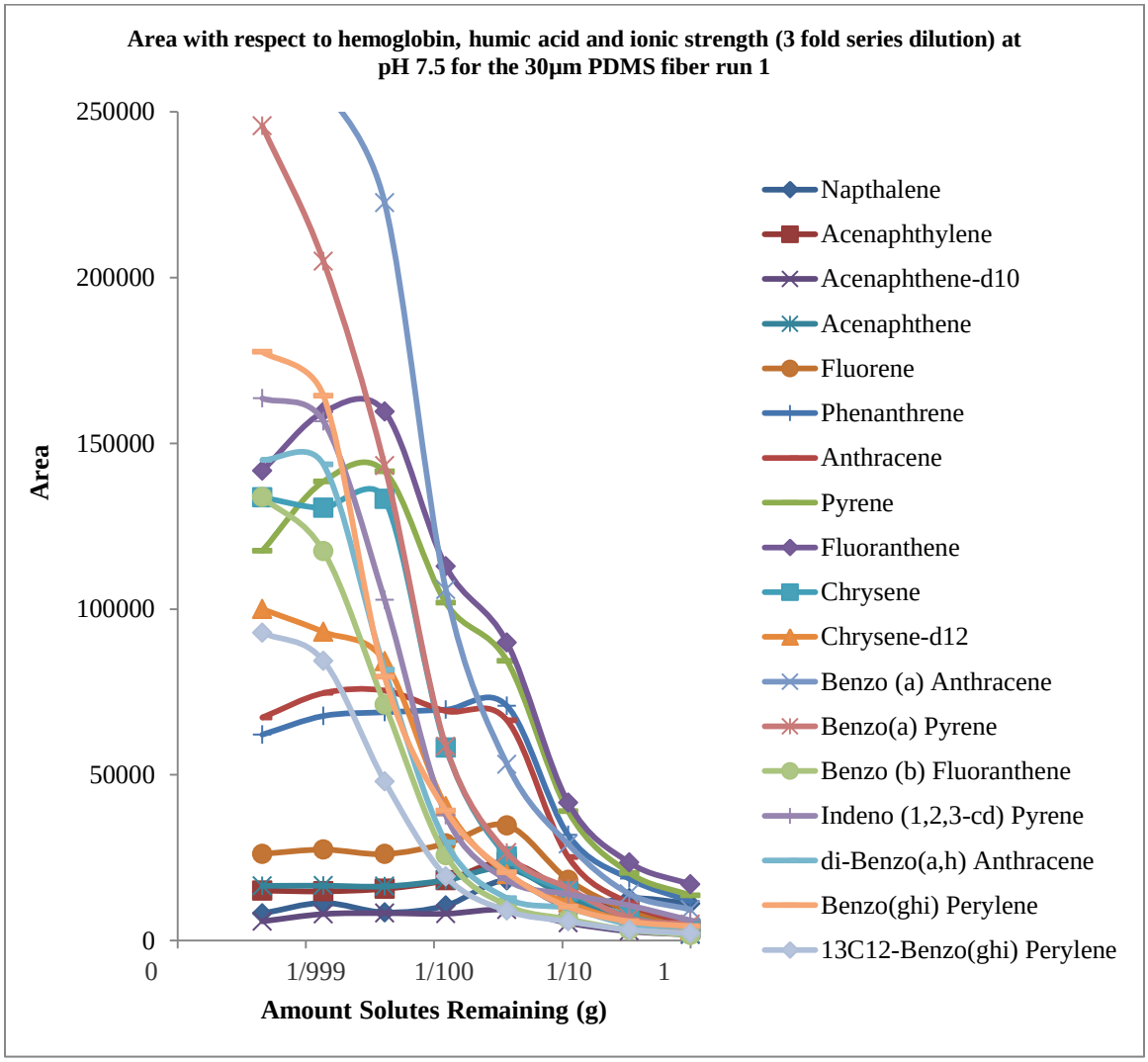

Figure 85 Area with respect to ionic strength, humic acid and hemoglobin at a pH 7.5 (3 fold series dilution) using the 30 µm PDMS fiber run 1.

`

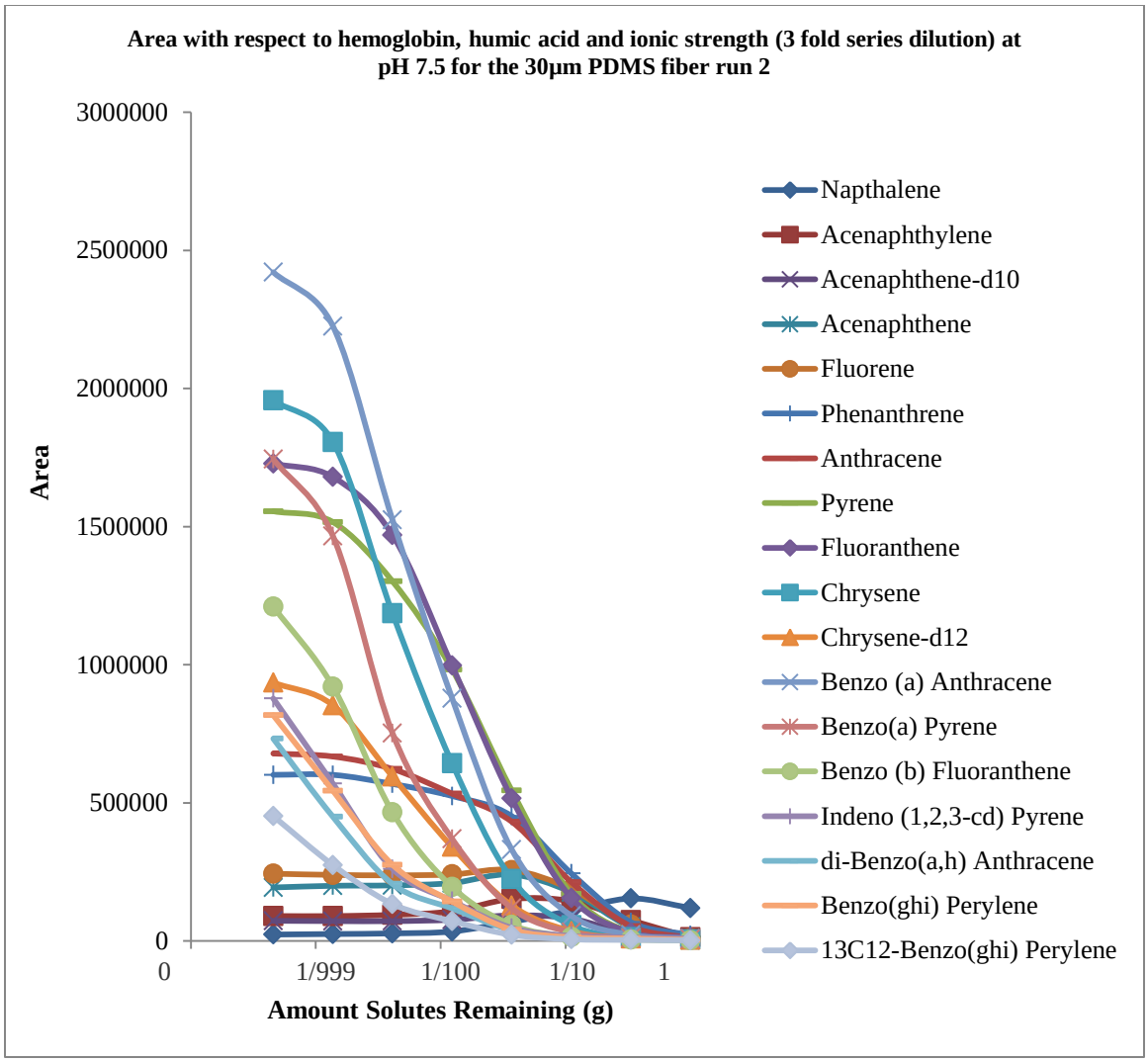

Figure 86 Area with respect to ionic strength, humic acid and hemoglobin at a pH 7.5 (3 fold series dilution) using the 30 µm PDMS fiber run 2.

`

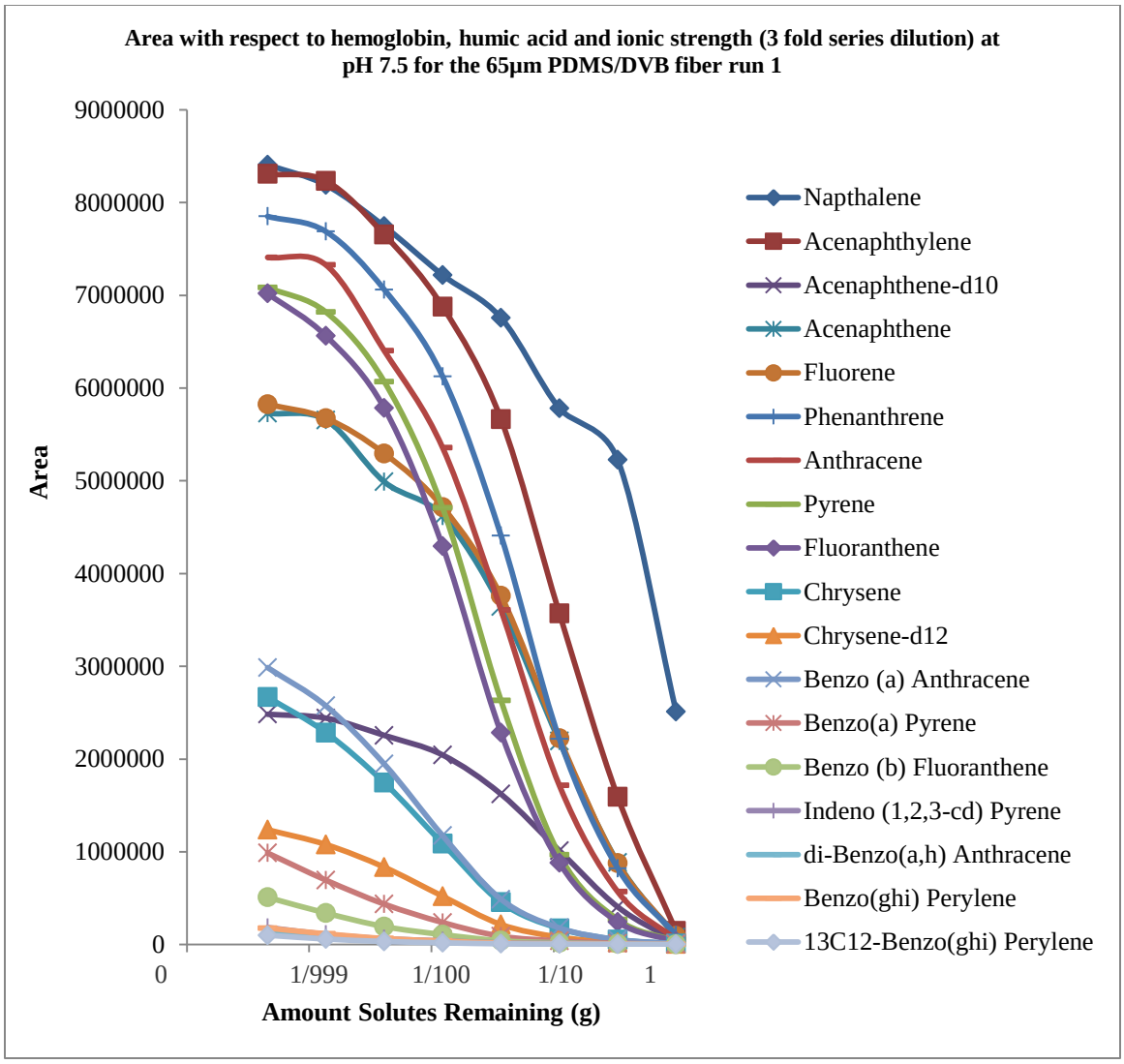

Figure 87 Area with respect to ion strength, humic acid and hemoglobin at a pH 7.5 (3 fold series dilution) using the 65 µm PDMS/DVB fiber run 1.

`

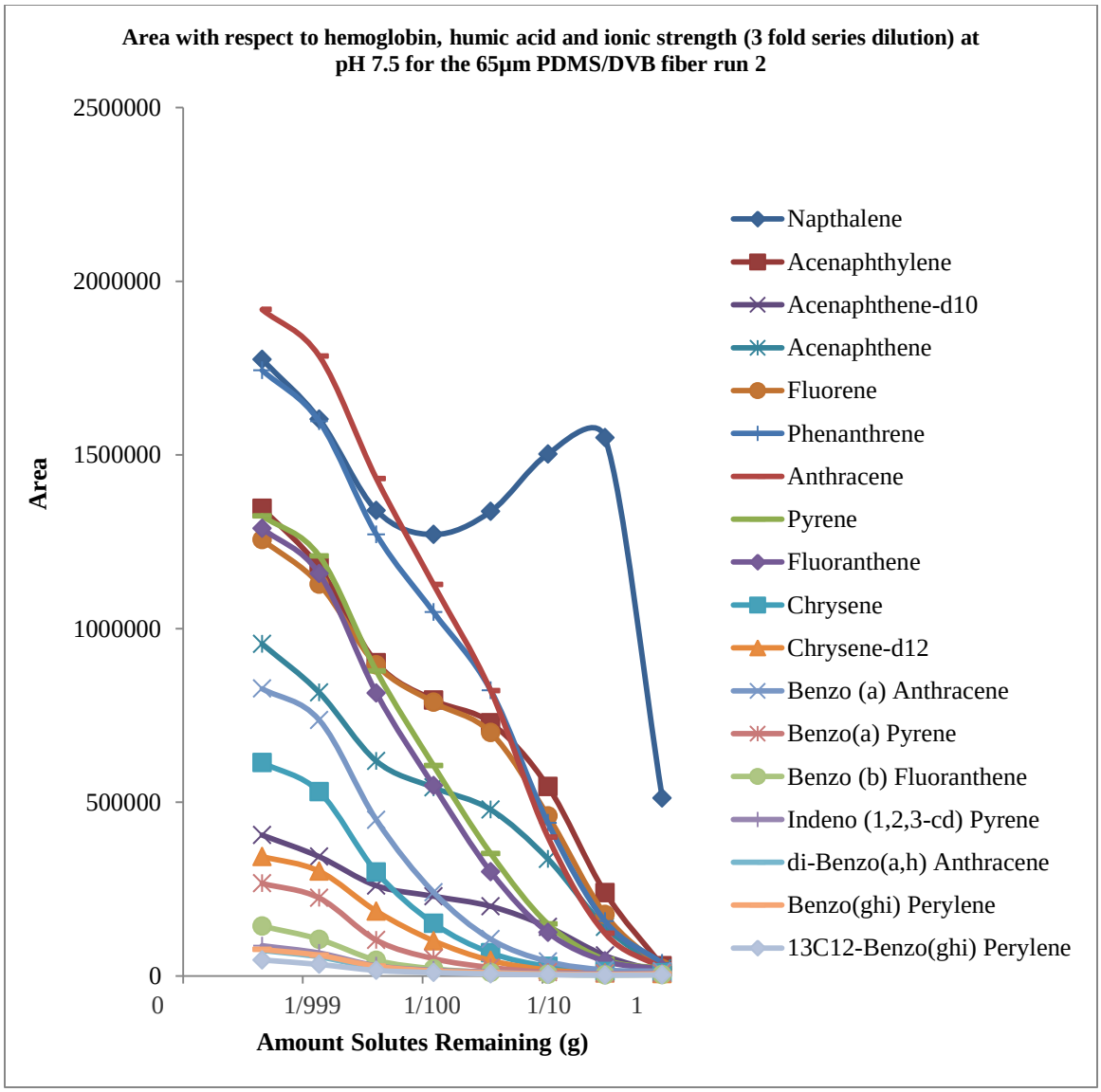

Figure 88 Area with respect to ion strength, humic acid and hemoglobin at a pH 7.5 (3 fold series dilution) using the 65 µm PDMS/DVB fiber run 1.

`

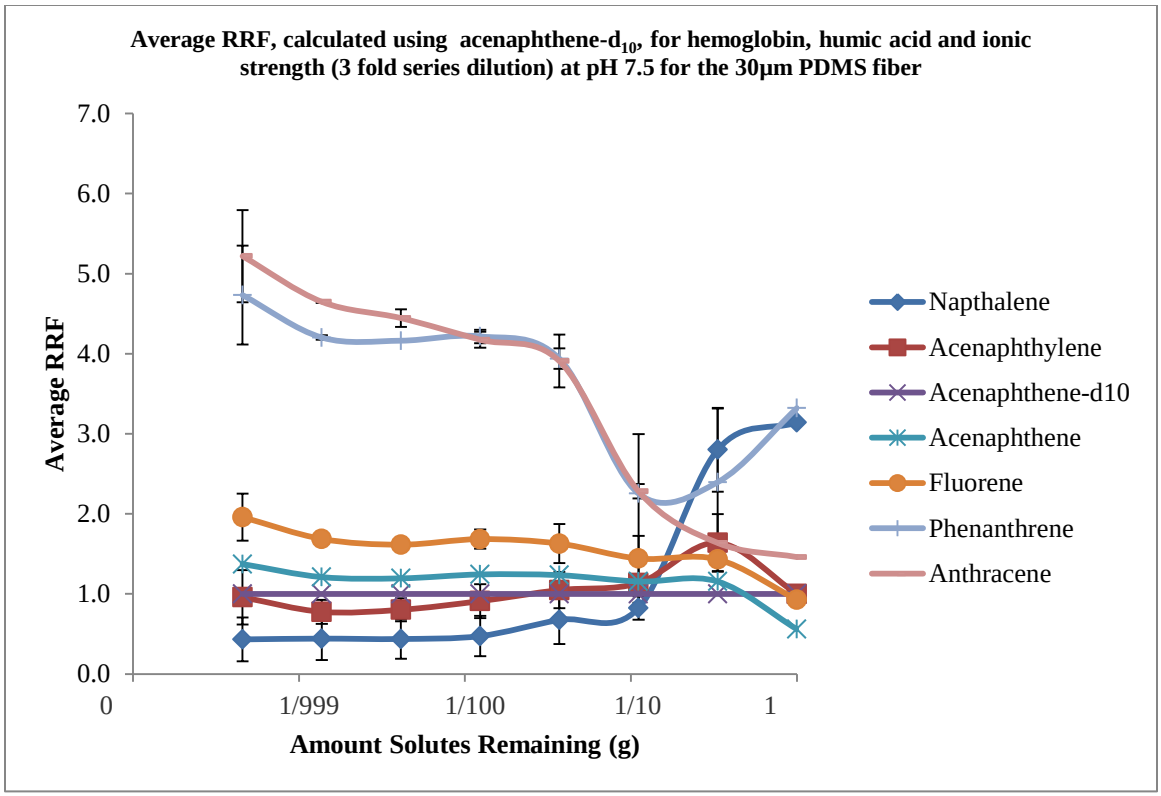

Figure 89 Average RRF (acenaphthene-d_{10}), using the 30 µm PDMS fiber for hemoglobin, humic acid and ionic strength (3 fold series dilution) at pH 7.5. (RRF = relative response factor)

`

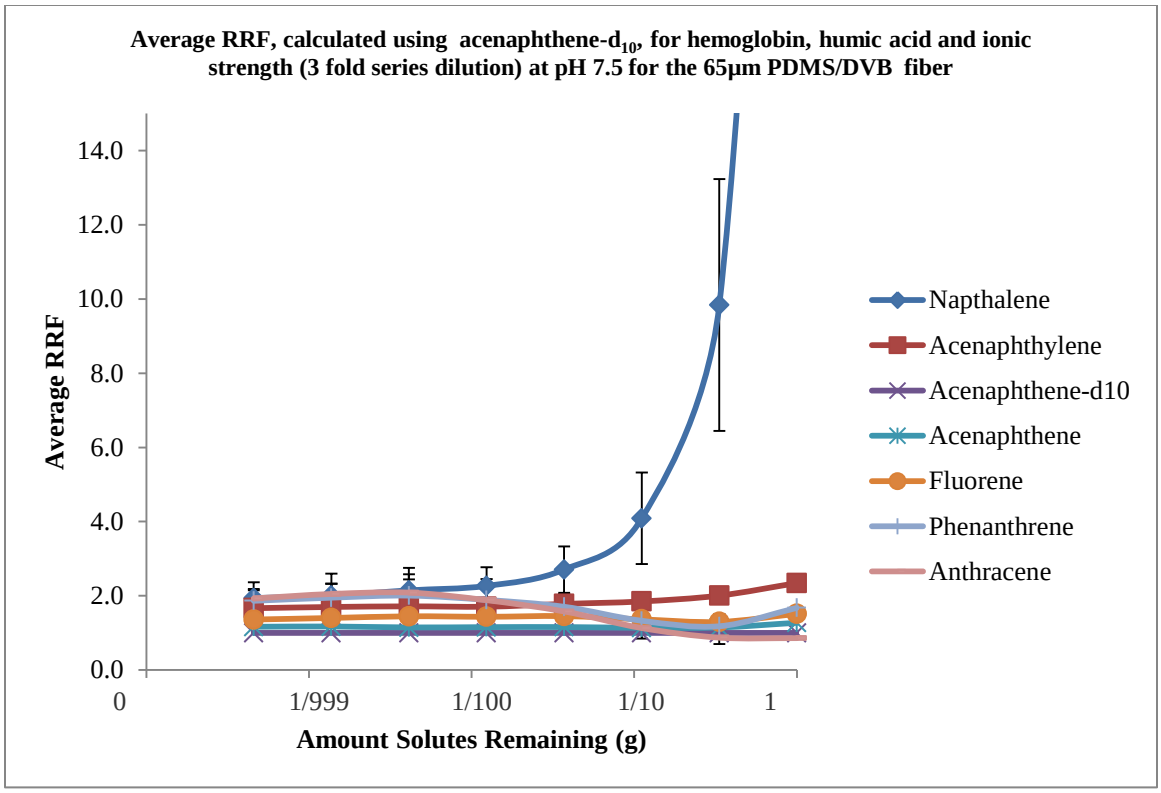

Figure 90 Average RRF (acenaphthene-d_{10}), using the 65 µm PDMS/DVB fiber for hemoglobin, humic acid and ionic strength (3 fold series dilution) at pH 7.5. (RRF = relative response factor)

`

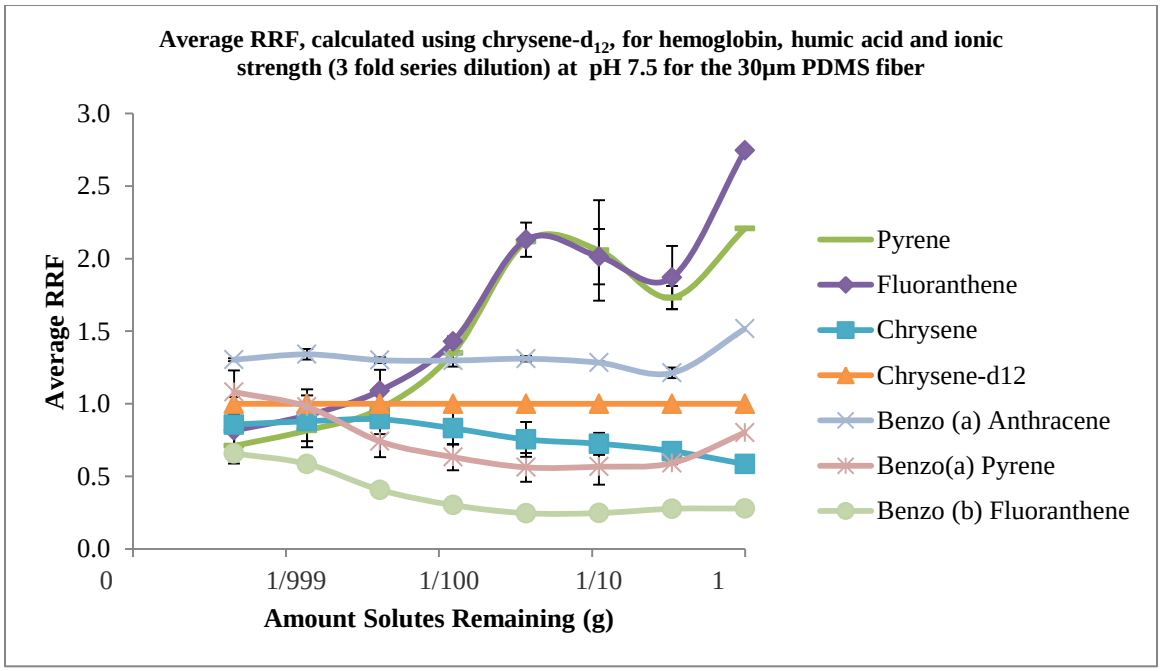

Figure 91 Average RRF (chrysene-d_{12}), using the 30 µm PDMS fiber for hemoglobin, humic acid and ionic strength (3 fold series dilution) at pH 7.5. (RRF = relative response factor)

`

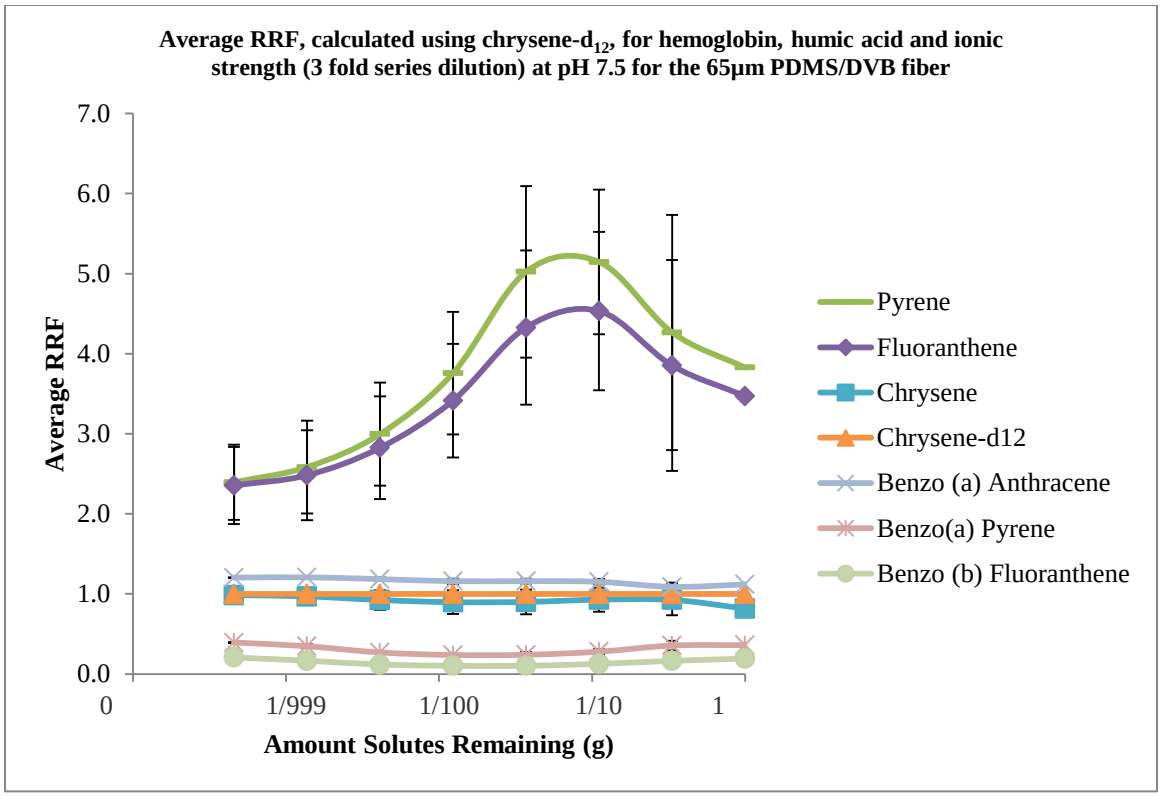

Figure 92 Average RRF (chrysene-d_{12}), using the 65 µm PDMS/DVB fiber for hemoglobin, humic acid and ionic strength (3 fold series dilution) at pH 7.5. (RRF = relative response factor)

`

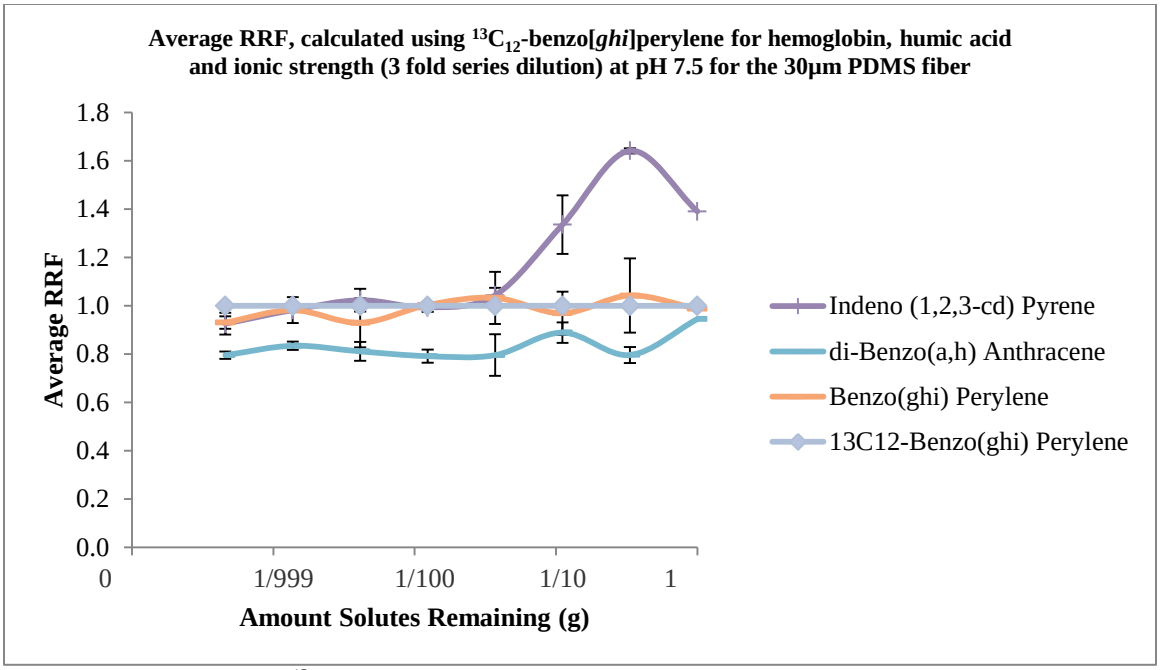

Figure 93 Average RRF ($^{13}C_{12}$- benzo[*ghi*]perylene), using the 30 µm PDMS fiber for hemoglobin, humic acid and ionic strength (3 fold series dilution) at pH 7.5. (RRF = relative response factor)

`

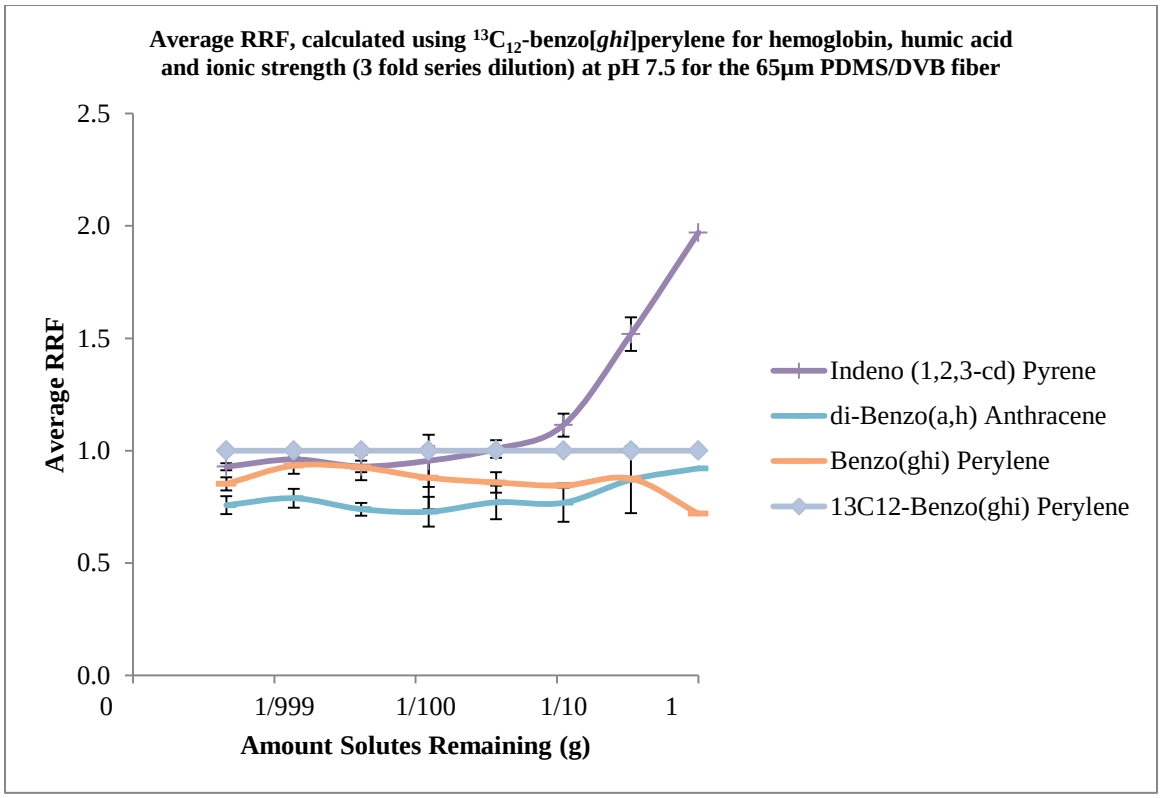

Figure 94 Average RRF ($^{13}C_{12}$- benzo[*ghi*]perylene), using the 65 µm PDMS/DVB fiber for hemoglobin, humic acid and ionic strength (3 fold series dilution) at pH 7.5. (RRF = relative response factor)

`

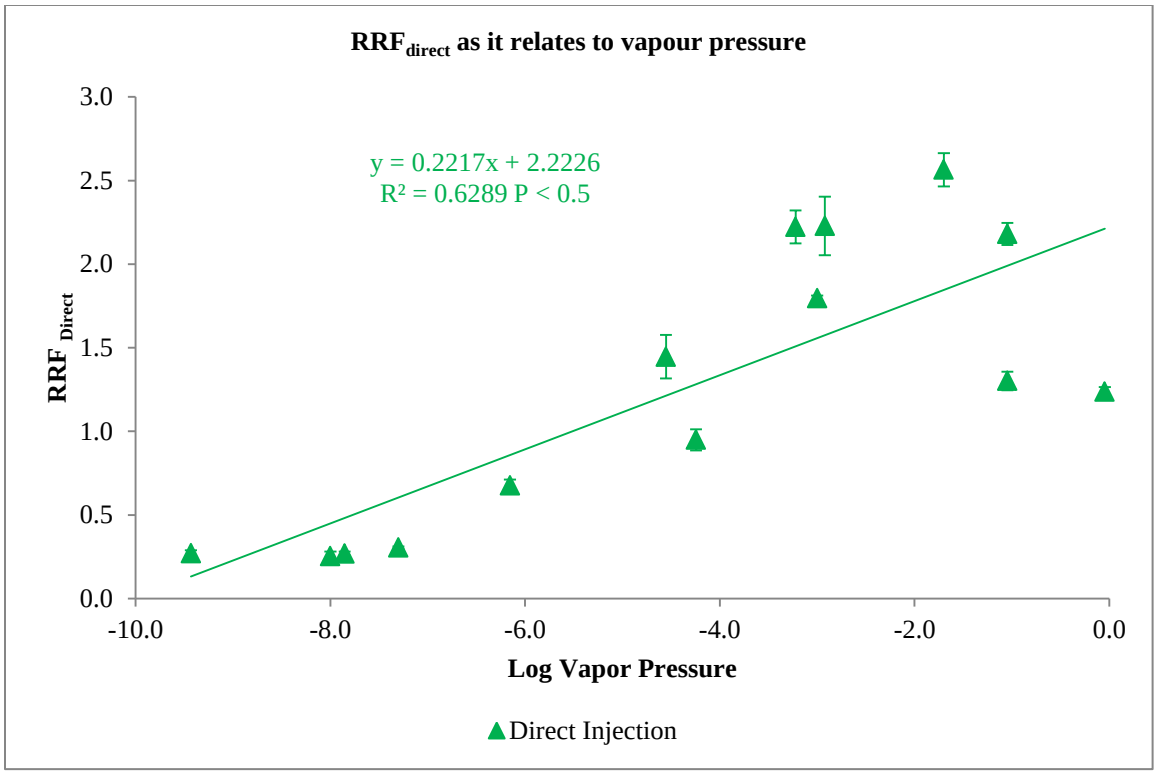

Figure 95 Relationship of RRF_{direct} to the log vapor pressure (Pa) for direct injection. (RRF_{direct} = relative response factor direct injection)

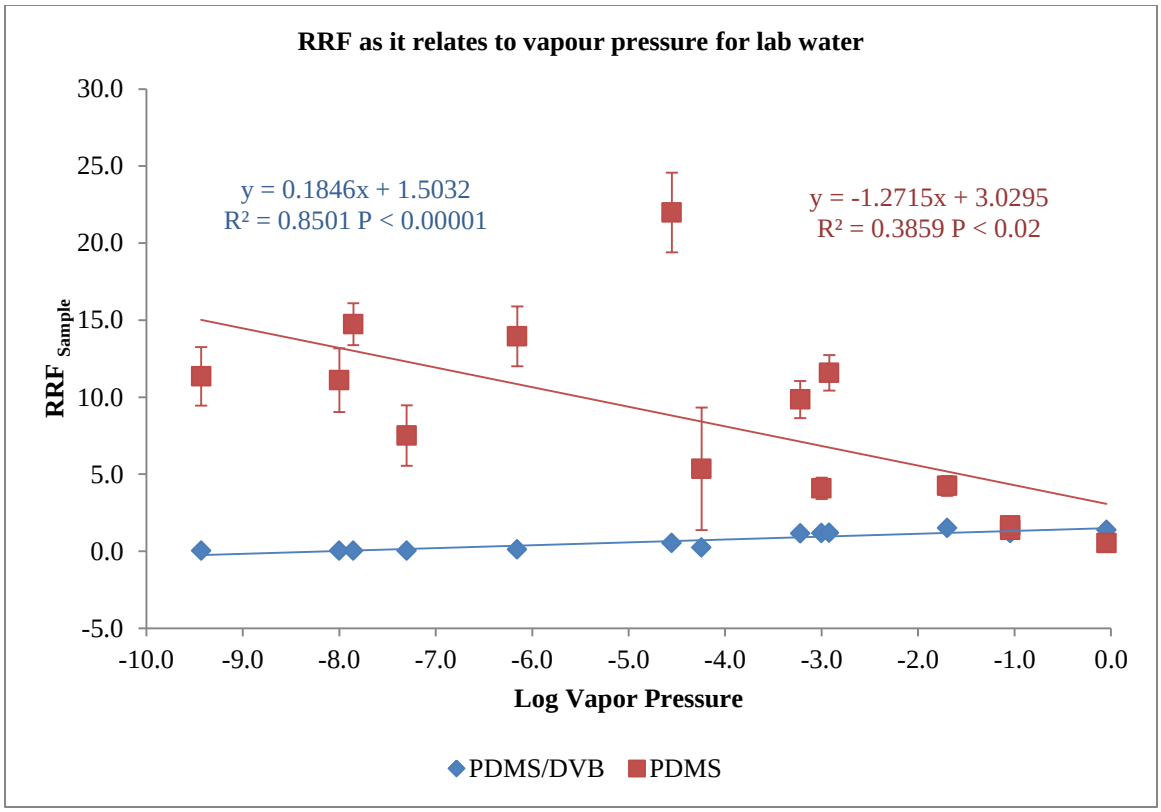

Figure 96 Relationship of RRF to the log vapor pressure (Pa) for laboratory water. (RRF_{direct} = relative response factor direct injection, RRF_{sample} = relative response factor SPME sample injection)

`

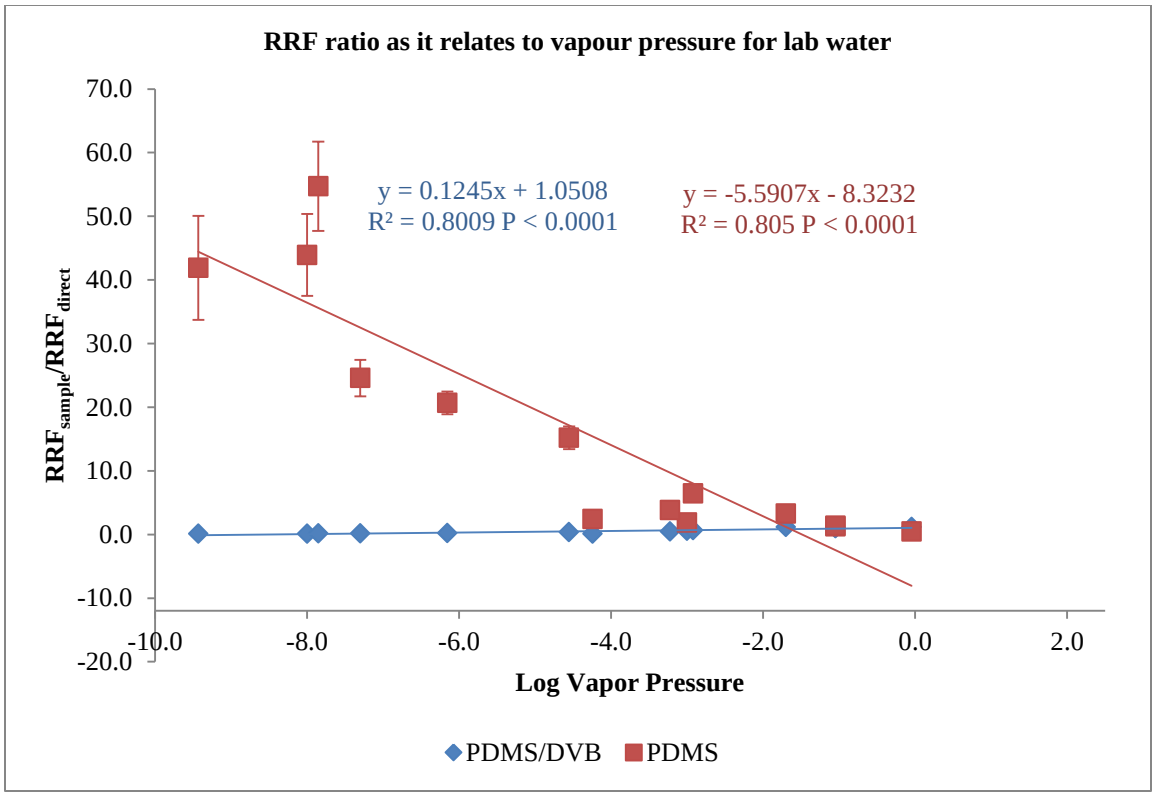

Figure 97 Relationship of the RRF ratio to the log vapor pressure (Pa) for laboratory water. (RRF_{direct} = relative response factor direct injection, RRF_{sample} = relative response factor SPME sample injection

`

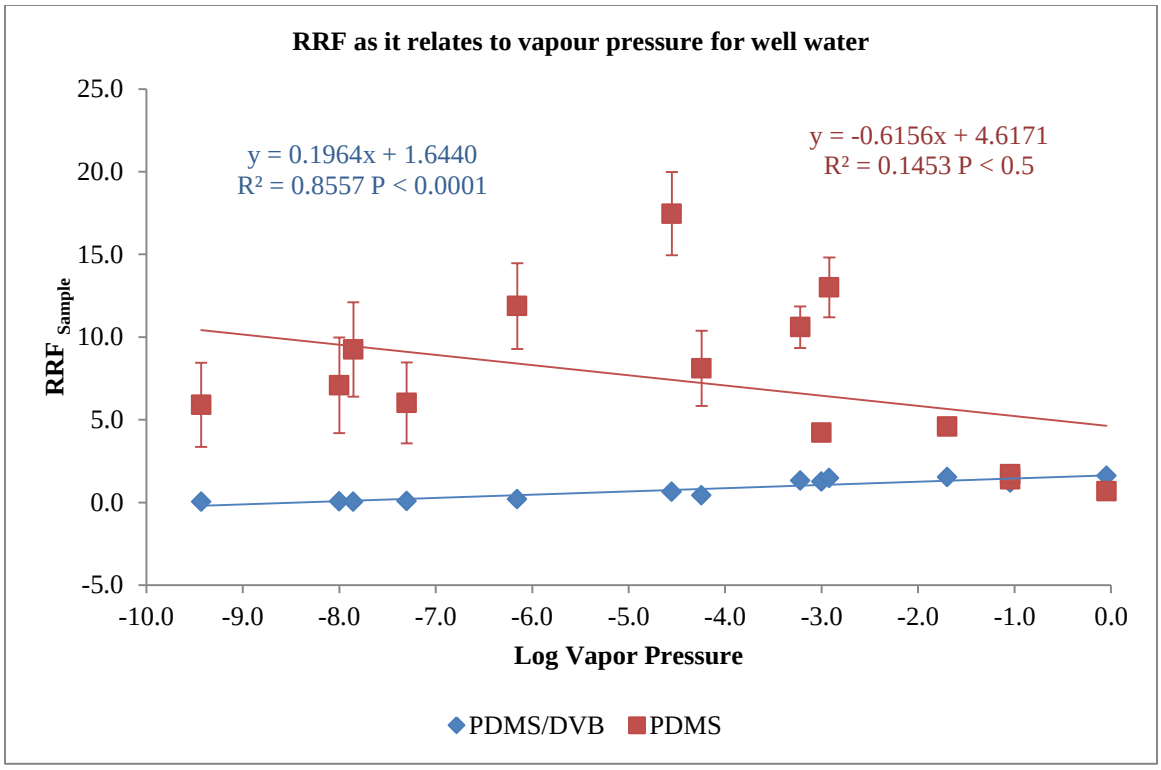

Figure 98 Relationship of RRF to the log vapor pressure (Pa) for well water. (RRF_{sample} = relative response factor SPME sample injection)

`

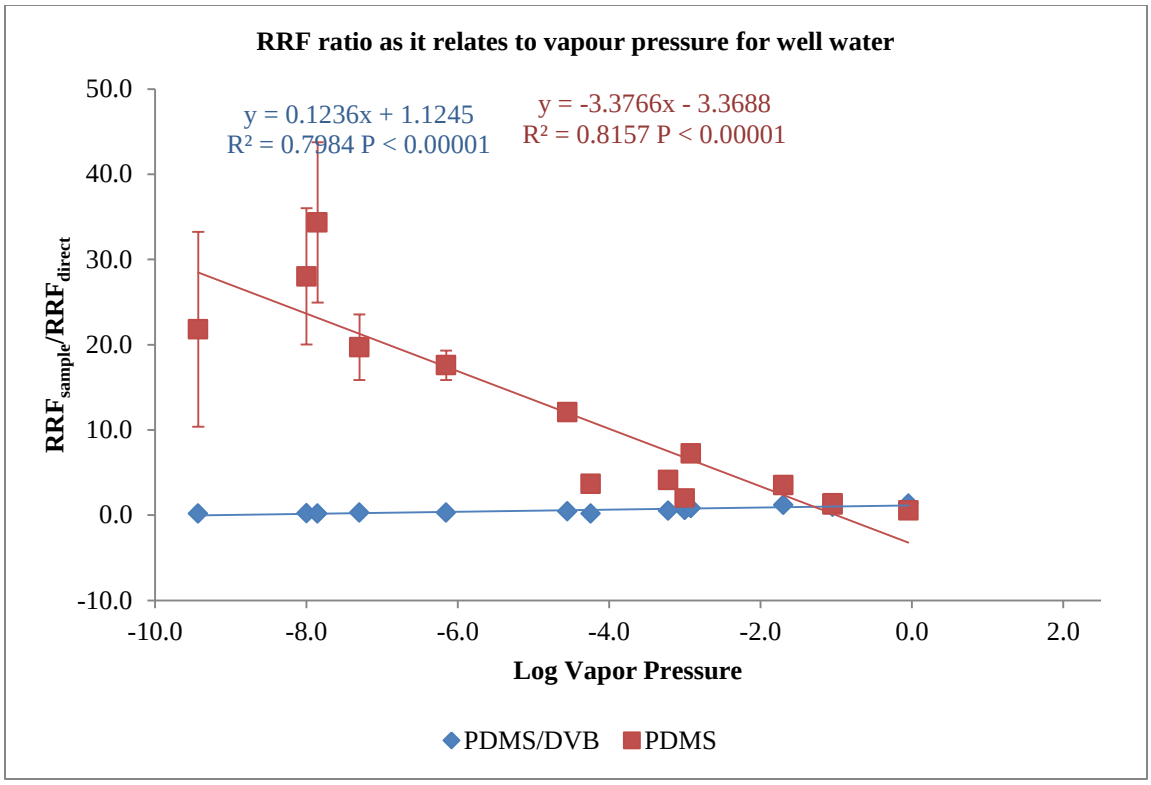

Figure 99 Relationship of the RRF ratio to the log vapor pressure (Pa) for well water. (RRF_{direct} = relative response factor direct injection, RRF_{sample} = relative response factor SPME sample injection)

`

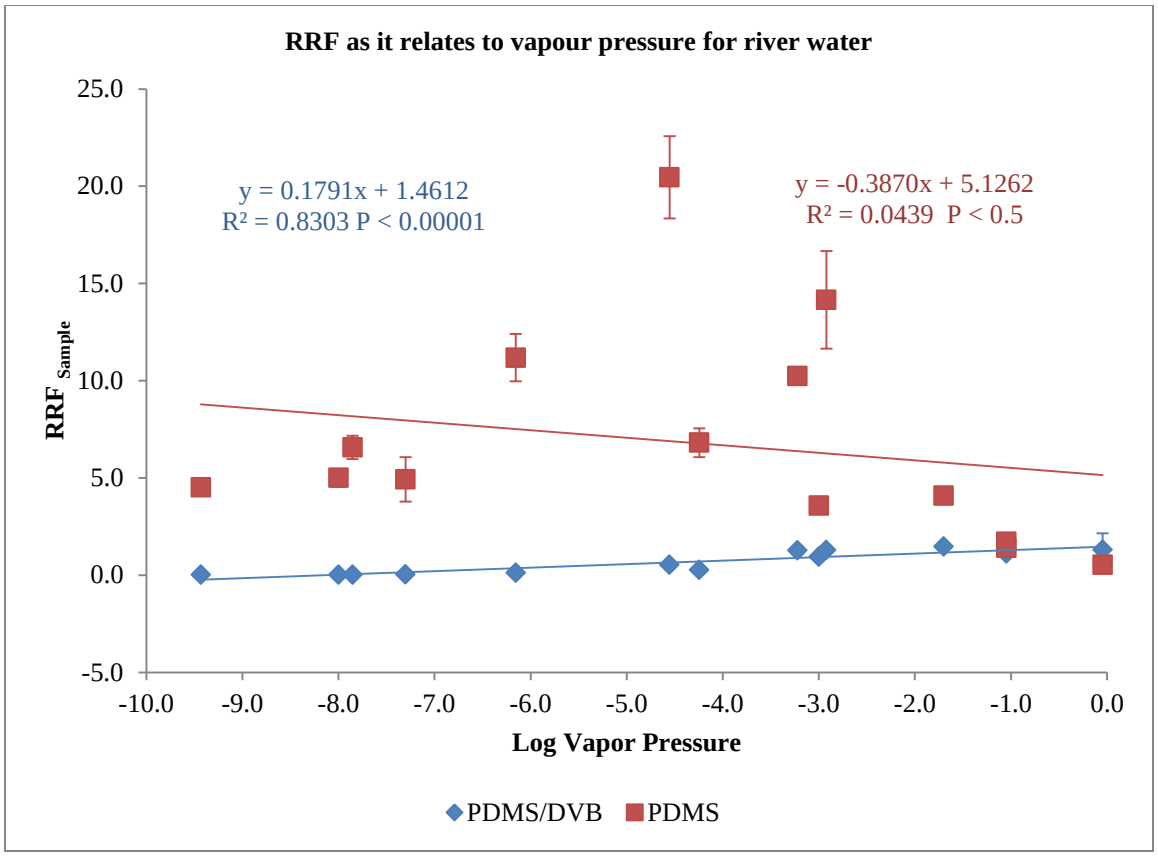

Figure 100 Relationship of RRF to the log vapor pressure (Pa) for river water. (RRF_{sample} = relative response factor SPME sample injection)

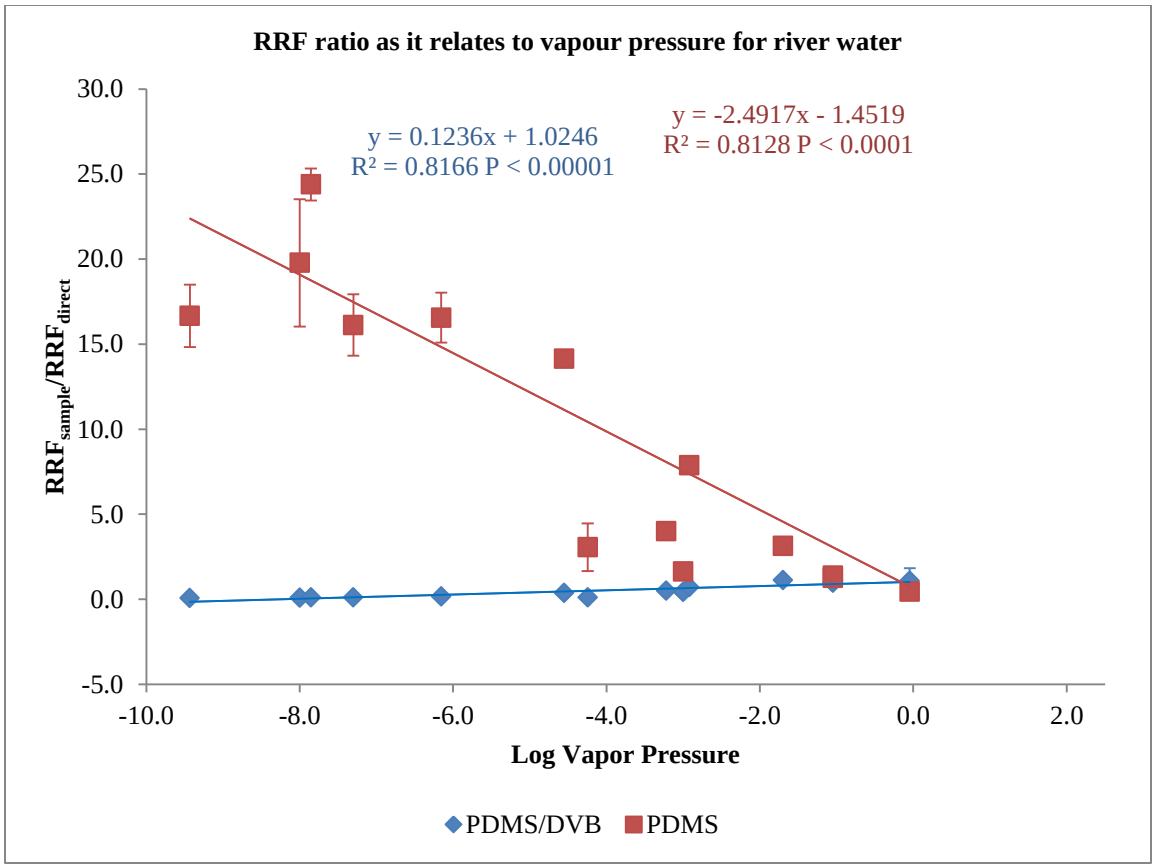

Figure 101 Relationship of the RRF ratio to the log vapor pressure (Pa) for river water. (RRF_{direct} = relative response factor direct injection, RRF_{sample} = relative response factor SPME sample injection)

`

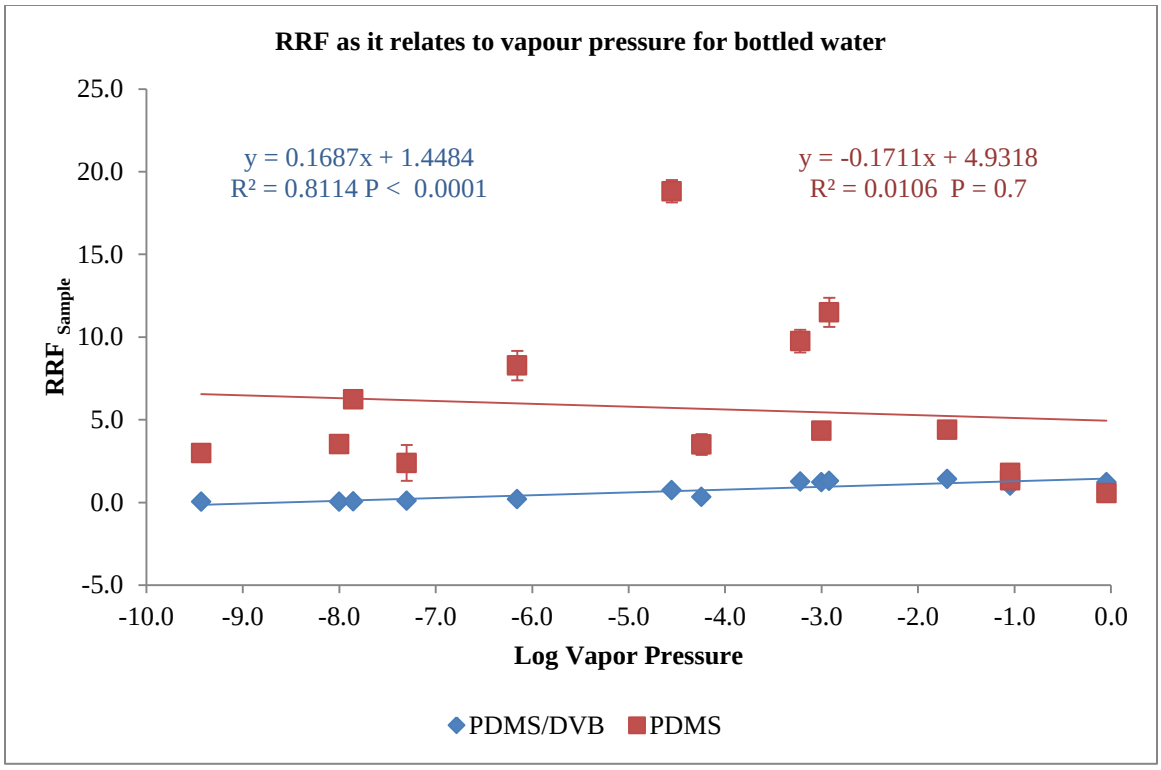

Figure 102 Relationship of the RRF to the log vapor pressure (Pa) for bottled water. (RRF_{sample} = relative response factor SPME sample injection)

`

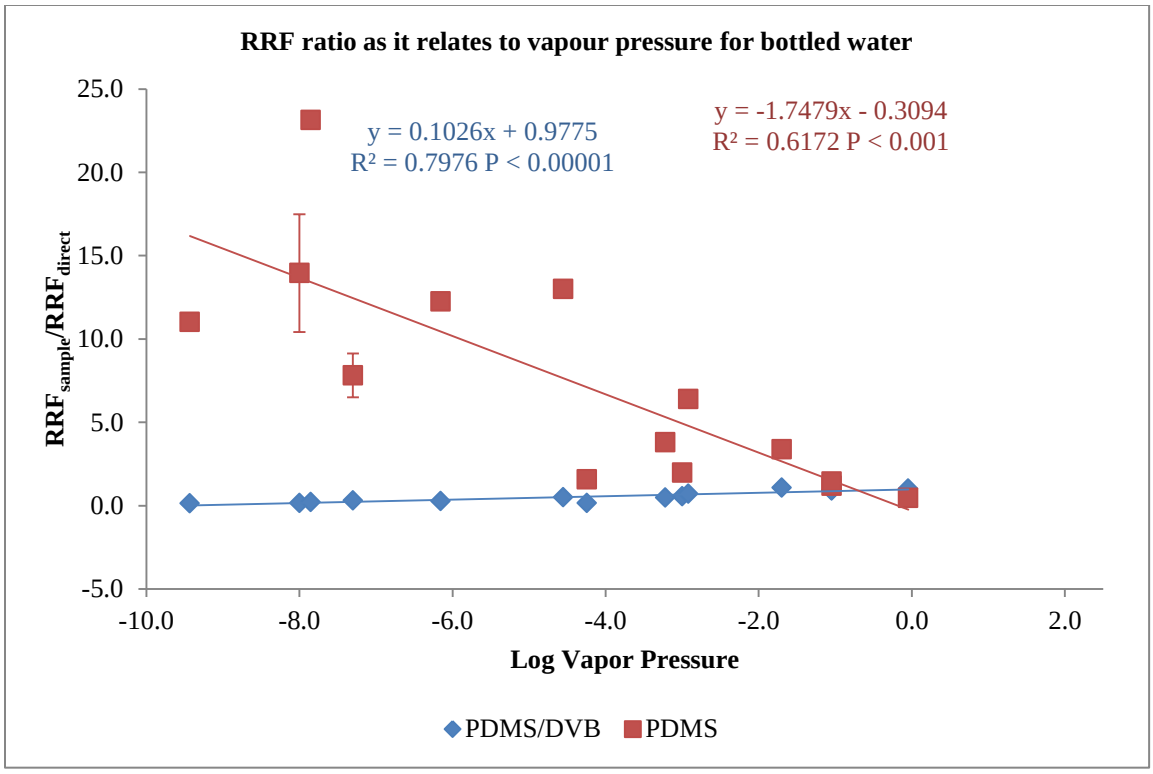

Figure 103 Relationship of the RRF ratio to the log vapor pressure (Pa) for bottled water. (RRF_{direct} = relative response factor direct injection, RRF_{sample} = relative response factor SPME sample injection)

`

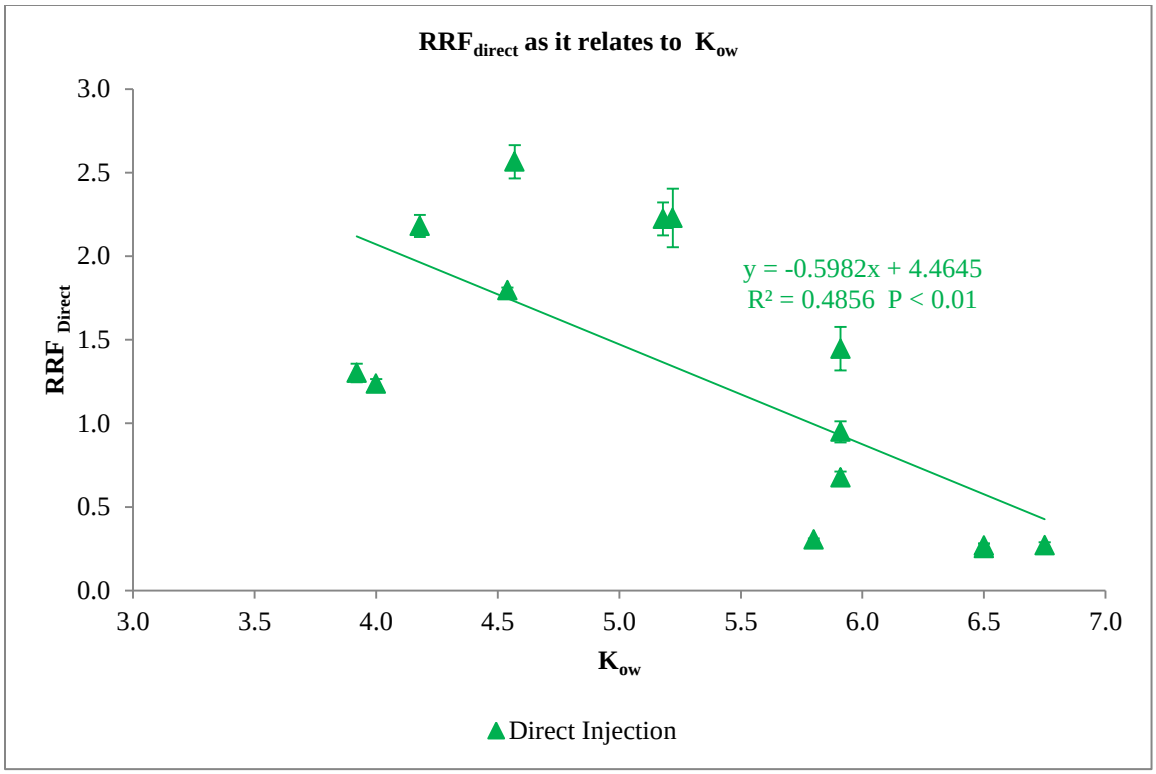

Figure 104 Relationship of the RRF_{direct} to the octanol/water coefficient (K_{ow}) for direct injection. (RRF_{direct} = relative response factor direct injection)

`

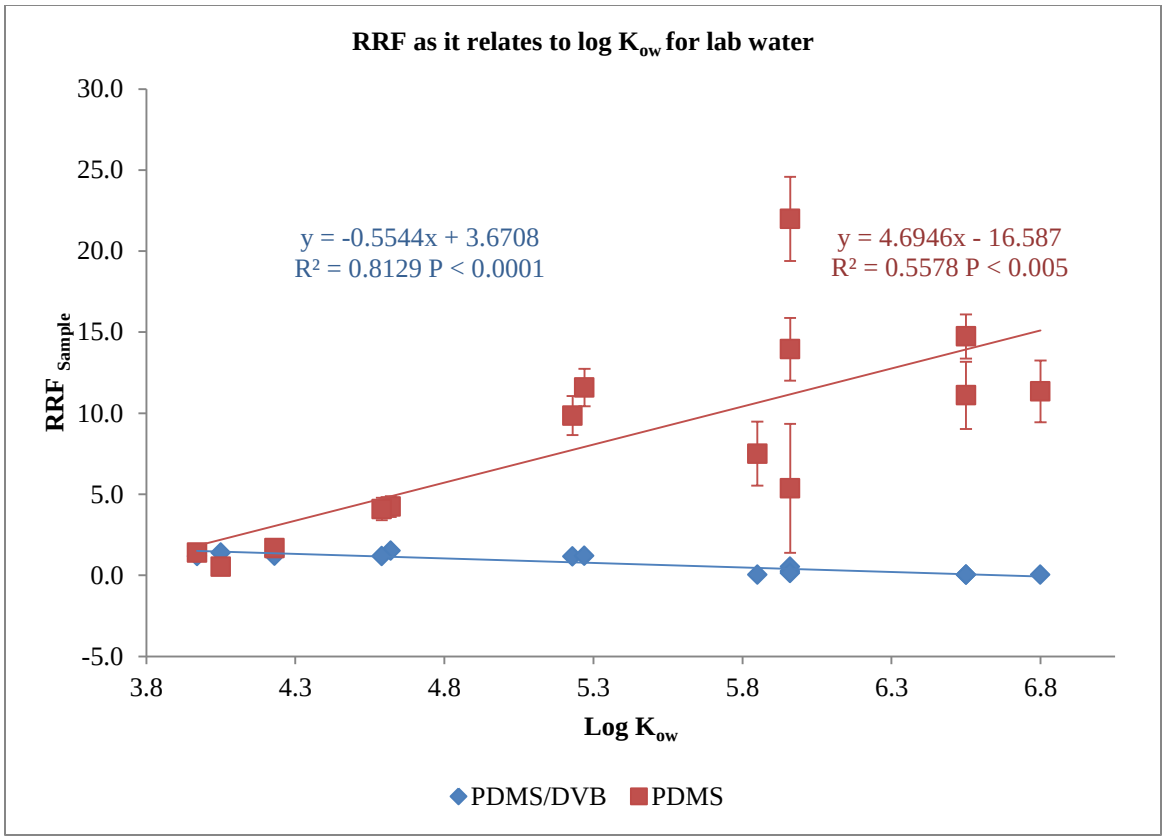

Figure 105 Relationship of the RRF to the octanol/water coefficient (K_{ow}) for laboratory water. (RRF_{sample} = relative response factor SPME sample injection)

`

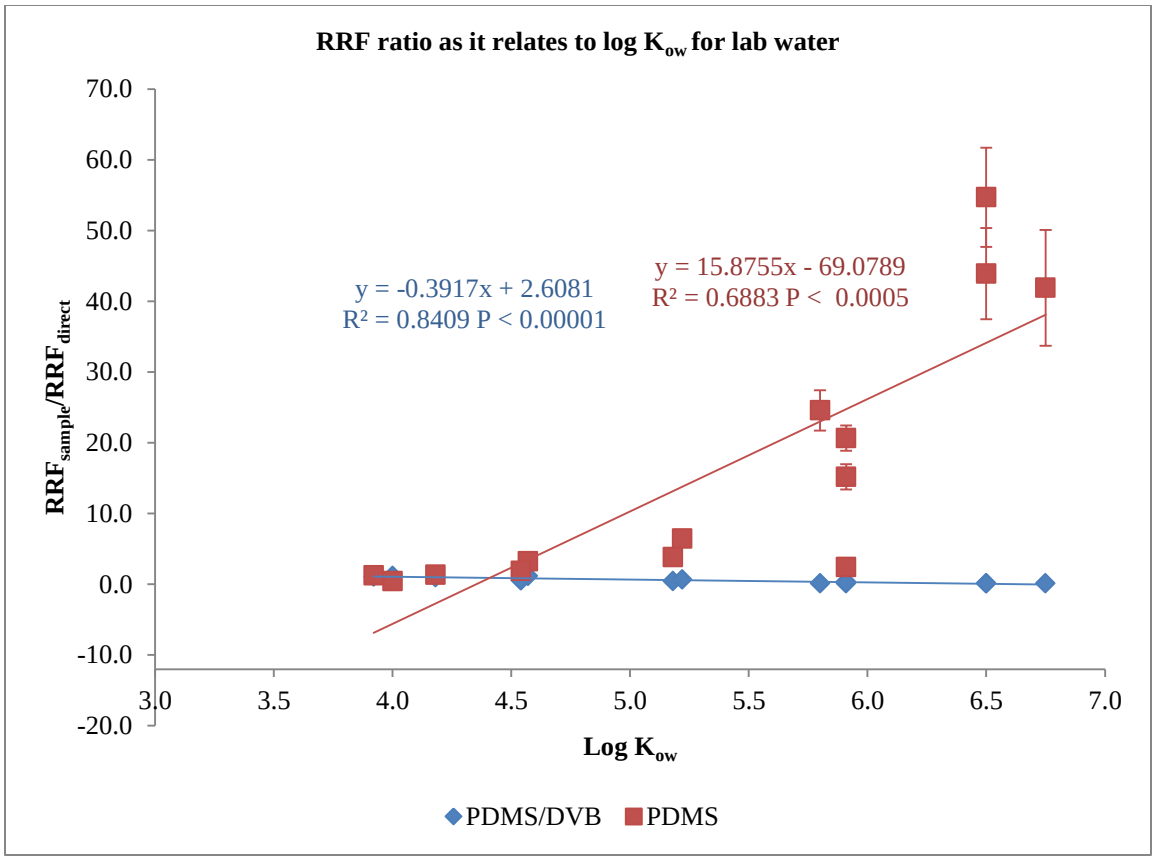

Figure 106 Relationship of the RRF ratio to the octanol/water coefficient (K_{ow}) for laboratory water. (RRF_{direct} = relative response factor direct injection, RRF_{sample} = relative response factor SPME sample injection)

`

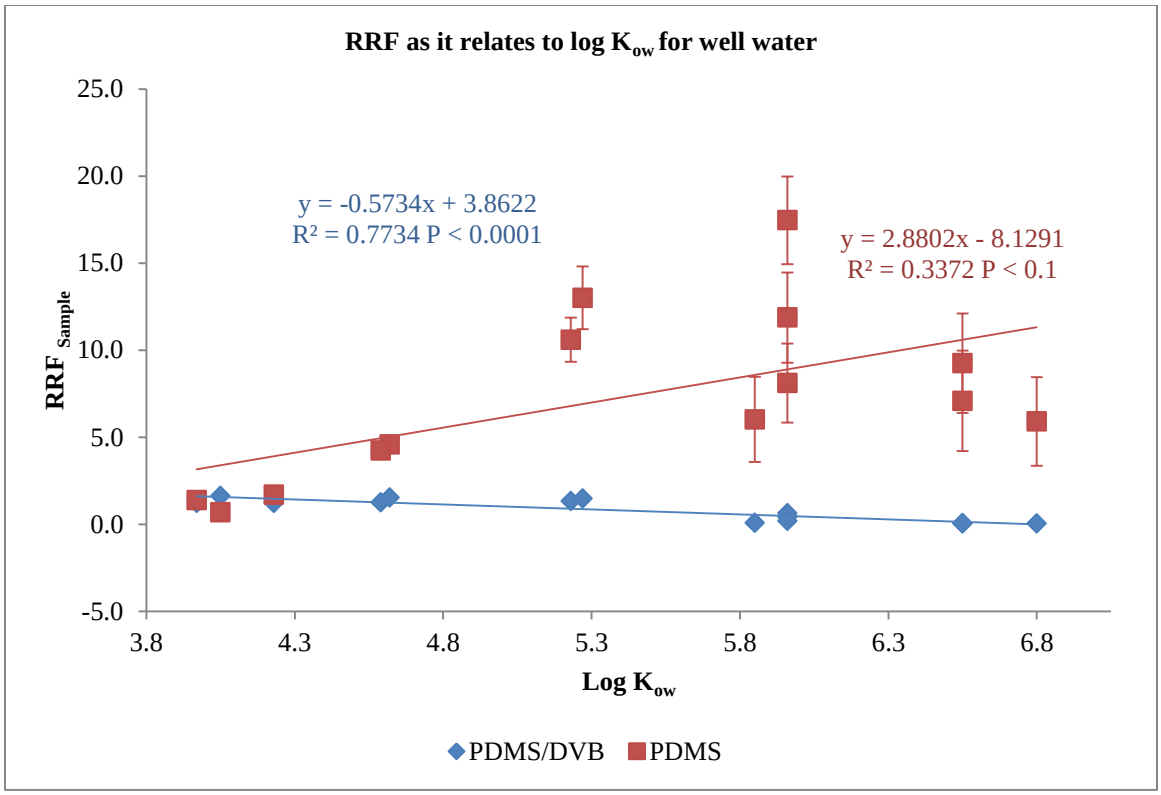

Figure 107 Relationship of the RRF to the octanol/water coefficient (K_{ow}) for well water. (RRF_{sample} = relative response factor SPME sample injection)

`

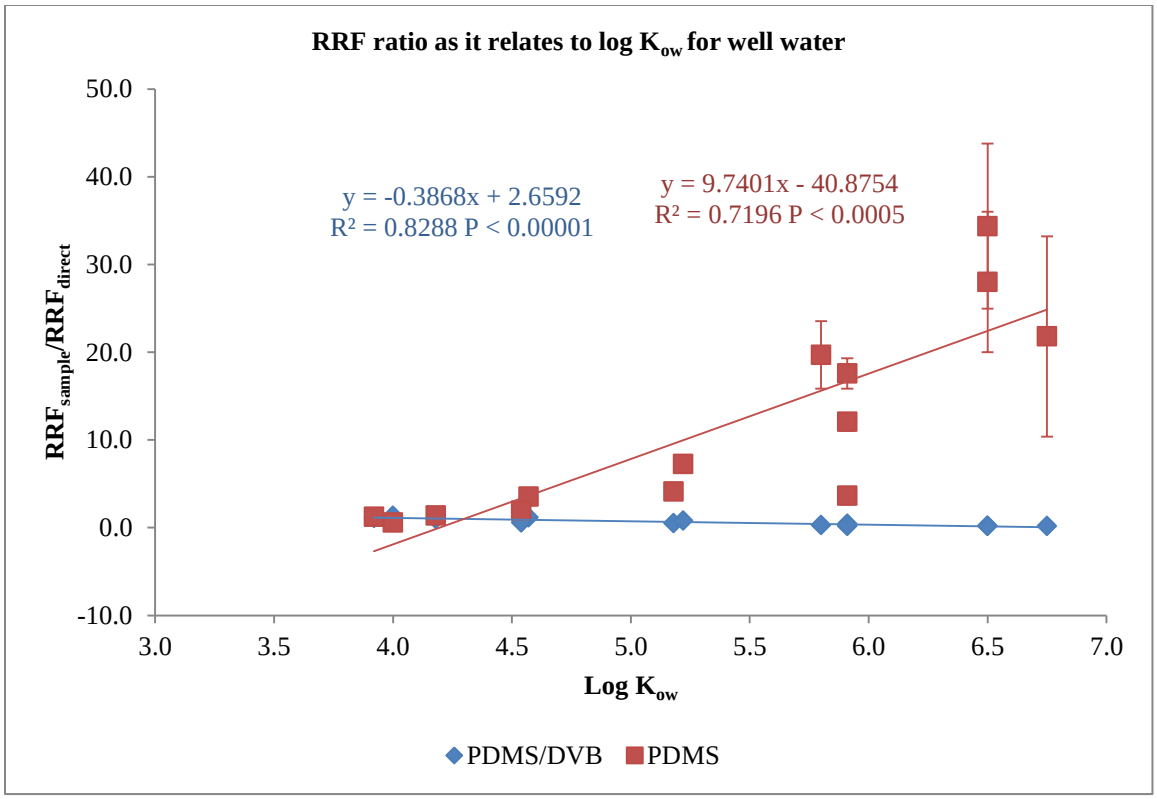

Figure 108 Relationship of the RRF ratio to the octanol/water coefficient (K_{ow}) for well water. (RRF_{direct} = relative response factor direct injection, RRF_{sample} = relative response factor SPME sample injection)

`

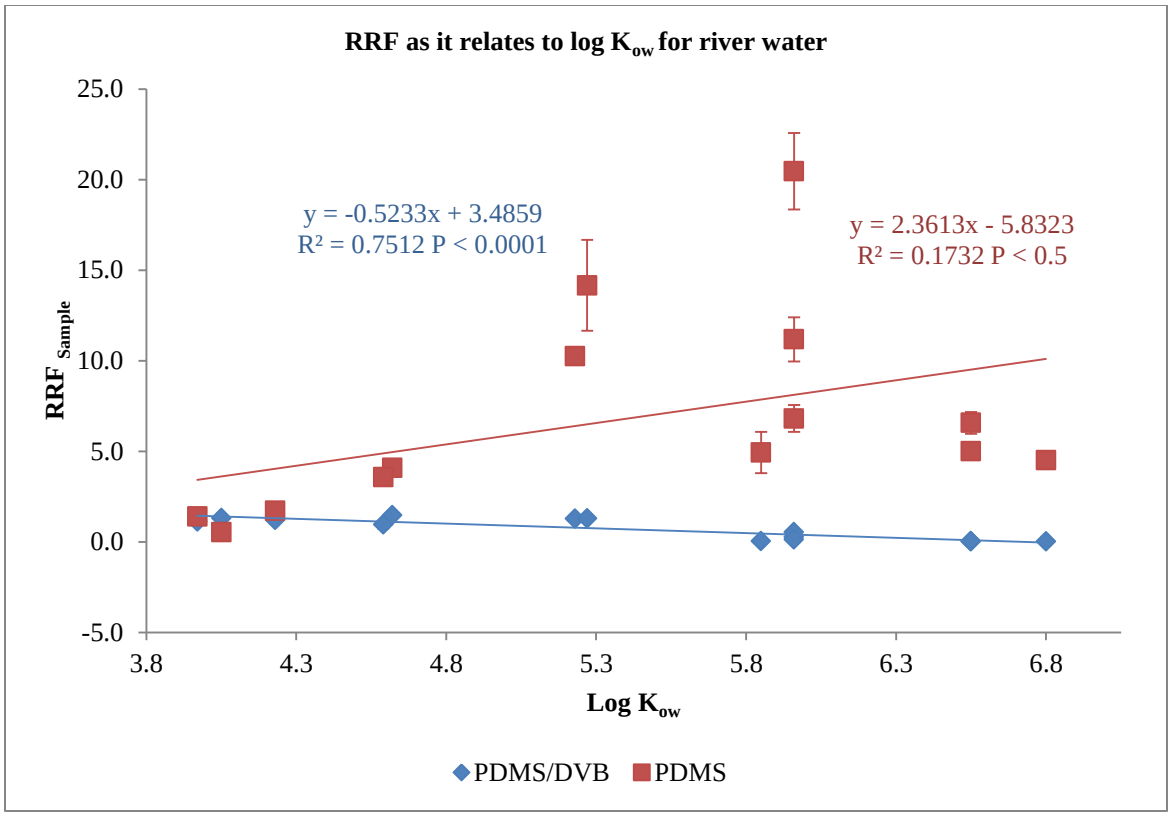

Figure 109 Relationship of the RRF to the octanol/water coefficient (K_{ow}) for river water. (RRF_{sample} = relative response factor SPME sample injection)

`

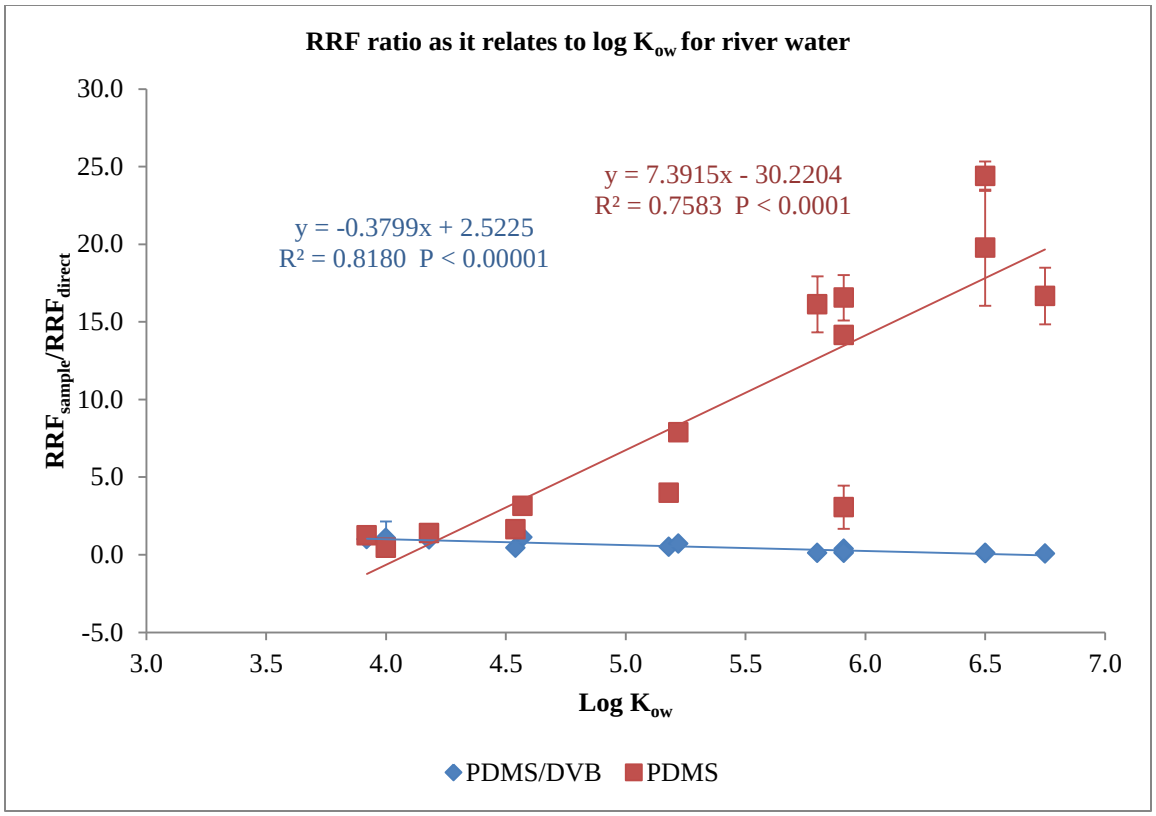

Figure 110 Relationship of the RRF ratio to the octanol/water coefficient (K_{ow}) for river water. (RRF_{direct} = relative response factor direct injection, RRF_{sample} = relative response factor SPME sample injection)

`

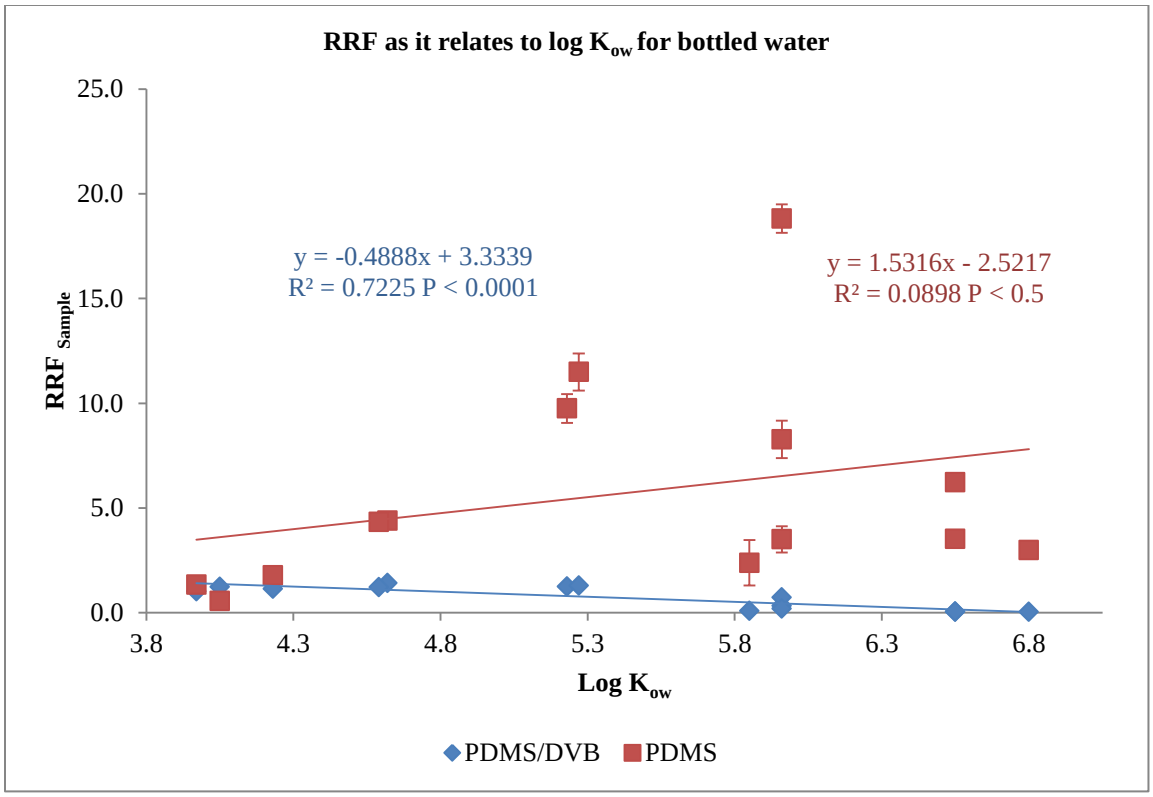

Figure 111 Relationship of the RRF to the octanol/water coefficient (K_{ow}) for bottled water. (RRF_{sample} = relative response factor SPME sample injection)

`

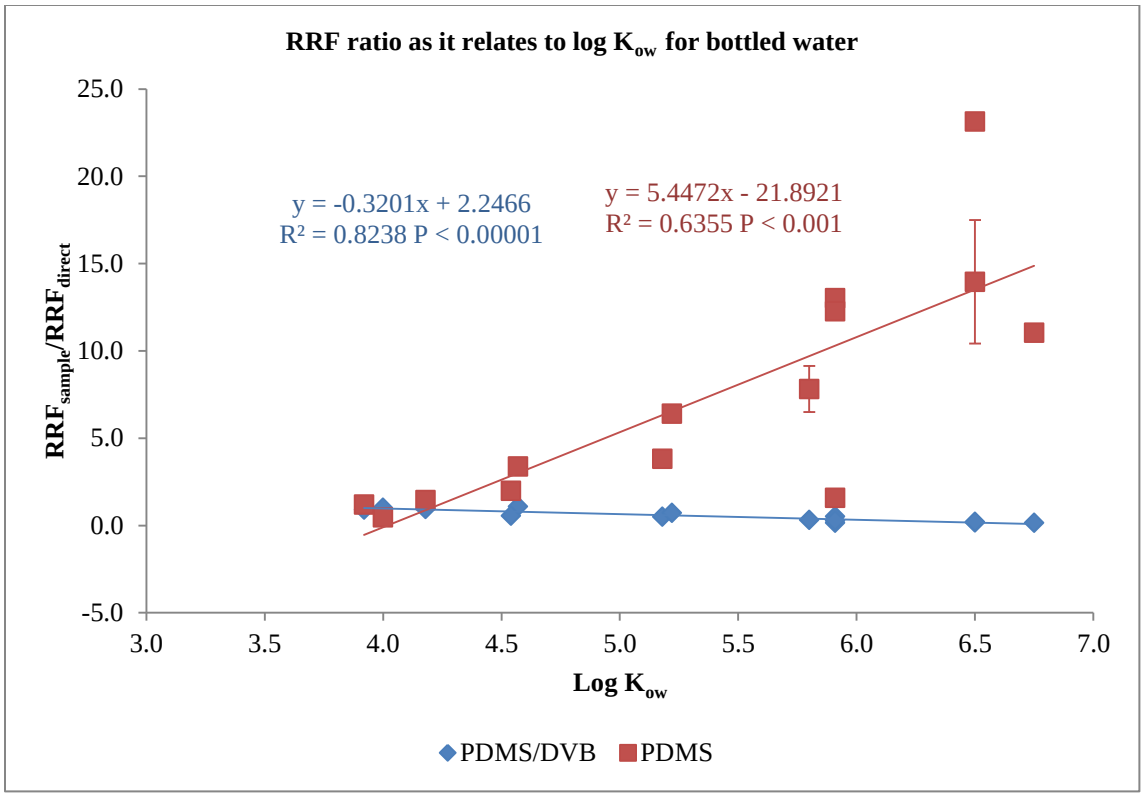

Figure 112 Relationship of the RRF ratio to the octanol/water coefficient (K_{ow}) for bottled water. (RRF_{direct} = relative response factor direct injection, RRF_{sample} = relative response factor SPME sample injection)

`

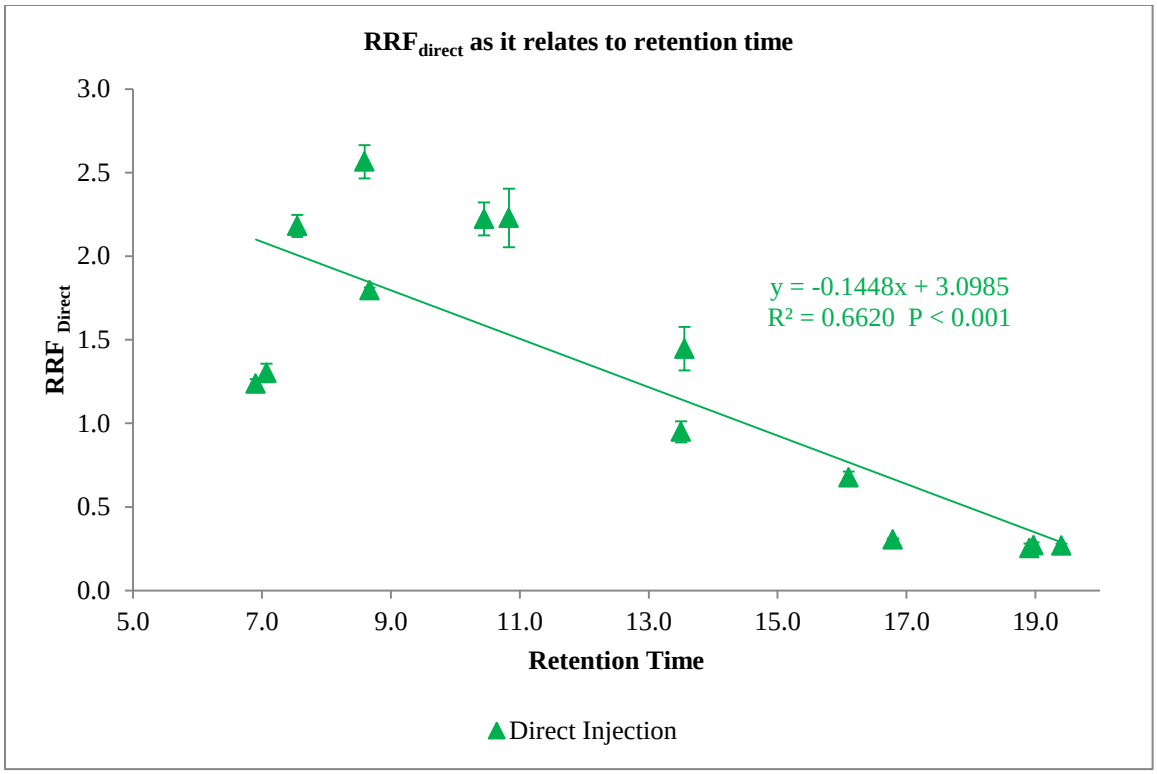

Figure 113 Relationship of the RRF_{direct} to the instrument retention time for direct injection. (RRF_{direct} = relative response factor direct injection)

`

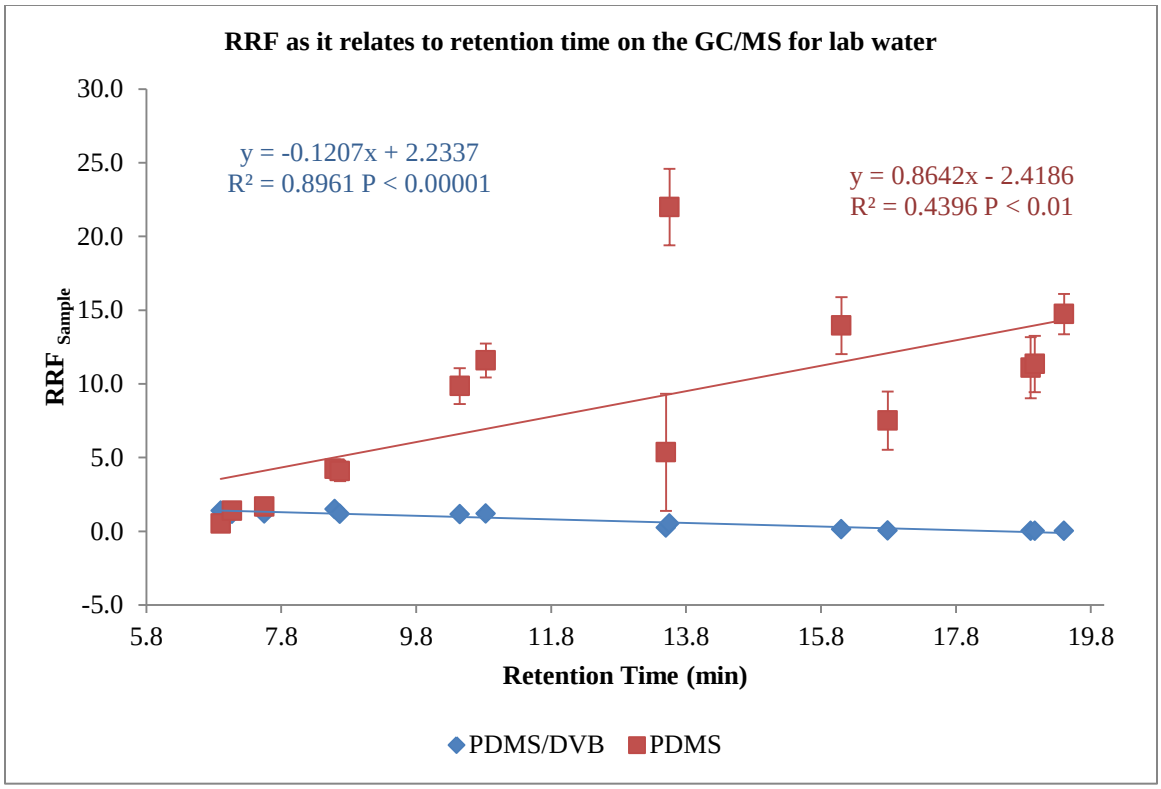

Figure 114 Relationship of the RRF to the instrument retention time for laboratory water. (RRF_{sample} = relative response factor SPME sample injection)

`

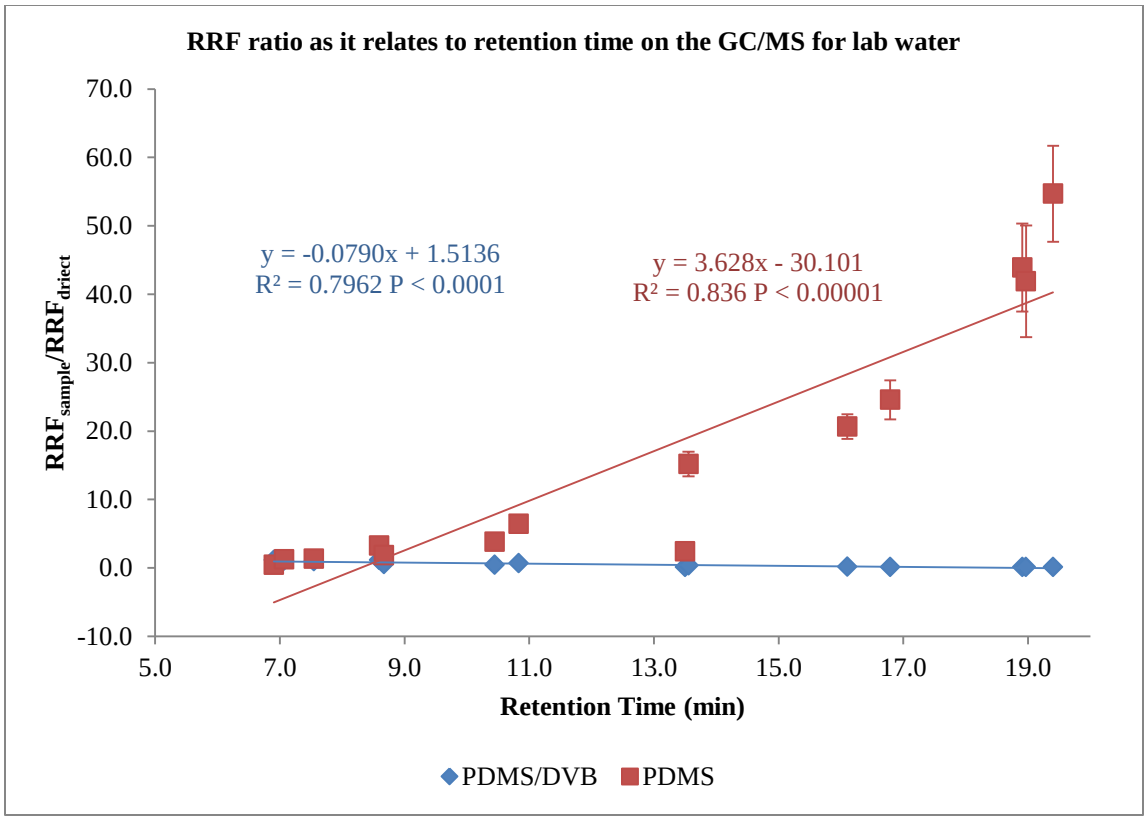

Figure 115 Relationship of the RRF ratio to the instrument retention time for laboratory water. (RRF_{direct} = relative response factor direct injection, RRF_{sample} = relative response factor SPME sample injection)

`

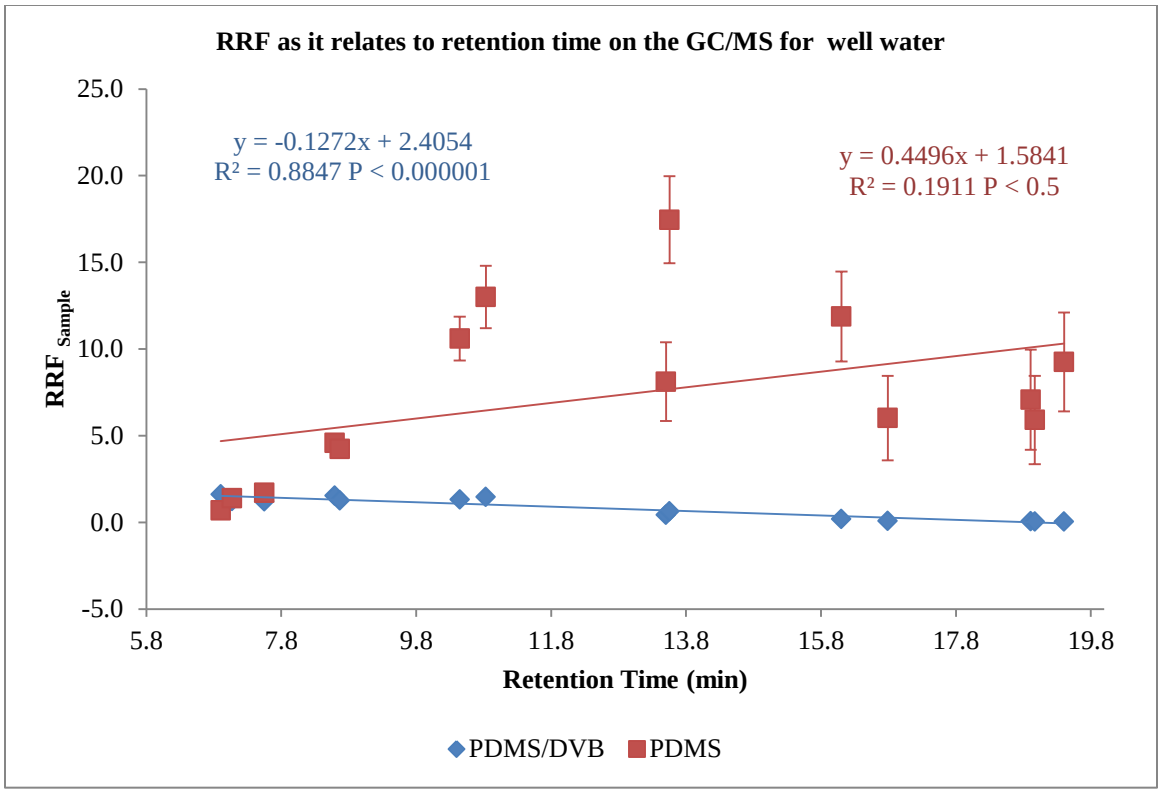

Figure 116 Relationship of the RRF to the instrument retention time for well water. (RRF_{sample} = relative response factor SPME sample injection)

`

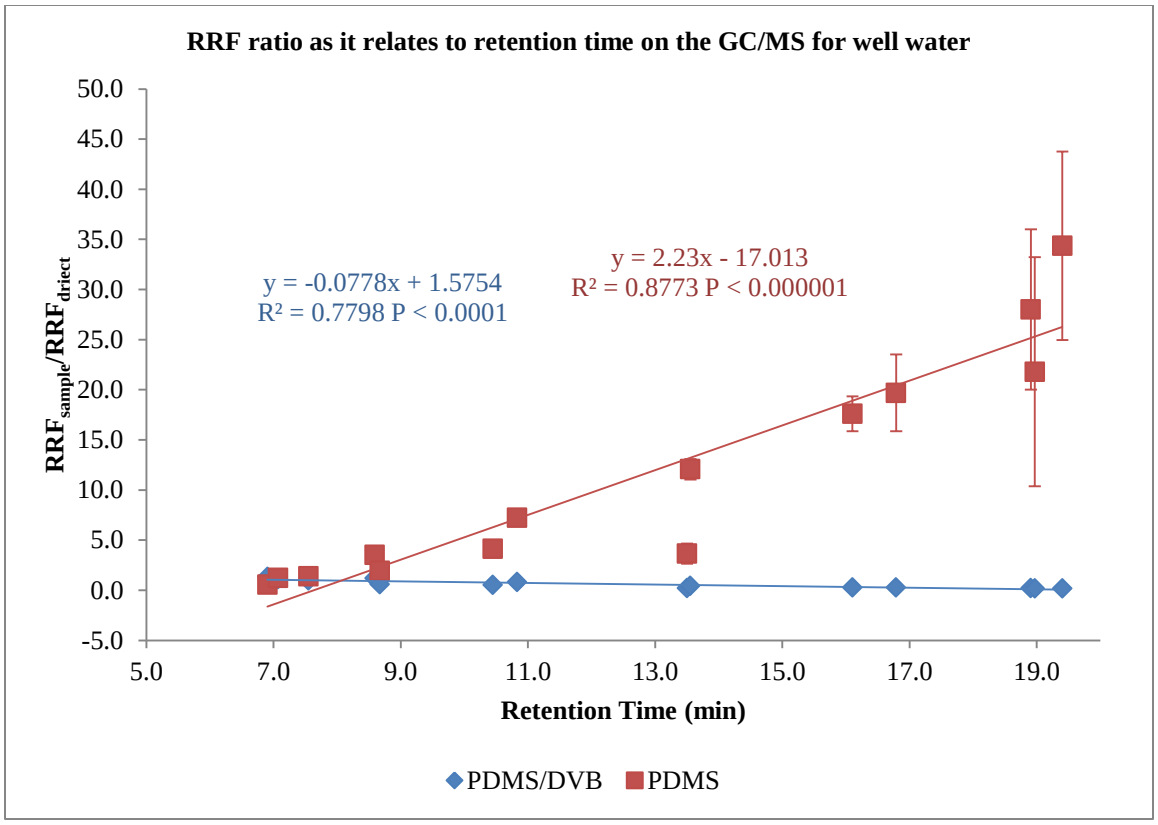

Figure 117 Relationship of the RRF ratio to the instrument retention time for well water. (RRF_{direct} = relative response factor direct injection, RRF_{sample} = relative response factor SPME sample injection)

`

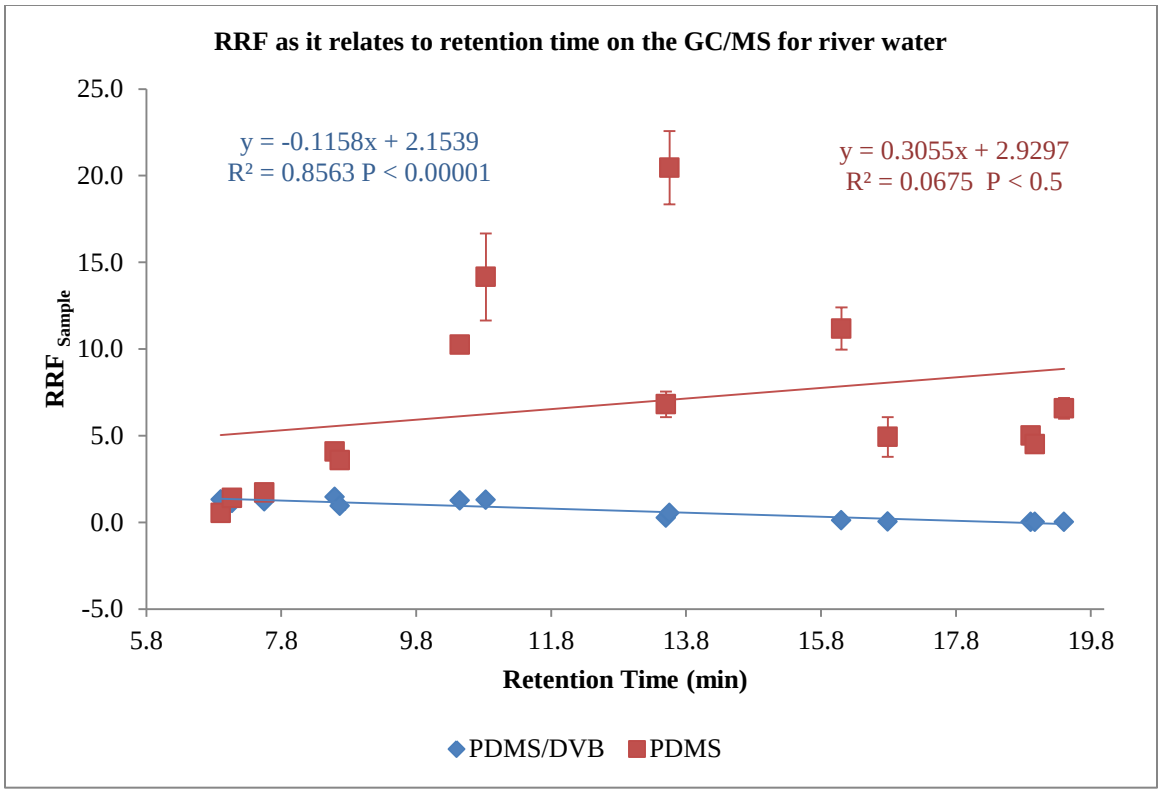

Figure 118 Relationship of the RRF to the instrument retention time for river water. (RRF_{sample} = relative response factor SPME sample injection)

`

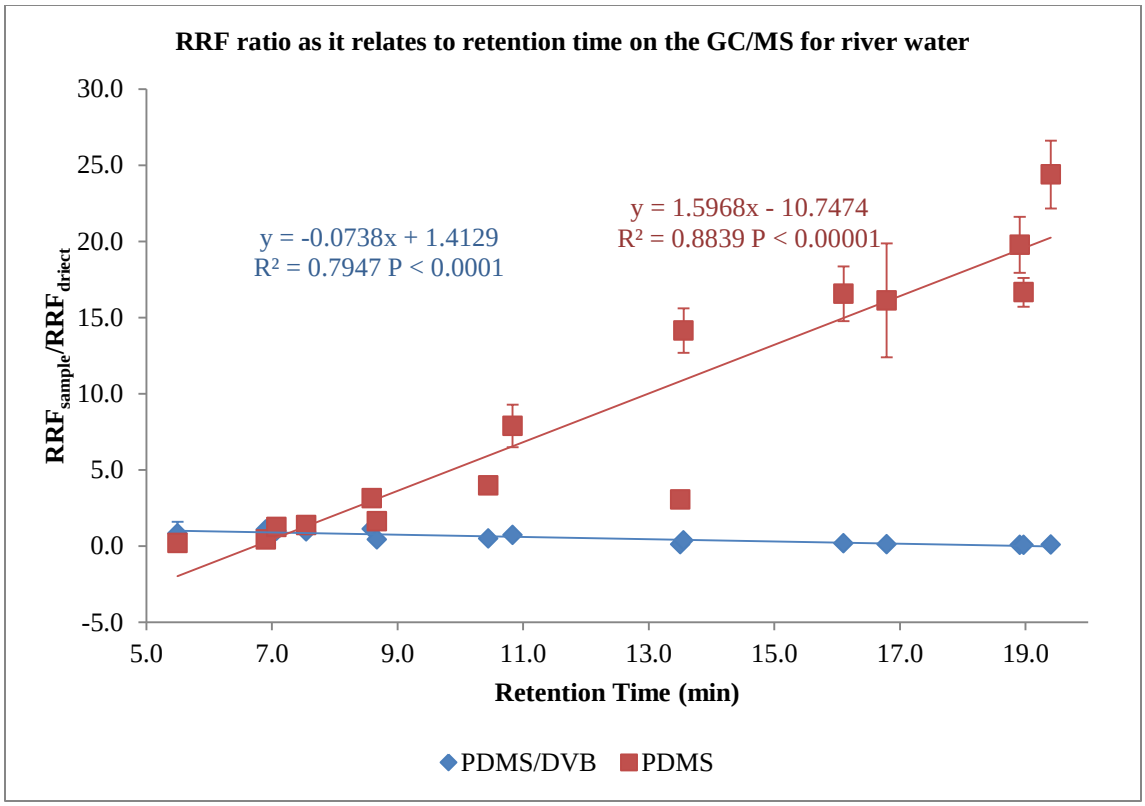

Figure 119 Relationship of the RRF ratio to the instrument retention time for river water. (RRF_{direct} = relative response factor direct injection, RRF_{sample} = relative response factor SPME sample injection)

`

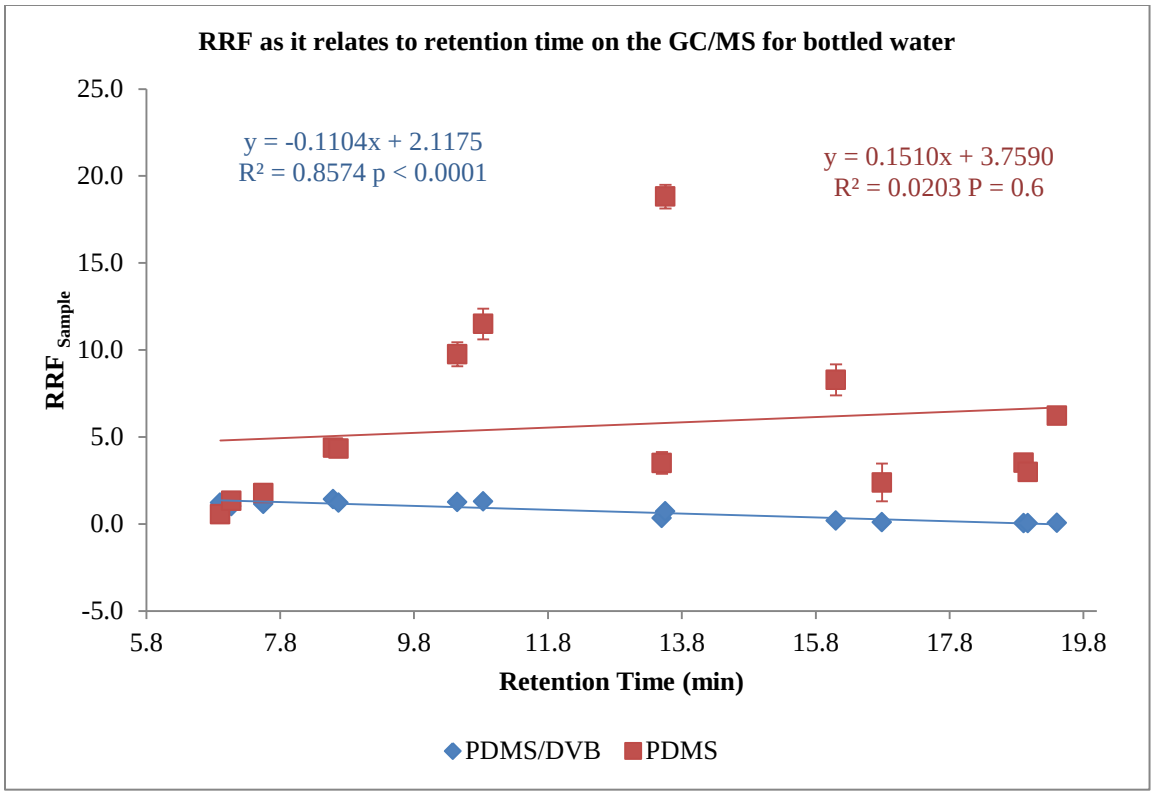

Figure 120 Relationship of the RRF to the instrument retention time for bottled water. (RRF_{sample} = relative response factor SPME sample injection)

`

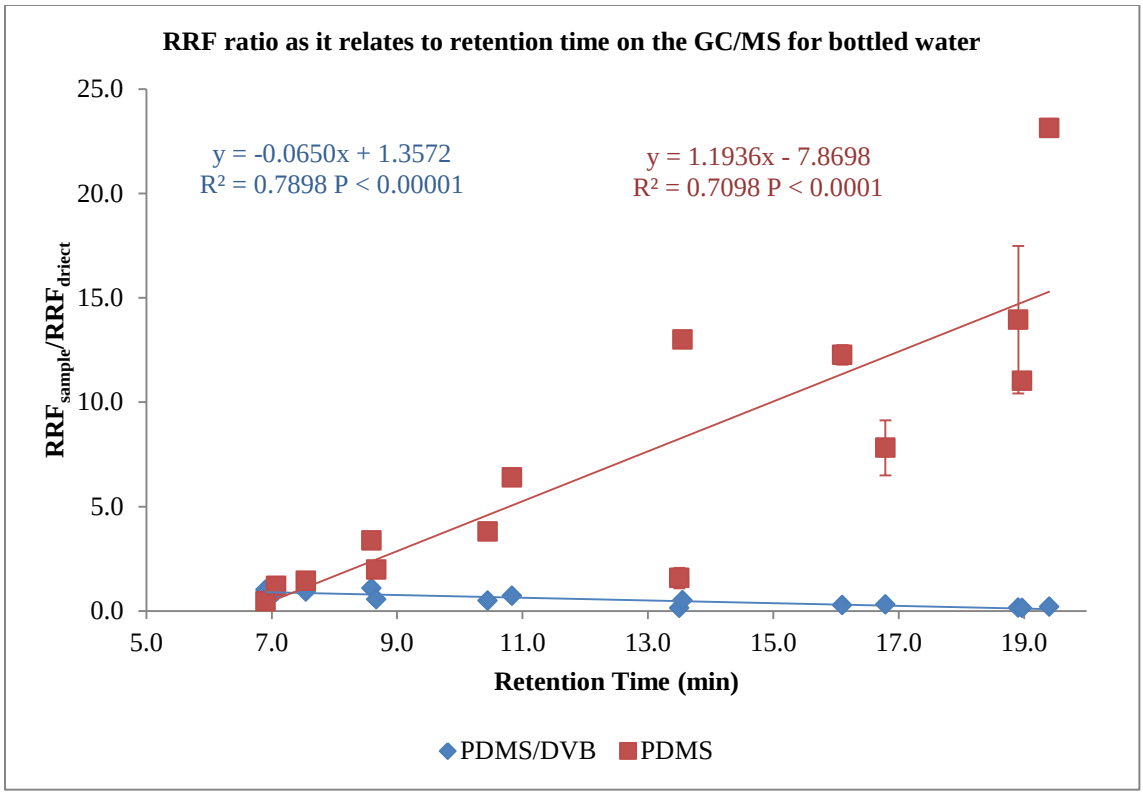

Figure 121 Relationship of the RRF ratio to the instrument retention time for bottled water. (RRF_{direct} = relative response factor direct injection, RRF_{sample} = relative response factor SPME sample injection)

`

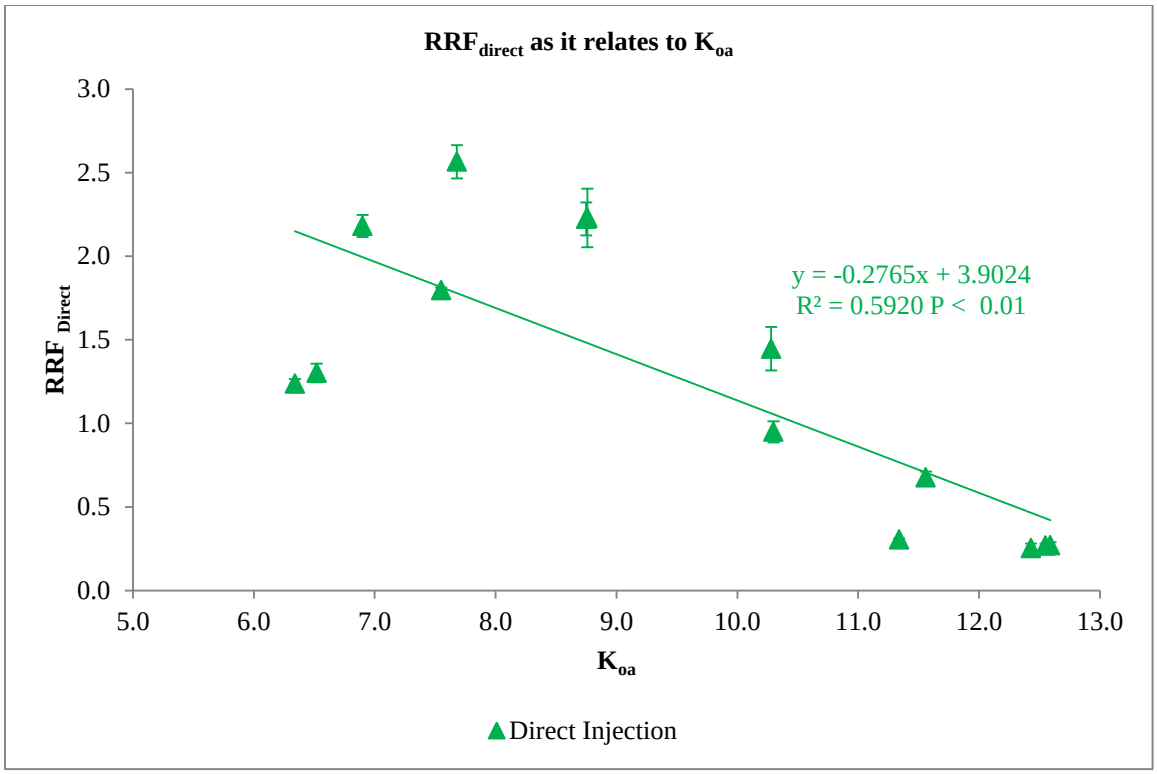

Figure 122 Relationship of the RRF_{direct} to the K_{oa} for direct injection. (RRF_{direct} = relative response factor direct injection)

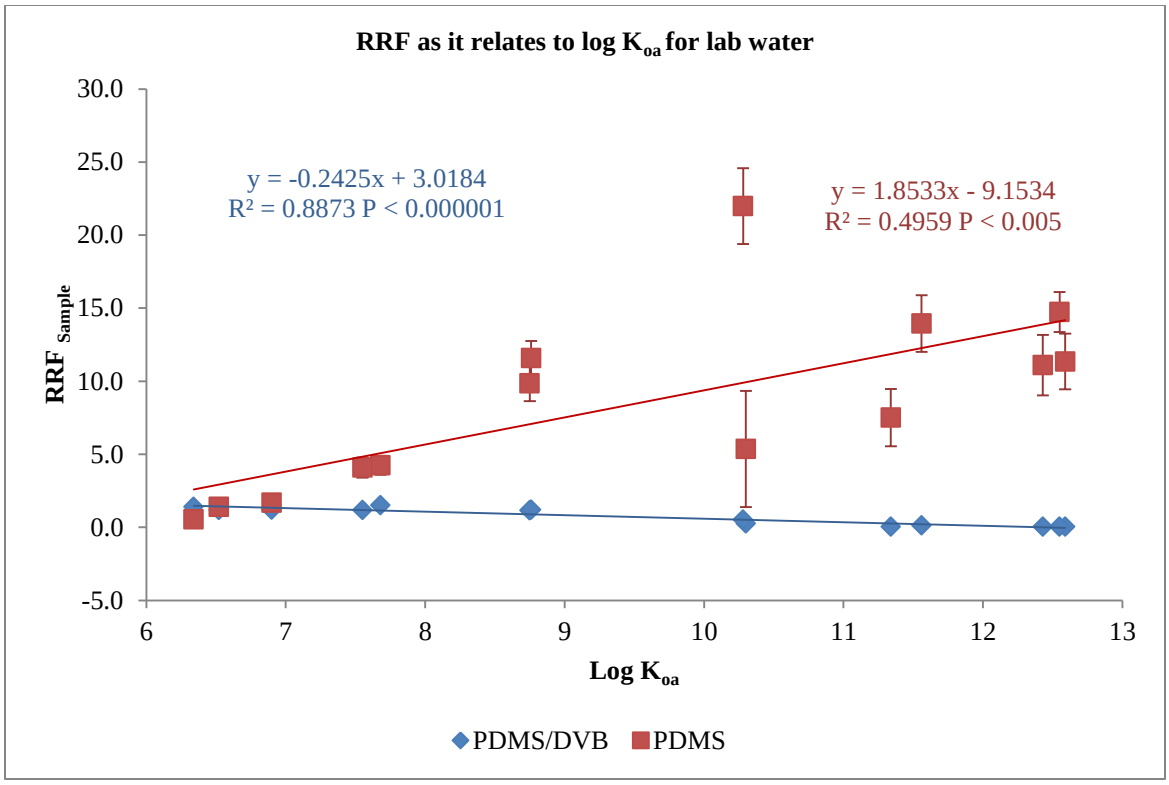

Figure 123 Relationship of the RRF to the K_{oa} for laboratory water. (RRF_{sample} = relative response factor SPME sample injection)

`

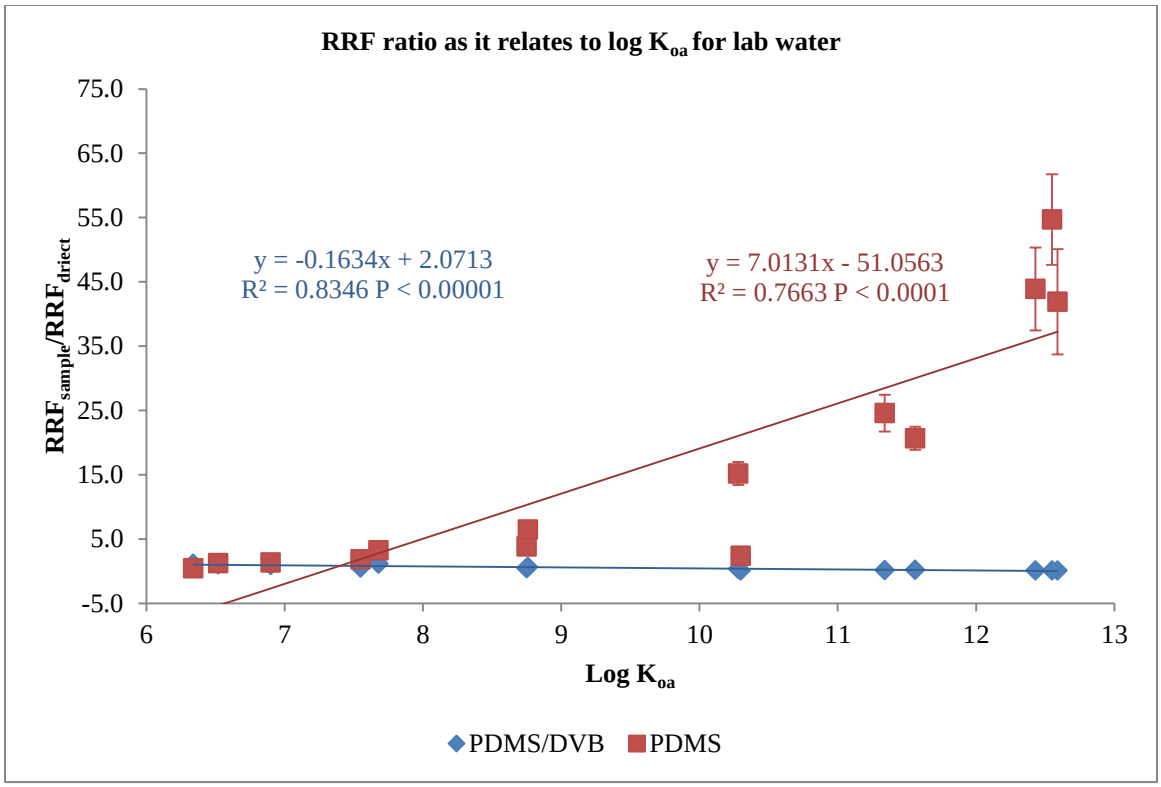

Figure 124 Relationship of the RRF ratio to the K_{oa} for laboratory water. (RRF_{direct} = relative response factor direct injection, RRF_{sample} = relative response factor SPME sample injection)

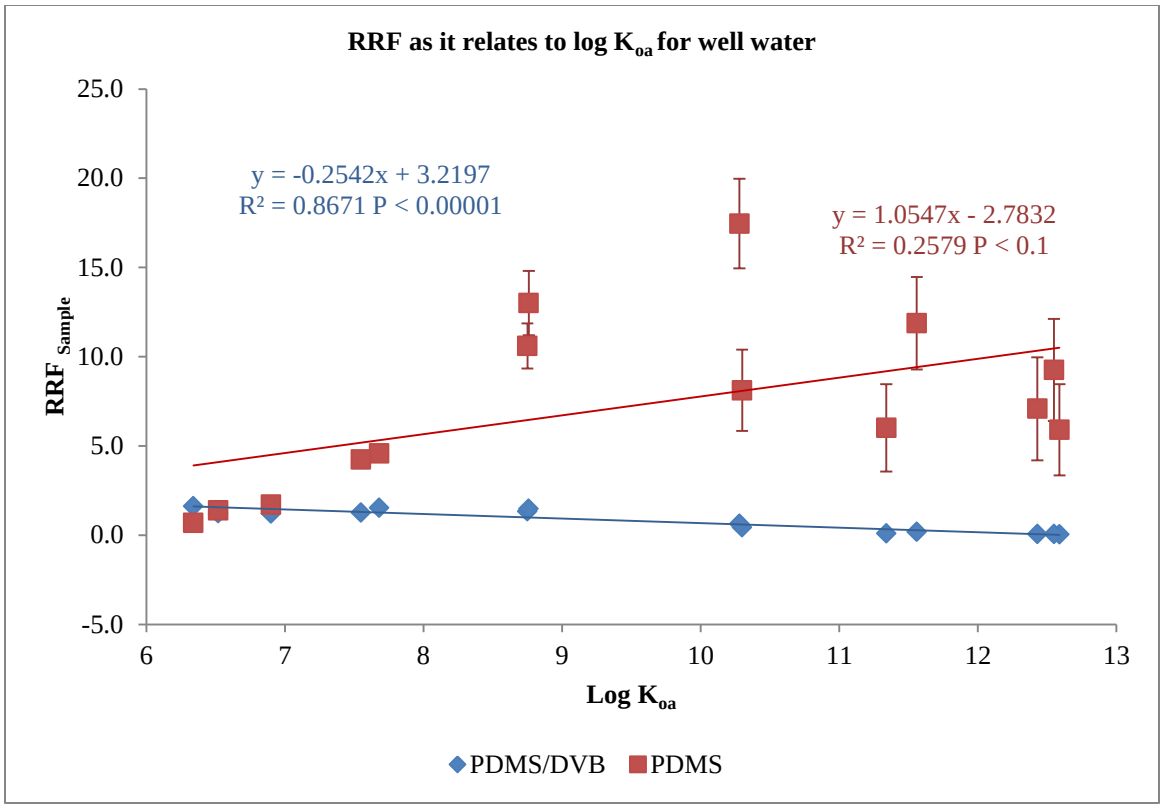

Figure 125 Relationship of the RRF to the K_{oa} for well water. (RRF_{sample} = relative response factor SPME sample injection)

`

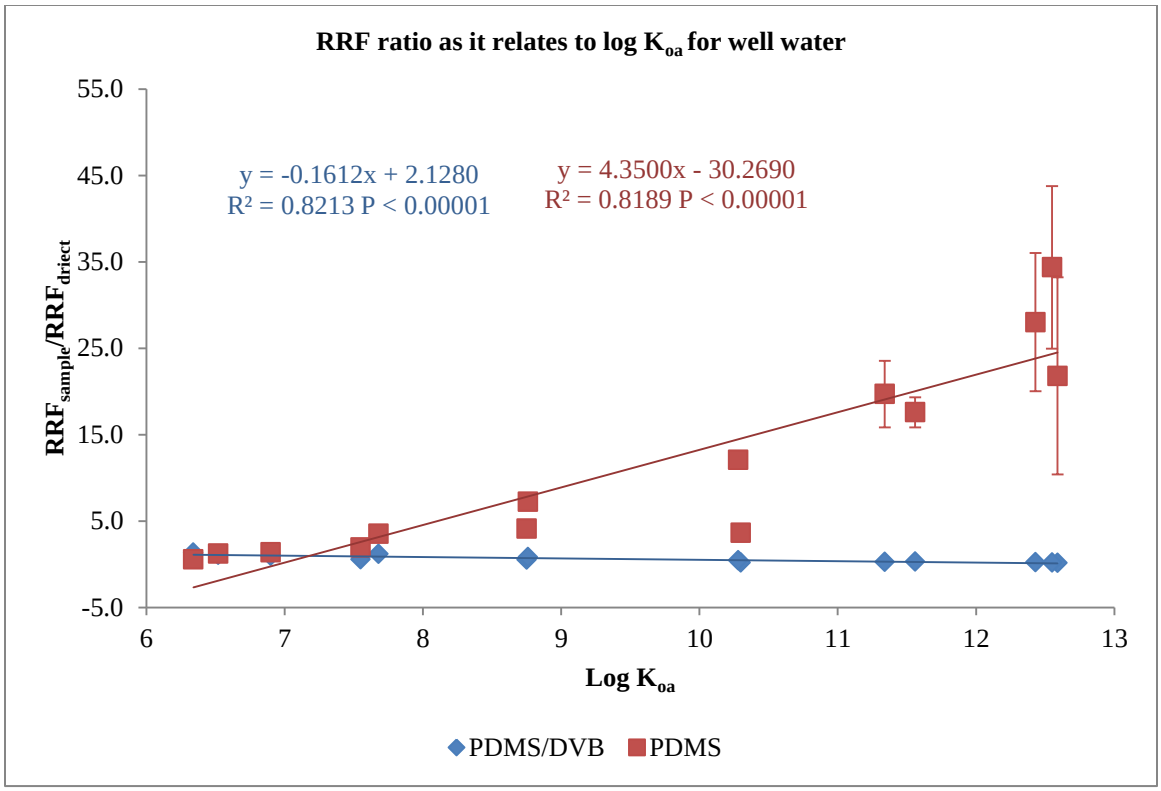

Figure 126 Relationship of the RRF ratio to the K_{oa} for well water. (RRF_{direct} = relative response factor direct injection, RRF_{sample} = relative response factor SPME sample injection)

`

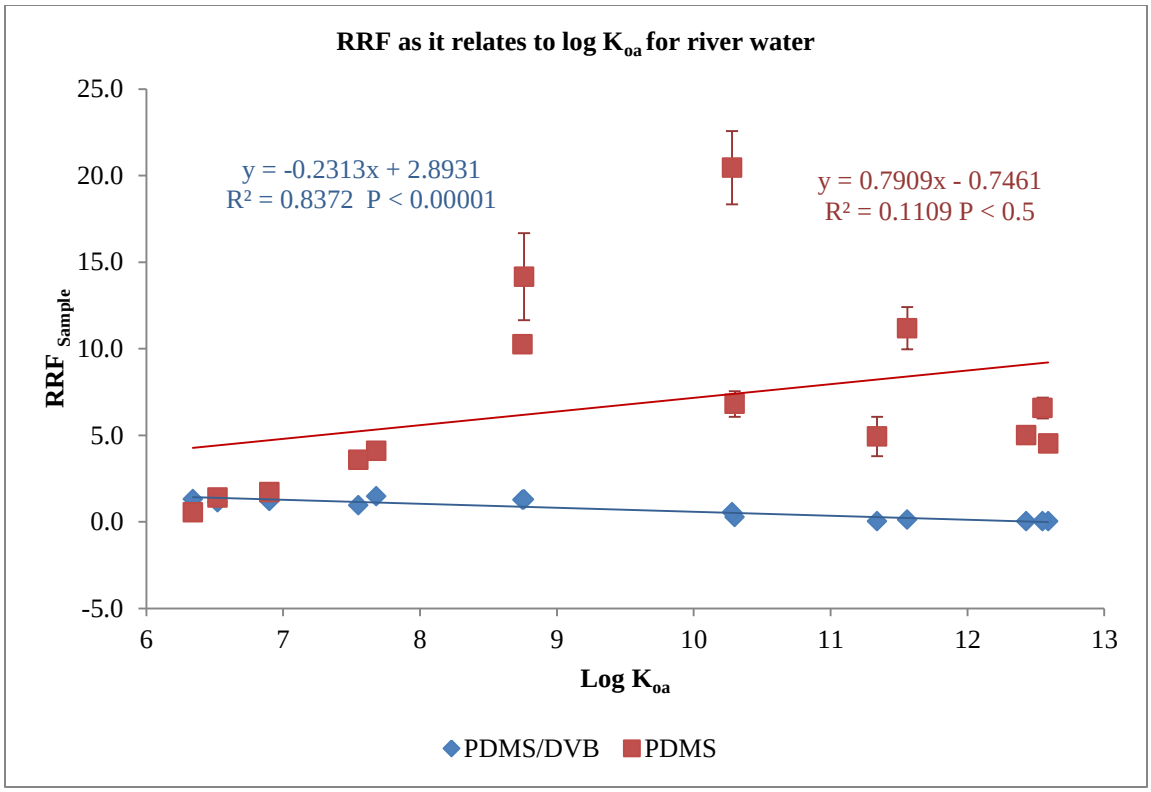

Figure 127 Relationship of the RRF to the K_{oa} for river water. (RRF_{sample} = relative response factor SPME sample injection)

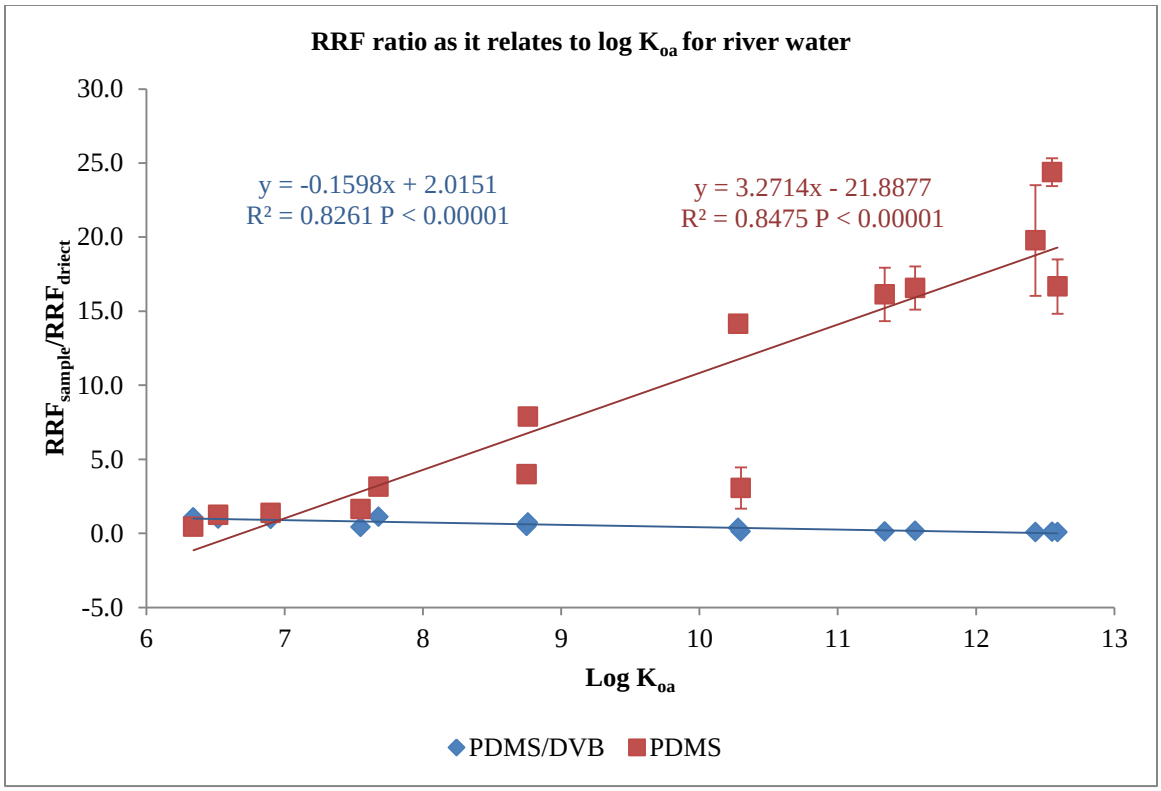

Figure 128 Relationship of the RRF ratio to the K_{oa} for river water. (RRF_{direct} = relative response factor direct injection, RRF_{sample} = relative response factor SPME sample injection)

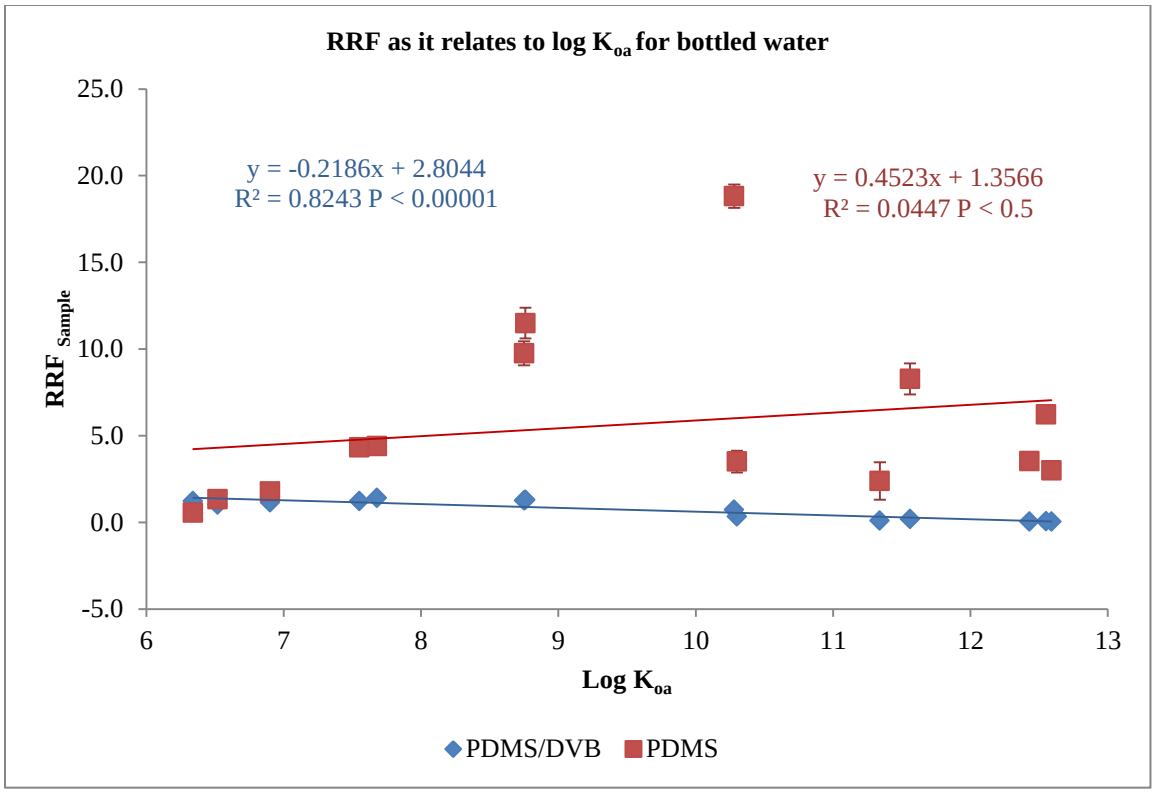

Figure 129 Relationship of the RRF to the K_{oa} for bottled water. (RRF_{sample} = relative response factor SPME sample injection)

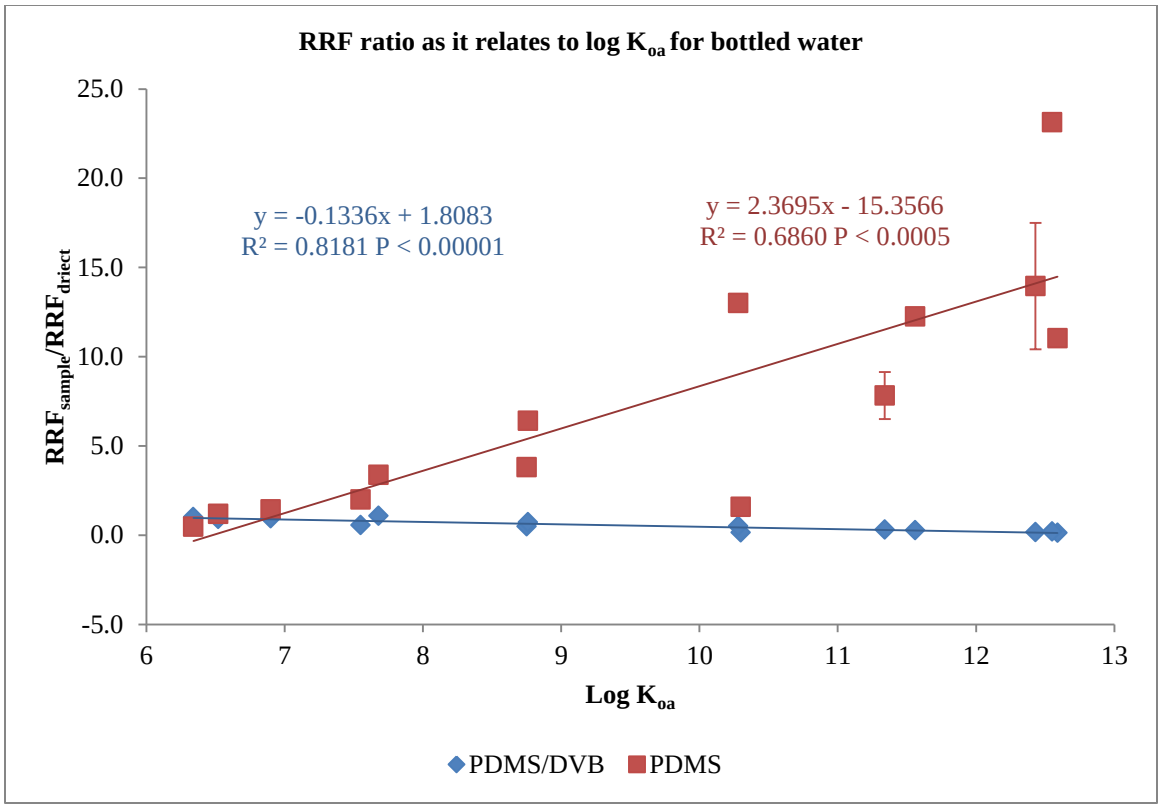

Figure 130 Relationship of the RRF ratio to the K_{oa} for bottled water. (RRF_{direct} = relative response factor direct injection, RRF_{sample} = relative response factor SPME sample injection)

`

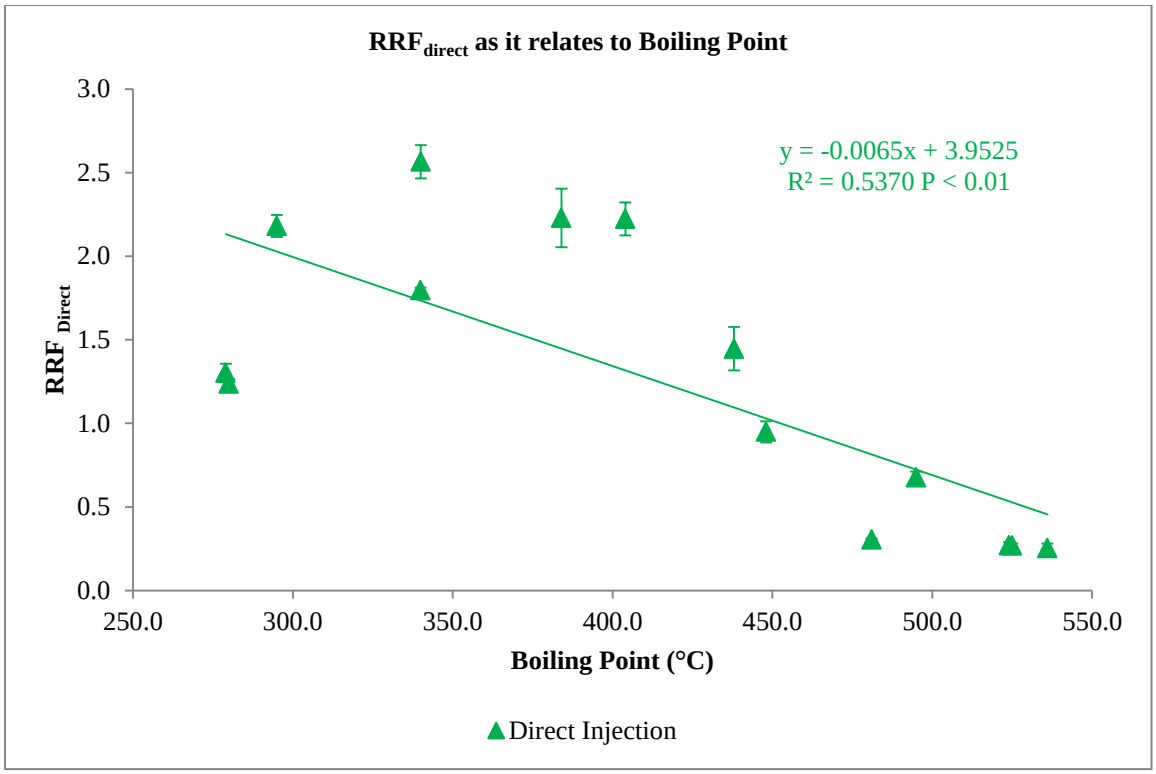

Figure 131 Relationship of the RRF_{direct} to the boiling points of PAHs as it relates to direct injection. (RRF_{direct} = relative response factor direct injection)

`

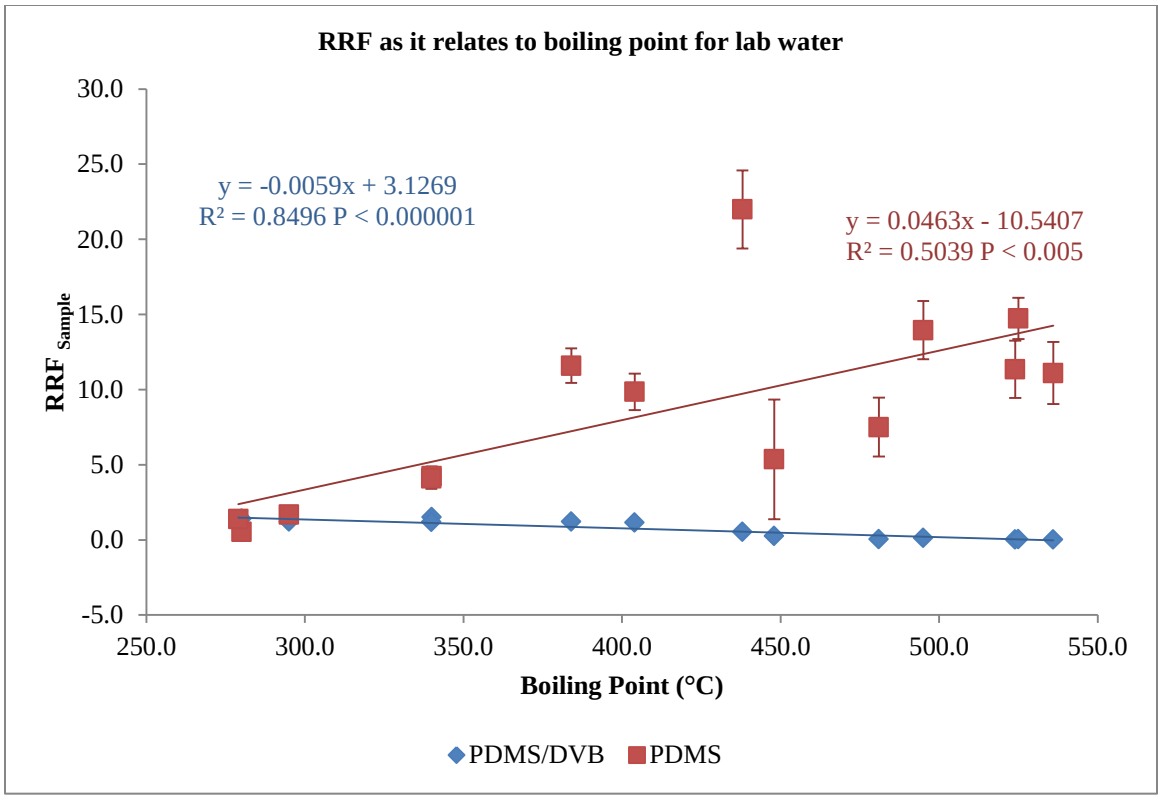

Figure 132 Relationship of the RRF to the boiling points of PAHs using laboratory water. (RRF_{sample} = relative response factor SPME sample injection)

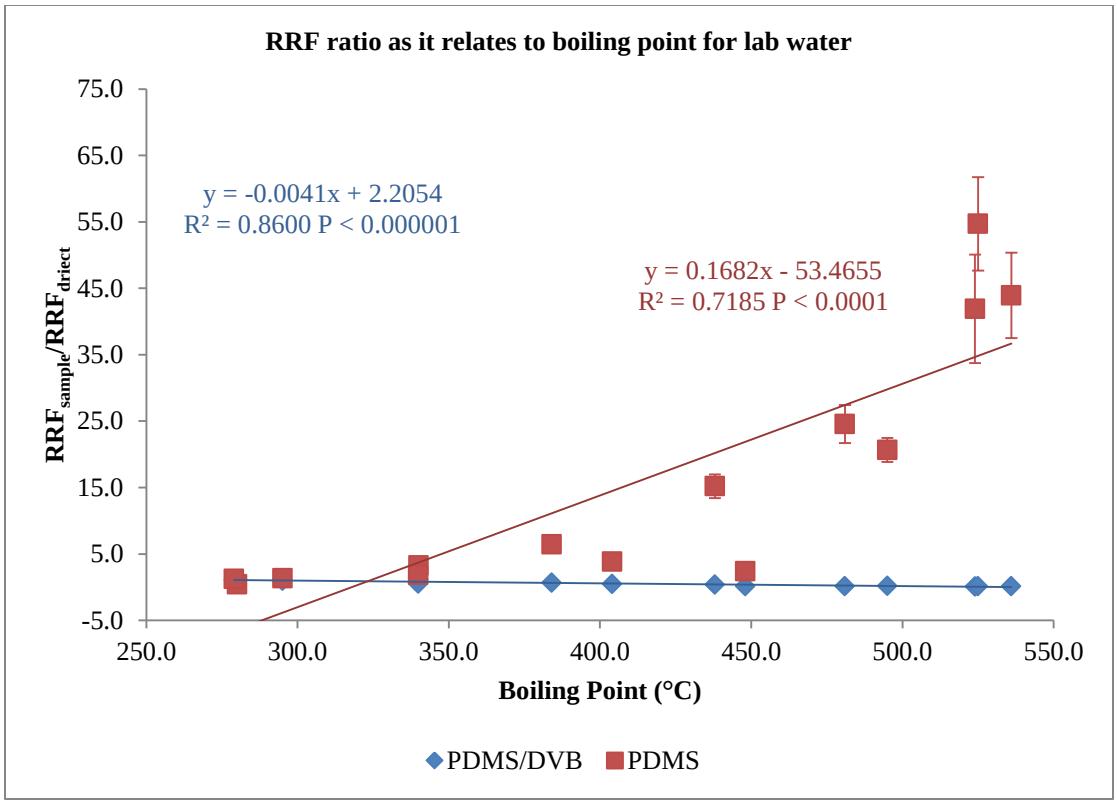

Figure 133 Relationship of the RRF ratio to the boiling points of PAHs using laboratory water. (RRF_{direct} = relative response factor direct injection, RRF_{sample} = relative response factor SPME sample injection)

`

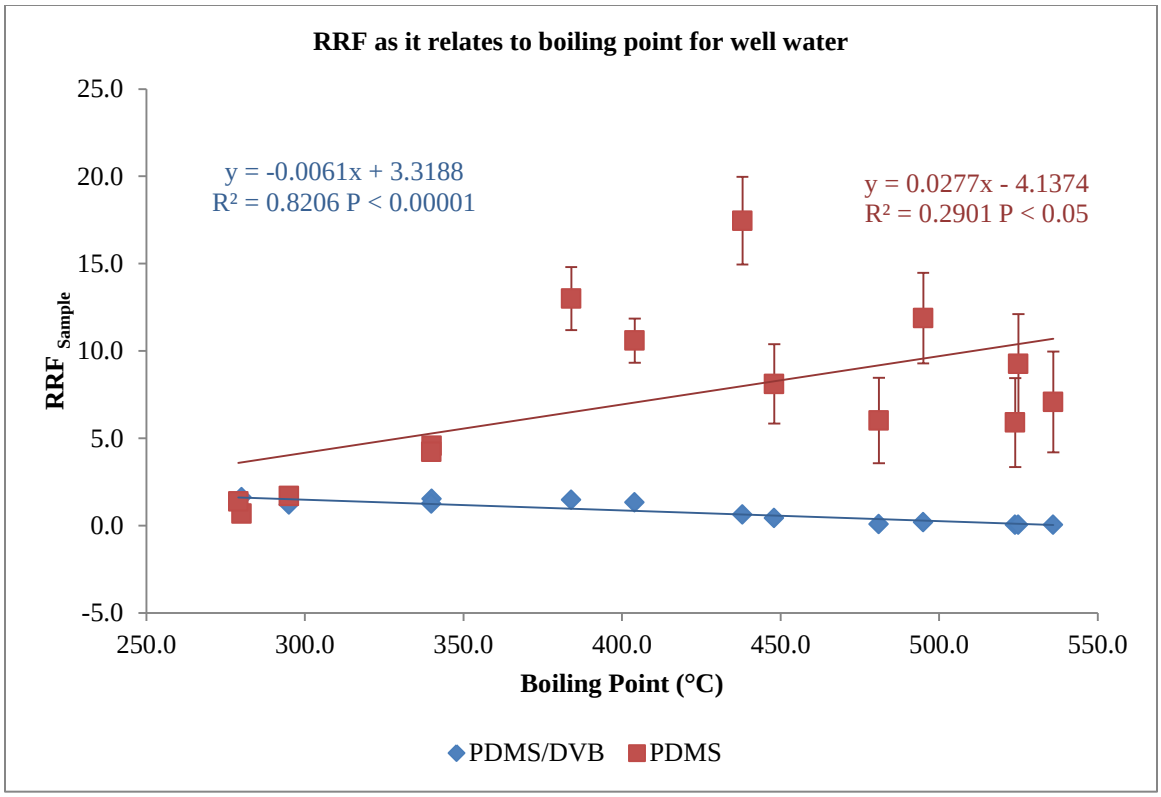

Figure 134 Relationship of the RRF to the boiling points of PAHs using well water. (RRF_{sample} = relative response factor SPME sample injection)

`

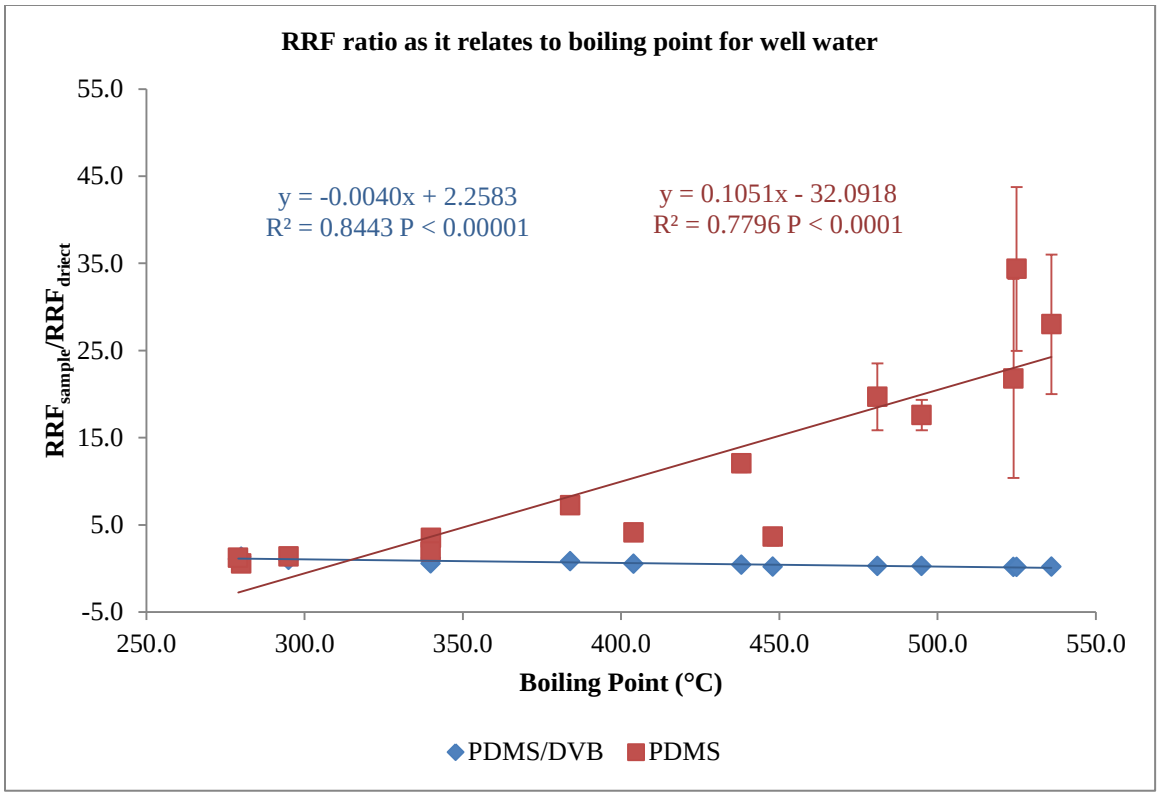

Figure 135 Relationship of the RRF ratio to the boiling points of PAHs using well water. (RRF_{direct} = relative response factor direct injection, RRF_{sample} = relative response factor SPME sample injection)

`

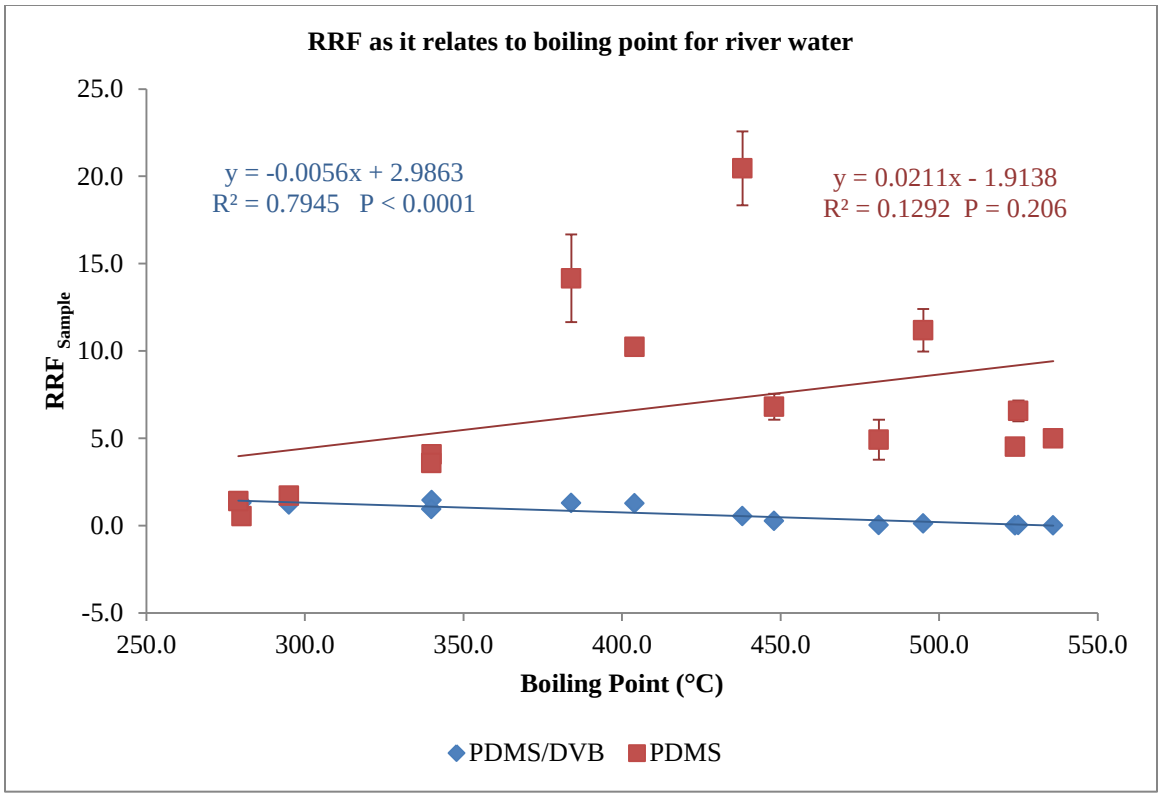

Figure 136 Relationship of the RRF to the boiling points of PAHs using river water. (RRF_{sample} = relative response factor SPME sample injection)

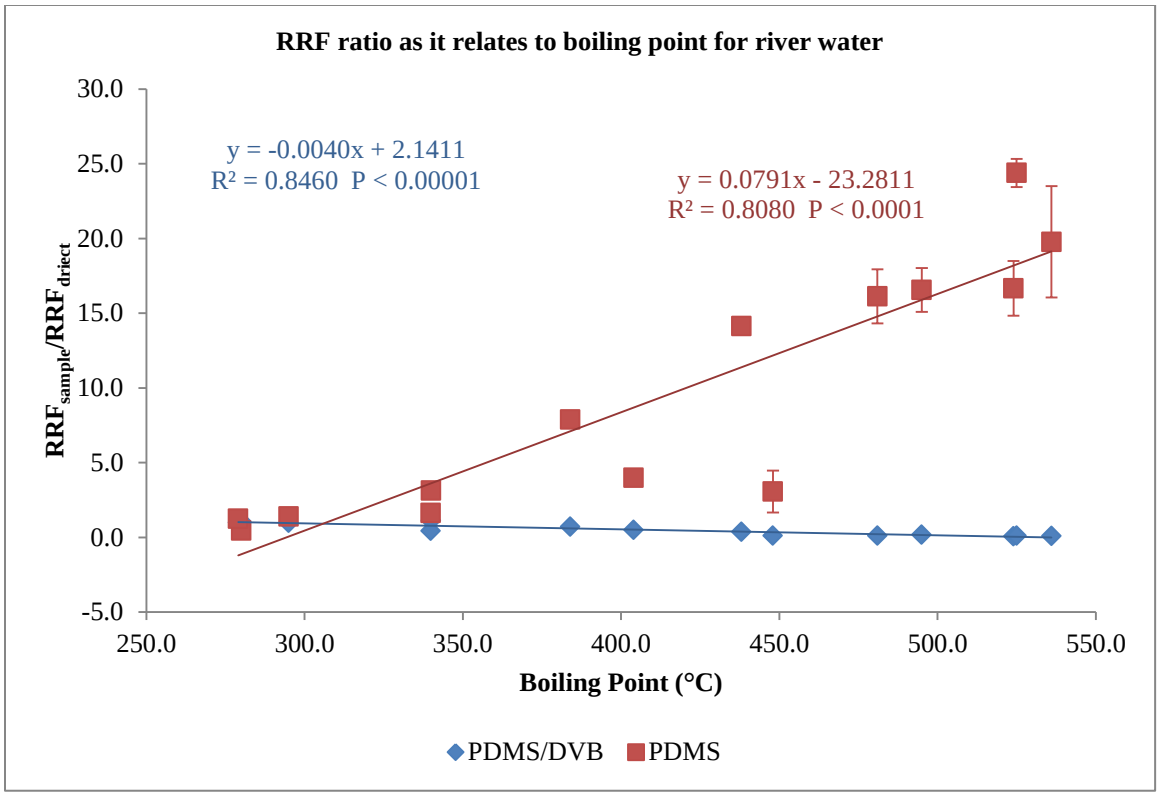

Figure 137 Relationship of the RRF ratio to the boiling points of PAHs using river water. (RRF_{direct} = relative response factor direct injection, RRF_{sample} = relative response factor SPME sample injection)

`

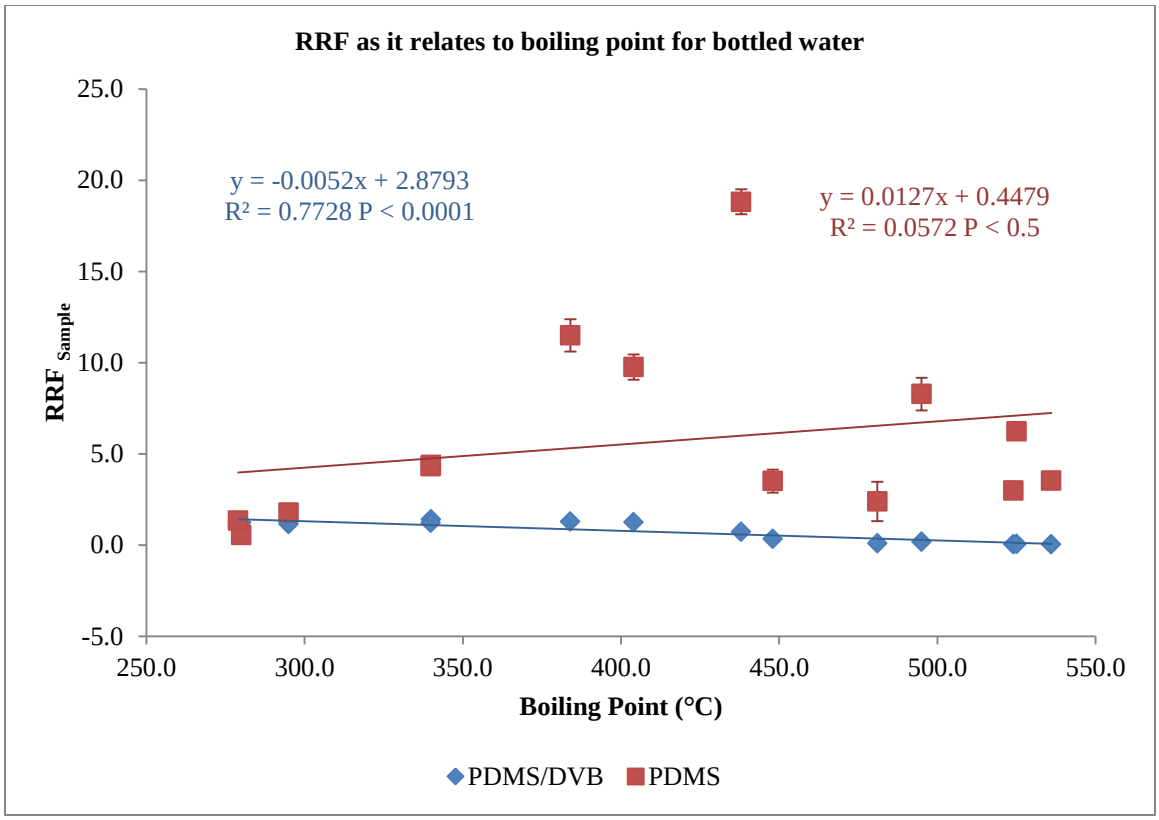

Figure 138 Relationship of the RRF to the boiling points of PAHs using bottled water. (RRF_{sample} = relative response factor SPME sample injection)

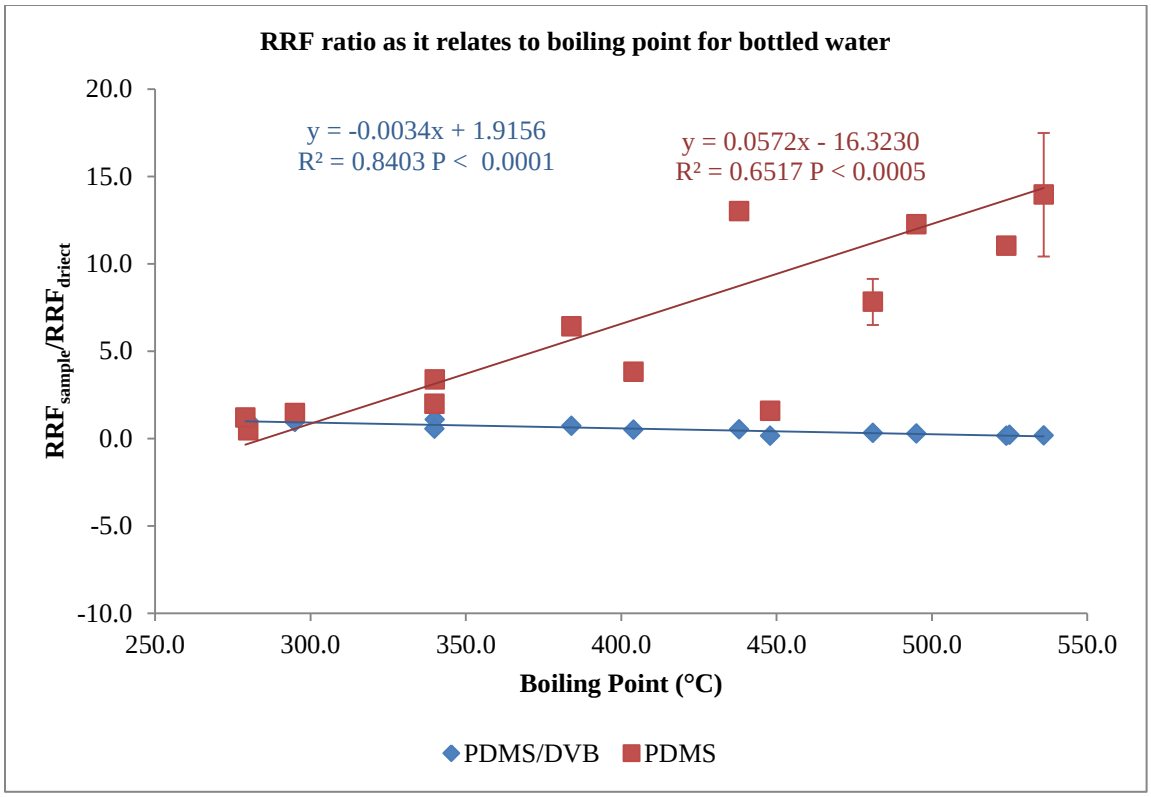

Figure 139 Relationship of the RRF ratio to the boiling points of PAHs using bottled water. (RRF_{direct} = relative response factor direct injection, RRF_{sample} = relative response factor SPME sample injection

`

Bibliography

1. Baklanov, A. et al. Integrated systems for forecasting urban meteorology, air pollution and population exposure. *Atmospheric Chemistry and Physics* 7, 855–874 (2007).

2. Menzie, C. A., Potocki, B. B. & Joseph, S. Exposure to Carcinogenic PAHs in The Environment. *Environmental Science and Technology* 26, 1278–1284 (1992).

3. Arey, J. and Atkinson, R. (2003). Photochemical Reactions of PAHs in the Atmosphere. In Peter E. T. Douben (1st ed) *PAHs: An Ecotoxicological Perspective*. (pp. p47–63) John Wiley & Sons West Sussex, England

4. DiToro, D. M. & McGrath, J. a. Technical basis for narcotic chemicals and polycyclic aromatic hydrocarbon criteria.I. *Water and tissue. Environmental Toxicology and Chemistry 19*, 1951–1970 (2000).

5. International Agency for Research on Cancer. IARC Monographs on the Evaluation of Carcinogenic Risks to Humans, volume 92.*Some Non-heterocyclic Polycyclic Aromatic Hydrocarbons and Some Related Exposures*. Lyon, France: IARC 2010.

6. CCME. *Carcinogenic and other Polycyclic Aromatic Hydrocarbons (PAHs) (Environmental and Human Health Effects) Scientific Criteria Document (revised).* Canadian Council of Ministers of the Environment, 216 pp (2010).

7. Masih, J., Singhvi, R., Kumar, K., Jain, V. K. & Taneja, A. Seasonal variation and sources of polycyclic aromatic hydrocarbons (PAHs) in indoor and outdoor air in a semi-arid tract of Northern India. *Aerosol and Air Quality Research* 12, 515–525 (2012).

`

8. Akyüz, M. & Çabuk, H. Gas-particle partitioning and seasonal variation of polycyclic aromatic hydrocarbons in the atmosphere of Zonguldak, Turkey. *Science of the Total Environment* 408, 5550–5558 (2010).

9. Armstrong, B., Hutchinson, E., Unwin, J. & Fletcher, T. Lung cancer risk after exposure to polycyclic aromatic hydrocarbons: A review and meta-analysis. *Environmental Health Perspectives* 112, 970–978 (2004).

10. World Health Organization. *Polynuclear aromatic hydrocarbons in Drinking-water*. Background document for development of WHO Guidelines for Drinking-water Quality 2, 1–27 (1998).

11. Tolosa, I., Bayona, J. M. & Albaigés, J. Aliphatic and polycyclic aromatic hydrocarbons and sulfur/oxygen derivatives in Northwestern Mediterranean sediments: Spatial and temporal variability, fluxes, and budgets. *Environmental Science and Technology* 30, 2495–2503 (1996).

12. Masih, A. & Taneja, A. Polycyclic aromatic hydrocarbons (PAHs) concentrations and related carcinogenic potencies in soil at a semi-arid region of India. *Chemosphere* 65, 449–456 (2006).

13. Seo, J. S., Keum, Y. S., Harada, R. M. & Li, Q. X. Isolation and characterization of bacteria capable of degrading Polycyclic Aromatic Hydrocarbons (PAHs) and organophosphorus pesticides from PAH-contaminated soil in Hilo, Hawaii. *Journal of Agricultural and Food Chemistry* 55, 5383–5389 (2007).

14. Zhang, Y. & Tao, S. Global atmospheric emission inventory of polycyclic aromatic hydrocarbons (PAHs) for 2004. *Atmospheric Environment* 43, 812–819 (2009).

15. Wang, Z. *et al.* Forensic source differentiation of petrogenic, pyrogenic, and biogenic hydrocarbons in Canadian oil sands environmental samples. *Journal of Hazardous Materials* 271**,** 166–177 (2014).

16. Environment Canada. Toxic substances list: PAHs - Canada.ca. Government of Canada[online] Ec.gc.ca. Available at: http://www.ec.gc.ca/toxiques-toxics/Default.asp?lang=En&n=9C252383-1 [Accessed 29 Jun. 2018].

17. Government of British Columbia. *Water Quality* Province of British Columbia. Env.gov.bc.ca. (2018) [online]
Available at :http://www.env.gov.bc.ca/wat/wq/BCguidelines/pahs/pahs-03.htm
[Accessed 29 Jun. 2018].

18. Sánchez-Avila, J., Fernandez-Sanjuan, M., Vicente, J. & Lacorte, S. Development of a multi-residue method for the determination of organic micropollutants in water, sediment and mussels using gas chromatography-tandem mass spectrometry. *Journal of Chromatography A* 1218**,** 6799–6811 (2011).

19. Alexander, J. et al. Polycyclic Aromatic Hydrocarbons in Food Scientific Opinion of the Panel on Contaminants in the Food Chain (Question N° EFSA-Q-2007-136). *The EFSA Journal* 724, 1–114 (2008).

20. Gomez-Eyles, J. L., Collins, C. D. & Hodson, M. E. Using deuterated PAH amendments to validate chemical extraction methods to predict PAH bioavailability in soils. *Environmental Pollution* 159, 918–923 (2011).

21. Ortmann, A., Anders, J. & Shelton, N. et al. Dispersed oil disrupts microbial pathways in pelagic food webs. *PLoS ONE* 7, (2012).

`

22. Weber, R. *et al.* Dioxin- and POP-contaminated sites - Contemporary and future relevance and challenges: Overview on background, aims and scope of the series. *Environmental Science and Pollution Research* 15**,** 363–393 (2008)

23. Cruzan, G. & Kirkpatrick, D. Tertiary-butyl acetate metabolism, toxicity, and human health considerations. *Toxicological & Environmental Chemistry* 88, 405–421 (2006).

24. Wang, X., Lin, L., Luan, T., Yang, L. & Tam, N. F. Y. Determination of hydroxylated metabolites of polycyclic aromatic hydrocarbons in sediment samples by combining subcritical water extraction and dispersive liquid-liquid microextraction with derivatization. *Analytica Chimica Acta* 753, 57–63 (2012).

25. Yebra-Pimentel, I., Fernández-González, R., Martínez-Carballo, E. & Simal-Gándara, J. A critical review about the health risk assessment of pahs and their metabolites in foods. *Critical Reviews in Food Science and Nutrition* 55, 1383–1405 (2015)

26. Król, S., Zabiegała, B. & Namieśnik, J. Monitoring and analytics of semivolatile organic compounds (SVOCs) in indoor air. *Analytical and Bioanalytical Chemistry* 400, 1751–1769 (2011).

27. Warren, J. *Needle Trap Device and Solid Phase Microextraction Combined with Portable GC-MS for On-Site Applications*. University of Waterloo, Thesis, 91 (2011).

28. Hyötyläinen, T. & Riekkola, M. L. Potential of effective extraction techniques and new analytical systems for profiling the marine environment. *TrAC - Trends in Analytical Chemistry* 26, 788–808 (2007).

`

29. Tarantini, A. et al. Relative contribution of DNA strand breaks and DNA adducts to the genotoxicity of benzo[a]pyrene as a pure compound and in complex mixtures. *Mutation Research - Fundamental and Molecular Mechanisms of Mutagenesis* 671, 67–75 (2009).

30. Spink, D. C. et al. Induction of CYP1A1 and CYP1B1 by benzo(k)fluoranthene and benzo(a)pyrene in T-47D human breast cancer cells: Roles of PAH interactions and PAH metabolites. *Toxicology and Applied Pharmacology* 226, 213–224 (2008).

31. Hainaut, P. & Pfeifer, G. P. Patterns of p53 G→T transversions in lung cancers reflect the primary mutagenic signature of DNA-damage by tobacco smoke. *Carcinogenesis* 22, 367–374 (2001).

32. Jung, K. H. Kim, J. & Noh, J. et al. Characteristic molecular signature for the early detection and prediction of polycyclic aromatic hydrocarbons in rat liver. *Toxicology Letters* 216, 1–8 (2013).

33. World Health and Safety, International Program on Chemical Safety. *Selected non-heterocyclic polycyclic aromatic hydrocarbons*. [online] Apps.who.int. Available at: http://apps.who.int/iris/handle/10665/41958 [Accessed 29 Jun. 2018].

34. Yan, J., Wang, L., Fu, P. P. & Yu, H. Photo mutagenicity of 16 polycyclic aromatic hydrocarbons from the US EPA priority pollutant list. *Mutation Research - Genetic Toxicology and Environmental Mutagenesis* 557, 99–108 (2004).

35. Government of Canada, Health Canada, Healthy Environments and Consumer Safety Branch, Policy and Planning Directorate, Office of Business Services, HECS Publishing. ARCHIVED - *Canadian Environmental Protection Act: Priority Substances List Assessment Report: Polycyclic Aromatic Hydrocarbons*. (2004).

`

36. Wild, S. R. & Jones, K. C. Polynuclear aromatic hydrocarbons in the United Kingdom environment: A preliminary source inventory and budget. *Environmental Pollution* 88, 91–108 (1995).

37. Mackay, D. *Handbook of Physical-Chemical Properties and Environmental Fate for Organic Chemicals On Cd-Rom*. (CRC Press, 2006).

38. Haarstad, K., Bavor, H. J. & Mæhlum, T. Organic and metallic pollutants in water treatment and natural wetlands: A review. *Water Science and Technology* 65, 76–99 (2012).

39. Wu, M., Xu, H. & Ding, Y. Occurrence and removal efficiency of six polycyclic aromatic hydrocarbons in different wastewater treatment plants. *Water Science & Technology* 68, 1844–1851 (2013).

40. Dabrowska, D., Kot-Wasik, A. & Namieśnik, J. Stability studies of selected polycyclic aromatic hydrocarbons in different organic solvents and identification of their transformation products. *Journal of Environmental Studies* 17, 17–24 (2008).

41. Fasnacht, M. P. & Blough, N. V. Aqueous photodegradation of polycyclic aromatic hydrocarbons. *Environmental Science and Technology* 36, 4364–4369 (2002).

42. Yan, B. Abrajano, T. & Bopp, R. et al. Molecular tracers of saturated and polycyclic aromatic hydrocarbon inputs into Central Park Lake, New York City. *Environmental Science and Technology* 39, 7012–7019 (2005).

43. Finlayson-Pitts, B. J. & Pitts, J. N. Tropospheric air pollution: Ozone, airborne toxics, polycyclic aromatic hydrocarbons, and particles. *Science* 276, 1045–1052 (1997).

`

44. Lehto, K.-M., Vuorimaa, E. & Lemmetyinen, H. Photolysis of polycyclic aromatic hydrocarbons (PAHs) in dilute aqueous solutions detected by fluorescence. *Journal of Photochemistry and Photobiology* A: Chemistry 136, 53–60 (2000).

45. Dabrowska, D., Namieśnik, J. & Kot-Wasik, A. Stability studies of selected polycyclic aromatic hydrocarbons in different organic solvents and identification of their transformation products. *Polish Journal of Environmental Studies* 17, 17–24 (2008).

46. Avcibasi, N., Icli, S., & Gilbert, A. Photochemical reactions of alpha-terpinene and acenaphthene under concentrated sunlight. *Turkish Journal of Chemistry*, 27(1), 1–7. (2003).

47. Rivas, F. J., Beltrán, F. J. & Acedo, B. Chemical and photochemical degradation of acenaphthylene. Intermediate identification. *Journal of Hazardous Materials* 75, 89–98 (2000).

48. Miller, J. S. & Olejnik, D. Photolysis of polycyclic aromatic hydrocarbons in water. *Water Research* 35, 233–243 (2001).

49. Woo, O. T., Chung, W. K., Wong, K. H., Chow, A. T. & Wong, P. K. Photocatalytic oxidation of polycyclic aromatic hydrocarbons: Intermediates identification and toxicity testing. *Journal of Hazardous Materials* 168, 1192–1199 (2009).

50. Teng, Y. Luo, Y. & Sun, M. et al. Effect of bioaugmentation by Paracoccus sp. strain HPD-2 on the soil microbial community and removal of polycyclic aromatic hydrocarbons from an aged contaminated soil. *Bioresource Technology* 101, 3437–3443 (2010).

`

51. Moody, J. D., Freeman, J. P., Fu, P. P. & Cerniglia, C. E. Degradation of Benzo[a]pyrene by Mycobacterium vanbaalenii PYR-1. *Applied and Environmental Microbiology* 70, 340–345 (2004).

52. Haritash, A. K. & Kaushik, C. P. Biodegradation aspects of Polycyclic Aromatic Hydrocarbons (PAHs): A review. *Journal of Hazardous Materials* 169, 1–15 (2009).

53. Šepič, E., Bricelj, M. & Leskovšek, H. Toxicity of fluoranthene and its biodegradation metabolites to aquatic organisms. *Chemosphere* 52, 1125–1133 (2003).

54. Environmental Protection Agency. *Method 610: Polynuclear aromatic hydrocarbons*. United States Environmental Protection Agency 1–13 (1986). doi:10.1159/000330408

55. Poster, D. L., Schantz, M. M., Sander, L. C. & Wise, S. A. Analysis of polycyclic aromatic hydrocarbons (PAHs) in environmental samples: A critical review of gas chromatographic (GC) methods. *Analytical and Bioanalytical Chemistry* 386, 859–881 (2006).

56. Eicheelberger, J. W., Behymer, T. D. & Budde, W. L. *Method 525.2 Determination of organic compounds in drinking water by liquid-solid extraction and capillary column gas chromatography/mass spectrometry*. National Exposure Research Laboratory Office of Research and Development, *USEPA*, Cincinnati, Ohio 45268 0, 60 (1995).

57. Lerda, D. Polycyclic Aromatic Hydrocarbons (PAHs) Factsheet. *JRC Technical Notes* 3, 1–25 (2010).

58. Cheng, J., Matsadiq, G., Liu, L., Zhou, Y.-W. & Chen, G. Development of a novel ultrasound-assisted surfactant-enhanced emulsification microextraction method and

its application to the analysis of eleven polycyclic aromatic hydrocarbons at trace levels in water. *Journal of Chromatography A* 1218, 2476–2482 (2011).

59. Tugulea, A. (2011). *Principles of SPME- Chromedia*. [online] Chromedia.org. Available at: http://www.chromedia.org/chromedia?waxtrapp=npuhcHsHiemBpdmBlIEcCKJ&subNav=abffyDsHiemBpdmBlIEcCtBDF [Accessed 30 Jun. 2018].

60. Pawliszyn, J. (2012). *Handbook of solid phase microextraction*. 1st ed. Waltham, MA: Elsevier, pp.13-59. doi:10.1016/B978-0-12-416017-0.00002-4

61. Campo, L., Fustinoni, S. & Bertazzi, P. Quantification of carcinogenic 4- to 6-ring polycyclic aromatic hydrocarbons in human urine by solid-phase microextraction gas chromatography-isotope dilution mass spectrometry. *Analytical and Bioanalytical Chemistry* 401, 625–634 (2011).

62. Menezes, H. C. Palva, M. & Santos, R. et al. A sensitive GC/MS method using cold fiber SPME to determine polycyclic aromatic hydrocarbons in spring water. *Microchemical Journal* 110, 209–214 (2013).

63. Yamada, T. M., Souza, D. A., Morais, C. R. & Mozeto, A. A. Validation of a method for the analysis of PAHs in bulk lake sediments using GC-MS. *Journal of Chromatographic Science* 47, 794–799 (2009).

64. Dolan, J. *Internal Standards #2: What Makes a Good Internal Standard?* Separation Science HPLC Solutions [online] Blog.sepscience.com. Available at: http://blog.sepscience.com/separationscience/hplc-solutions-135-internal-standards-part-2-what-makes-a-good-internal-standard [Accessed 29 Jun. 2018].

`

65. Lange, V., Picotti, P., Domon, B. & Aebersold, R. Selected reaction monitoring for quantitative proteomics: A tutorial. *Molecular Systems Biology 4*, (2008).

66. Chen, H.-W. Determination of polycyclic aromatic hydrocarbons in water by solid-phase microextraction and liquid chromatography. *Analytical sciences : the international journal of the Japan Society for Analytical Chemistry* 20, 1383–8 (2004).

67. Bagheri, H., Babanezhad, E. & Es-haghi, A. An aniline-based fiber coating for solid phase microextraction of polycyclic aromatic hydrocarbons from water followed by gas chromatography-mass spectrometry. *Journal of Chromatography A* 1152, 168–174 (2007).

68. Zuazagoitia, D., Millán, E. & Garcia, R. A Screening Method for Polycyclic Aromatic Hydrocarbons Determination in Water by Headspace SPME with GC-FID. *Chromatographia 66*, 773–777 (2007).

69. López-Darias, J., Pino, V., Meng, Y., Anderson, J. L. & Afonso, A. M. Utilization of a benzyl functionalized polymeric ionic liquid for the sensitive determination of polycyclic aromatic hydrocarbons; parabens and alkylphenols in waters using solid-phase microextraction coupled to gas chromatography-flame ionization detecti. *Journal of Chromatography A* 1217, 7189–7197 (2010).

70. Steffen, A. & Pawliszyn, J. Analysis of Flavor Volatiles Using Headspace Solid-Phase Microextraction. *Journal of Agricultural and Food Chemistry* 44, 2187–2193 (1996).

71. Aryal, R. K., Furumai, H., Nakajima, F. & Boller, M. Dynamic behavior of fractional suspended solids and particle-bound polycyclic aromatic hydrocarbons in highway runoff. *Water Research 39*, 5126–5134 (2005).

`

72. Leversee, G. J., Landrum, P. F., Giesy, J. P. & Fannin, T. Humic acids reduce bioaccumulation of some polycyclic aromatic hydrocarbons. *Canadian Journal of Fisheries and Aquatic Sciences* 40, s63–s69 (1983).

73. Jones, K. D. & Tiller, C. L. Effect of solution chemistry on the extent of binding of phenanthrene by a soil humic acid: A comparison of dissolved and clay bound humic. *Environmental Science and Technology* 33, 580–587 (1999).

74. Curtosi, A., Pelletier, E., Vodopivez, C. L. & Mac Cormack, W. P. Distribution of PAHs in the water column, sediments and biota of potter cove, south Shetland Islands, Antarctica. *Antarctic Science* 21, 329–339 (2009).

75. Kobayashi, T. & Sumida, H. Effects of humic acids on the sorption and bioavailability of pyrene and 1,2-dihydroxynaphthalene. *Soil Science and Plant Nutrition* 61, 113–122 (2015).

76. Ghosh, U., Talley, J. W. & Luthy, R. G. Particle-scale investigation of PAH desorption kinetics and thermodynamics from sediment. *Environmental Science and Technology* 35, 3468–3475 (2001).

77. Rockne, K. J., Shor, L. M., Young, L. Y., Taghon, G. L. & Kosson, D. S. Distributed sequestration and release of PAHs in weathered sediment: The role of sediment structure and organic carbon properties. *Environmental Science and Technology* **36,** 2636–2644 (2002).

78. Nikanorov and L.V. Brazhnikova, 2003, *Types and Properties of Water*, Vol. II, pages 42-80 in Encyclopedia of Life Support Systems (EOLSS), Developed under the Auspices of the UNESCO, Eolss Publishers, Paris, France, [http://www.eolss.net]

`

79. European Commission & Scientific Committee on Food. Polycyclic Aromatic Hydrocarbons – Occurrence in foods, dietary exposure and health effects. Brussels, Belgium: *European Commission*; 2002 Annex A1–A194.

80. Chen, X. Zang, H. &Wang, X. et al. Metal–organic framework MIL-53(Al) as a solid-phase microextraction adsorbent for the determination of 16 polycyclic aromatic hydrocarbons in water samples by gas chromatography–tandem mass spectrometry. *The Analyst* 137, 5411 (2012).

81. Havenga, W. J. & Rohwer, E. R. The use of SPME and GC-MS for the chemical characterisation and assessment of PAH pollution in aqueous environmental samples. *International Journal of Environmental Analytical Chemistry* 78, 205–221 (2000).

82. Krüger, O., Olberg, S., Senz, R. & Simon, F. G. Comparison of Stir Bar Sorptive Extraction (SBSE) and Solid Phase Microextraction (SPME) for the Analysis of Polycyclic Aromatic Hydrocarbons (PAH) in Complex Aqueous Soil Leachates. *Water, Air, and Soil Pollution* 226, (2015).

83. García-Falcón, M. S., Pérez-Lamela, M. & Simal-Gándara, J. Comparison of strategies for extraction of high molecular weight polycyclic aromatic hydrocarbons from drinking waters. *Journal of Agricultural and Food Chemistry* 52, 6897–6903 (2004).

84. Risticevic, S. et al. Protocol for the development of automated high-throughput SPME-GC methods for the analysis of volatile and semivolatile constituents in wine samples. *Nature Protocols* 5, 162–176 (2010).

85. Patrolecco, L., Ademollo, N., Capri, S., Pagnotta, R. & Polesello, S. Occurrence of priority hazardous PAHs in water, suspended particulate matter, sediment and

common eels (Anguilla anguilla) in the urban stretch of the River Tiber (Italy). *Chemosphere* 81, 1386–1392 (2010).

86. Rügner, H., Schwientek, M., Beckingham, B., Kuch, B. & Grathwohl, P. Turbidity as a proxy for total suspended solids (TSS) and particle facilitated pollutant transport in catchments. *Environmental Earth Sciences* 69, 373–380 (2013).

87. Countway, R. E., Dickhut, R. M. & Canuel, E. A. Polycyclic aromatic hydrocarbon (PAH) distributions and associations with organic matter in surface waters of the York River, VA Estuary. *Organic Geochemistry* 34, 209–224 (2003).

88. Cheng, X., Forsythe, J. & Peterkin, E. Some factors affecting SPME analysis and PAHs in Philadelphia's urban waterways. Water Research 47, 2331–2340 (2013).

89. de Perre, C., Le Ménach, K., Ibalot, F., Parlanti, E. & Budzinski, H. Development of solid-phase microextraction to study dissolved organic matter-Polycyclic aromatic hydrocarbon interactions in aquatic environment. *Analytica Chimica Acta* 807, 51–60 (2014).

90. Chiou, C. T., Kile, D. E., Rutherford, D. W., Sheng, G. & Boyd, S. A. Sorption of selected organic compounds from water to a peat soil and its humic-acid and humin fractions: Potential sources of the sorption nonlinearity. *Environmental Science and Technology* 34, 1254–1258 (2000).

91. Zhu, L., Chen, Y. & Zhou, R. Distribution of polycyclic aromatic hydrocarbons in water, sediment and soil in drinking water resource of Zhejiang Province, China. *Journal of Hazardous Materials* 150, 308–316 (2008).

92. Planas, C., Puig, A., Rivera, J. & Caixach, J. Analysis of alkyl and 2-6-ringed polycyclic aromatic hydrocarbons by isotope dilution gas chromatography/mass

spectrometry. Quality assurance and determination in Spanish river sediments. *Journal of Chromatography A* 1113, 220–230 (2006).

93. Aldaeus, F., Thewalim, Y. & Colmsjö, A. Prediction of retention times of polycyclic aromatic hydrocarbons and n-alkanes in temperature-programmed gas chromatography. *Analytical and Bioanalytical Chemistry* 389, 941–950 (2007).